2015

Passivity control of bilateral and multilateral teleoperation systems

Da Sun
University of Wollongong, ds744@uowmail.edu.au

UNIVERSITY OF WOLLONGONG

School of Electrical, Computer and Telecommunications Engineering

Passivity Control of Bilateral and Multilateral Teleoperation Systems

Da Sun

**"This thesis is presented as part of the requirements for the
Award of the Degree of
Doctor of Philosophy
From
University of Wollongong"**

November, 2015

ABSTRACT

Teleoperation systems, characterized as bilateral and multilateral, allow an operator to perform complex tasks remotely via a slave manipulator. Such systems can extend human sensing, decision making and manipulation to a remote object and make the control system more flexible than a fully automated system.

The performance of a teleoperation system is primarily assessed by two criteria, stability and transparency. High transparency provides an operator with the genuine feeling of the remote environment but may increase the closed-loop gain, thereby causing instability. Stability is also undermined by time delay in a teleoperation system. Achieving a trade-off between stability and transparency in the presence of time delay is a major challenge in teleoperation systems. This challenge is also present in multilateral teleoperation systems that use more than one user to remotely operate the slave robot as well as systems with multiple slaves that collaborate to perform a manipulation task.

In this thesis we explore how passivity-based methods can be deployed to achieve simultaneous transparency and stability in bilateral and multilateral teleoperation systems under variable time delay. This will be an improvement to the passivity-based methods proposed in the literature that cannot produce high transparency in the presence of time delay.

During the course of the thesis a number of novel passivity-based methods are proposed and validated. A new architecture that can address two intrinsic problems, wave reflection and position drift, is developed and applied to linear and nonlinear bilateral teleoperation systems.

The reduced wave reflection architecture is further extended to a Single-Master-Multi-Slave teleoperation system in order to allow one master robot to control multiple slave robots and simultaneously derive improved force reflection.

A new approach that combines the wave variable method and Time Delay Passivity Approach (TDPA) with novel wave-based passivity observers and controllers is also proposed. Compared with other passivity-based methods, this approach can effectively enhance the system transparency and simultaneously maintain stability in the presence of time varying delays. The wave-based TDPA is then further extended with the

Prescribed Performance Control (PPC) method in order to achieve prescribed transient tracking behaviour of position, velocity and external force signals in the presence of time-varying delays.

Innovative methods applying sliding-mode control, neural networks and fuzzy logic methods are also deployed to estimate and eliminate the dynamic uncertainties and enhance the system synchronization performance in finite time.

The flexibility, stability and tracking accuracy of the multilateral teleoperation systems are also studied in this thesis. A dual-master-dual-slave teleoperation system with variable dominance factor is proposed to largely enhance the shared control training system's flexibility. The dual-user system is further extended to multi-user shared control system that allows the mentor to simultaneously lead multiple trainees in different places with different time-varying delays to collaboratively perform the remote task. All of the proposed systems are validated through experimental work using platforms consisting of 1-DOF and 3-DOF manipulators.

ACKNOWLEDGEMENTS

First and foremost, I would like to express my sincere appreciation to my supervisors, Professor Fazel Naghdy and Associated Professor Haiping Du for their guidance, encouragement and constant support throughout the course of this thesis.

Special thanks goes to my precious parents, Yiquan Sun and Manjuan Shen for their unconditional love, inspiration and endless support in all life of my life. To them, I dedicate this thesis.

Da Sun

November, 2015

TABLE OF CONTENTS

LIST OF FIGURES

LIST OF TABLES

1 INTRODUCTION

1.1 Background and Motivation

Teleoperation, in which a human operator interacts with the environment remotely, extends human sensing, decision-making and operation beyond direct physical contact. Since the 1940's, teleoperation systems have been deployed in numerous domains ranging from space exploration [1]-[2], underwater operation [3], mining [4], nuclear reactor [5]-[6] where human operators are protected from dangerous situations, to medical training [7], rehabilitation [8]-[10] and minimally invasive surgery [11]-[14] where through key-hole surgery a patient suffers less trauma. [15]. A teleoperation system consists of five elements of the human operator, the master, communication channels, the slave and the environment. From the teleoperator's point of view, a teleoperation system can be bilateral or multilateral.

A bilateral teleoperation system, comprising single master and single slave, provides the operator with a sense of presence in the remote environment (haptic sensation) by feeding back the force signal from a slave robot to a master through a communication network, such as Ethernet or Internet. The performance of bilateral teleoperation system is evaluated in terms of three objectives: stability, feeling of presence, and transparency. System stability of passivity is the basis of a system to normally function. Feeling of presence is a subjective process, indicating the operator's feeling of being present in the remote environment. Ideally, the operator should not fee any difference between present in a remote place and the real world. Compared to feeling of presence, transparency in a teleoperation system is an objective element, indicating that the technical medium between operator and environment is not felt, i.e. that the dynamics of master and slave are canceled out.

Teleoperation controllers are designed to ensure stability of contact and to achieve a desired performance. Incorporation of force feedback, is a double-edged sword as it injects extra energy into the overall system and jeopardizes the system stability [16] in addition to providing force information to the operator. With the network technologies advancing at a staggering rate, teleoperation can be conducted by using commercially

available communication networks. When the local and remote platforms are connected via commercial networks, the forward and feedback control signals between the master and the slave will be inevitably associated with time delay. For the remote control and manipulation, without proper control algorithms, even a small time delay may destabilize and degrade the tracking performance of a teleoperation system. Due to sensitivity of bilateral teleoperation systems to time delay, even a small time delay can de-stabilize the system [17].

Numerous methods have been proposed [18]-[21] to minimize the effect of time delay. A system designed by Lee and Spong uses direct position feedback to eliminate position drift [22]. Nunõ et al. use P-like, PD-like and scattering controllers to analyse the stability of the nonlinear teleoperation system with the classic assumptions of passivity [23]. In further development, they introduce a general Lyapunov-like function to unify stability analysis on the passivity-based control for the nonlinear teleoperation system [24]. An adaptive coordination control law based on the scattering approach is introduced by Chopra et al. to ensure position synchronization in the nonlinear teleoperation systems [25]. Yang et al. design a new fuzzy PD-like controller to deal with the system dynamics uncertainties [26]. However, all of the P-like and PD-like system require pre-set dampers with constant gains relating to the value of the time delay to guarantee the system's stability by reducing transparency. Due to different types of time delay, these method may be over-conservative in some situations.

The passivity-based approaches aim to robustly guarantee the system passivity under time delay. The idea of passivity characterized by mechanical energy, which uses force and velocity as efforts and flow variables, is an effective tool for establishing stability of bilateral teleoperation interaction. However, all of the passivity-based systems have a major challenge that is the largely reduced system transparency can seriously influence the system's performances especially in the presence of large time delays. Therefore, enhancing transparency and meanwhile maintaining system stability under random time delays is the primary goal for the passivity-based system design.

Several applications, including rehabilitation, surgical training and signal modification require the teleoperation systems with more than one user to remotely operate the slave robot [27]-[29]. These applications can be more effective with the collaboration of multiple robots where a single robot does not have the required level of manipulation dexterity, mechanical strength, robustness to single point failure, or safety (e.g. distributed kinetic energy). Therefore, an emerging research area is multilateral cooperative telerobotics where multiple robots interact with each other to cooperatively perform the remote task in different environments. The slave robots can manipulate the environment through an intervening tool or directly. Depending on the application, diverse configurations of master and slave robots are structured to build a cooperative teleoperation system.

The Single-Master-Multiple-Slave (SMMS) teleoperation system is a major direction of research in multilateral teleoperation. In SMMS teleoperation systems, a single operator collectively controls multiple slave robots. The slave robots are provided with local intelligence to avoid collision when performing a task. The applications of the SMMS teleoperation system include multi-finger grasping [30], tele-manipulation in remote or inaccessible environments [31], formation of a group of robotic agents [32], flexible and dexterous micro-assembling [33], and haptic guidance in tele-micromanipulation with increased human operability [34].

The multi-user teleoperation system is another major direction in the multilateral teleoperation research. In a multi-user teleoperation system, multiple operators control the slave robot by providing control information. Each operator can feel the mixed dynamics of the environment and the other operators. Multi-user teleoperation systems have found applications in surgical training simulators [35]-[37], control of a kinematically redundant robot [38], and rehabilitation [39].

As an extension of bilateral teleoperation, multilateral teleoperation is another approach with control challenges similar to bilateral teleoperation. Especially, dealing with the trade-off between stability and transparency in the presence of random time delays is a major objective in multilateral teleoperation systems. In the work conducted in [40], it is demonstrated that the optimized controller gains can be set to maintain stability by sacrificing system transparency. Sirouspour extend the bilateral nonlinear

adaptive control architecture that proposed earlier for multilateral teleoperation systems using a μ-synthesis based robust control [41]-[42]. Khademian et al. propose a four-channel controller for dual-master-single-slave teleoperation to achieve high transparency [43]. However, in the above works, two most important elements, i.e., the nonlinearity in the robot dynamics and time delays in the communication channels are ignored. Ghorbanian et al. explore the nonlinear trilateral teleoperation under time-varying delays using proportion-differential plus damping (PD+d) control architecture [44]. Li et al. propose an adaptive fuzzy control scheme to eliminate the nonlinearities and dynamics uncertainties of the trilateral teleoperation system under random time delays [45]. A framework for force-velocity control architecture is proposed in [46] for the development of a stability-guaranteed network of multilateral teleoperation by introducing the notion of absolute k-stability. The issue of balancing the trade-off between transparency and stability in the presence of time delay is still the main problem faced by the multilateral teleoperation systems.

1.2 Aims, Contributions and Publications of Thesis

In this Section, the primary aim of the thesis is initially introduced. Then the original contributions of the work relative to the existing works are presented. Finally, the major publications produced on the outcomes of the thesis will be described.

1.2.1 Aims

The primary aim of this thesis has been to investigate how concurrent transparency and stability in the presence of time delay can be maintained in bilateral and multilateral teleoperation systems using passivity-based approach. Towards realising this aim, a number of objectives have been pursued. In particular, we have explored wave variable transformation architecture to solve two intrinsic problems in the conventional wave variable transformation, wave reflection and position drift. We have succeeded to develop a new controller that could significantly reduce wave reflections and eliminate position drift thereby enhancing the system transparency. As mentioned before, variable time delay has been a challenge in traditional wave variable

transformation. This issue has been studied in our research and novel techniques have been proposed to enhance the wave-based system's performance in the presence of arbitrary time delay. Specifically, the methods developed in this thesis can improve system tracking accuracy in the worst case scenario where a system experiences large time delay at high rate. This approach can also enhance the system synchronization performance under time varying delays in finite time. The work has been further extended to guarantee the position, velocity and torque tracking of a bilateral system through novel control algorithm that can rapidly converge a system with a pre-defined boundary in the presence of random time delays. The uncertainties of the nonlinear dynamics are estimated and eliminated by deploying different methods. We have also studied multi-master multi-slave telerobotic systems. Multilateral systems can extend the human operational ability to remotely control more than one slave robot or allow multiple users to collaboratively drive the remote slave robot. In the thesis, the tracking accuracy, flexibility, synchronization and stability of multilateral teleoperation system in the presence of time varying delays are studied in order to further extend the multilateral robotic system capability and practicability.

1.2.2 Contributions

The major contributions of this thesis are as follows:

1) We have developed a novel wave variable transformation for bilateral teleoperation system that unlike the conventional wave variable transformation can effectively reduce wave reflections as well as the related signal perturbations using a proposed position, velocity and force encoding method. By adding direct position signal transmission channels, position drift as another intrinsic problem of conventional wave-based systems is addressed. The proposed wave transformations can also robustly guarantee the passivity of the communication channels under constant time delay.
2) An innovative wave-based system that can be effectively combined with the Time Delay Passivity Approach (TDPA) is proposed. The developed system can simultaneously enhance transparency while maintaining overall system stability in the presence of large constant and time-varying delays. This method can robustly

guarantee the channel passivity under constant delays. Moreover, the combined wave-based TDPA in this approach can address instability of wave-based system under time-varying delays and simultaneously enhance transparency of the overall system.

3) An extended Prescribed Performance Control (PPC) approach is proposed to further extend the wave-based TDPA system and restrict the boundary of position, velocity and torque tracking errors with a pre-set value. Therefore, the new system can achieve highly accurate tracking performance in the presence of large time-varying delays, compared with previous passivity-based systems.
4) A novel sliding-mode control method deploying Radial Basic Function (RBF) neural networks and Fuzzy Logic (FL) control method is developed to estimate and eliminate the system dynamic uncertainties.
5) A multilateral system applying the reduced wave-reflection architecture is proposed to allow one master robot to remotely control multiple slave robots under time-varying delays. Since the wave reflections are largely reduced, all of the slave robots can accurately follow the motion of the master robot. Moreover, the proposed algorithm provide the multilateral teleoperation system accurate torque tracking, which allows a single human operator to genuinely feel the mixed dynamics of the multiple slave robots.
6) A Dual-Master-Dual-Slave (DMDS) teleoperation system with a series of variable dominance factors is designed to enhance the overall system's flexibility in the presence of time-varying delays. With the variable dominance factors, the efficiency of the cooperation of the two users is enhanced. Moreover, as a flexible training system, the proposed algorithm allows one mentor to guide and evaluate the motion of a single trainee.
7) A novel multi-user shared control teleoperation system with extended wave-based TDPA is proposed to allow one mentor to simultaneously lead multiple trainees in different location at different time delays in order to collaboratively perform the remote tasks. The proposed approach can robustly guarantee stability of multiple robots. High flexibility and accurate motion synchronization of multiple robots can also be achieved in this system.

1.2.3 Publications

The research outcomes produced in this thesis have been published extensively in top tier journal and conferences. Here is the list of publications:

a) Sun, D., Naghdy, F., & Du, H. (2014). Application of wave-variable control to bilateral teleoperation systems: A survey. *Annual Reviews in Control,* Vol. 38, No. 1, pp.12-31.
b) Sun, D., Naghdy, F., & Du, H. (2014). Transparent four-channel bilateral control architecture using modified wave variable controllers under time delays. *Robotica*.
c) Sun, D., Naghdy, F., & Du, H. (2015). Wave-variable-based Passivity Control of Four-channel Nonlinear Bilateral Teleoperation System under Time Delays. *Mechatronics, IEEE Trans. on. Online-first.*
d) Sun, D., Naghdy, F., & Du, H. (2015) Enhancing Flexibility of the Dual-Master-Dual-Slave Multilateral Teleoperation System. *IEEE Multi conference, Sydney, accept.*
e) Sun, D., Naghdy, F., & Du, H. (2015). Stability Control of Force-Reflected Nonlinear Multilateral Teleoperation System under Time-Varying Delays. *Journal of Sensors, 501, 682736.*
f) Sun, D., Naghdy, F., & Du, H. A Novel Approach for Stability and Transparency Control of Nonlinear Bilateral Teleoperation System with Time Delays. *Control Engineering Practice, accept.*
g) Sun, D., Naghdy, F., & Du, H. Neural Network based Passivity Control of Teleoperation System under Time-Varying Delays. *Cybernetics, IEEE Trans. on, under review.*
h) Sun, D., Naghdy, F., & Du, H. An Innovative Framework for Nonlinear Multi-user Shared Control of Teleoperation System with Time-varying Delays. *Industrial Electronics, IEEE Trans. on, under review.*

i) Sun, D., Naghdy, F., & Du, H. Passivity Control for Nonlinear Networked Bilateral Teleoperation System with Prescribed Performance under Arbitrary Time Delays. *Industrial Electronics, IEEE Trans. on, under review.*

1.3 Thesis structure

This thesis is organized in 6 chapters as follows:

Chapter 2 provides a review of the studies conducted on the wave variable control algorithms over the last 20 years. An analysis of the properties of the wave-variable control method is conducted and various approaches proposed for its improvement are evaluated.

Chapter 3 introduces the proposed reduced wave reflections bilateral architectures. The proposed systems has a better performance in reducing wave reflection and eliminating position drift than compared to the previous work.

In Chapter 4, the innovative wave-based TDPA systems are introduced. The proposed systems can have high transparency and robust stability in the presence of random time delays.

In Chapter 5, Single-Master-Multi-Slave teleoperation system applying deploying the reduced wave reflections architecture, a flexible dual-user-dual-slave system, and a multi-user teleoperation system applying deploying the wave-based TDPA are introduced described and modelled and analysed.

Chapter 6 draws some conclusions and provides an outline for the future work.

The developed algorithms are validated in each chapter.

2 BACKGROUND

2.1 Overview

As one of the major passivity-based methods, wave variable control is quite unique as it provides a physical description of system passivity while it does not require the knowledge of the remote robot. The concepts associated with standard wave variable control were introduced around 20 years ago. Since then, various algorithms have been proposed to enhance the performance of wave variable control in bilateral teleoperation. In this chapter, a review of various applications of wave variable control in telerobotics is conducted and an evaluation of different methods proposed to compensate for intrinsic problems of the approach such as position drift, wave reflection and sensitivity to time varying delay is carried out. A critical analysis and evaluation of the advantages and disadvantages of the wave-variable control method will be conducted and various and different methods proposed in the literature for its improvement will be reviewed.

2.2 Theoretical Foundations of the Wave Variable Method

2.2.1 2-port Network

Representing the effective relationship between force and velocity with voltage and current [47], a two-port network model of a teleoperation system can be represented as cascaded feedback interconnection of the component shown in Figure 2.1, where the models of the master, communication network and slave are represented by two ports, and the operator and environment by a single port [48].

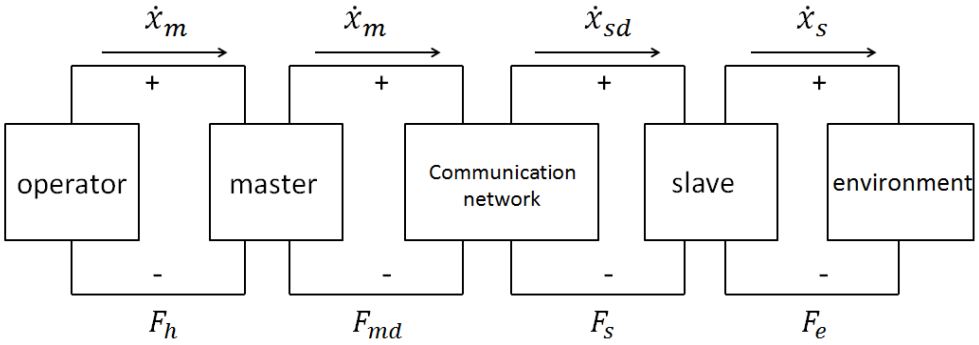

Figure 2.1. 2-port network model of a teleoperation system [142]

The property of a 2-port system can be described by the relationship between effort and flow. In terms of a linear time-invariant single port system, this relationship can be defined by (2.1):

$$F(s) = Z(s)v(s) \tag{2.1}$$

Where F(s) and v(s) are the Laplace transforms of effort F(t) and flow v(t), respectively. Z(s) is an impedance matrix defining the relationship between force and flow. For a linear time-invariant 2-port system, this relationship can be also presented by the hybrid matrix H(s):

$$\begin{bmatrix} F_1(s) \\ -v_2(s) \end{bmatrix} = \begin{bmatrix} h_{11}(s) & h_{12}(s) \\ h_{21}(s) & h_{22}(s) \end{bmatrix} \begin{bmatrix} v_1(s) \\ F_2(s) \end{bmatrix} = H(s) \begin{bmatrix} v_1(s) \\ F_2(s) \end{bmatrix} \tag{2.2}$$

Where the properties of the output effort F_1, the input effort F_2, the input flow v_1 and the output flow v_2 are shown in Figure 2.2.

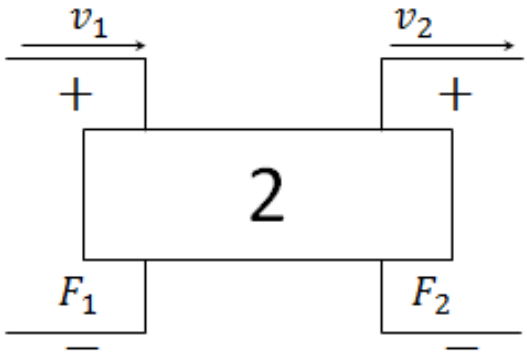

Figure 2.2. 2-Port model [143]

In (2), Hybrid matrix H(s) is defined by [49], which can be interpreted as $\mathrm{H}(\mathrm{s}) = \begin{bmatrix} h_{11}(s) & h_{12}(s) \\ h_{21}(s) & h_{22}(s) \end{bmatrix} = \begin{bmatrix} Z_{in} & Force\ scalling \\ Velocity\ Scalling & Z_{out}^{-1} \end{bmatrix}$, in which Z_{in} and Z_{out} are the input and the output impedances, respectively. The hybrid parameters $h_{ij}, \mathrm{i,j} = 1,2$ are functions of the master and slave dynamics and the control parameters [49]. The main effect of $\mathrm{H}(\mathrm{s})$ is to present kinesthetic feedback between the human operator and the environment, and to build a relationship between force and velocity.

According to the 2-port network model shown in Figure 2.1, the system's hybrid matrix model can be written as:

$$\begin{bmatrix} F_h(s) \\ -\dot{x}_s(s) \end{bmatrix} = \begin{bmatrix} h_{11}(s) & h_{12}(s) \\ h_{21}(s) & h_{22}(s) \end{bmatrix} \begin{bmatrix} \dot{x}_m(s) \\ F_e(s) \end{bmatrix} = H(s) \begin{bmatrix} \dot{x}_m(s) \\ F_e(s) \end{bmatrix} \tag{2.3}$$

Where F_h and F_e are the force applied by the operator and the interaction force between the slave and the environment, respectively. Since x represents position, $\dot{x}$ the differential of x, is the velocity. Therefore, $\dot{x}_m$ and $\dot{x}_s$ represent the velocities of master and slave.

The 2-port network model provides a reference model for analysis of energy flow in teleoperation systems. Hence, it has been deployed as the default model in the subsequent application of passivity theory in teleoperation.

2.2.2 Passivity Theory

Passivity is a property presented in many physical systems (electronic systems, electromechanical system etc.). It reveals the system stability property from the input/output energy perspective, and has been developed as a general design approach and theory in system stability control. According to [50] and [51], passivity is a sufficient condition for the stability of a system. If a teleoperation system is passive, it is guaranteed to be stable. However, if a system is stable, it is not necessarily a passive system.

Remark 1 [52]: the inner product of system input vector x and output vector y is the input power P_{in}, which is also equal to the sum of the variation of system storage

energy E_{store} (lower-bounded) and the system dissipative power P_{diss}. This can be written as:

$$P_{in} = x^T y = \frac{dE_{store}}{dt} + P_{diss} \tag{2.4}$$

The power defined in this relationship is not the actual physical quantity. Therefore, this relationship is satisfactory when the dimensions of input/output vectors are appropriate. For instance, the input power of the 2-port model shown in Figure 2.2 can be defined as v^TF.

Under the condition that the power is either stored or dissipated, the total energy supplied by the system up to time t, which corresponds to a negative energy transfer into the system, can be limited to the initial stored energy. That is, the energy transfer is lower bounded by the negative initial energy.

$$\int_o^t P_{in}\, d\tau = \int_0^t x^T \mathrm{y}\ d\tau = E_{store}(t) - E_{store}(0) + \int_o^t P_{diss}\, d\tau \geq -E_{store}(0) \tag{2.5}$$

Remark 2 [52]: A control system is passive at any time if (2.5) is true. If the dissipated power P_{diss} is positive when the system storage energy E_{store} does not reach its lower bound, the system can be defined strictly passive. If the dissipated power P_{diss} remains constantly zero, the system is lossless.

Treating the system storage power E_{store} as a Lyapunov-like function, it can be shown that in the absence of an external input, the passive system is stable and the strictly passive system is asymptotically stable [52].

A passivity-based system illustrates that the output energy of a system will not exceed the sum of the input energy and the initial stored energy of the system [27].

It should be noticed that one of the major challenges for passivity maintenance of the teleoperation system is the largely unknown human and environment dynamics, both of which are part of the global control loop in Figure 2.1. Therefore, in most teleoperation control systems, the dynamics of the human operator and the environment are assumed to be passive. That is $E_h = -\int_0^t \dot{x}_m^T F_h\, d\tau + k_m \geq 0, E_e =$

$\int_0^t \dot{x}_s^T F_e \, d\tau + k_s \geq 0 \left(k_{m,s} \in R_+\right)$, where E_h and E_e denotes the energy of the human and the environment. [24]

2.2.3 Scattering Approach

Remark 3 [50]: R_+ is a non-negative real number. R^n is the n-dimensional Euclidean space. $L_2^n(R_+)$ is the Hilbert space composed of Lebesque square integrable function f: $R_+ \to R^n$, which is $\|f\|_2 \triangleq \left(\int_0^\infty |f(t)|^2 dt\right)^{1/2} > \infty$. If operator T: $L_2^n(R_+) \to L_2^n(R_+)$ has boundary ($L_2^n(R_+)$ is the Hilbert space of Lebesque measurable functions $R_+ \to R^n$), its norm can be defined as:

$$\|T\| = \sup_{\substack{x \in L_2^n(R_+) \\ \|x\| \neq 0}} \frac{\|Tx\|_2}{\|x\|_2} \tag{2.6}$$

where "sup" denotes supremum (the least upper bound).

Remark 4 [18]: For ∀F, v ∈ $L_2^n(R_+)$, scattering operator S: $L_2^n(R_+) \to L_2^n(R_+)$ is defined as:

$$\mathrm{F} - \mathrm{v} = \mathrm{S}(\mathrm{F} + \mathrm{v}) \tag{2.7}$$

From (2.7), the scattering operator S is deployed to map the sum of effort and flow into the difference between effort and flow. For linear time-invariant systems, scattering operator S can be represented by the scattering matrix S(s) in the frequency domain:

$$\mathrm{F}(\mathrm{s}) - \mathrm{v}(\mathrm{s}) = \mathrm{S}(\mathrm{s})[\mathrm{F}(\mathrm{s}) + \mathrm{v}(\mathrm{s})] \tag{2.8}$$

As to the two-port system, the scattering matrix can be derived from hybrid matrix H(s):

$$\begin{bmatrix} F_1(s) - v_1(s) \\ F_2(s) + v_2(s) \end{bmatrix} = \begin{bmatrix} 1 & 0 \\ 0 & -1 \end{bmatrix} \left(\begin{bmatrix} F_1(s) \\ -v_2(s) \end{bmatrix} - \begin{bmatrix} v_1(s) \\ F_2(s) \end{bmatrix} \right) = \begin{bmatrix} 1 & 0 \\ 0 & -1 \end{bmatrix} (H(s) - I) \begin{bmatrix} v_1(s) \\ F_2(s) \end{bmatrix} \tag{2.9}$$

where I is the identity matrix. Likewise:

$$\begin{bmatrix} F_1(s)+v_1(s) \\ F_2(s)-v_2(s) \end{bmatrix} = \begin{bmatrix} F_1(s) \\ -v_2(s) \end{bmatrix} + \begin{bmatrix} v_1(s) \\ F_2(s) \end{bmatrix} = (H(s)+I)\begin{bmatrix} v_1(s) \\ F_2(s) \end{bmatrix} \quad (2.10)$$

Based on (2.8)-(2.10):

$$\mathrm{S(s)} = \begin{bmatrix} 1 & 0 \\ 0 & -1 \end{bmatrix}(H(s)-I)(H(s)+I)^{-1} = \mathrm{diag}(1,-1)\big[[H(s)-I]H(s)+I\big]^{-1} \quad (2.11)$$

Theory 1 [18]: the necessary and sufficient condition of passivity in teleoperation system (3) is that the norm of the scattering matrix (11) must not exceed 1. That is, $\|S\| \le 1$. It is also illustrated as $sup\lambda^{1/2}[S^*(\mathrm{j}\omega)\mathrm{S}(\mathrm{j}\omega)] \le 1$, where $\lambda^{1/2}$ represents the square root of the largest characteristic value. This theory is proved as follows [28]:

Proof: $\|S\| \le 1 \Leftrightarrow \frac{\|F-v\|_2}{\|F+v\|_2} \le 1 \Leftrightarrow \|F+v\|_2 - \|F-v\|_2 \ge 0 \Leftrightarrow \int_0^\infty (F+v)^T(F+v) - (F-v)^T(F-v)\mathrm{dt} \ge 0 \Leftrightarrow 2\int_0^\infty (v^TF + F^Tv)dt \ge 0 \Leftrightarrow 4\int_0^\infty (F^T\,\mathrm{v})\mathrm{dt} \ge 0$ (2.12)

The relationship (10) can be also presented in a form similar to (3): $\mathrm{H(s)}=\begin{bmatrix} 0 & e^{-sT} \\ -e^{-sT} & 0 \end{bmatrix}$, where T is the communication time delay. Thus, after substituting H(s) into (11), the scattering matrix of the system can be derived: $\mathrm{S(s)} = \begin{bmatrix} -\tanh(sT) & \mathrm{sech}(sT) \\ \mathrm{sech}(sT) & \tanh(sT) \end{bmatrix}$, then $\|S\|=\infty$ can be proved [18].

$$\begin{aligned} \|S\| &= sup_\omega \lambda^{\frac{1}{2}}\left(\begin{bmatrix} jtan(\omega T) & \sec(\omega T) \\ \sec(\omega T) & jtan(\omega T) \end{bmatrix}\begin{bmatrix} -jtan(\omega T) & \sec(\omega T) \\ \sec(\omega T) & jtan(\omega T) \end{bmatrix}\right) \\ &= sup_\omega \lambda^{\frac{1}{2}}\left(\begin{bmatrix} tan^2(\omega T)+\sec^2(\omega T) & 2jtan(\omega T)\sec(\omega T) \\ -2jtan(\omega T)\sec(\omega T) & tan^2(\omega T)+\sec^2(\omega T) \end{bmatrix}\right) \end{aligned} \quad (2.13)$$

Thus:

$$\|S\| = sup_\omega(|tan(\omega T)+\sec(\omega T)|) = \infty \quad (2.14)$$

As the scattering matrix norm S for direct transmission force and velocity variables is infinite, it is proved that the signal transmission model with time delay is not passive.

2.2.4 Wave Variable and Wave Controller

2.2.4.1 Wave Variables and Wave Transformation

Based on the passivity theory and scattering approach, the concept of the wave variables approach as a notion of energy is introduced [52], which is a passive control algorithm. Its effect is to modify and extend the passivity theory in order to alleviate the negative effects of time delay in a control system. Scattering matrix maps the relationship between the velocity and force signals to the system. As this approach is mainly deployed in nonlinear systems manipulated in an unstructured environment, it has high potential in practical applications.

The scattering operator is proved to be unbounded when there is time delay in a transmission channel. This influences the passivity of a teleoperation system. The wave variable method introduced by [52] compensates for this drawback to a great extent.

If correction modules are added to the signal transmission module shown in Figure 2.1 to render $H(s) = \begin{bmatrix} b\tanh(sT) & -\operatorname{sech}(sT) \\ \operatorname{sech}(sT) & \frac{1}{b}\tanh(sT) \end{bmatrix}$, its scattering operator will be $S(s) = \begin{bmatrix} 0 & e^{-sT} \\ e^{-sT} & 0 \end{bmatrix}$ [18].

Therefore, $\|S\| = sup\lambda^{1/2}[S^*(j\omega)S(j\omega)] = sup\lambda^{1/2}\left(\begin{bmatrix} 0 & e^{sT} \\ e^{sT} & 0 \end{bmatrix}\begin{bmatrix} 0 & e^{-sT} \\ e^{-sT} & 0 \end{bmatrix}\right) = sup\lambda^{1/2}\left(\begin{bmatrix} 1 & 0 \\ 0 & 1 \end{bmatrix}\right) = 1$. Accordingly, the transmission module satisfies the passivity condition and becomes lossless after correction. For this purpose, the following wave variables are introduced:

$$u = \frac{b\dot{x} + F}{\sqrt{2b}} \quad v = \frac{b\dot{x} - F}{\sqrt{2b}} \tag{2.15}$$

where b is defined as the characteristic impedance or wave impedance. This parameter can be a positive constant or a symmetric positive definite matrix and is the only adjustable parameter in the force and velocity model. Different values of b can prompt the system to have different properties from damping to freedom. Parameter u is the forward moving wave from master to slave, while v is the returning wave from slave to master. These two parameters are symmetrical relative to each other, which eliminates the difference between velocity and force.

In the transmission module illustrated in Figure 2.3(a) (2.15), transformation from power variables to wave variables ($(\dot{x}, F) \rightarrow (u, v)$) is reversible. The inverse transmission as illustrated in Figure 2.3(b) can be written as:

$$\dot{x} = \frac{1}{\sqrt{2b}}(u + v), \mathrm{F} = \sqrt{\frac{b}{2}}(u - v) \tag{2.16}$$

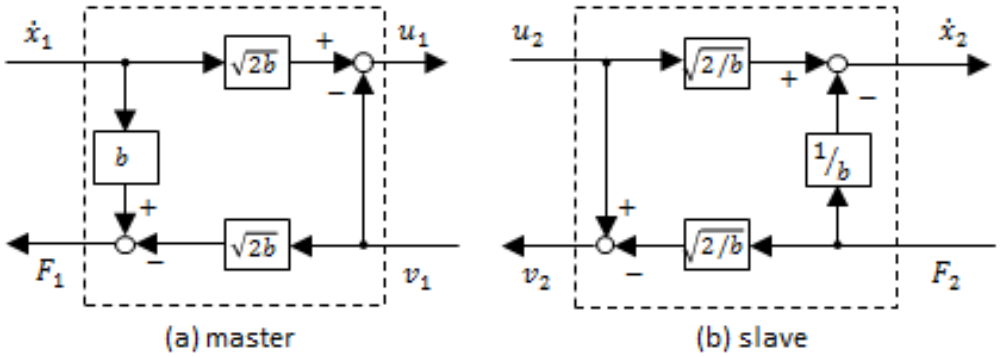

Figure 2.3. Wave variable transformation

Therefore, the power in any part of the teleoperation system (Figure 2.1) can be re-defined by:

$$\mathrm{P} = \dot{x}^T \mathrm{F} = \frac{1}{2}u^T u - \frac{1}{2}v^T v \tag{17}$$

From (17), forward wave u provides power to the system, while backward wave v dissipates power from the system.

Substituting (17) into (5) results in $\int_0^t \frac{1}{2} u^T u \, d\tau - \int_0^t \frac{1}{2} v^T v \, d\tau \geq -E_{store}(0)$. Thus, the passivity condition (5) can also be re-written as:

$$\int_0^t \frac{1}{2} v^T v d\tau \leq \int_0^t \frac{1}{2} u^T u d\tau + E_{store}(0), \forall t \geq 0 \tag{18}$$

Wave variables, unlike physical entities such as velocity and force, have no intuitive physical significance and cannot be easily measured. The unit $\sqrt{watt}$ of wave variables is also quite unusual [29].

2.2.4.2 Conventional wave transformation

The structure of the wave controller on the basis of the communication loop is shown as Figure 2.4.

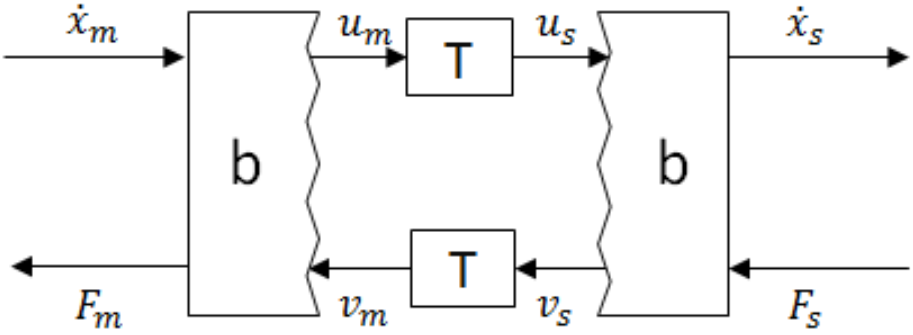

Figure 2.4. Structure of wave controller [52]

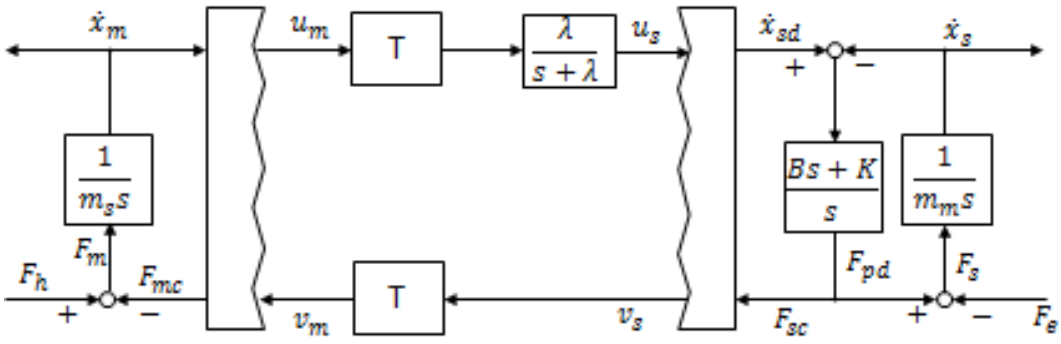

Figure 2.5. Wave-based teleoperator [52]

As an example, the transfer function diagram of a 1-DOF teleoperation system, in which the slave side uses a PD-controller: $F_s = -B(\dot{x}_s - \dot{x}_{sd}) - K(x_s - x_{sd})$, where B and K are damping parameter and stiffness gain, respectively, is shown as Figure 2.5.

Based on (16), the wave transformation of the wave controller [52] can be defined by:

$$u_m(t) = \frac{b\dot{x}_m(t) + F_{mc}(t)}{\sqrt{2b}}, u_s(t) = \frac{b\dot{x}_{sd}(t) + F_{sc}(t)}{\sqrt{2b}} \tag{2.19}$$

$$v_m(t) = \frac{b\dot{x}_m(t) - F_{mc}(t)}{\sqrt{2b}}, v_s(t) = \frac{b\dot{x}_{sd}(t) - F_{sc}(t)}{\sqrt{2b}} \tag{2.20}$$

Where $\dot{x}_m$, $\dot{x}_{sd}$, F_{mc} and F_{sc} denote the master velocity, the desired slave velocity, the master control force and the slave control force, respectively. When the communication channel transmitting wave variables has a constant time delay T, the following relationship holds:

$$u_s(t) = u_m(t - T), v_m(t) = v_s(t - T) \tag{2.21}$$

Assuming a two-port device as shown in Figure 2.2, the power flow P can be defined by $P = \dot{x}_1^T F_1 - \dot{x}_2^T F_2$ [52]. Based on scattering theory, the total power flow [52] in the communication link is:

$$P_{in} = \dot{x}_m^T F_m - \dot{x}_s^T F_s = \frac{1}{2}u_m^T u_m - \frac{1}{2}v_s^T v_s - \frac{1}{2}u_s^T u_s + \frac{1}{2}v_m^T v_m \tag{2.22}$$

After substituting (2.19)-(2.21) into (2.22) and then integrating (2.22), the energy casually stored during the wave transmission procedure is represented by:

$$E_{store}(t) = \int_{t-T}^{t} (\frac{1}{2}u_m^T u_m + \frac{1}{2}v_s^T v_s) d\tau > 0 \tag{2.23}$$

2.3 Properties of Standard Wave-variable-based Teleoperation System

2.3.1 Indices of Teleoperation System

2.3.1.1 Dissipativity and Finite Gain L_2-Stability

Involving the model knowledge of human and environment closed-loop dynamics into design of the teleoperation control system can enhance transparency but may degrade system stability [55]. Therefore, applying the approximate knowledge of the damping properties of the human operator, manipulators and environment can improve transparency without jeopardizing system stability. [56]-[60] denote these subsystems to be dissipative with a quadratic supply rate (QSR-dissipative).

Theory 2 [56]: a control system is called QSR-dissipative if there exists a storage function V: $\mathrm{R}^n \to R_+$, which is positive-semidefinite, as follows:

$$\mathrm{V}(\mathrm{x(t)}) - \mathrm{V}(\mathrm{x(0)}) \leq \int_0^t \begin{bmatrix} a \\ y \end{bmatrix}^T P \begin{bmatrix} a \\ y \end{bmatrix} d\tau \tag{2.24}$$

with the dissipativity matrix: $\mathrm{P} = \begin{bmatrix} Q & S \\ S^T & R \end{bmatrix}$ $(Q \in R^{p\times p}, R \in R^{q\times q}, S \in R^{p\times q})$ where x, a, y are the state, input and output vectors of the control system, respectively. [61] illustrates that input-feedforward-output feedback passive systems (IF-OFP), which is a subclass of the QSR-dissipative system, are represented by: $\mathrm{P} = \begin{bmatrix} -\delta I & \frac{1}{2}I \\ \frac{1}{2}I & -\varepsilon I \end{bmatrix}$ $(\delta, \varepsilon \in R)$ This system is lossless under the condition $\delta = \varepsilon = 0$, output-feedback strictly passive (OFP(ε)) under the condition $\delta = 0, \varepsilon > 0$, and input-feedforward strictly passive (IFP(δ)) under the condition $\delta > 0, \varepsilon = 0$. Under the condition that one or both of δ, ε are negative, the passivity of this system is not satisfied.

Theory 3 [62]: a control system is called finite gain L_2-Stable if there exists a positive-semidefinite function V: $\mathrm{R}^n \to R_+$ and a scalar constant $\gamma > 0$ such that for each admissible a and each $\mathrm{t} \geq 0$

$$\mathrm{V}(\mathrm{x}(\mathrm{t})) - \mathrm{V}(\mathrm{x}(0)) \leq \int_0^t \gamma^2 a^T a - y^T y \, d\tau \tag{2.25}$$

$$\|y_t\|_{L_2} \leq \gamma^2 \|u_t\|_{L_2} + \sqrt{V(x(0))} \tag{2.26}$$

Where $\|y_t\|_{L_2}$ denotes the L_2-norm of the truncated signal y. That is, $\|y_t\|_{L_2} = \sqrt{\int_0^t y(\tau)^T y(\tau)}$. The smallest parameter γ in (26) is said to be the L_2-gain of the control system. When $\gamma \leq 1$, this system is called to own the small gain property.

2.3.1.2 Transparency

Transparency is an abstract concept because this index represents the property of a teleoperation system from the concept of 'human feelings'. A teleoperation system is defined to be transparent if the human operator perceives the remote environment accurately and performs the remote task with ease [63].

Specifically, transparency is also defined as the matching equality between operator-perceived mechanical impedance Z_h and the environment impedance Z_e [64]-[65]; that is: $Z_h = Z_e$. According to (1), the impedance of the human operator or the environment is the ratio between the effort (force, voltage) and the flow (velocity, current) in the Laplace domain. Transparency can be analyzed by a 2-port network model where the hybrid matrix is used to build the relationship between the forces and velocities of the master and slave as shown in (3)

Also, from (1), the slave force can be derived using the environmental impedance Z_e:

$$\mathrm{F}_s = Z_e v_s \tag{2.27}$$

From (2.27) and (2.3), force F_m on the master side can be derived as:

$$F_m = \left(\frac{h_{12}h_{21}}{1 - h_{22}Z_e} Z_e + h_{11}\right) v_m \tag{2.28}$$

P_r and P_o can be defined by [66]:

$$P_r = \frac{h_{12}h_{21}}{1 - h_{22}Z_e}, P_o = h_{11} \tag{2.29}$$

Therefore, (2.28) can be rewritten as:

$$F_m = (P_r Z_e + P_o)v_m \tag{2.30}$$

Where P_r and P_o denote reproducibility and operationality, which are two sub-indices of transparency. Reproducibility means the precision of the master side reproducing the environment while operationality means the degree of smoothness at which the human operator manipulates the master robot [146]. To achieve the ideal Transparency, reproducibility and operationality should satisfy $|P_r| = \left|\frac{h_{12}h_{21}}{1-h_{22}Z_e}\right| = 1$ and $P_o = h_{11} = 0$, respectively [66]. Therefore, the following conditions should be maintained:

$$h_{11} = h_{22} = 0, h_{12}h_{21} = 1 \tag{2.31}$$

Accordingly, the hybrid matrix for the ideal transparency is $H_{ideal}(s) = \begin{bmatrix} 0 & 1 \\ -1 & 0 \end{bmatrix}$. Considering the time delay, the best transparency is achievable when $Z_h = e^{-iTs}Z_e$, therefore, the hybrid matrix for the best transparency can be written as [64]:

$$H_{ideal}(s) = \begin{bmatrix} h_{11}(s) & h_{12}(s) \\ h_{21}(s) & h_{22}(s) \end{bmatrix} = \begin{bmatrix} 0 & e^{Ts} \\ -e^{Ts} & 0 \end{bmatrix} \tag{2.32}$$

Each element of the hybrid matrix H(s) also has its own physical meaning. h_{11} denotes the input impedance in the free-motion condition while a non-zero value of h_{11} means force feedback is still received on the master side even when the slave is in free motion, which offers the human operator a sticky feeling for the free motion. h_{12} and h_{21} represent the measure of force scaling and velocity scaling, respectively. h_{22} denotes the output admittance of master locked in motion while non-zero values of h_{22} means the slave robot keeps moving even when the master robot's motion is stopped.

Trade-off between stability and transparency is an inherent problem in teleoperation systems. This is due to the property of the bilateral teleoperation contending with the system passivity as a result of the possible instabilities caused by force feedback [66], [67]. Hence, guaranteeing the system stability usually implies the degradation of transparency [50]. Since wave variable is a conservative approach to system stability that excessively pursues the passivity of the teleoperation system, the transparency of the standard wave-variable-based system is degraded. Additionally, this method has two intrinsic problems: wave reflection and position drift. Therefore, increasing transparency is a critical target for the design of wave-variable-based teleoperation systems.

2.3.2 Intrinsic Problems of Wave-based System

2.3.2.1 Wave Reflection

Wave reflection occurs in the wave-based teleoperation systems when the junction impedance is not perfectly matched [68]. This can be revealed by analyzing the standard wave-based teleoperation architecture. According to a standard teleoperation system with wave controller, there are three independent signal feedback channels as shown in Figure 2.6: the straight feedback of the master (dashed line 1), the feedback from the slave (dashed line 2) and wave reflections (dashed line 3).

In Channel 1, the signal returns in the form of the damping b$\dot{x}_m$ as (2.33) which is a transformation of (2.15):

$$F_m = b\dot{x}_m - \sqrt{2b}v_m \tag{2.33}$$

For the human operator, this signal is like a signal damper, which is the only signal without time-delay.

Channel 2 sends back the signal from slave to the local operator with the PD controller, and also provides the expected information. Both the free motion and environment contact will be described by the position and velocity of the slave, and presented in the tracking error. The force of the slave encodes this information in order to provide the

approximate representation of a practical contact force, and then feedback to the operator, which is also the main aim of a bilateral teleoperator.

The phenomenon of wave reflection is shown as channel 3. Re-writing (2.19) and (2.20) results in:

$$u_m = -v_m + \sqrt{2b}\dot{x}_m \, , v_s = u_s - \sqrt{\frac{2}{b}} F_S \tag{2.34}$$

As can be seen from (2.34), each input wave $v_m$or u_s will be reflected and returned, then left as the output wave u_m and v_s.

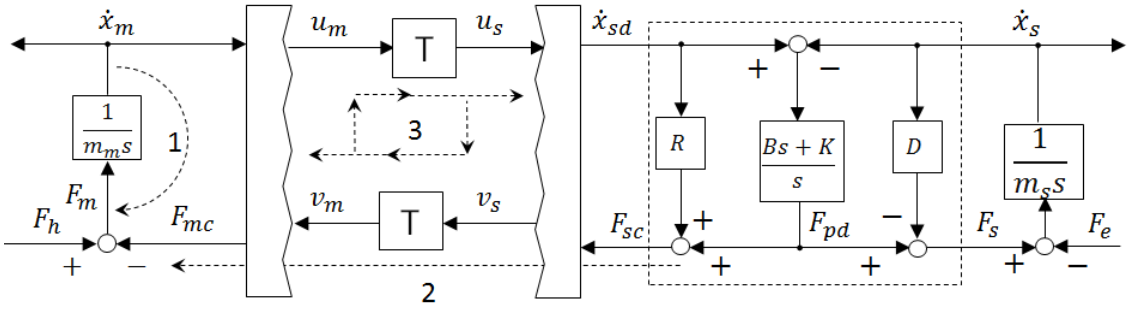

Figure 2.6. Three feedback channels of the wave-based system [69]

In the 3-channel mode, the second channel contains important data which must be protected. The first channel produces a certain amount of damping to enhance the stability of the system at the expense of losing telepresence. However, the wave reflection of the third channel will result in significant problems and adversely affect the other two channels. Therefore, in practical applications of the wave variables approach, the influence of wave reflection must be eliminated.

The other interpretation of wave reflection is on the basis of a standing wave phenomenon in which wave reflections on boundaries can superimpose and interfere in order to generate continual oscillations. The boundary conditions determine the particular resonant frequency. In addition, the operator may be forced by the slow decay of the wave reflections to wait for a long time before continuing manipulation [70].

In [71], wave reflection is analyzed in the frequency domain. Based on Figure 2.5, the dynamic model standard wave-based teleoperation architecture in the frequency domain can be written as [71]:

$$\mathrm{G}_m^{-1} X_m = F_m - F_{mc} \tag{2.35}$$

$$\mathrm{G}_s^{-1} X_s = F_s - F_e, F_s = C_v(s)(sX_{sd} - sX_s) \tag{2.36}$$

Where $G_m = \frac{1}{M_m s^2}$ and $G_s = \frac{1}{M_s s^2}$ are the transfer functions of the master and the slave. M_m and M_s are the inertia masses of master and slave. F_{mc} and X_{sd} represent the desired force of the master and the desired slave position, respectively. $C_v = \frac{Bs+K}{s}$ is the slave velocity controller. B and K are the differential parameter and proportional parameter, respectively. The operator s is the Laplace operator.

In addition, the reference signal in the frequency domain of this architecture can be derived based on (2.15), (2.16) and (2.21) in the presence of time delay

$$\mathrm{F}_{mc} = F_s e^{-T_2 s} + b(sX_m - sX_{sd} e^{-T_2 s}) \tag{2.37}$$

$$sX_{sd} = sX_m e^{-T_1 s} + \frac{1}{b}(\mathrm{F}_{mc} e^{-T_1 s} - F_s) \tag{2.38}$$

Where T_1 and T_2 are the time delays in the feed-forward and feedback path.

Substituting (2.37) and (2.38) into (2.35) and (2.36), the dynamics model of master and slave can be re-written as:

$$\mathrm{G}_m^{-1} X_m = F_m - F_s e^{-T_2 s} + b(X_{sd} e^{-T_2 s} - sX_m) \tag{2.39}$$

$$\mathrm{G}_s^{-1} X_s = C_v(s)(sX_m e^{-T_1 s}) - sX_s + \frac{C_v(s)}{b}(\mathrm{F}_{mc} e^{-T_1 s} - F_s) - F_e \tag{2.40}$$

Moreover, the dynamic model of master and slave can be expressed as:

$$F_{mc} = F_m - \mathrm{G}_m^{-1} X_m \tag{2.41}$$

$$F_s = F_e + \mathrm{G}_s^{-1} X_s \tag{2.42}$$

$$sX_{sd} = \frac{G_s^{-1}X_s + F_e}{C_v(s)} + sX_s \tag{2.43}$$

Substituting (2.41), (2.42) and (2.43) into (2.39) and (2.40):

$$G_m^{-1}X_m = \left(\frac{bG_s^{-1}}{C_v(s)} - G_s^{-1} + bs\right)X_s e^{-T_2 s} - bsX_m - F_h - \left(1 - \frac{b}{C_v(s)}\right)F_e e^{-T_2 s} \tag{2.44}$$

$$G_s^{-1}X_s = C_v(s)\left(s - \frac{G_m^{-1}}{b}\right)X_m e^{-T_1 s} - C_v(s)\left(s + \frac{G_s^{-1}}{b}\right)X_s - \frac{C_v(s)}{b}F_h e^{-T_1 s} - \left(\frac{C_v(s)}{b} + 1\right)F_e \tag{2.45}$$

After substituting (39) and (40) into (44) and (45), [71] finally results in:

$$\begin{aligned} G_m^{-1}X_m &= b\left(\frac{e^{-(T_1+T_2)s} - 1}{e^{-(T_1+T_2)s} + 1}\right)sX_m - F_h - \frac{2G_s^{-1}X_s e^{-T_2 s}}{e^{-(T_1+T_2)s} + 1} - \frac{2F_e e^{-T_2 s}}{e^{-(T_1+T_2)s} + 1} \\ &= b\left(e^{-(T_1+T_2)s} - 1\right)sX_m - 2G_s^{-1}X_s e^{-T_2 s} - \left(e^{-(T_1+T_2)s} + 1\right)F_h \\ &\quad - 2F_e e^{-T_2 s} - G_m^{-1}X_m \end{aligned} \tag{2.46}$$

$$\begin{aligned} G_s^{-1}X_s &= \frac{2C_v(s)sX_m e^{-T_1 s}}{e^{-(T_1+T_2)s} + 1} - C_v(s)sX_s + \frac{C_v(s)}{b}\left(\frac{e^{-(T_1+T_2)s} - 1}{e^{-(T_1+T_2)s} + 1}\right)F_e - F_e \\ &= 2C_v(s)sX_m e^{-T_1 s} - \left(e^{-(T_1+T_2)s} + 1\right)F_e - \left(e^{-(T_1+T_2)s} + 1\right)C_v(s)sX_s \\ &\quad - \frac{C_v(s)}{b}\left(e^{-(T_1+T_2)s} + 1\right)F_e - G_s^{-1}X_s e^{-(T_1+T_2)s} \end{aligned} \tag{2.47}$$

The relationships of (2.46) and (2.47) represent the delayed dynamics of the master $G_m^{-1}X_m e^{-(T_1+T_2)s}$ and the slave $G_s^{-1}X_s e^{-(T_1+T_2)s}$ in the master control and the slave control, respectively. They illustrate that the wave reflection phenomenon is caused by the oscillation in the response of the teleoperation system.

Wave reflection does not contain any useful information, and gradually disappears after several loops. It can easily result in unpredictable disturbance and disorder, and even destabilize the whole system. Therefore, developing effective methods to deal

with wave reflection is one of the active research areas in wave-variable-based teleoperation systems.

2.3.2.2 Position Drift

In the conventional wave-variable-based system, data transmitted from master/slave is a combination of the wave signal and the implied information of velocity and force rather than the direct position feedback. Therefore, a slow position drift may be generated from the master/slave site due to discrete sampling rate, calculation error (the position information derived by integrating the velocity) and temporary loss of data, etc.

In [71], the reason for this position drift in the frequency domain is identified through mathematical analysis. Re-considering (2.46), one can see that the position control of the master is expressed by the term $b\left(e^{-(T_1+T_2)s}-1\right)sX_m - 2\mathrm{G}_s^{-1}X_s e^{-T_2 s}$. However, the existence of the bias term $-\left(e^{-(T_1+T_2)s}+1\right)F_h - 2F_e e^{-T_2 s} - \mathrm{G}_m^{-1}X_m e^{-(T_1+T_2)s}$ results in position drift.

Furthermore, [72]-[74] interpret the position drift in the velocity dimension in the time domain. Considering the standard wave-variable-based architecture, the PD controller employed at the slave side and the reference velocity at the slave side are expressed in the time domain by (2.48) and (2.49) using (2.19)-(2.21) [72]-[74]:

$$\mathrm{F}_{sc}(t) = \left(\dot{x}_{sd}(t) - \dot{x}_s(t)\right) \otimes L^{-1}\left(\frac{Bs+K}{s}\right) \tag{2.48}$$

$$\dot{x}_{sd}(t) = L^{-1}\left(\frac{\lambda}{s+\lambda}\right) \otimes \dot{x}_m(t-T) - \frac{1}{b}\left[\mathrm{F}_{sc}(t) - L^{-1}\left(\frac{\lambda}{s+\lambda}\right) \otimes F_{mc}(t-T)\right] \tag{2.49}$$

Where $\otimes$ denotes the convolution operation. $\frac{\lambda}{s+\lambda}$ is a low-pass filter where λ denotes the cut-off frequency. From (2.49), it can be seen that the desired velocity at the slave side $\dot{x}_{sd}(t)$ drifts away from the transmitted delayed master velocity $\dot{x}_m(t-T)$. As to the PD controller at the slave side shown in (2.48), $\dot{x}_s(t)$ is expected to track the desired velocity $\dot{x}_{sd}(t)$.

By transforming (2.48), $\dot{x}_{sd}(t)$ can be derived as:

$$\dot{x}_{sd}(t) = L^{-1}\left(\frac{s}{Bs+K}\right)\otimes \mathrm{F}_{sc}(t) + \dot{x}_s(t) \tag{2.50}$$

The actual velocity $\dot{x}_s(t)$ can be achieved by substituting (2.50) into (2.49):

$$\dot{x}_s(t) = L^{-1}\left(\frac{\lambda}{s+\lambda}\right)\otimes \dot{x}_m(t-T) - \frac{1}{b}\mathrm{F}_{sc}(t) + \frac{1}{b}L^{-1}\left(\frac{\lambda}{s+\lambda}\right)\otimes F_{mc}(t-T) - L^{-1}\left(\frac{s}{Bs+K}\right)\otimes \mathrm{F}_{sc}(t) \tag{2.51}$$

It can be seen from (2.51) that the actual velocity $\dot{x}_s$ drifts away from the master velocity $\dot{x}_m$ by adding the bias term $-\frac{1}{b}\mathrm{F}_{sc}(t) + \frac{1}{b}L^{-1}\left(\frac{\lambda}{s+\lambda}\right)\otimes F_{mc}(t-T) - L^{-1}\left(\frac{s}{Bs+K}\right)\otimes \mathrm{F}_{sc}(t)$. The bias term arithmetically expresses the reason for position drift in a wave-based teleoperation system. Various analyses in frequency and time domains indicate that position drift is caused by asymmetry in the position controller.

2.3.3 Influence on Communication Channels

2.3.3.1 Time Delay

Due to constraints such as signal transmission speed, and channel bandwidth, there is always time delay between the master and slave in a teleoperation system. Time delays of any duration may result in the instability of a system and disturb smooth bilateral teleoperation [50] -[54]. Re-considering the passivity condition (2.5), system passivity depends on the inner product of the system input and output variables. If the time delay exists in the output variable, the inner product will be influenced to the extent that the system passivity will be negatively affected. However, in condition (2.18), if the output variables have time delay, the power generated by the delay will be casually saved in the wave so that the system passivity will not be influenced.

For instance, assume $\mathrm{v(t)} = \mathrm{u(t-T)}$, $E_{store}(t) = \int_{t-T}^{t}\frac{1}{2}u^T u d\tau$, which meets condition (2.5). Then, the input power during the time delay is saved as energy. Moreover, the dissipated power is 0 and the system is lossless. The communication

channel has become a temporary energy storage element by using the wave variable approach. Hence, when using wave variables to transmit the signals, the teleoperation system can maintain passivity and be stable for an arbitrary time delay [75]. It should be noted that the above analysis is based on constant time delay. However in practice, time delay in communication channels is asymmetric and time-varying. Therefore, the performance of the standard wave-variable-based teleoperation system under the condition of time-varying delay should be analyzed.

In [76], the passivity of a wave-variable-based teleoperation system under time delay condition is investigated. It should be noted that (2.23), though true for a passive communication channel with arbitrary constant delays, robust passivity is no longer valid under the varying time delay condition $\mathrm{T} = \mathrm{T(t)}$. Rewriting (2.22):

$$\mathrm{E} = \int_0^t P_{in} d\tau = \frac{1}{2}\left[\int_{t-T_1(t)}^{t} u_m^T u_m d\tau + \int_{t-T_2(t)}^{t} v_s^T v_s d\tau + \int_0^{t-T_1(t)} u_m^T u_m d\tau + \int_0^{t-T_2(t)} v_s^T v_s d\tau - \int_0^t (u_s^T u_s + v_m^T v_m d\tau)\right] \tag{2.52}$$

Where $T_1(t)$ and $T_2(t)$ denote the time varying delay of forward path and backward path.

Rewriting (2.21), considering the time-varying delay condition:

$$\begin{cases} u_s(t) = u_m(t - T_1(t)) \\ v_m(t) = v_s(t - T_2(t)) \end{cases} \tag{2.53}$$

By substituting (2.53) and the following change of variable $\sigma = \tau - T_i(\tau) = g_i(\tau)$ into (2.52) where:

$$T_i'(\sigma) = \frac{dT_i}{d\tau}|_{\tau = g^{-1}(\sigma)} \tag{2.54}$$

Then, the total energy in the standard wave-variable-based teleoperation system can be expressed as [77]:

$$\mathrm{E} = \int_0^t P_{in} d\tau = \frac{1}{2}\left[\int_{t-T_1(t)}^{t} u_m^T u_m d\tau + \int_{t-T_2(t)}^{t} v_s^T v_s d\tau - \int_0^{t-T_1(t)} \frac{T_1(\sigma)}{1-T_1(\sigma)} u_m^T u_m d\tau - \int_0^{t-T_2(t)} \frac{T_2(\sigma)}{1-T_2(\sigma)} v_s^T v_s d\tau\right] \quad (2.55)$$

In (2.55), the last two integrals are passive if the value of the delay is increasing ($T_i' > 0$) and the energy in the communication channels is generated rather that dissipated due to increased time delays. Accordingly, the passivity property of the wave-based system suffers degradation. From the term $\frac{T_i(\sigma)}{1-T_i(\sigma)}$ in (2.55), it can be concluded that the standard wave-based teleoperation system can only be guaranteed to be passive during intervals of decreasing time delay.

2.3.3.2 Data Loss

Data loss is a condition generally occurring in Internet-based teleoperation systems. In networked teleoperation systems, UDP (User Datagram Protocol) is the most popular protocol. However, without acknowledgement, UDP protocol has the drawback of data loss for different teleoperation architectures including wave-based teleoperation systems [78]-[80]. In [81], the influence of data loss as well as time delay on different criteria for the standard wave-based scheme is studied. The results are illustrated in Table 2.1

Free motion			Restricted motion			
	Transient position error	Steady-state position error		Steady-state position error	Perceived stiffness	Mean force error
Data loss	⇑	⇑	Data loss	⇑	⇓	–
Delay	⇑	–	Delay	–	⇓	–

Time varying delay	⟰	⟰	Time varying delay	–	⟱	–

Table 2.1 effect of data loss and delay on different criteria

In Table 2.1, the first column denotes different parameters such as data loss and delay. The first row denotes the criteria to be assessed. The symbol "⟰" means that a specific criterion increases proportional to a certain parameter while "⟱" means the opposite. The symbol " − " indicates that no conclusion could be drawn.
Therefore, it can be concluded that the increasing data loss as well as delays can increase the position error in the wave-based systems since the standard wave variable method neither provides the explicit position feedback (wave variables contain velocity and force) nor compensates for data loss. In addition, the increasing data loss and time delay also degrade the performance of perceived stiffness. Accordingly, data loss and time varying delays are major barriers to achieve system transparency.

2.3.3.3 Discrete Communication

The passivity of the time delayed communication in a discrete wave-based system is studied in [82]. In the discrete wave-based system, during the transmission of the kth samples, (2.22) can be re-written as $\mathrm{E[k]} = \frac{T_s}{2}\sum_{i=1}^{k} P[i] = \frac{T_s}{2}\sum_{i=1}^{k}(u_m^2[i] - u_s^2[i] + v_s^2[i] - v_m^2[i])$, where i is the sample instant at which the power enters the communication channel. T_s is the sampling rate. For constant time delay ($\mathrm{T} = \mathrm{n}T_s$), where $u_s^2[i] = u_m^2[i-n]$ and $v_m^2[i] = v_s^2[i-n]$, the energy in the communication channel is given as:

$$\frac{T_s}{2}\sum_{i=1}^{k}(u_m^2[i] - u_m^2[i-n] + v_s^2[i] - v_s^2[i-n]) = \frac{T_s}{2}\sum_{i=k-n+1}^{k}(u_m^2[i] + v_s^2[i]) \geq 0 \quad (2.56)$$

Based on (2.56), the system is passive, independent of the constant time delay. Considering data loss, a lost packet in a discrete system will result in an empty sampling instance. [82] states that the passivity of the communication channel is related to the strategy adopted by the controller to handle the event. Applying the strategy assuming a null packet for an empty sampling instance on the slave side ($u_s = 0$), the energy in the communication channel can be expressed as:

$$\mathrm{E[k]} = \frac{T_s}{2}\sum_{i=k-n+1}^{k}(u_m^2[i] + v_s^2[i]) + \frac{T_s}{2}\sum_{i=1}^{k-n}(u_m^2[i]\beta_{Lm}[i] + v_s^2[i]\beta_{Ls}[i]) \geq 0 \tag{2.57}$$

Where $\beta_{Lm}[i], \beta_{Ls}[i] = 0$, if the packet is not lost or 1, otherwise. Based on (57), the controller adopting a null packet on an empty sampling instance can guarantee system passivity in the presence of constant time delay. On the other hand, taking the strategy that the controller reuse the previous packet's value in this sample time, the energy is expressed as:

$$\begin{aligned}\mathrm{E[k]} = \frac{T_s}{2}\sum_{i=k-n+1}^{k}(u_m^2[i] + v_s^2[i]) \\ + \frac{T_s}{2}\sum_{i=1}^{k-n}(u_m^2[i] - u_m^2[i-1])\beta_{Lm}[i] + (v_s^2[i] \\ - v_s^2[i-1])\beta_{Ls}[i]\end{aligned} \tag{2.58}$$

Since E[k] in (2.58) can be less than 0, the time delayed system passivity cannot be guaranteed by applying this strategy.

Under time varying delays ($\mathrm{T[k]} = \mathrm{n[k]}T_s$), the empty sampling instances can be caused by either data loss or the increasing time delay. Taking the strategy of adopting a null packet, the packet finally arrives, but not at its prearranged sampling instance. Accordingly, (2.57) can be rewritten as:

$$\begin{aligned}\mathrm{E[k]} = \frac{T_s}{2}\sum_{i=k-n[k]+1}^{k}(u_m^2[i] + v_s^2[i]) + \frac{T_s}{2}\sum_{i=1}^{k-n[k]}(u_m^2[i]\beta_{Lm}[i] + v_s^2[i]\beta_{Ls}[i]) \\ - \frac{T_s}{2}\sum_{i=1}^{k-n[k]}(u_m^2[i]\beta_{Am}[i] + v_s^2[i]\beta_{As}[i])\end{aligned} \tag{2.59}$$

Where $\beta_{Am}[i], \beta_{As}[i] = 1$ when the assumed lost packet is delayed but not lost due to the increasing delay or 0 otherwise. Note: $\frac{T_s}{2}\sum_{i=1}^{k-n[k]}(u_m^2[i]\beta_{Lm}[i] + v_s^2[i]\beta_{Ls}[i]) \geq \frac{T_s}{2}\sum_{i=1}^{k-n[k]}(u_m^2[i]\beta_{Am}[i] + v_s^2[i]\beta_{As}[i])$, E[k] in (2.59) is not less than 0. Hence, the system is guaranteed to be passive.

On the other hand, applying the strategy that the controller repeats the value of the previous sample in the current empty instance, the energy flow in (2.60) can be expressed as:

$$\begin{aligned} \mathrm{E[k]} = \frac{T_s}{2}\sum_{i=k-n[k]+1}^{k}(u_m^2[i] + v_s^2[i]) \\ + \frac{T_s}{2}\sum_{i=1}^{k-n[k]}(u_m^2[i] - u_m^2[i-1])\beta_{Lm}[i] + (v_s^2[i] \\ - v_s^2[i-1])\beta_{Ls}[i] - \frac{T_s}{2}\sum_{i=1}^{k-n[k]}(u_m^2[i]\beta_{Am}[i] - u_m^2[i-1]\beta_{As}[i]) \end{aligned} \tag{2.60}$$

Since E[k] cannot be guaranteed to be less than 0 in (2.60), the passivity can no longer be guaranteed in the discrete case. Therefore, based on the above analysis, the passivity of the wave-based system in the presence of time varying delay and data loss is highly dependent on the mechanism applied by the controller to handle the lost packets. Discrete scattering can be used to implement passive packet switching transmission line in the presence of time varying delays and data loss [83].

2.4 Applications of Wave Variable in Telerobotics

2.4.1 Trajectory Tracking

In wave-variable-based teleoperation systems, though steady-state tracking is ensured [84], the trajectory tracking is distorted due to the presence of bias terms. Distortion also increases in parallel with an increase in time delay. For many applications such as tele-surgery, the slave trajectory must strictly and closely follow the master trajectory. To enhance steady-state position tracking, [85] introduces a wave-based architecture which applies new channels to directly transmit position signal. Unlike [85], the bias

term compensation method is introduced in [74] which uses an extra term Δu to compensate for the second term in the right-hand side of (2.49) as shown in (2.61).

$$\Delta \mathrm{u} = \frac{1}{\sqrt{2b}}\left[F_{sc} - L^{-1}\left(\frac{\lambda}{s+\lambda}\right) \otimes F_{mc}(t-T)\right] \tag{2.61}$$

This added term is inserted into the feed-forward path at the slave side to achieve: $u_s = u_m(t-T) \otimes L^{-1}\left(\frac{\lambda}{s+\lambda}\right) + \Delta u$. Substituting (2.19) and (2.61) into the above equation gives:

$$\begin{aligned} u_s &= \frac{1}{\sqrt{2b}}(b\dot{x}_{sd} + F_{sc}) \\ &= \frac{1}{\sqrt{2b}} L^{-1}\left(\frac{\lambda}{s+\lambda}\right) \otimes \left(\dot{x}_m(t-T) + F_{mc}(t-T)\right) \\ &+ \frac{1}{\sqrt{2b}}\left[F_{sc} - L^{-1}\left(\frac{\lambda}{s+\lambda}\right) \otimes F_{mc}(t-T)\right] \\ &= u_m(t-T) \otimes L^{-1}\left(\frac{\lambda}{s+\lambda}\right) + \Delta u \end{aligned} \tag{2.62}$$

Therefore, the bias term of the velocity transmission is eliminated and the best trajectory tracking is derived as $\dot{x}_{sd}(t) = L^{-1}\left(\frac{\lambda}{s+\lambda}\right) \otimes \dot{x}_m(t-T)$.

Hu et al [72] make further improvement to (2.62). The corrected velocity for tracking the master in [74] is the reference velocity of slave $\dot{x}_{sd}$ but not the actual velocity $\dot{x}_s$. The trajectory tracking is improved by adding a correction term for the actual slave velocity. Re-considering the computation of the actual slave velocity $\dot{x}_s$ (2.51), the correction term is set as $\Delta \mathrm{U} = \sqrt{\frac{1}{2b}} F_{sc}(s) - \sqrt{\frac{1}{2b}} \frac{\lambda}{s+\lambda} F_{mc}(s) e^{-sT} + \sqrt{\frac{b}{2}} F_{sc}(s) \frac{s}{Bs+K}$.

Therefore, (2.63) in the frequency domain representing the best tracking from actual slave velocity to master velocity is derived by adding this correction term to (2.51):

$$\sqrt{\frac{b}{2}}\dot{X}_s(s) = \sqrt{\frac{b}{2}}\frac{\lambda}{s+\lambda}\dot{X}_m(s)e^{-sT} - \sqrt{\frac{b}{2}}F_{sc}(s)\frac{s}{Bs+K} - \sqrt{\frac{1}{2b}}F_{sc}(s)$$

$$+ \sqrt{\frac{1}{2b}}\frac{\lambda}{s+\lambda}F_{mc}(s)e^{-sT} + \Delta\mathrm{U(s)} = \sqrt{\frac{b}{2}}\frac{\lambda}{s+\lambda}\dot{X}_m(s)e^{-sT} \qquad (2.63)$$

Substituting (19) and (20) into the correction term ΔU, ΔU can be rewritten as:

$$\Delta\mathrm{U(s)} = \frac{1}{2}\big(U_s(s) - V_s(s)\big) + \sqrt{\frac{b}{2}}F_{sc}(s)\frac{s}{Bs+K} - \frac{1}{2}\big(U_m(s) - V_m(s)\big)\frac{\lambda}{s+\lambda}e^{-sT} \qquad (2.64)$$

In view of the added correction term, the passivity of the proposed system must be reexamined. The transfer functions of $V_s(s)/U_s(s)$ and $V_m(s)/U_m(s)$ are derived from [73] as follows:

$$|G_{se}(s)| = \left|\frac{V_s(s)}{U_s(s)}\right| = \left|\frac{bG_{pd}(s) + \big(ms + G_{env}(s)\big)\Big(b - G_{pd}(s)\Big)}{bG_{pd}(s) + \big(ms + G_{env}(s)\big)\Big(b + G_{pd}(s)\Big)}\right| \leq 1 \qquad (2.65)$$

$$\left|\frac{V_m(s)}{U_m(s)}\right|$$

$$= \left|\frac{(Bs+K)}{\Big(\frac{s}{\lambda}+1\Big)(Bs - bs + K)\frac{1}{G_{se}(s)} + \Big(\frac{s}{\lambda}+1-e^{-2sT}\Big)(Bs+K) + bs\big(\frac{s}{\lambda}+1\big)}\right| \qquad (2.66)$$

Where $G_{pd}(s)$ and $G_{env}(s)$ are the transfer functions of the slave PD controller and the environment, respectively. According to (66), if the parameter of the forward low-pass filter λ is tuned properly, the transfer function $V_m(s)/U_m(s)$ can be smaller than 1. Therefore, the passivity of the system is guaranteed.

In [86] and [87], it is shown that forward low-pass filter $\frac{\lambda}{s+\lambda}$ has a unity gain at steady state frequencies. Thus this filter is not able to guarantee system passivity at those frequencies, especially for stiff contact. Hence, in [86] and [87], a positive amplifying gain α is added to the force feedback channel of the structure proposed by Ye et al. [74] to minimize the steady state force tracking errors and to ensure passivity.

The wave-based system with bias term compensation augmentation is a successful improvement of the standard wave-based architecture which enforces the trajectory tracking without affecting the system passivity. Hence, the trade-off between stability and transparency of the wave-based teleoperation is enhanced.

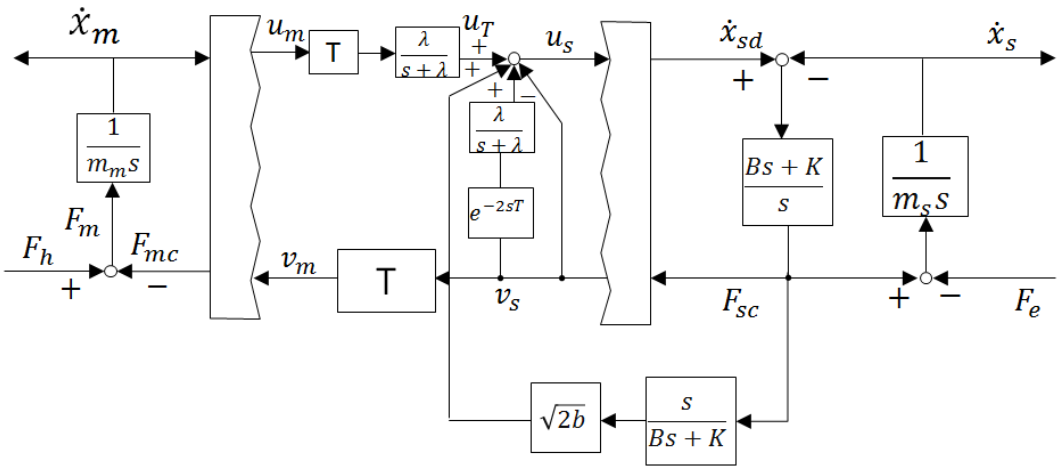

Figure 2.7. Proposed wave-based architecture for trajectory tracking [72]

2.4.2 Wave Integral

As mentioned before, wave variables encode force and velocity signals rather than direct position information. Therefore, controller in the wave-based system does not receive the position feedback, which will result in slow position drift. In order to add position signal to wave variables, Niemeyer and Slotine propose the concept of wave integral [88].

Wave integral, just as its name implies, is the integration of velocity and force information present in the wave variable. After integral of (2.15), the integrated wave variables are defined by (2.67):

$$\mathrm{U}(t) = \int_0^t u(\tau)\, d\tau = \frac{bx + p}{\sqrt{2b}}, V(t) = \int_0^t v(\tau)\, d\tau = \frac{bx - p}{\sqrt{2b}} \qquad (2.67)$$

Where x and p are position and momentum, respectively. It is obvious from (2.67) that the wave integral method explicitly provides the teleoperator with direct position feedback and enforce position convergence between master and slave.

Since time varying delays can cause wave distortion, the desired results cannot be achieved and the stability and performance of the wave-based system is degraded. Namely, either the wave integral which guarantees correct position tracking or the wave energy which determines system passivity will not be preserved. To deal with this problem, both the wave integral U_{in} and the wave energy E_{in} are designed to be transmitted through the communication channel instead of only transmitting the wave signal. That is:

$$\begin{aligned} U_{delay}(t) &= U_{in}\big(t - T(t)\big) = \int_0^{t-T(t)} u_{in}(\tau)\, d\tau \\ E_{delay}(t) &= E_{in}\big(t - T(t)\big) = \int_0^{t-T(t)} u_{in}^2(\tau)\, d\tau \end{aligned} \qquad (2.68)$$

Where U_{delay} and E_{delay} denote the delayed wave integral and energy signals. To achieve signal tracking, the output wave signal is designed to be reconstructed to track the delayed wave signal. Furthermore, to derive passivity, the output energy is designed to be less than the delayed energy. Therefore, a reconstruction filter is deployed to obtain a stable performance by preserving the passivity of the communication channel under time varying delays and data loss. This reconstruction filter is designed as:

$$u_{out}(t) = \begin{cases} \alpha \dfrac{E(t)}{U(t)} & (U(t) \neq 0) \\ 0 & (U(t) = 0) \end{cases} \qquad (2.69)$$

Where α is a tunable parameter.

In [81], the performance of a scheme based on wave integral with the reconstruction filter is examined. The overall performance of wave-integral-based scheme is better than the standard wave-based scheme under the condition of time delay and data loss since the wave-integral-based scheme directly compensates for position tracking and preserves system stability under the condition of time delay by employing a reconstruction filter. However, in the presence of time-varying delay, steady-state position error still exists in the wave-integral-based scheme even though it provides explicit position compensation. Moreover, time varying delay also increases the mean force error in this scheme as the integrated wave variables do not contain direct force reflection.

Yokokohji and Yoshikawa improve the wave integral theory to deal with the problem of time varying delay by designing compensators on the feed-forward and feedback channels [89]-[91]. They analyze the position deviation by:

$$x_m(t) - x_s(t) = \frac{1}{\sqrt{2b}}\left(\int_{t-T_1}^{t} u_m(\tau)d\tau - \int_{t-T_2}^{t} v_s(\tau)d\tau\right) \tag{2.70}$$

Based on (2.70), a compensator is designed to achieve the corrected waveform $u_s^{correct}$ as:

$$\mathrm{u}_s^{correct}(t) = \tilde{u}_s(t) + K\left(\int_0^t u_s'(\tau) - \int_0^t u_s(\tau)d\tau\right) \tag{2.71}$$

where $\tilde{u}_s(t)$ and $u_s'(\mathrm{t})$ are the distorted waveform and the ideal waveform, respectively. K represents a positive-diagonal feedback gain matrix. It should be noted that $u_s'(\mathrm{t})$ is equal to $u_m(t-T_1)$. At the time when the wave variable of the master side $u_m(t)$ is transmitted into the communication channel, the current time is stamped on the waveform, which is used to calculate the integral of $u_s'(\mathrm{t})$. Therefore:

$$\int_0^t u_s'(\tau)d\tau = \int_0^{t_m^{last}(t)} u_m(\tau)d\tau \tag{2.72}$$

where $t_m^{last}(t)$ represents the last stamped time in the communication channel of the master side. Moreover, an online energy observer is employed in [91] to monitor the energy balance as well as to adopt correct actions based on the level of activity. Using the energy monitor, the transmitting wave flow can be controlled to guarantee the system passivity constantly.

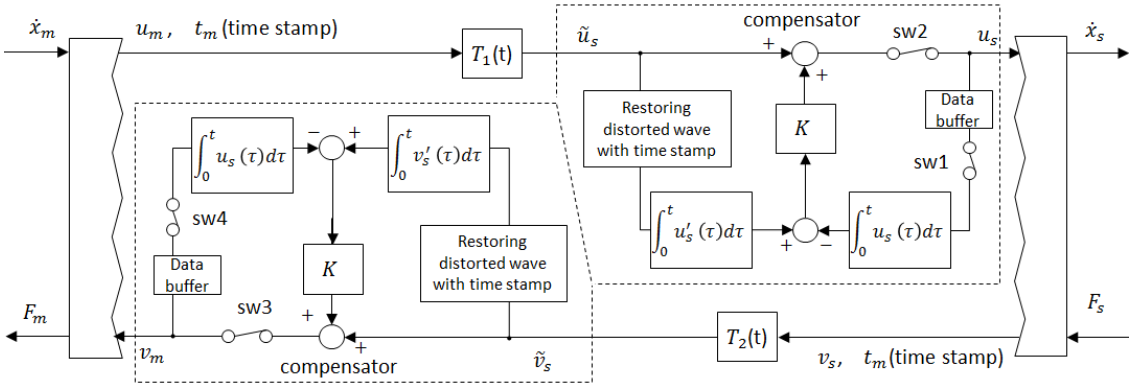

Figure 2.8. Wave-based architecture with wave integral compensator [90]

As mentioned by Yokokohji and Yoshikawa, the system (Figure 2.8) can be well compensated for by tuning the positive-diagonal feedback gain matrix K. Accordingly, Zhang and Li include an on-line time delay identification algorithm to tune the wave integral gain K of the proposed compensator [92]. They find that the gain K must vary with the time-varying delay to achieve minimum error. This implies that K must be more negative when time delay becomes large and more positive when the time delay becomes small. Using the proposed time delay identification algorithm, the value of K is derived.

2.4.3 Wave Prediction

One of the limitations of wave variables is the degradation of their performance in the presence of increased time delay [76]. Therefore, a classic approach called ‘wave prediction’ is proposed to enhance the performance of wave-based teleoperation systems.

The concept of wave prediction was initially introduced by Niemeyer and Slotine [52], and then developed further by Munir and Book, with the aim of improving a wave-based system under constant delay [93], where the predictor proposed in [93] is deployed to drive the slave model. Similar idea was also introduced by [95]. Different to [93], Arioui et al. propose a master-model based predictor to stabilize the bilateral teleoperation system and improve performance under a large delay constant. Later, Munir and Book extend the approach proposed in [93] to guarantee the system passivity in the presence of time varying delay [94].

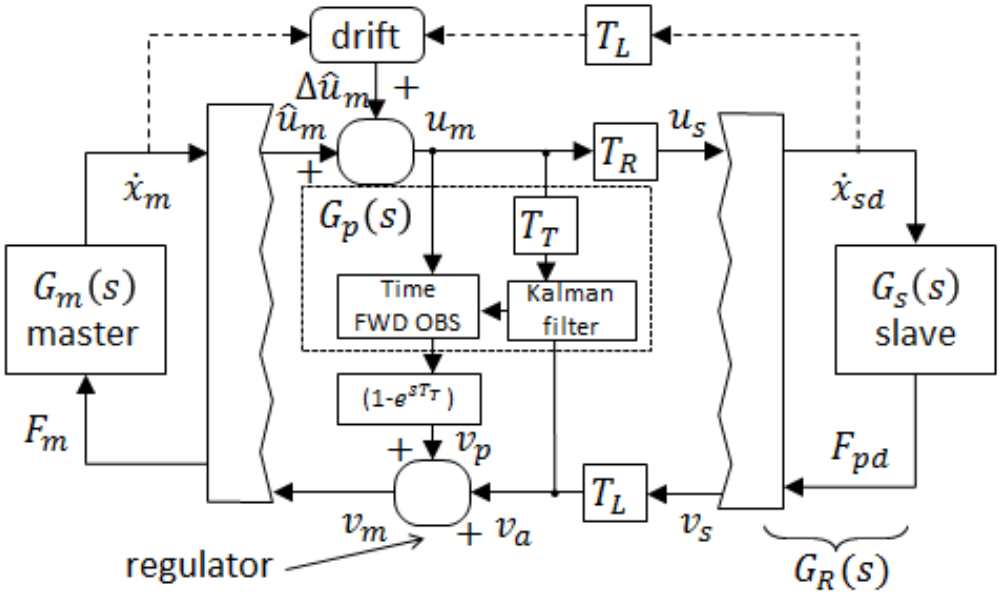

Figure 2.9. wave-based architecture using wave prediction algorithm [93]

Wave prediction is based on the Smith predictor [96], with the key idea of installing the predictor on the master side between the wave variable controllers. Since the role of the Smith predictor is immediate feedback of the predicted response and the error of prediction after measuring the real response [57], the Smith predictor estimates the incoming wave variable without the entire time delay.

Figure 2.9 shows the wave prediction architecture proposed in [94]. In this study, a Kalman filter is deployed to estimate the states of the entire right side $G_R(s)$ combined with the PD controller, the slave plant and wave transformation. The Kalman filter is an important element in this design, improving the prediction performance by

enhancing the accuracy of matching between the initial condition and the model of the entire right- hand plant. The estimated states are applied as the initial conditions of the predictor to predict the states after the entire transmission delay time T_T. As the initial conditions of the Smith predictor are delayed by T_T, the current state is predicted based on the previous states. Moreover, the present states of the slave estimated by the predictor are employed to compute a new current incoming wave variable which is used to compare with that value on the basis of the initial condition of the predictor. Accordingly, the predictor can be expressed as:

$$v_p = (1 - e^{-sT_T})G_p(s)u_m \tag{2.73}$$

Where $G_p(s)$ is the transfer function of the right side. v_p is merged with the actual feedback v_a to achieve v_m. Assuming that the model used by the predictor is absolutely accurate to predict the present slave states, no transmission time delays can be seen by the master.

Incorporating the correction v_p derived by the Smith predictor into the feedback variable v_a is a challenge in the wave prediction algorithm. Although a simple summation junction should theoretically suffice, the junction may generate energy and degrade the passivity of the system. Hence, an energy-reservoir-based regulator estimating v_m as the sum of v_a and v_p, is proposed in [94]:

$$E_\gamma(t) = \int_0^t [v_a^2(\tau) - v_m^2(\tau)]\,\mathrm{d}\tau \tag{2.74}$$

The aim of the proposed regulator is to diminish the "distance-to-go", which means integrating the difference between incoming and outgoing wave variable flow of the regulator (2.75).

$$D_{tg}(t) = \int_0^t [v_a(\tau) + v_p(\tau) - v_m(\tau)]d\tau \tag{2.75}$$

In order to converge $D_{tg}(t)$ to zero, [93] and [94] set a control law to derive v_m on the basis of the energy in the reservoir:

$$v_m(t) = \alpha\left[1 - e^{-\beta E_\gamma(t)}\right] D_{tg}(t) \tag{2.76}$$

Where α and β are constant tuning parameters. The system passivity is obtained by $\left[1 - e^{-\beta E_\gamma(t)}\right]$ as the energy reservoir since if the energy reservoir is completely drained, the regulator would shut down after driving the output wave variable v_m to 0. Hence, if the value of β is large for a given value of E_γ, v_m will not be severely choked by the regulator. On the other hand, the large value of α makes v_m converge faster to the sum of v_a and v_p. Suppose the system has been running for a certain time, and the energy reservoir is sufficiently large so that $\left[1 - e^{-\beta E_\gamma(t)}\right] \approx 1$. For the steady state condition:

$$\lim_{t\to\infty} v_p(t) = \lim_{t\to\infty} v_0(t) = 0 \tag{2.77}$$

The regulator control law can be simplified to a stable first-order differential equation with v_m as the variable (2.78).

$$\frac{d}{dt} D_{tg}(t) = -v_m(t) \tag{2.78}$$

This will drive D_{tg} to zero. That is, the output wave variable v_m will approach the corrected wave variable by the predictor.

Nevertheless, keeping an upper limit on the energy reservoir is a prudent way to guarantee system performance, as it takes a long time for a large amount of energy accumulated in the reservoir to drain. This may violate the passivity of the regulator in the short term and may result in an unstable system.

The wave prediction algorithm must be guaranteed by two prerequisites: constant time delay and accurate slave model. If either of these two requisites is not reached, position drift will occur in the wave-based architecture. In practice, an absolutely accurate model is impossible to obtain in the physical system. A predictor with an inaccurate model will produce an incorrect correction to the incoming wave variable which will cause the steady–state error.

To overcome the shortcoming of the wave prediction algorithm proposed by Munir and Book [93] [94], Ching and Book propose adaptive predictors [98].Since the predictor model introduced in [94] is determined beforehand and is a constant value, its accuracy of prediction is doubtful when the environment is changed because it is impossible for the single slave model $G_p(s)$ mentioned in (2.73) to reflect the changed environment precisely. With an inaccurate predictor model, wrong prediction of the returning wave will occur to the extent that the force feedback on the master side and the velocity command on the slave side will be adversely affected. Considering the above situation, [98] suggests a semi-adaptive predictor to provide more accurate force feedback to the human operator. Moreover, a fully adaptive predictor is employed to compensate for arbitrary environmental force. Using this approach, different types of environments can be modeled with more accuracy. In addition, considering the position drift, another wave compensation channel is proposed in [98] on the wave prediction architecture given in [94] to directly compensate for the position drift caused by time varying delay.

In conclusion, the wave prediction algorithm deploys the Smith predictor to estimate the behavior of the slave and to compensate for the side-effects of time delays. In addition, a position-correcting input and an energy regulator are employed to mitigate the position error and limit the generated energy of the Smith predictor, respectively. In [81], the performance of the wave prediction architecture is evaluated by conducting several experiments. That is, the system stability employing this algorithm is robust as the proposed regulator guarantees the system passivity. Even with an explicit position compensation, time delay still affects the steady-state position error of the wave prediction system. The data loss also adversely affects the performance of this system. However, compared with standard wave-based architecture, the wave prediction architecture provides considerably better response under data losses and high delays at the expense of high computational complexity.

2.4.4 Perceptual Feedback

The interaction between human and environment is extremely asymmetric. Although the frequency of human motion is usually less than 10Hz, the high frequency power from 10 Hz to 1 kHz is more important in the case of human's perception of the environment [99]. Accordingly, high frequency haptic feedback, which provides information about macroscopic material properties and precise surface features, is particularly useful for teleoperation systems. Without high frequency haptic feedback, all remote objects manipulated by the human operator feels like soft, smooth foam. Hence, the operator has to rely on visual or auditory cues to perceive material properties [100].

The majority of the proposed delay-capable controllers guarantee system stability under time delays by seriously restricting the system bandwidth [101]-[103]. The largest disadvantage of bandwidth restriction is depriving the human operator of significant high frequency feedback information. In both continuous and discrete time domains, the wave variable transformation suffers from performance degradation due to wave reflection and limited frequency content and the high frequency portions of the wave reflections can be very disruptive as it distracts from real interaction signals [104].

Considering that power flows are separated by the wave variable constructed into the distinct forward and reverse paths, Tanner and Niemeyer propose that different bandwidths can be set in the forward and reverse paths to allow high frequency feedback signals from the slave to provide a useful feedback to operators and enhance fidelity [105]. Therefore, feeding back the perceptual information, based on the property of human perception, the interaction between the teleoperation system and the environment is divided into two discrete bands: the manipulation band and the perception band [84]. The manipulation band, which contains the motion of low frequency and force signal, is bi-directional, while the perception band is unilateral where vibrations can only be derived rather than controlled or commanded. Therefore, when adding a unilateral channel of perspective feedback based on the traditional wave controller, it can actually feed the high frequency contact force back to the operator to

improve the telepresence of the remote environment and enhance the manipulation performance of the system.

Inspired by the successful feedback of high frequency acceleration presented to the operator through vibro-tactile displays [106], Tanner and Niemeyer further extended their approach on perceptual feedback by feeding the high frequency acceleration information rather that the high frequency contact force back to the master [107]. A slave accelerometer is employed to measure the slave tip acceleration $\ddot{x}_s$ of any contact and scale the feedback to vary the operator's experience. Then this signal is incorporated into the returning wave after passing through a scaling element $\mathrm{M(s)}$ set as the mass of the slave $\mathrm{m(s)}$ and a high-pass filer $\mathrm{H(s)}$. Wave impedance $1/\sqrt{2b}$ is used to scale the acceleration signal in order to match the signal against the units of the wave variables. Figure 2.10 shows the wave-based architecture with the augmentation of high frequency acceleration feedback.

In Figure 2.10, the high-pass filter $\mathrm{H(s)}$ processes the equivalent force F_{eq} to isolate the perception band signals and avoid interference. However, high frequency energy will be injected by the augmentation of the additional feedback into the system, and as a result adversely affect the passivity of the integrated system. Since the extra energy must remain uni-directional without creating closed-loop instability, a forward low-pass filter $\mathrm{L(s)}$ is added in the feed-forward channel to dissipate the high frequency energy. Therefore, by appropriately tuning the adversely affecting low-pass filter $\mathrm{L(s)}$, high pass filter $\mathrm{H(s)}$ and the scaling element $\mathrm{M(s)}$, system stability can be obtained with balanced energy amplification and dissipation. Moreover, to clearly separate the manipulation band and the perception band, both the high-pass filter and the low -pass filter are selected as second-order filters in which all poles are set at a non-dimensional frequency.

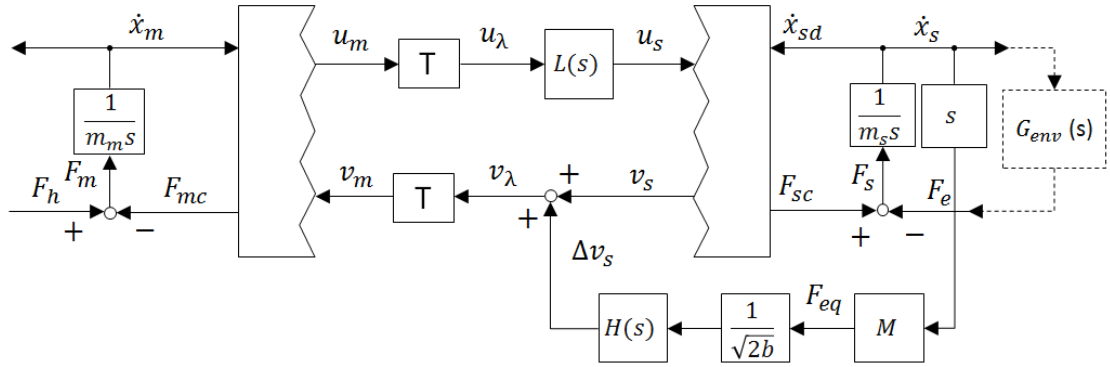

Figure 2.10. Wave-based architecture with high frequency acceleration feedback [107]

2.4.5 Combination with 4-CH Architecture

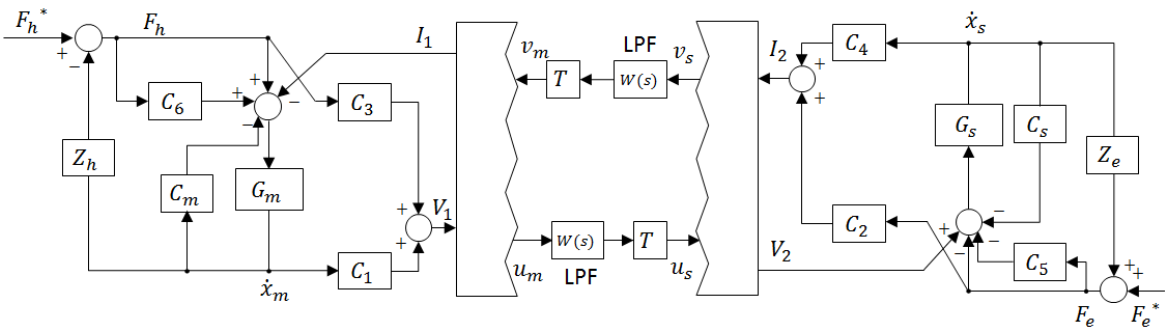

Figure 2.11. 4-CH architecture applying wave transmission [108]

It is demonstrated that 4-CH architecture which possesses the extra “degrees of freedom” (control parameters) is the best teleoperation system from a transparency point of view under the condition of no time delay [50], [109]. Nevertheless, while achieving high transparency, the 4-CH system suffers the penalty of stability degradation in the presence of time delay. Considering that the largest advantage of the wave variable method is to guarantee system passivity, Aziminejad et al extend the wave transmission to the 4-CH architecture in order to improve the overall performance of the teleoperation system [108]. Similar architecture is also proposed in [110]. To combine the wave transmission with the 4-CH architecture, the

communication channel part of the extended Lawrence 4-CH system illustrated in [65] must be segregated as a two-port network, which is shown as Figure 2.11.

In Figure 2.11, the nonphysical input and output effort and flow of the communication channel are expressed as:

$$V_1 = C_3F_h + C_1\dot{x}_m, V_2 = F_e(1 + C_5) + \dot{x}_s(M_s s + C_s) \tag{2.79}$$

$$I_1 = F_h(1 + C_6) - \dot{x}_m(M_m s + C_m), I_2 = C_2F_e + C_4\dot{x}_s \tag{2.80}$$

In this scheme, the wave variables can be written as:

$$\mathrm{u} = \frac{bI + V}{\sqrt{2b}}, \mathrm{v} = \frac{bI - V}{\sqrt{2b}} \tag{2.81}$$

By extending the wave-variable method into the 4-CH architecture, the trade-off between stability and transparency of the bilateral teleoperation is enforced, compared with the conventional 4-CH architecture.

The stability of the architecture shown in Figure 2.12 is guaranteed by the low-pass filters in the communication channel which can limit the system bandwidth and restrict high frequency information transmission. Yalcin and Ohnishi designed a 4-CH architecture based on the wave variable method to enhance the overall performance of the bilateral teleoperation in [111], [112]. Inspired by [107], Yalcin and Ohnishi also employed the high frequency acceleration to provide perceptual feedback in their proposed architecture. Moreover, they propose to employ direct rather than feedback force and position information of the master and slave robots to create the 'acceleration' waves, which is different from the combination of conventional wave transmission channels and the high frequency acceleration feedback proposed in [107]. Therefore, the feedback in communication channels shown in Figure 2.3 is canceled. Katsura et al state that the acceleration controller can provide satisfactory accuracy for position and force tracking in bilateral control [113]. Therefore, instead of the conventional PD controller used in the standard wave-based system, Yalcin and Ohnishi choose acceleration controllers for the master and slave robots in the acceleration dimension.

In [111] and [112], acceleration is presented in terms of position-dependent acceleration $\ddot{x}_m^p$ and force-dependent acceleration $\ddot{x}_m^f$. Force control C_f relies on a force control gain K_f, while position control C_p relies on acceleration K_a, velocity K_v and position K_p (2.82).

$$C_p(s) = K_a s^2 + K_v s + K_p, C_f(s) = K_f \tag{2.82}$$

Disturbance observers (DOB) and reaction force observers (RFOB) are also applied in [111] and [112]. DOB is widely used to attenuate the disturbance elements. A fast DOB structure based on acceleration is very beneficial as it can estimate and feedback the disturbance to the system in order to derive a more stable and robust structure [114]. RFOBs are applied in the proposed structure ([111], [112]) to replace force sensors as they possess more transmission bandwidth than force sensors [115], which is appropriate for this architecture with the privileged aim of improving user perception. RFOB is mainly used to estimate reaction force. By combining DOB and RFOB, the estimated master and slave forces $\hat{F}_m$ and $\hat{F}_s$ are derived with little disturbance.

Considering that in the conventional wave-variable method, master and slave robots are treated as the sources of either force or velocity, a 4-CH data transmission scheme is introduced as both robots are the sources of force and velocity. That is, the scheme of velocity feed-forward and force feedback is superposed with that of force feed-forward and velocity feedback by two asymmetric character impedances.

The scaling parameters α and β of the proposed architecture in Figure 2.12 are applied to scale the accelerations in order to give the operator flexibility in control issues, e.g. to deal with drift problems during environmental contact. The arrows with dotted lines denote the cancelled feedback in the communication channels, which improve the system transparency at the expense of passivity degradation. Accordingly, the asymmetric dampers b_1 and b_2 are used to maintain the system stability. Hence, in the acceleration dimension, the wave variables with different character impedances are written as:

$$u_{m_1} = \frac{b_1 \ddot{x}_m^p - \ddot{x}_m^f}{\sqrt{2b_1}}, u_{m_2} = \frac{b_2 \ddot{x}_m^p + \ddot{x}_m^f}{\sqrt{2b_2}} \tag{2.83}$$

$$v_{s_1} = \frac{-b_1\ddot{x}_m^p + \ddot{x}_m^f}{\sqrt{2b_1}}, v_{s_2} = \frac{-b_2\ddot{x}_m^p - \ddot{x}_m^f}{\sqrt{2b_2}} \tag{2.84}$$

In the end, the authors obtain the master and slave robot acceleration references $\ddot{x}_m^{ref}$ and $\ddot{x}_s^{ref}$ with scaling in the presence of time delay as:

$$\ddot{x}_m^{ref} = C_p(x_s e^{-sT_2} - \beta x_m) - C_f(\alpha F_m + F_s e^{-sT_2}) \tag{2.85}$$

$$\ddot{x}_s^{ref} = C_p(\alpha\beta x_m e^{-sT_1} - \alpha x_s) - C_f(\beta F_s + \alpha\beta F_m e^{-sT_1}) \tag{2.86}$$

Where the master and slave acceleration references $\ddot{x}_m^{ref}$ and $\ddot{x}_s^{ref}$ are the necessary parameters for the DOB and RFOB to derive position and force signals.

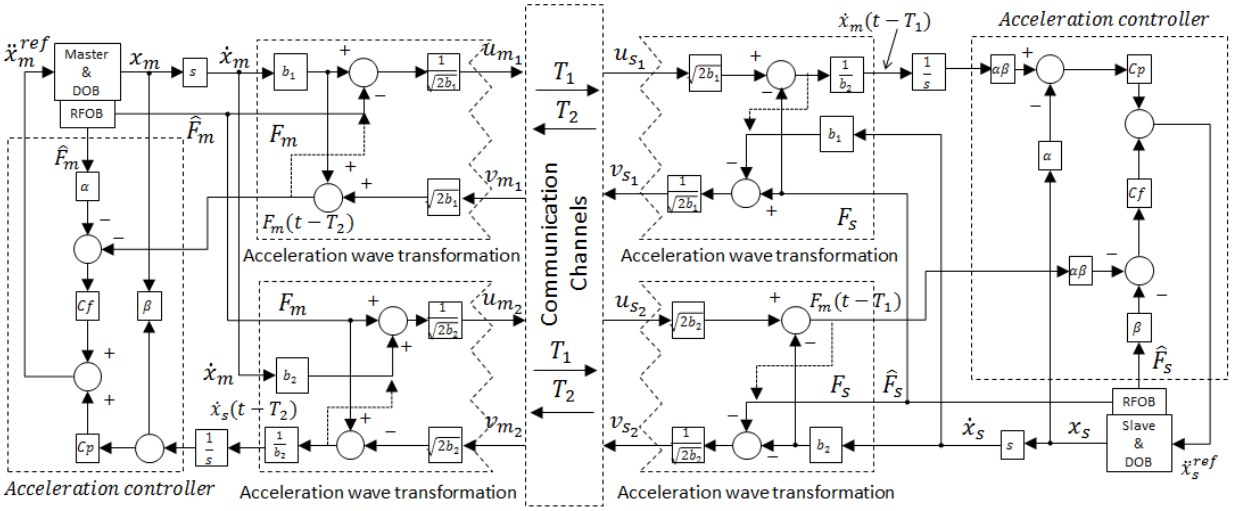

Figure 2.12. Scaled 4-CH acceleration-wave transmission architecture [112]

This architecture, combined with acceleration wave transmission, considerably enforces the trade-off between stability and transparency for the 4-CH architecture by properly tuning the scaling parameters α and β. As shown by the result of their experiment, force and position tracking are achieved with high accuracy by applying a combination of acceleration controllers, DOBs and RFOBs. Without using force sensors, this architecture derives high system bandwidth and also provides the operator with more authentic perceptions of the remote environment by using acceleration wave

transmission to transmit high frequency information. Therefore, Yalcin and Ohnishi conclude that the higher the acceleration feedback and the better the perception of the environment, the higher transmission bandwidth and the more accurate high-frequency acceleration matching the system can be achieved.

In conclusion, the combination of a wave variable approach with 4-CH architecture is a promising development direction for the wave variable method. Since the most notable property of 4-CH architecture is achieving high transparency and the wave-variable method can provide systems robust passivity, the combination of these two methods can compensate for their respective shortcomings.

2.4.6 Methods for Wave Reflection

The phenomenon of wave reflection was initially discovered by Niemeyer and Slotine [68]. An approach proposed to match the impedance of the master with that of the slave is to add damping elements R and D at both sides of the PD controller, as shown in Figure 2.6 [68]-[69], [116]. The two damping elements and the PD controller constitute an impedance controller whose parameters satisfy (2.87):

$$D = \lambda m_s, B = \lambda m_s, K = \lambda^2 m_s, , R = b - \lambda m_s \tag{2.87}$$

Where λ is the expected bandwidth of the slave PD controller. However, the predetermined damping elements are not able to deal with the unanticipated impedance changes of the operator and environment. In particular, when unknown changes appear in the task environment, the wave reflections can be reinstated.

Niemeyer and Slotine introduce the method of wave filtering [88]. Then, the wave filtering method, the essence of which is adding a low-pass filter in the communication channels, is applied in numerous studies to process unknown impedance changes through restricting the teleoperation systems' bandwidth [72]-[74], [84], [107], [108],[117]-[118].

The integration of wave filtering and impedance matching can considerably suppress the wave reflections in which wave filtering and the impedance matching minimize the wave reflections from the human operator/task environment and in free space,

respectively. A notable drawback of wave filtering is that its property of teleoperator bandwidth restriction can impede the transmission of high frequency information. Furthermore, the predetermined wave filter needs the precise estimation of the communication time delay.

Notably, when a teleoperation system is perfectly matched, the wave variable at the master side u_m only contains velocity information while that at the slave side v_s only possesses force information as follows:

$$u_m = \frac{b\dot{x}_m}{\sqrt{2b}}, v_s = \frac{F_s}{\sqrt{2b}} \tag{2.88}$$

In the wave teleoperator with perfect wave matching, the outgoing wave signals u_m and v_s no longer comprise the incoming wave signals u_s and v_m. Hence, the wave reflection problem can be successfully prevented. Nevertheless, [52] and [98] state that velocity tracking and force reflection will be corrupted by the additional impedance matching terms as shown in (2.89) and (2.90):

$$\dot{x}_s(t) = \frac{\dot{x}_m(t-T)}{2} - \frac{F_s(t)}{2b} \tag{2.89}$$

$$F_m(t) = \frac{F_s(t-T)}{2} + \frac{b}{2}\dot{x}_m(t) \tag{2.90}$$

To circumvent these problems, Bate et al propose a new scheme that does not require transcendental knowledge of the remote environment [132], which is later improved in [133]. Through decoupling force and velocity at the slave side, the velocity tracking and force reflection are derived as:

$$\dot{x}_s(t) = \dot{x}_m(t-T) + \frac{F_s(t-2T) - F_s(t)}{b} \tag{2.91}$$

$$F_m(t) = b\dot{x}_m(t) + F_s(t-T) \tag{2.92}$$

Compared with conventional impedance matching teleoperation described by (2.89) and (2.90), (2.91) and (2.92) clarify that the proposed architecture provides an

improvement in velocity tracking and force feedback with little corruption under the condition of hard contact. However, this method has an obvious drawback. That is, in free motion and soft contact, the bias term $b\dot{x}_m$ in (2.92) will considerably influence the force tracking performance of this method.

Furthermore, the main effect of this architecture is the circumvention of wave reflection. The wave variables of this architecture are derived by:

$$u_m(t) = \frac{b\dot{x}_m(t) + F_s(t-T)}{\sqrt{2b}}, v_s(t) = \frac{F_s(t)}{\sqrt{2b}} \tag{2.93}$$

Unlike the wave formulas in the standard wave variable method (2.19) and (2.20), in (2.93), the velocity information is not possessed by the new wave variable v_s any longer. This means that the wave variable u_s is no longer reflected at the junction of v_s. Using this method, the wave reflections are avoided by decoupling force and velocity at the slave side without the need for active modeling or impedance matching.

2.4.7 Force Reflection

Force reflection is a critical objective in teleoperation systems in which the human operator can kinesthetically couple to the remote environment to considerably enhance task performance. With the advantage of maintaining stability under arbitrary communication delays, wave-variable-based controllers can support the stable operation of force-reflecting operators. Nevertheless, transparency in the wave-based teleoperator always has to be compromised in order to maintain stability.

Considering the standard teleoperator, the velocity feed-forward and force feedback are given by:

$$\dot{x}_{sd}(t) = \dot{x}_m(t-T), F_{mc} = F_{sc}(t-T) \tag{2.94}$$

According to (2.94), the force transmission is ideal when the slave driving force is replicated at the master side. However, this system suffers from non-passivity [66]. The communication channel of the wave-based teleoperator obtains passivity. However, this conservative system achieves passivity at the expense of the biased

force feedback shown by (2.38). Accordingly, the bias term must be minimized in order to improve the force reflection of the wave-based system.

Kawashima et al introduce a velocity scaling method to enhance the force tracking process. Normally the control parameters of the standard wave variable controllers F_{mc} and $\dot{x}_{sd}$ are given as (2.37) and (2.38). To achieve better force tracking, [119] modifies the wave variable with velocity scaling:

$$\mathrm{F}_{mc} = F_s e^{-T_2 s} + \sqrt{b}\left(\dot{X}_m - \dot{X}_{sd} e^{-T_2 s}\right) \tag{2.95}$$

$$\dot{X}_{sd} = \dot{X}_m e^{-T_1 s} + \frac{1}{b}\left(\mathrm{F}_{mc} e^{-T_1 s} - F_s\right) \tag{2.96}$$

By using $\sqrt{\mathrm{b}}$ to scale velocity, the bias term $\dot{X}_m - \dot{X}_{sd} e^{-T_2 s}$ in (2.95) that affects the force tracking is diminished. As the characteristic impedance b is deployed to preserve the passivity of the wave-based system, changing this element may influence the system stability. Accordingly, the authors verify the passivity of the proposed system and show that the system passivity cannot be satisfied when b is too large. However, when the value of b is too small, the tracking error will be improved although the passivity condition is satisfied. Therefore, selecting a correct value of b is critical to ensure good force tracking and maintain passivity.

Ye and Liu [117] adopt another measure of bias term compensation to improve wave reflection by adding an augmentation channel (Figure 2.13).

Considering that the bias term is $\frac{1}{b}\left(\mathrm{F}_{mc} e^{-Ts} - F_s\right)$, the compensation term is derived as:

$$\Delta v_m = \frac{\sqrt{b/2}\lambda}{0.5s + \lambda}\left(\dot{x}_m - \dot{x}_s e^{-Ts}\right) \tag{2.97}$$

Hence, by adding $\frac{\lambda}{0.5s+\lambda}$, the bias term is partially eliminated, and the force reflection equation can be written as:

$$F_{mc}(s) = F_{sc}(s) e^{-Ts} + \frac{bs}{0.5s + \lambda}\left[\dot{x}_m(\mathrm{s}) - \dot{x}_{sd}(\mathrm{s}) e^{-Ts}\right] \tag{2.98}$$

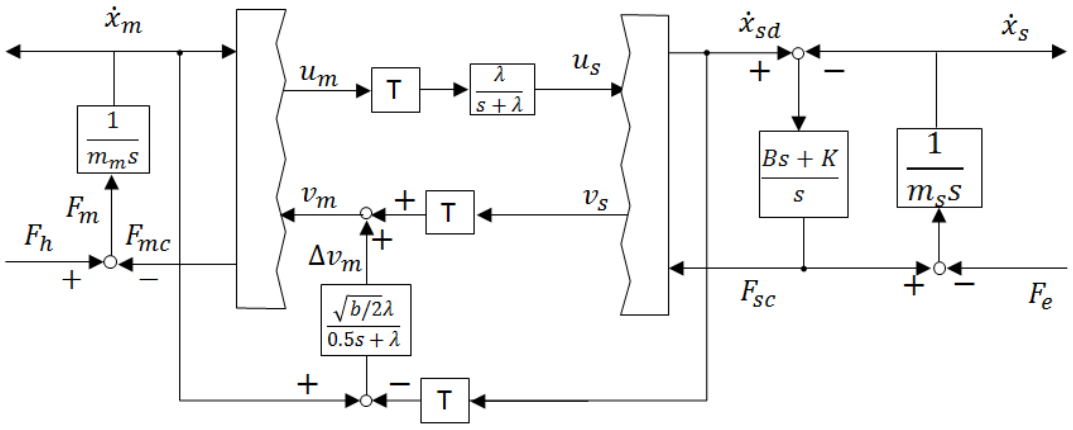

Figure 2.13. Cancelling force feedback bias term [117]

The augmentation of the additional path will inevitably inject energy to degrade the system passivity. To guarantee passivity, the low-pass wave filter $\frac{s}{0.5s+\lambda}$ is adopted to limit the energy inserted. As the bandwidth of the canceling effort 2λ is twice that of the wave variable in the feed-forward path, highly authentic force reflection is derived within the bandwidth 2λ. As to whether the augmentation will affect the system's stability, the stability analyzed under constant delay can be achieved by properly tuning the parameter of the low-pass filter λ.

These methods for force reflection are similar to high frequency feedback schemes introduced by Tanner and Niemeyer [84], [92], but their purpose is totally different. The method for improving force reflection is to minimize the inherent bias of the wave-based system while [84] and [107] aim at enhancing the high frequency force feedback. However, these two purposes can be unified to further enforce the haptic perception in the wave-based system.

2.4.8 Generalized Wave Variable Transformation

Generalized wave variable transformation is applied to guarantee stability with communication unreliability , especially the finite gain L_2-stability for the small gain operators, large time delays and data loss [120]-[122]. Like the notation in (2.19) and (2.20), the left-hand side and right-hand side generalized wave variables u_l, v_l, u_r, v_r are given as:

$$\begin{bmatrix} u_l \\ v_l \end{bmatrix} = S_G \begin{bmatrix} x_m \\ F_{mc} \end{bmatrix}, \begin{bmatrix} u_r \\ v_r \end{bmatrix} = S_G \begin{bmatrix} x_s \\ F_{sc} \end{bmatrix} \tag{2.99}$$

where the matrix S_G represents the generalized wave variable transformation, which is parameterized using a rotation matrix R_θ and a scaling matrix B ($\det B \neq 0$):

$$S_G = R_\theta B = \begin{bmatrix} cos\theta I & sin\theta I \\ -sin\theta I & cos\theta I \end{bmatrix} \begin{bmatrix} b_{11} & 0 \\ 0 & b_{22} \end{bmatrix} \tag{2.100}$$

Where $\theta \in [-\frac{\pi}{2}, \frac{\pi}{2}]$. The parameters$b_{11}, b_{22} > 0$ are free tuning.

Remark 5 [61]: For a teleoperation system consisting of the networked negative feedback of an OFP(ε_l) and an IFP(δ_r) system with $\varepsilon_l, \delta_r > 0$, communication channels and the input-output transformation (2.100), the finite gain L_2-stability can be guaranteed for any small gain operator in the network if and only if $\theta \in [\theta_l, \theta_r]$ for each B, where θ_l, θ_r are one of the solutions of

$$\cot 2\theta_i = \frac{\varepsilon_{B_i} - \delta_{B_i}}{2\eta_{B_i}}, \mathrm{i} \in (\mathrm{l}, \mathrm{r}) \tag{2.101}$$

which simultaneously satisfies:

$$\mathrm{a}(\theta_i) = 2\eta_{B_i} sin\theta_i cos\theta_i - \delta_{B_i} cos^2\theta_i - \epsilon_{B_i} sin^2\theta_i \geq 0 \tag{2.102}$$

ϵ_{B_i} and δ_{B_i} are given by the matrix P_{B_i}

$$P_{B_i} = \begin{bmatrix} -\delta_{B_i} I & \eta_{B_i} I \\ \eta_{B_i} I & \epsilon_{B_i} I \end{bmatrix} = B^{-T} P_i B^{-1} = \begin{bmatrix} -\frac{\delta_i}{b_{22}^2} I & \frac{1}{2b_{11}b_{22}} I \\ \frac{1}{2b_{11}b_{22}} I & -\frac{\epsilon_i}{b_{11}^2} I \end{bmatrix}, \mathrm{i} \in (\mathrm{l}, \mathrm{r}) \tag{2.103}$$

It should be noted that the standard wave variable transmission can be derived by setting $\theta = 45^{\mathrm{o}}$, $b_{11} = \sqrt{b}$ and $b_{22} = \frac{1}{\sqrt{b}}$.

The generalized wave variable transformation is applied to guarantee the stability with communication unreliabilities especially the finite gain L_2-stability for any small gain

network operators, including the large time delays and the appropriately handled packet loss [55].

2.4.9 Multi-DOF Wave-Variable-based System

To apply the wave variable method to a multi-DOF system, Niemeyer and Slotine [88] substitute the characteristic impedance b with a symmetric positive–definite impedance matrix. A geometric-based approach based on the geometric scattering variables is used in [123]. As in [123], a generalization of wave variables is proposed in [93], [94] to deal with the Multi-DOF case, which are re-written from (2.19) and (2.20) as follows:

$$u_m = A_w \dot{x}_m + B_w F_{mc}, u_s = A_w \dot{x}_{sd} + B_w F_{sc} \tag{2.104}$$

$$v_m = C_w \dot{x}_m - D_w F_{mc}, v_S = C_w \dot{x}_{sd} - D_w F_{sc} \tag{2.105}$$

where A_w, B_w, C_w and D_w are defined as the $\mathrm{n} \times \mathrm{n}$ scaling matrices ($\mathrm{n}-\mathrm{DOF}$). Substituting (2.104) and (2.105) into (2.22), the scaling matrices should hold the following requirement in order to guarantee system passivity:

$$C_w^T C_w = A_w^T A_w, D_w^T D_w = B_w^T B_w \tag{2.106}$$

$$\mathrm{I} = A_w^T B_w + C_w^T D_w \tag{2.107}$$

To satisfy (2.106), the scaling matrices should be nonsingular and $C_w = A_w$, $D_w = B_w$. Therefore, (2.107) reduces to:

$$\mathrm{I} = 2A_w^T B_w \tag{2.108}$$

A_w is defined in [93] to be symmetric but not necessarily positive-definite. Moreover, the system stability is ensured by using the norm of the scattering matrix where $B_w = \frac{1}{2} A_w^{-1} = \frac{1}{2} A_w^{-T}$. ($A_w^{-T}$ is the inverse transposition of A_w.) By replacing b with a positive-definite matrix B, the scaling matrices are expressed as:

$$A_w = C_w = \sqrt{\frac{B}{2}}, B_w = D_w = \sqrt{\frac{1}{2}B} \tag{2.109}$$

[124] extends the family of the scaling matrices proposed in [93], [94] and summarizes the necessary and sufficient conditions for A_w, B_w, C_w and D_w as follows:

1) The scaling matrix A_w is nonsingular.

2) $B_w = \frac{1}{2}(I + S_w)A_w^{-T}$. ($S_w$ is any n × n skew-symmetric matrix.)

3) $C_w = QA_w$. (Q is any n × n orthogonal matrix.)

4) $D_w = \frac{1}{2}Q(I - S_w)A_w^{-T}$.

Through defining the scaling matrices to satisfy the above four conditions, [85] has proved that the defined scaling matrices can robustly guarantee the passivity of the standard multi-DOF wave-based system.

2.4.10 Time Varying Delay

System performance under time varying delay is an inevitable criterion for a proposed wave-based method. Reconstruction filter is added in the wave-integral-based system proposed by Niemeyer et al to guarantee passivity and no drift under time varying delays [75]. The wave integral compensator proposed by Yokokohji et al is to minimize the performance degradation caused by variation of time delays [88]-[90]. Munir and Book extend their wave prediction approach to the Internet where time delay is unpredictable and fluctuating [94]. However, when the delay time becomes larger, the aforementioned methods may not guarantee system stability.

Some studies directed at the time varying delay propose new approaches based on the wave-based method. As analyzing the system passivity is violated by the last two terms of (2.55) under time varying delay, Boukhnifer et al [76] modify the controller structure initially proposed by Niemeyer [75] by adding adaptive gains α in the communication channels to preserve the passivity-performance trade-off. Therefore, the reflected waves are written as:

$$\mathrm{u}_s(t) = \alpha_1 u_m\big(t - T_1(t)\big), v_m(t) = \alpha_2 v_s\big(t - T_2(t)\big) \tag{2.110}$$

Therefore, [76] derives the total energy as:

$$\begin{aligned} \mathrm{E} = \int_0^t P_{in} d\tau = \frac{1}{2}\Bigg[& \int_{t-T_1(t)}^{t} u_m^T u_m d\tau \\ & + \int_{t-T_2(t)}^{t} v_s^T v_s d\tau - \int_0^{t-T_1(t)} \frac{1 - T_1' - \alpha_1}{1 - T_1'} u_m^T u_m d\tau \\ & - \int_0^{t-T_2(t)} \frac{1 - T_2' - \alpha_2}{1 - T_2'} v_s^T v_s d\tau \Bigg] \end{aligned} \tag{2.111}$$

From (2.111), the total energy can be always positive for all delays by tuning the gains α to satisfy:

$$\alpha_i^2 \leq 1 - \frac{dT_i}{dt} \ (i = 1, 2) \tag{2.112}$$

By properly tuning the gains, system stability can be achieved under time varying delay. However, according to (2.110), velocity tracking and force tracking are inevitably degraded, which is the biggest drawback of this approach.

Wave filtering is also a popular approach to handle time delay problems. Yang et al [125] add a second order filter in the forward and feedback paths of the communication link to derive a similar effect to the adaptive gains proposed in [76]. Apparently, such an approach limits the transmission bandwidth of the whole system so that the system transparency is violated.

Hashemzadeh et al introduce an innovative idea for time varying delay control, where the time varying delay can be modeled as a constant time delay along with an additive disturbance [126]. Considering the communication channels, where $\mathrm{u}_s(t) = u_m\big(t - T_1(t)\big), v_m(t) = v_s\big(t - T_2(t)\big)$. $T_1(t)$ and $T_2(t)$ are the actual time varying delays:

$$u_s(t) = u_m(t - T_{1c}) + D_1(t), v_m(t) = v_s(t - T_{2c}) + D_2(t) \tag{2.113}$$

where T_{1c} and T_{2c} are the constant time delay. $D_1(t) \triangleq u_m\big(t - T_1(t)\big) - u_m(t - T_{1c})$ and $D_2(t) \triangleq u_m\big(t - T_2(t)\big) - u_m(t - T_{2c})$ are defined as the disturbances. Then, a disturbance estimator is proposed in each of the feed-forward and feedback paths to estimate the distance in order to compensate for the time-varying delay effects in terms of force and velocity tracking performance. Since the disturbances are estimated, the time varying delays in the proposed system can effectively act as the constant delays. By using this method, the whole proposed system will have better stability and transparency.

2.4.11 Data Loss

Data loss, as the main unreliability of the communication channels, can not only destabilize the teleoperation system, but also distort the human haptic perception of the environmental objects [61]. Different methods have been proposed to deal with data loss. [82] introduces a buffering and interpolation scheme for packet switching in the communication network to preserve system passivity with communication unreliabilities. [83] proposes a strategy handling packet loss to allow power scaling based on the discrete scattering. Moreover, since high packet rate which stresses the underlying network resources can intensify data loss, decreasing data rate is one of the popular methods to deal with the data loss problem.

The deadband approach, introduced in [127] and [128], is an effective method for reduction of the data rate in a packet-switched communication network. As a lossy perceptual coding approach, the deadband approach employs Weber's Law of Just Noticeable Differences (JND) [129], [130] to exploit human haptic perception limits, the principle of which is to eliminate data considered to be unperceivable by human in order to reduce data rate.

Using the deadband approach, data is sent only if the difference between the most recent sample $\mathrm{x}(\mathrm{t}')$ and the current sample $\mathrm{x}(\mathrm{t})$ is larger than a predetermined threshold $\Delta_{x(t')}$. That is:

$$|\mathrm{x}(\mathrm{t}') - \mathrm{x}(\mathrm{t})| > \Delta_{x(t')} \tag{2.114}$$

By using the insights of Weber's law, this threshold is set to grow proportionally with the magnitude of the signal x:

$$\Delta_{x(t')} = \mathcal{K}|x(t')| > 0 \tag{2.115}$$

where $0 < \mathcal{K} < 1$ is a factor which affects the size of the deadband [55] Hirche, S., & Buss, M. (2012). Human-oriented control for haptic teleoperation. *Proceedings of the IEEE*, *100*(3), 623-647..

When the deadband method is applied to the wave-based teleoperator, the added coding scheme will not insert additional energy into the overall system to violate passivity. In [131], a deadband passifier is proposed to guarantee the passivity of the deadband coding scheme. By using the deadband approach, the packets rate is reduced and the data loss in the network-based teleoperator can be effectively alleviated.

2.5 Discussion and Summary

In Chapter 2, different properties of the wave-variable-based system have been reviewed. As a conservative method for passivity maintenance, the wave variable method is able to robustly guarantee the stability of the teleoperation system. This is useful for different practical industrial applications such as handling hazardous material, tele-surgery, underwater vehicles, space robots, etc. [66] However, two of the intrinsic problems of this method, i.e., wave reflection and position drift, are the major barriers to reach high transparency, especially under large time delays. Furthermore, time varying delay and data loss are also two main elements in the communication that influences passivity and work performance of the wave-variable-based system.

Among the studies reviewed in this chapter, some intend to enhance the performance of the wave-based systems in terms of trajectory and force tracking by transmitting high frequency information and minimizing wave reflection. Methods such as wave prediction and compensation for wave integral are proposed to deal with the time delay problem especially for variable time delay. Combining the wave variable method with 4-CH architecture is also an effective way to optimize the trade-off between stability

and transparency. Based on the dissipativity theory, generalized wave variable transformation is applied to guarantee small gain L_2-stability in the presence of communication unreliabilities such as time delays and data loss. The multi-DOF wave-based system is also surveyed in this Chapter.

In spite of various methods proposed in the literature to enhance the performance the wave-based systems, a significant amount of research is still required. As mentioned earlier, wave reflection significantly influences the force feedback and limits frequency content of the rendered force to the user. Although high frequency information transmission has been explored by Niemeyer and Slotine applying wave filtering in [84], [107], restriction of bandwidth and incorrect force feedback under large time delays are the main drawbacks of this approach. Therefore, developing a wave reflection reducing controller like [132] for accurate force feedback and high frequency information transmission without using wave filtering is also a valuable future study.

Secondly since most of the studies on the wave variable method are based on linear teleoperator dynamics, which is not suitable for complex multi-DOF teleoperators, a nonlinear wave-variable-based teleoperation system is a valuable direction for exploration. Some studies have theoretically proved that the wave variable method can guarantee the nonlinear teleoperation systems' passivity [134], [135]. However, without practical experiments on complex multi-DOF system, transparency and work performance of the nonlinear multi-DOF systems using the wave variable method still need investigation and exploration.

Thirdly, [108] demonstrates that a combination of the wave variable method and 4-CH architecture can enhance system transparency since extra human and environmental force sources are introduced into the system. However, [136] has pointed out that wave-based system stability can be destroyed by the extra force sources. Accordingly, the 4-CH wave-variable-based teleoperation system applying force observers [137] is considered to simultaneously guarantee system stability and transparency, which can also be used in nonlinear teleoperation systems. The force observer in [137] can derive highly accurate force signals and the Kalman filter applied in the observer also effectively suppress the measurement noises.

Fourthly, the conventional wave variable method can only guarantee passivity in the presence of time-varying delays. Most of the wave-based systems lack the capability of dealing with the time-varying delay issues. Several wave-based methods were proposed to guarantee passivity under time varying delays [25], [77]. However, these methods over-dissipate energy to guarantee the passivity of the teleoperation system by considering the worst-case scenario. Guaranteeing stability and simultaneously enhancing the system transparency in the presence of time-varying delays in still a challenging issue in the wave variable method.

Finally, several applications, including rehabilitation, surgical training and signal modification require the teleoperation system with more than one user to remotely operate the slave robot [138]-[140]. These applications can be more effective with the collaboration of multiple robots where a single robot does not have the required level of manipulation dexterity, mechanical strength, robustness to single point failure, or safety (e.g. distributed kinetic energy) [141]. Therefore, Application of the wave variable method to maintain stability of the multilateral teleoperation systems such as the Single-Master-Multiple-Slave (SMMS) system and the multi-user system is also valuable direction of work.

3 REDUCED WAVE REFLECTION SYSTEMS

3.1 Overview

As mentioned in Chapter 2, decay of transparency is the main drawback of the passivity based systems. For a wave-based system, wave reflections and position drift are the two main issues that can seriously affect the system transparency. In this chapter, reduced wave reflection architectures for the linear system with constant time delay and for the nonlinear system with time-varying delays are proposed which can reduce the wave reflection and address the position drift issue, and eventually largely enhance the system transparency compared with previous wave-based systems.

The proposed reduced wave reflection architecture for the linear system is implemented on a HILINK microcontroller board driving 4 one degree-of-freedom (1-DOF) motors. The proposed reduced wave reflection architecture for the non-linear system is implemented on a teleoperation platform consisting of two three Degree-Of-Freedom (3-DOF) haptic devices. More information about the experimental setups will be provided in this chapter.

3.2 Review of Reduced Wave Reflection Architectures

As reviewed in Chapter 2, a number of wave-based control systems are proposed in the literature for reduced wave reflections. While these systems can reduce wave reflections to some extent, they suffer from some deficiencies.

The phenomenon of wave reflection is due to the imperfectly matched junction impedance. The standard wave-variable-based system shown in Figure 2.2 consists of three independent channels: the master's direct feedback (dotted line 1), the wave-variable-based reflections (dotted line 2) and the slave's force feedback to master (dotted line 3). In channel 1, the master velocity signals directly return as the damping $b\dot{x}_m$, which can be treated as a simple damper. A certain amount of damping produced in channel 1 enhances the system stability via sacrificing transparency. Channel 3 feeds force information back to the operator from the remote slave side. The phenomenon of wave-variable-based reflection occurs in the channel 2. According to

(2.34), each incoming wave variable v_m and u_s is reflected and returned as the outgoing wave variable u_m and v_s. Wave-variable-based reflection lasts several cycles in the communication channels and then gradually disappears. This phenomenon can easily generate unpredictable interferences and disturbances that can destabilise the system.

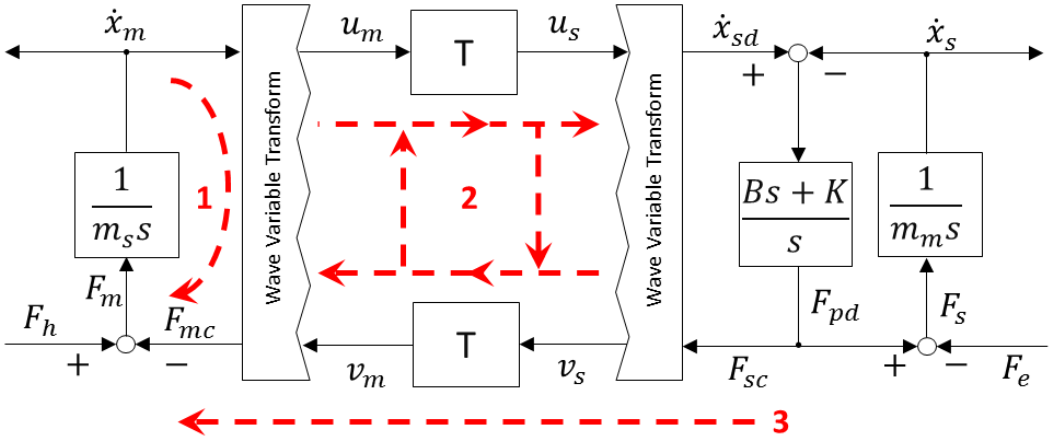

Figure 3.1. Wave-based reflection due to impedance junctions

The velocity and force tracking of the standard wave -based system in Figure 3.1 are written as (2.37) and (2.38). The wave reflections in channel 2 adversely influence the transmitted force and velocity signals so that $F_{sc}(s)$ and $\dot{x}_m(s)$ are not equal to $F_{mc}(s)e^{-sT}$ and $\dot{x}_{sd}(s)e^{-sT}$, respectively. Hence, the bias terms $-\frac{1}{b}[F_{sc}(s) - F_{mc}(s)e^{-sT}]$ in (2.37) and $b[\dot{x}_m(s) - \dot{x}_{sd}(s)e^{-sT}]$ in (2.38) can degrade the large delay based system's transparency, especially during the transient state of the system. Under the ideal condition when the teleoperation system impedance is perfectly matched, the feed-forward wave variable u_m and the feedback wave variable v_s only contain velocity information and force information, respectively:

$$u_m(s) = \frac{b\dot{x}_m(s)}{\sqrt{2b}}, v_s(s) = \frac{F_{sc}(s)}{\sqrt{2b}} \tag{3.1}$$

When the impedance is perfectly matched, u_m and v_s will not be influenced by the input wave variables u_s and v_m. Hence, the wave reflections can be avoided. The

remaining problem is that the added impedance matching terms can significantly degrade the velocity and force tracking performance. Based on Figure 3.3, $\dot{x}_s$ and F_m are expressed as:

$$\dot{x}_{sd}(s) = \frac{b\dot{x}_m(s)e^{-sT} - F_s(s)}{2b} \tag{3.2}$$

$$F_{mc}(s) = \frac{b\dot{x}_m(s) - F_{sc}(s)e^{-sT}}{2} \tag{3.3}$$

Based on (3.2) and (3.3), if F_s decays to zero, $\dot{x}_s$ will be equal to $\frac{\dot{x}_m}{2}$. On the other hand, if the master manipulator moves slowly and finally the master velocity decays to zero, F_m will converge to $-\frac{F_s}{2}$. In this situation, the velocity and the force tracking performances will be largely degraded.

Slave impedance matching is a method to deal with the wave-variable-based reflections by adding predetermined damping elements [147]. Nevertheless, the predetermined damping elements are not able to address the unknown impedance changes of the operator and the environment to the extent that the wave-variable-based reflections are reinstated.

Another method to handle the unknown changes of the operator and the environment impedances is wave filtering through adding a low-pass filter to the feed-forward path [147]. Combined with impedance matching, either the wave-variable-based reflection in free space or the wave reflection brought about by the operator or the remote environment can be reduced to some extent. Nevertheless, this approach has the obvious disadvantage that the located low-pass filters can significantly restrict the bandwidth of the communication channel.

A new scheme for reduced wave reflections is proposed in [132]. The outgoing wave variables of this scheme are expressed as (2.93).

Unlike the conventional wave transformation, with containing no velocity information, the slave outgoing wave variable v_s in (2.93) retains no information from the incoming wave variable u_s. Therefore, the wave-variable-based reflections can be circumvented. Based on (2.93), the velocity and force tracking equations are written as:

$$b\dot{x}_{sd}(s) = b\dot{x}_m(s)e^{-sT} + [F_{sc}(s)e^{-2sT} - F_{sc}(s)] \quad (3.4)$$

$$F_{mc}(s) = \mathrm{b}\dot{x}_m(s) + F_{sc}(s)e^{-sT} \quad (3.5)$$

According to (3.4), precise velocity tracking can be achieved under constant time delay or delay with slowly time varying condition. Under the completely hard environment contact condition (no movement of the master manipulator), (3.5) indicates that accurate force reflection can also be achieved. However, if master manipulator still has velocity during contact with the environment, this system will generate inaccurate force tracking due to the bias term $\mathrm{b}\dot{x}_m(s)$ in (3.5). Furthermore, the inaccurate force tracking can also adversely affect the position tracking when contacting to the environment so that large position drift will occur in this architecture.

It is demonstrated that the 4-CH architecture with the extra "degrees of freedom" (control parameters) is the best teleoperation system from a transparency point of view when the communication channels have no time delay [50]. Nevertheless, the 4-CH system suffers from stability degradation in the presence of time delays [27]. In order to guarantee the delay-based channels' stability, Aziminejad et al [108] extend the wave transmission to the extended Lawrence 4-CH architecture in [65] as shown in Figure 2.11.

In Figure 2.3, the nonphysical input and output effort and flow of the communication channel are expressed as (2.79)-(2.80) and in this scheme, the wave variables can be written as (2.81). By extending the wave-variable method into the 4-CH architecture, the trade-off between stability and transparency of the bilateral teleoperation is enforced, compared with the conventional wave-variable-based system. Since the application of the extended Laurence architecture allows for the transmission of the position signals, position drift problem of the wave-variable-based system can be reduced to some extent. In order to overcome the oscillatory behavior caused by the wave-variable-based reflection and guarantee the delay-based stability, [108] still applies the wave-filtering approach where the cutoff frequency f_{cut} of the first-order low-pass filters $\mathrm{W(s)} = \frac{2\pi f_{cut}}{(s+2\pi f_{cut})}$ located at the transmission paths should be set as a small value. Therefore, the bandwidth of the communication channels is seriously

restricted. Moreover, even applying extra control parameters of the 4-CH architecture, the bias terms of the wave-variable-based system in (2.37) and (2.38) are still not thoroughly compensated. Substituting (2.79) and (2.80) into (2.81), the signal transmission in this system can be written as

$$(1 + C_5 + \mathrm{b}C_2)F_e = (C_3 + \mathrm{b} + \mathrm{b}C_6)F_h \times e^{-sT}W + [(M_s s + C_s + \mathrm{b}C_4)\dot{x}_s - (C_1 - bM_m s - bC_m)\dot{x}_m \times e^{-sT}W] \quad (3.6)$$

$$(bM_m s + bC_m + C_1)\dot{x}_m = (M_s s + C_s - bC_4)\dot{x}_s \times e^{-sT}W + [(b + bC_6 - C_3)F_h \times e^{-sT}W - (bC_2 - 1 - C_5)F_e] \quad (3.7)$$

Based on (19) and (20), both the velocity and force tracking performance of the system in [108] are degraded by the bias terms $[(M_s s + C_s + \mathrm{b}C_4)\dot{x}_s - (C_1 - bM_m s - bC_m)\dot{x}_m \times e^{-sT}W]$ and $[(b + bC_6 - C_3)F_h \times e^{-sT}W - (bC_2 - 1 - C_5)F_e]$ during the signal transmission between the master and the slave. Therefore, even with extra control parameters, it is impossible for the system in [108] to achieve ideal transparency in the presence of large time delays.

3.3 Proposed Architecture for the Linear System under Constant Time Delays

3.3.1 Design

In this work, a new 4-CH linear system with modified wave variable transformation is proposed in Figure 3.2. The goal of the developed architecture is to reduce the wave-based reflection, enhance the system transparency and simultaneously guarantee the system stability in the presence of constant time delays.

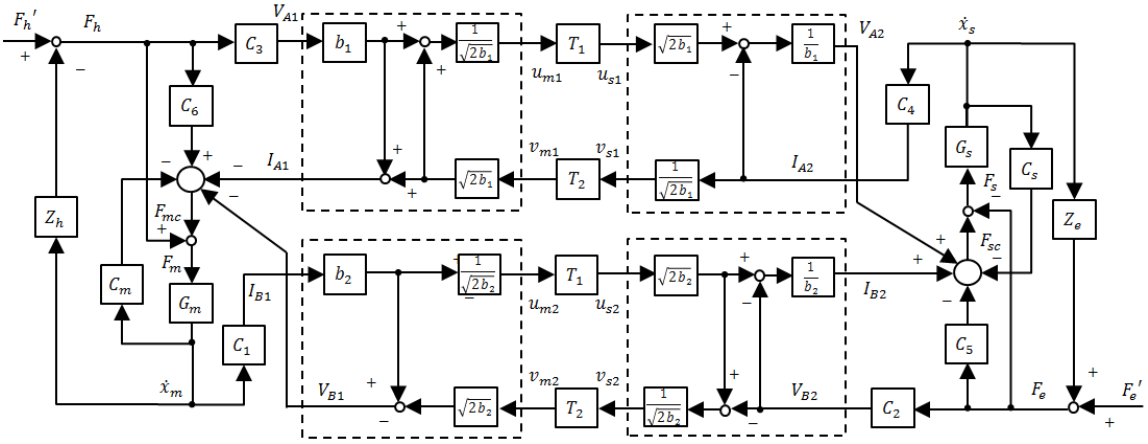

Figure 3.2. Proposed 4-CH Architecture with Modified Wave Controllers

In Figure 3.2, two modified reduced wave reflection wave transformation schemes are applied to guarantee the stability of the delay-based communication channels. The wave controller with the characteristic impedance b_1 is used to encode the controlled human operator's force V_{A1} and the controlled slave velocity I_{A2}. The wave variables in this wave controller are defined as:

$$u_{m1}(s) = \frac{b_1 V_{A1}(s) + I_{A2}(s)e^{-sT_1}}{\sqrt{2b_1}}, u_{s1}(s) = \frac{b_1 V_{A2}(s) + I_{A2}(s)}{\sqrt{2b_1}} \tag{3.8}$$

$$v_{m1} = \frac{I_{A2}(s)e^{-sT_2}}{\sqrt{2b_1}}, v_{s1}(s) = \frac{I_{A2}(s)}{\sqrt{2b_1}} \tag{3.9}$$

Since v_{s1} in (3.9) no longer contains the force information so that the slave outgoing wave variable v_{s1} does not retain any information from the incoming wave variable u_{s1}. Therefore the wave-variable-based reflections in the first two channels can be circumvented.

The controlled environmental force V_{B2} and the controlled master velocity I_{B1} are encoded by the wave controller with the characteristic impedance b_2. The wave variables in this wave controller are defined as:

$$u_{m2}(s) = \frac{b_2 I_{B1}(s)}{\sqrt{2b_2}}, u_{s2}(s) = \frac{b_2 I_{B1}(s)e^{-sT_1}}{\sqrt{2b_2}} \tag{3.10}$$

$$v_{m2}(s) = \frac{b_2 I_{B1}(s) - V_{B1}(s)}{\sqrt{2b_2}}, v_{s2}(s) = \frac{b_2 I_{B1}(s)e^{-sT_1} - V_{B2}(s)}{\sqrt{2b_2}} \tag{3.11}$$

As shown in (3.10), the feed-forward wave variables u_{m2} and u_{s2} do not contain any force information to the extent that any information of the feedback wave variable v_{m2} are no longer included in the outgoing master wave variable u_{m2}. Therefore, since the proposed wave transform controller at the master side decouples the velocity and force information, circulating wave reflections in the last two channels can be prevented.

The wave transmissions between the master and slave side in this system are expressed as (3.12).

$$\begin{cases} u_{m1}(s)e^{-sT_1} = u_{s1}(s) \\ v_{m1}(s) = v_{s1}(s)e^{-sT_2} \\ u_{m2}(s)e^{-sT_3} = u_{s2}(s) \\ v_{m2}(s) = v_{s2}(s)e^{-sT_4} \end{cases} \tag{3.12}$$

Substituting (3.10)-(3.11) into (3.12), the controlled force and velocity transmission in the proposed system can be expressed by:

$$V_{A2}(s) = V_{A1}(s)e^{-sT_1} + \frac{1}{b_1}\left[I_{A2}(s)e^{-s(T_1+T_2)} - I_{A2}(s)\right] \tag{3.13}$$

$$I_{A1}(s) = b_1 V_{A1}(s) + I_{A2}(s)e^{-sT_2} \tag{3.14}$$

$$V_{B1}(s) = V_{B2}(s)e^{-sT_2} + b_2\left[I_{B1}(s) - I_{B1}(s)e^{-s(T_1+T_2)}\right] \tag{3.15}$$

$$I_{B2}(\mathrm{s}) = I_{B1}(s)e^{-sT_1} - \frac{1}{b_2}V_{B2}(s) \tag{3.16}$$

According to (3.13) and (3.15), since the effect of the wave-variable-based reflections is cancelled in the feed-forward and feedback controlled velocity transmission channels, the bias term $\frac{1}{b_1}\left[I_{A2}(s)e^{-s(T_1+T_2)} - I_{A2}(s)\right]$ and $b_2\left[I_{B1}(s) - I_{B1}(s)e^{-s(T_1+T_2)}\right]$ is near zero. Under the constant time delay or time delay with slow variation condition, (3.13) and (3.15) show a highly accurate force tracking performance. This advantage allows the proposed teleoperator to handle different kinds of unknown environment and provide the operator accurate perception of the

remote environment. The major disadvantage of the two modified wave transform controllers is shown in (3.14) and (3.16) that the bias terms $b_1 V_{A1}(s)$ and $-\frac{1}{b_2} V_{B2}(s)$ can degrade the trajectory tracking performance especially during the environmental contact with a large force values of V_{A1} and $V_{B2}(s)$. Therefore, position drift can occur if only using either of the two wave transform controllers in a 2-CH channel architecture. However, the bias terms $b_1 V_{A1}(s)$ and $-\frac{1}{b_2} V_{B2}(s)$ cannot be cancelled since they are treated as the dampers to guarantee the delay-based system stability. Accordingly, the controllers of the 4-CH architectures are applied to compensate for the bias terms and enhance the overall system's transparency.

On the master and slave side, $G_m = \frac{1}{M_m s}$ and $G_s = \frac{1}{M_s s}$ are the transfer functions of the master and slave manipulators where M_m and M_s are the masses of the slave and master, respectively. C_2, C_3, C_5 and C_6 are the force control gains and C_1, C_4, C_s and C_m are the velocity controllers. The dynamics of the slave and the master manipulators can be expressed as:

$$(G_m^{-1} + C_m)\dot{x}_m(s) = (1 + C_6)F_h(s) - I_{A1}(s) - V_{B1}(s) \tag{3.17}$$

$$(G_s^{-1} + C_s)\dot{x}_s(s) = I_{B2}(s) + V_{A2}(s) - (1 + C_5)F_e(s) \tag{3.18}$$

Where $V_{A1}(s) = \mathrm{C}_3 F_h(s),\ I_{B1}(s) = \mathrm{C}_1 \dot{x}_m(s),\ I_{A2}(s) = \mathrm{C}_4 \dot{x}_s(s), V_{B2}(s) = \mathrm{C}_2 F_e(s)$. Substituting (3.13)-(3.16) to (3.17) and (3.18), the dynamic equations of the overall system can be expressed by (3.19) and (3.20):

$$\begin{aligned}\left[G_m^{-1} + C_m + b_2 \mathrm{C}_1\left(1 - e^{-s(T_1+T_2)}\right)\right]\dot{x}_m(s) \\ = -\mathrm{C}_4 e^{-sT_2}\dot{x}_s(s) + (1 + C_6 - b_1 \mathrm{C}_3)F_h(s) \\ - \mathrm{C}_2 e^{-sT_2} F_e(s)\end{aligned} \tag{3.19}$$

$$\begin{aligned}\left[G_s^{-1} + C_s + \frac{\mathrm{C}_4}{b_1}(1 - e^{-s(T_1+T_2)})\right]\dot{x}_s(s) \\ = \mathrm{C}_1 e^{-sT_1}\dot{x}_m(s) + \mathrm{C}_3 e^{-sT_1} F_h(s) - (\frac{\mathrm{C}_2}{b_2} + 1 + C_5)F_e(s)\end{aligned} \tag{3.20}$$

3.3.2 Transparency Analysis and Controller Parameters Setting

A teleoperation system is defined to be transparent if the human operator perceives the remote environment by fidelity and can easily perform the remote tasks. The system transparency can be illustrated by the hybrid matrix H(s) of a bilateral teleoperation system given in (2.3). Based on (2.3), hybrid matrix H(s) is defined by [49], which can be interpreted as: $\mathrm{H(s)} = \begin{bmatrix} H_{11}(s) & H_{12}(s) \\ H_{21}(s) & H_{22}(s) \end{bmatrix} = \begin{bmatrix} Z_h & Force\ scalling \\ Velocity\ Scalling & Z_e^{-1} \end{bmatrix}$. The hybrid parameters $h_{ij}, \mathrm{i,j} = 1,2$ are functions of the master and slave dynamics and the control parameters. The main effect of H(s) is to present kinesthetic feedback between human operator and environment, and build a relationship between force and velocity. $H_{11}(s)$ and $H_{22}(s)$ denote the operator impedance and environment admittance. In the ideal transparency condition, the technical medium between the operator and the environment is not felt. That is, Z_h and Z_e^{-1} equal to zero. H_{12} and H_{21} represent the measure of force scaling and velocity scaling, respectively. In order to achieve the ideal transparency in a bilateral teleoperation system in the presence of time delay, the delayed kinematic correspondence and the delayed interaction force correspondence are expressed as $\dot{x}_s(s) = \dot{x}_m(s)e^{-sT}$ and $F_h(s) = F_e(s)e^{-sT}$, respectively. Accordingly, the hybrid matrix in the time-delay-based ideal transparency is expressed as:

$$H_{ideal}(s) = \begin{bmatrix} 0 & e^{Ts} \\ e^{-Ts} & 0 \end{bmatrix} \tag{3.21}$$

After transformation, the dynamic equations (3.19) and (3.20) of the overall system can be expressed by (2.3) to demonstrate the transparency of the proposed system. The parameters of the hybrid matrix H(s) are shown in (3.22)-(3.26) where Den denotes the denominator of each term:

$$H_{11} = \left[G_m^{-1} + C_m + b_2\mathrm{C}_1\left(1 - e^{-s(T_1+T_2)}\right)\right]\left[G_s^{-1} + C_s + \frac{\mathrm{C}_4}{b_1}\left(1 - e^{-s(T_1+T_2)}\right)\right] + \mathrm{C}_4\mathrm{C}_1 e^{-s(T_1+T_2)} \tag{3.22}$$

$$H_{12} = -\mathrm{C}_4 e^{-sT_2}\left(\frac{\mathrm{C}_2}{b_2} + 1 + C_5\right) + \mathrm{C}_2 e^{-sT_2}[G_s^{-1} + C_s + \frac{\mathrm{C}_4}{b_1}\left(1 - e^{-s(T_1+T_2)}\right)] \quad (3.23)$$

$$H_{21} = -(1 + C_6 - b_1\mathrm{C}_3)\mathrm{C}_1 e^{-sT_1} - \mathrm{C}_3 e^{-sT_1}\left[G_m^{-1} + C_m + b_2\mathrm{C}_1\left(1 - e^{-s(T_1+T_2)}\right)\right] \quad (3.24)$$

$$H_{22} = -\mathrm{C}_2\mathrm{C}_3 e^{-s(T_1+T_2)} + \left(\frac{\mathrm{C}_2}{b_2} + 1 + C_5\right)(1 + C_6 - b_1\mathrm{C}_3) \quad (3.25)$$

$$\mathrm{Den} = -\mathrm{C}_4\mathrm{C}_3 e^{-s(T_1+T_2)} + (1 + C_6 - b_1\mathrm{C}_3)[G_s^{-1} + C_s + \frac{\mathrm{C}_4}{b_1}(1 - e^{-s(T_1+T_2)})] \quad (3.26)$$

According to (2.3), to achieve high transparency, the operator impedance and environmental admittance should be close to zero. To achieve highly accurate force and trajectory tracking at the presence of time delays, the force scaling and velocity scaling should be e^{sT} and e^{-sT}, respectively. Under constant time delay or slow time varying delay condition, the characteristic of the time delay element e^{-sT} in the frequency domain is described as $|e^{-sT}| = 1$.

Accordingly, based on (3.22), $|H_{11}| = \left|(G_m^{-1} + C_m)(G_s^{-1} + C_s) + \mathrm{C}_4\mathrm{C}_1 e^{-s(T_1+T_2)}\right|$. Therefore, by setting the velocity controllers C_4 and C_1 as (3.27) and (3.28), the operator impedance H_{11} is close to 0.

$$C_1 = G_m^{-1} + C_m \quad (3.27)$$

$$C_4 = -G_s^{-1} - C_s \quad (3.28)$$

Where the velocity controller C_m and C_s are defined as $C_{m,s} = \frac{1}{s}k_p + k_v$. k_p and k_v are the position and velocity control gains, respectively. Hence, C_1 and C_4 is defined as: $C_1 = \frac{1}{s}k_p + k_v + m_m s$, $C_4 = \frac{1}{s}k_p + k_v + m_s s$, respectively. Accordingly, the controllers C_1 and C_4 allows position information transmission which will enhance the trajectory tracking performance of the proposed 4-CH system.

Based on (3.25), the environmental admittance H_{22} is close to zero through the following equation:

$$C_3 = 1 + C_6 - b_1 \mathrm{C}_3 \tag{3.29}$$

$$\mathrm{C}_2 = \frac{\mathrm{C}_2}{b_2} + 1 + C_5 \tag{3.30}$$

Substituting (3.28), (3.29) and (3.30) into (3.23) and (3.26), the force scaling H_{12}/Den can be simplified as $\frac{H_{12}}{Den} = \frac{\mathrm{C}_2}{\mathrm{C}_3} e^{sT_1}$. Therefore, highly accurate force tracking can be achieved via setting:

$$\mathrm{C}_2 = \mathrm{C}_3 \tag{3.31}$$

Normally, the force signals transmission controllers C_2 and C_3 are designed as: $\mathrm{C}_2 = C_3 = 1$. Therefore, (3.29) and (3.30) can be simplified as:

$$C_6 = b_1 \tag{3.32}$$

$$C_5 = -\frac{1}{b_2} \tag{3.33}$$

Substituting (3.27)-(3.33) into (3.24), the velocity scaling H_{21}/Den can be simplified as: $\frac{H_{21}}{Den} = e^{-sT_1}$. Hence, the main drawback of the modified wave transform controllers i.e., position drift can be eliminated to the extent that highly accurate trajectory tracking performance is achieved.

Through setting the controller parameters to satisfy the above conditions, high transparency of the proposed architecture can be achieved at the presence of time delay.

3.3.3 Stability Analysis

This section analyzes the stability performance of the proposed 4-CH architecture in order to prove that this scheme is able to achieve high transparency without sacrificing system stability. Based on (3.13)-(3.16), the two modified wave transform controllers can be expressed in the form of the following hybrid matrixes:

$$\begin{bmatrix} V_{A1}(s) \\ -I_{A2}(s) \end{bmatrix} = \begin{bmatrix} H_{11}(s) & H_{12}(s) \\ H_{21}(s) & H_{22}(s) \end{bmatrix} \begin{bmatrix} I_{A1}(s) \\ V_{A2}(s) \end{bmatrix} = \begin{bmatrix} \frac{1}{b_1}\left[1 - e^{-s(T_1+T_2)}\right] & e^{-sT_2} \\ -e^{-sT_1} & b_1 \end{bmatrix} \begin{bmatrix} I_{A1}(s) \\ V_{A2}(s) \end{bmatrix} \tag{3.34}$$

$$\begin{bmatrix} V_{B1}(s) \\ -I_{B2}(s) \end{bmatrix} = \begin{bmatrix} H_{11}(s) & H_{12}(s) \\ H_{21}(s) & H_{22}(s) \end{bmatrix} \begin{bmatrix} I_{B1}(s) \\ V_{B2}(s) \end{bmatrix} = \begin{bmatrix} b_2\left[1 - e^{-s(T_1+T_2)}\right] & e^{-sT_2} \\ -e^{-sT_1} & \frac{1}{b_2} \end{bmatrix} \begin{bmatrix} I_{B1}(s) \\ V_{B2}(s) \end{bmatrix} \tag{3.35}$$

Anderson and Spong [18] state that a teleoperation system is passive if and only if the norm of the scattering matrix S(s) is equal to or less than one, where S(s) is expressed as (2.11). Therefore, the scattering norm $\|S\|$ is influenced by the angular frequency ω (s = jω) from the time delay component $e^{-sT_{1,2}}$. The periodicity of $e^{-sT_{1,2}}$ indicates that the scattering norm $\|S\|$ is periodic. Since the angular frequency can be considered as a factor of the product of $\omega T_{1,2}$, different time delay $T_{1,2}$ can be treated as the gains of the angular frequency to influence the scattering norm by which the scattering norm $\|S\|$ can be extended or compressed periodically. Accordingly, Figures 3.3 and 3.4 display the values of the scattering norm $\|S\|$ with ω changing. As shown in Figures 3.3 and 3.4, by setting the characteristic impedance b_1 and b_2 to be positive constants, the values of time delays only influence changes in the frequency of the waveform rather than the magnitude of the scattering norm. The vertex of the scattering norm remains unchanged. Accordingly, the scattering norm $\|S\|$ of the proposed scheme is uniformly no more than 1. Therefore, the passivity and stability of the communication channels in the proposed 4-CH architecture can be guaranteed.

Assuming the impedances of human operator and environment are passive, [108] has already proved that the modal spaces of master and slave are stable in common cases when the passivity of the delay-based communication channels is guaranteed. To further improve the stability of the master side and slave side, the velocity damping approach can be alternatively applied, since velocity damping by local velocity feedback is able to enhance the stability of each modal space [148]. However, setting a velocity damping controller to be a constant value can also degrade the overall

system's transparency. It is illustrated that the instability of the delay-based control system is caused by the time delay element e^{-sT}in the high frequency area [21]. In order to eliminate the high frequency perturbations in the master and slave side without sacrificing the system transparency, the velocity damping controller is designed to be a high-pass filter rather than a constant gain. Accordingly, the local velocity feedback controllers C_m and C_s can be rewritten as:

$$C_{m,s} = \frac{1}{s}k_p + k_v + \frac{s^2}{(s+p)^2} \tag{3.36}$$

Where p is the cut-off frequency of the high-pass filter. The reason of choosing a second order high-pass filter is that its bandwidth is better than that of the first-order high-pass filter [144]-[145]. By applying the high-pass filters, the high frequency vibrations of force and trajectory tracking of the proposed 4-CH architecture in the transient state can be mitigated in the presence of large time delay.

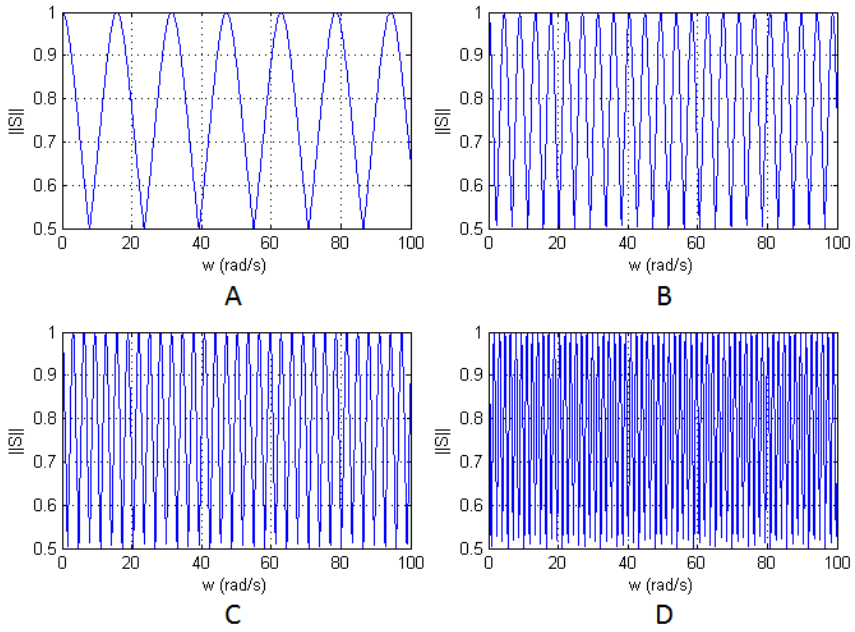

Figure 3.3. Scattering norm of the modified wave transform controller 1 with different time delays: A. 200 ms, B. 700 ms, C. 1000 ms, D. 2000 ms.

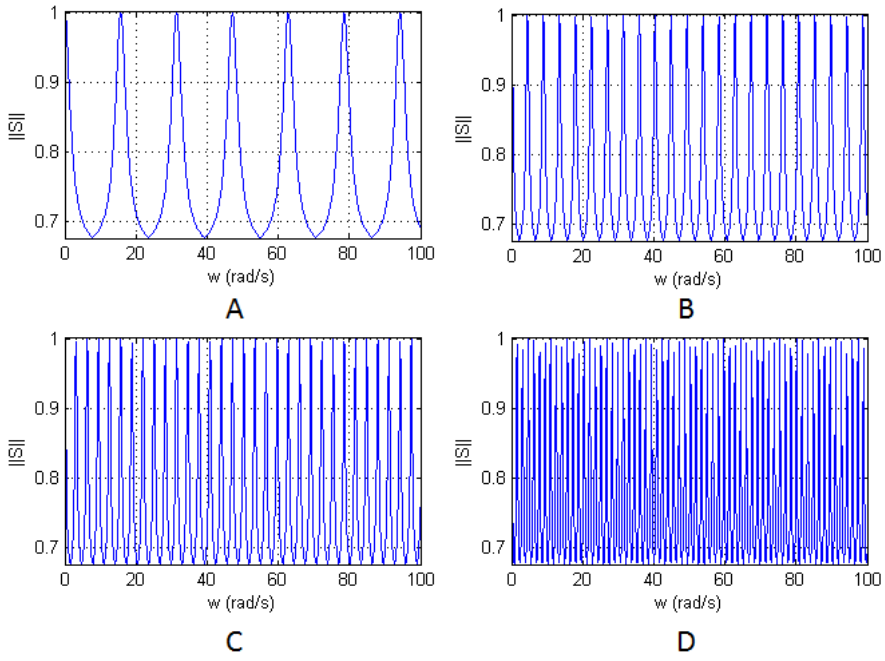

Figure 3.4. Scattering norm of the modified wave transform controller 2 with different time delays: A. 200 ms, B. 700 ms, C. 1000 ms, D. 2000 ms.

3.3.4 Experimental Results

This sub-section validates the proposed scheme through experimental work. Figure 3.5 shows the experimental platform which is a bilateral teleoperation set up for the study of the developed algorithms. The HILINK microcontroller board [149] is interfaced to a computer to control a set of DC motors in both of the master and the slave sides. The control algorithms are developed in Matlab/Simulink and downloaded to HLINK boards. The communication channel between the master computers and the slave computer is the Internet. In order to test the proposed system's work performance under larger time delays, the time delay blocks in the Simulink library are applied to the algorithms of the two computers. The time delay of these experiments is around 200 ms (400 ms round trip time); comparable to the round trip transit time of an Internet user Datagram Packet from Australia to the U.S. [150].

The four DC motors in Figure 3.5 represent the operator motor, the master motor, the slave motor and the environmental load motor. On the master side, the operator motor and the master motor are coupled mechanically so that the operator motor can act as

the human operator to physically control the master motor. Then, the Hilink board derives the velocity and force command signals generated from the master motor, and then the signals are transmitted to the computer on the slave side via the Internet. On the slave side, the slave motor and the environmental load motor are also mechanically coupled. The slave motor receives the velocity and force command signals and then moves accordingly. The environmental load motor can apply different environmental contact loads to the slave motor. Matlab/Simulink/Real-Time Workshop is the software applied for controlling the motors.

In the proposed control system, the sampling period is 0.1 ms. The two wave characteristic impedances b_1 and b_2 are set as 2.5 Ns/m. position gain k_p and velocity control gains k_v are set as 4.7 N/m and 2.3Ns/m. the value of the constant force control gains C_2, C_3, C_5 and C_6 are 1, 1, -0.4 and 2.5, respectively. The parameter p of the high-pass filter is 1.

In order to test the performance of the proposed 4-CH architecture in enhancing transparency, the force tracking, velocity tracking and position tracking of the proposed four-channel system are compared against two systems proposed in the previous work, the 4-CH architecture applying wave transformation [108] (system A) and the 2-CH reduced wave reflections teleoperation system in [132] (system B). The experiments are conducted for three scenarios of free space motion, hard contact with the environment, and high frequency contact with the environment. All gain values for the controllers and dynamics remain unchanged throughout the experiments.

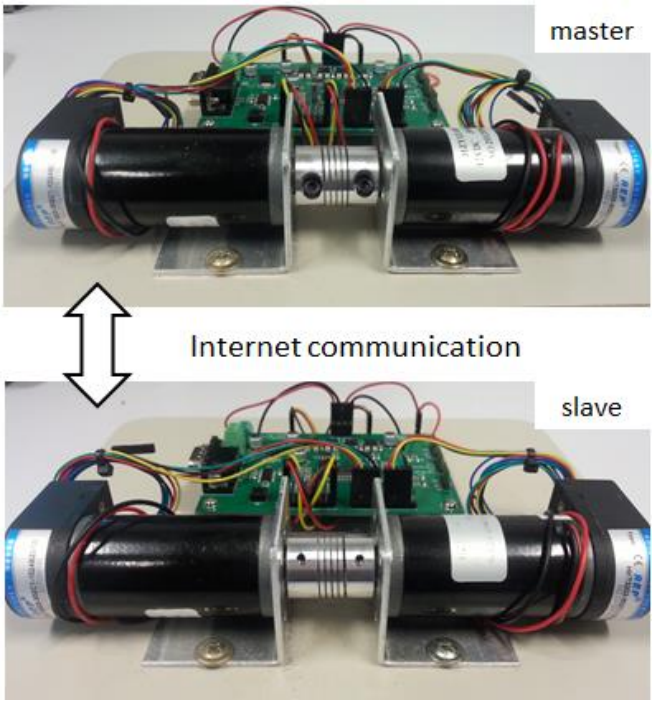

Figure 3.5. Experiment set up

3.3.4.1 Free Motion

In this experiment, a square signal at a frequency of 0.5 rad/s is applied to the motor representing the operator with zero input into the motor representing the environment, implying the free space movement. The performance of the systems A and B and our proposed 4-CH system in free motion are shown in Figures 3.6, 3.7 and 3.8, respectively. In Figure 3.6, the value of the low-pass filters located in the communication channels of the system should be set to be a small value in order to reduce the oscillatory behavior caused by the time delays and wave reflections. However, in the presence of large time delays, the delay-based bias term $[(b + bC_6 - C_3)F_h \times e^{-sT}W - (bC_2 - 1 - C_5)F_e]$ in (3.7) causes signal variations and adversely influences the accuracy of trajectory tracking as shown in Figure 3.6B and 3.6C. As shown in Figure 3.7B and 3.7C, accurate trajectory tracking can be achieved since the wave-variable-based reflections are reduced in system B. However, since the master motor has a velocity during free motion, the bias term $b\dot{x}_m(s)$ in (3.5) adversely affects the force feedback so that the force signals in Figure 3.7A have large

variations. In Figure 3.8, the oscillatory behaviour caused by wave-variable-based reflections is eliminated as shown in Figure 3.8A and high accuracy of trajectory tracking performance is achieved in the proposed 4-CH architecture as shown in Figure 3.8B and C.

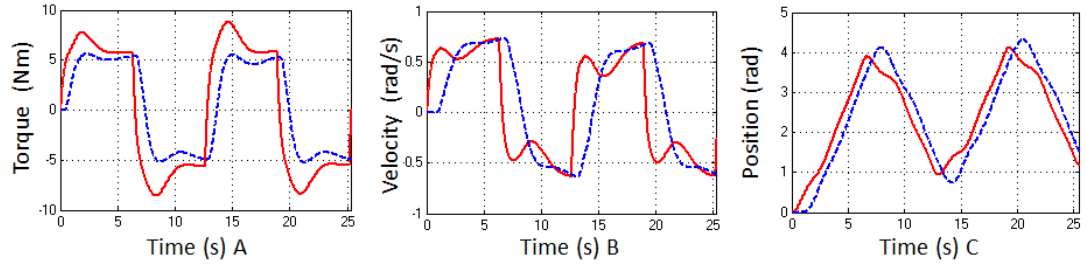

Figure 3.6. Free motion of the system A: A. Force tracking of master and slave motor, B. Velocity tracking of the master and slave motor, C. Position tracking of the master and slave motor (red curved-master, blue dotted-slave)

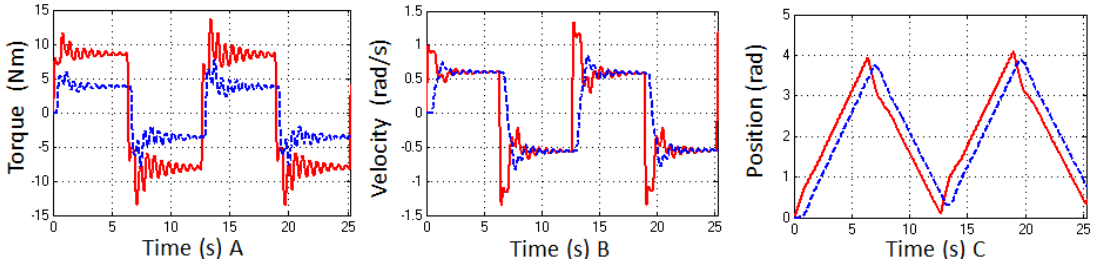

Figure 3.7. Free motion of the system B: A. Force tracking of master and slave motor, B. Velocity tracking of the master and slave motor, C. Position tracking of the master and slave motor (red curved-master, blue dotted-slave)

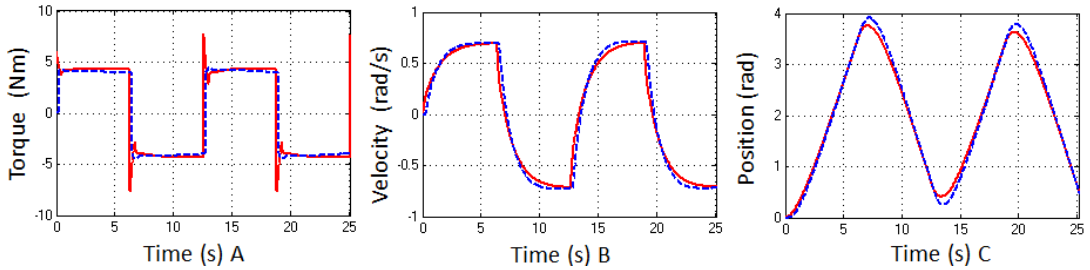

Figure 3.8. Free motion of the proposed 4-CH system: A. Force tracking of master and slave motor, B. Velocity tracking of the master and slave motor, C. Position tracking of the master and slave motor (red curved-master, blue dotted-slave)

3.3.4.2 Hard Environmental Contact

During the hard contact with the environment, a square signal command with 0.5 rad/s frequency is applied to the motor representing the operator, and an opposite square signal command with the same magnitude and frequency is applied to the environment motor. Figures 3.9, 3.10 and 3.11 illustrate the performances of systems A and B and our proposed 4-CH system in hard contact with the environment, respectively. As shown in Figure 3.9, the applied extra control parameters of the extended Laurence architecture provide system A the accurate force tracking performance. However, since the wave-based reflections still exist, the force tracking still has small variations even applying wave filtering as shown in Figure 3.9A. The trajectory tracking is adversely affected by the bias terms of the applied conventional wave transform controllers as shown in Figure 3.9B and C so that the position drift occurs. In Figure 3.10, during steady state contact with the environment, the velocities of the master and slave motors are zero. Therefore, the bias term $b\dot{x}_m(s)$ acts as a damping element to guarantee the accurate force tracking of system B. However, the bias term also leads to large position drift as shown in Figure 3.10C. Compared with these two systems, since the wave-based reflections are reduced and the bias terms of the modified wave transform controllers are compensated by the controllers in the master side and slave side, both of the trajectory tracking and force tracking of the proposed 4-CH system have better performance as shown in Figure 3.11.

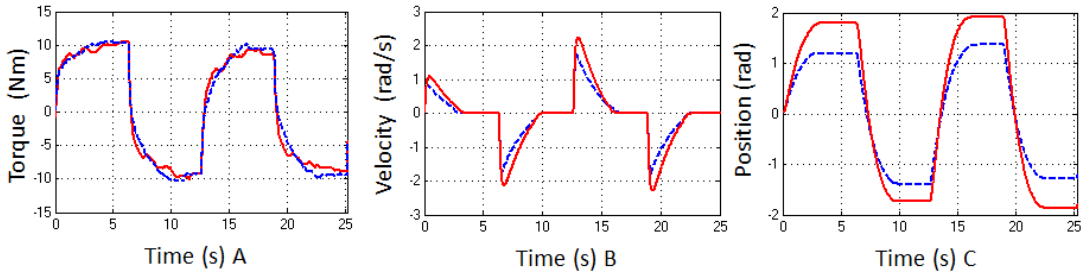

Figure 3.9. Hard environmental contact of the system A: A. Force tracking of master and slave motor, B. Velocity tracking of the master and slave motor, C. Position tracking of the master and slave motor (red curved-master, blue dotted-slave)

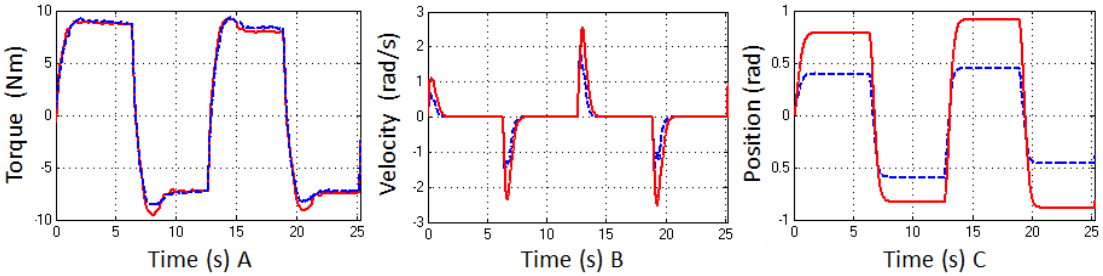

Figure 3.10. Hard environmental contact of the system B: A. Force tracking of master and slave motor, B. Velocity tracking of the master and slave motor, C. Position tracking of the master and slave motor (red curved-master, blue dotted-slave)

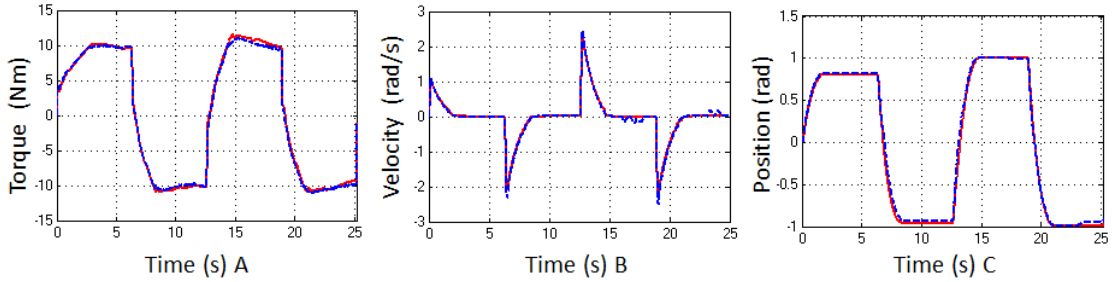

Figure 3.11. Hard environmental contact of the proposed 4-CH system: A. Force tracking of master and slave motor, B. Velocity tracking of the master and slave motor, C. Position tracking of the master and slave motor (red curved-master, blue dotted-slave)

3.3.4.3 High Frequency Environmental Contact

In this experiment, the human operator motor applies a constant force to the master, and at the same time, the environment motor applies an opposite force with high frequency vibration to the slave.

As shown in Figure 3.12, due to the limited bandwidth, the high frequency force signals from the environment is seriously degraded by the low pass filters during the communication channels as shown in Figure 3.12B. Figure 3.13 illustrates the

performance of system B. Since high frequency signal causes vibration in the whole system, large variance occurs in the velocities of the three systems (Figures 3.12C, 3.13C and 3.14C). Accordingly, the bias term $b\dot{x}_m(s)$ enlarges and distorts the master force signals of system B as shown in Figures 3.13A and 3.13B. Compared with these two systems, without using wave filtering, the proposed system has a satisfactory high frequency information transmission ability since accurate high frequency force tracking is achieved without distortion, magnification or degradation as shown in Figures 3.14A and 3.14B. Figures 3.14C and 3.14D illustrate that in spite of transmitting high frequency signals, the trajectory tracking performance of the proposed 4-CH system is not adversely affected by the high frequency perturbation.

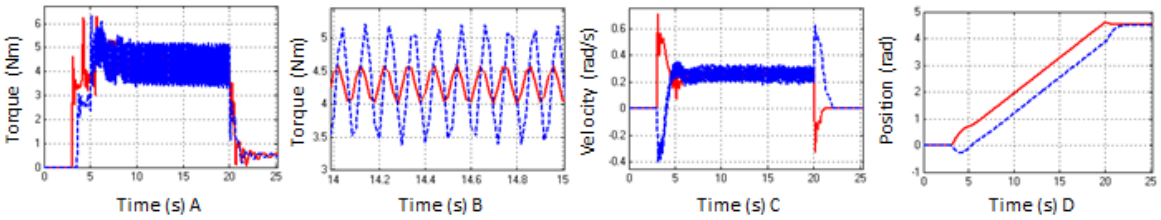

Figure 3.12. High frequency environmental contact of the system A: A. Force tracking of master and slave motor, B. Magnified drawing of the force signals C. Velocity tracking of the master and slave motor, D. Position tracking of the master and slave motor (red curved-master, blue dotted-slave)

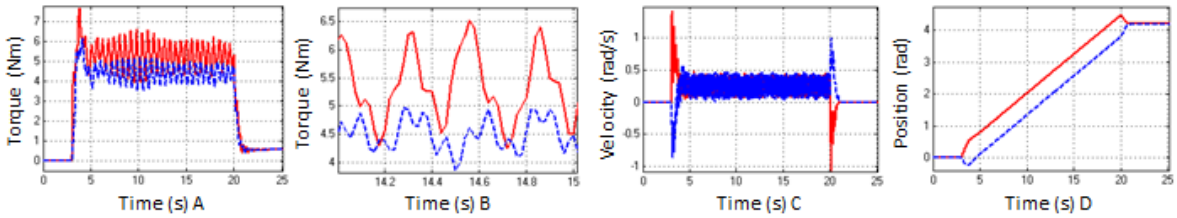

Figure 3.13. High frequency environmental contact of the system B: A. Force tracking of master and slave motor, B. Magnified drawing of the force signals, C. Velocity tracking of the master and slave motor, D. Position tracking of the master and slave motor (red curved-master, blue dotted-slave)

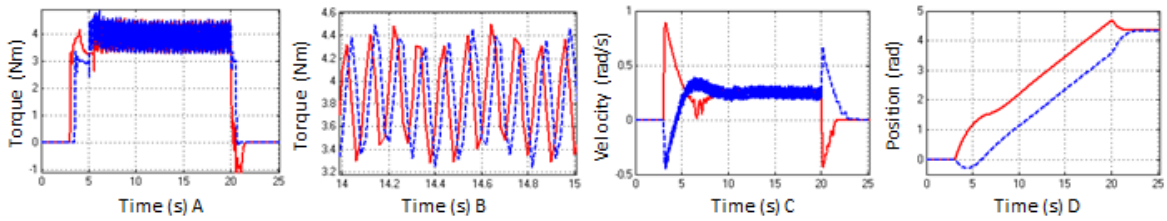

Figure 3.14. High frequency environmental contact of the proposed 4-CH architecture: A. Force tracking of master and slave motor, B. Magnified drawing of the force signals, C. Velocity tracking of the master and slave motor, D. Position tracking of the master and slave motor (red curved-master, blue dotted-slave)

The experimental results strongly confirm the effectiveness of the proposed 4-CH system in achieving an optimal trade-off between stability and transparency by reducing the wave-variable-based reflections. Furthermore, the experiment results for different environment situations (free space movement, hard environmental contact and high frequency environmental contact) also illustrate that compared with systems A and B, the proposed 4-CH system has superior performance in complex, unknown environment.

3.4 Proposed Architecture for the Non-linear System under Time-varying Delays

3.4.1 Modeling the n-DOF Teleoperation System

In Chapter 3.4, the proposed wave transformation architecture is extended to the non-linear teleoperation system in the presence of time-varying delays. The local (master) and the remote (slave) robots are modeled as a pair of n-DOF serial links with revolute joints. Their corresponding nonlinear dynamics are modeled as:

$$M_m(q_m)\ddot{q}_m + C_m(q_m, \dot{q}_m)\dot{q}_m + g_m(q_m) = \tau_m + \tau_h \tag{3.37}$$

$$M_s(q_s)\ddot{q}_s + C_s(q_s, \dot{q}_s)\dot{q}_s + g_s(q_s) = \tau_s - \tau_e \tag{3.38}$$

where $i = m, s$ for the master and slave. $\ddot{q}_i$, $\dot{q}_i$, $q_i \in R^n$ are the joint acceleration, velocity and position, respectively. $M_i(q_i) \in R^{n\times n}$ are the inertia matrices,

$C_i(q_i, \dot{q}_i) \in R^{n\times n}$ are Coriolis/centrifugal effects. $g_i(q_i) \in R^n$ are the vectors of gravitational forces and τ_i are the control signals. In addition, the forces exerted on the end-effector of the master and slave robots are related to equivalent torques in their joints by:

$$F_h = J_m \tau_h, F_e = J_s \tau_e \tag{3.39}$$

where J_i is the Jacobean of the robots and F_j stand for the human and environment forces, respectively. Important properties of the above nonlinear dynamic model, which will be used in this thesis, are as follows [151], [152]:

P1: The inertia matrix $M_i(q_i)$ for a manipulator is symmetric positive-definite which verifies: $0 < \sigma_{min}\left(M_i(q_i(t))\right) I \leq M_i(q_i(t)) \leq \sigma_{max}\left(M_i(q_i(t))\right) I \leq \infty$, where $I \in R^{n\times n}$ is the identity matrix. σ_{min} and σ_{max} denote the strictly positive minimum (maximum) eigenvalue of M_i for all configurations q_i.

P2: Under an appropriate definition of the Coriolis/centrifugal matrix, the matrix $\dot{M}_i - 2C_i$ is skew symmetric, which can also be expressed as:

$$\dot{M}_i(q_i(t)) = C_i(q_i(t), \dot{q}_i(t)) + C_i^T(q_i(t), \dot{q}_i(t)) \tag{3.40}$$

P3: The Lagrangian dynamics are linearly parameterizable:

$$M_i(q_i)\ddot{q}_i + C_i(q_i, \dot{q}_i)\dot{q}_i + g_i(q_i) = Y_i(q_i, \dot{q}_i, \ddot{q}_i)\theta_i \tag{3.41}$$

where θ_i is a constant p-dimensional vector of inertia parameters and $Y_i(q_i, \dot{q}_i, \ddot{q}_i) \in R^{n\times p}$ is the matrix of known functions of the generalized coordinates and their higher derivatives.

P4: For a manipulator with revolute joints, there exists a positive *L* bounding the Coriolis/centrifugal matrix as:

$$\left\| C_i\left(q_i(t), x(t)\right) y(t) \right\|_2 \leq L \|x(t)\|_2 \|y(t)\|_2 \tag{3.42}$$

P5: The time derivative of $C_i(q_i(t), \dot{q}_i(t))$ is bounded if $q_i(t)$ and $\dot{q}_i(t)$ are bounded.

3.4.2 Modified Wave Transformation

In this Sub-section, the proposed modified wave transformation schemes in Figure 3.2 is further extended as shown in Figure 3.15. Its major purpose is to reduce the wave reflection, enhance the accuracy of signals transmission and meanwhile guarantee the communication channels' passivity.

The two wave-based schemes are applied to encode the feed-forward signals V_{A1} and V_{B1} with the feedback signals Z_{A2} and Z_{B2}, where $V_{A1}(t) = D_1\tau_{th}(t)$, $V_{B1}(t) = \beta\big(\dot{q}_m(t) + \delta q_m(t)\big)$, $Z_{A2}(t) = -\beta(\dot{q}_s(t) + \delta q_s(t))$, $Z_{B2}(t) = D_2\tau_{te}(t)$. $D_{1,2}$, β, δ are diagonal positive-definite matrices. τ_{th} and τ_{te} are the measured human and environmental torques. The wave variables in the two schemes are defined as follows:

$$u_{m1}(t) = \frac{bV_{A1}(t) + \frac{\epsilon}{\lambda}Z_{A2}\big(t - T_2(t)\big)}{\sqrt{2b}}, u_{s1}(t) = \frac{bV_{A2}(t) + \frac{1}{\lambda}Z_{A2}(t)}{\sqrt{2b}} \tag{3.43}$$

$$v_{m1}(t) = \frac{Z_{A2}(t - T_2(t))}{\sqrt{2b}}, v_{s1}(t) = \frac{Z_{A2}(t)}{\sqrt{2b}} \tag{3.44}$$

$$u_{m2}(t) = \frac{bV_{B1}(t)}{\sqrt{2b}}, u_{s2}(t) = \frac{bV_{B1}(t - T_1(t))}{\sqrt{2b}} \tag{3.45}$$

$$v_{m2}(t) = \frac{\frac{b}{\lambda}V_{B1}(t) - Z_{B1}(t)}{\sqrt{2b}}, v_{s2}(t) = \frac{\frac{\epsilon b}{\lambda}V_{B1}(t - T_1(t)) - Z_{B2}(t)}{\sqrt{2b}} \tag{3.46}$$

where b and λ are the characteristic impedances, and $T_1(t)$ and $T_2(t)$ are the time-varying delays. $\epsilon = \sqrt{1 - \varepsilon}$. ε is the estimated upper bounds of $\dot{T}_{MAX}$ where $T_{MAX}(t) = T_1(t) + T_2(t)$. In this analysis, the time-varying delays are assumed not to increase or decrease faster than time itself, i.e. $|\dot{T}_{1,2}(t)| < 1$. Thus, the estimated upper bound ε is limited to be $0 \leq \varepsilon \leq 1$. Therefore, $0 \leq \epsilon = \sqrt{1 - \varepsilon} \leq 1$.

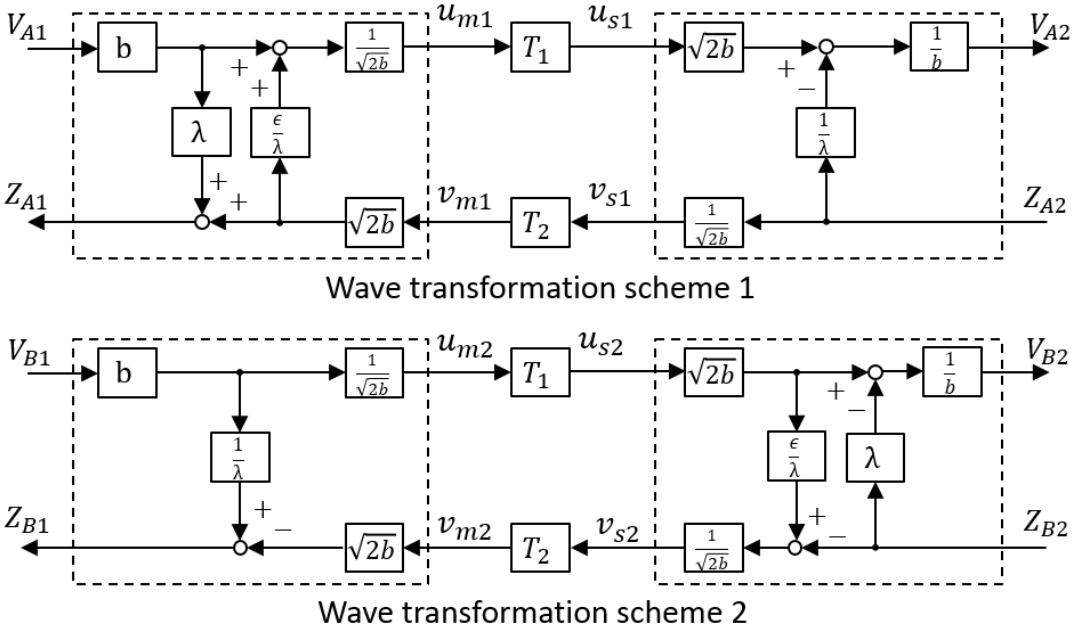

Figure 3.15. Modified wave variable transformation

Based on (3.43)-(3.46), the hybrid matrix H of the two schemes can be written as (3.47) and (3.48) in frequency domain, where H^A and H^B are the hybrid matrix of scheme 1 and 2, respectively.

$$\begin{bmatrix} Z_{A1}(s) \\ -V_{A2}(s) \end{bmatrix} = \begin{bmatrix} H_{11}^{A}(s) & H_{12}^{A}(s) \\ H_{21}^{A}(s) & H_{22}^{A}(s) \end{bmatrix} \begin{bmatrix} V_{A1}(s) \\ Z_{A2}(s) \end{bmatrix}$$

$$= \begin{bmatrix} b\lambda & e^{-sT_2} \\ -e^{-sT_1} & \frac{1}{b\lambda}\left[1 - \epsilon e^{-s(T_1+T_2)}\right] \end{bmatrix} \begin{bmatrix} V_{A1}(s) \\ Z_{A2}(s) \end{bmatrix} \quad (3.47)$$

$$\begin{bmatrix} Z_{B1}(s) \\ -V_{B2}(s) \end{bmatrix} = \begin{bmatrix} H_{11}^{B}(s) & H_{12}^{B}(s) \\ H_{21}^{B}(s) & H_{22}^{B}(s) \end{bmatrix} \begin{bmatrix} V_{B1}(s) \\ Z_{B2}(s) \end{bmatrix}$$

$$= \begin{bmatrix} \frac{b}{\lambda}\left[1 - \epsilon e^{-s(T_1+T_2)}\right] & e^{-sT_2} \\ -e^{-sT_1} & \frac{\lambda}{b} \end{bmatrix} \begin{bmatrix} V_{B1}(s) \\ Z_{B2}(s) \end{bmatrix} \quad (3.48)$$

Based on (2.11), A teleoperation system is defined to be passive, if and only if the norm of the scattering matrix S(s) is equal to or less than one. Substituting (3.47) and (3.48) into (2.11), the angular frequency ω ($s = j\omega$) of the time delay component

$e^{-sT_{1,2}}$ influences the value of the scattering norm ||S||. The scattering norm ||S|| for the scheme 1 and 2 are derived as:

$$\|S\| \; for \; scheme1 = \frac{|2b\lambda e^{-sT_{1,2}}| + \left|\lambda^2 b^2 + (\epsilon e^{-s(T_1+T_2)} - 1) + b\lambda(1-\epsilon)e^{-s(T_1+T_2)}\right|}{|2b\lambda + \lambda^2 b^2 + 1 - \epsilon e^{-s(T_1+T_2)} + b\lambda(1-\epsilon)e^{-s(T_1+T_2)}|} \tag{3.49}$$

$$\|S\| \; for \; scheme2 = \frac{|2b\lambda e^{-sT_{1,2}}| + \left|\lambda^2 - b^2 + b^2\epsilon e^{-s(T_1+T_2)} - b\lambda(1-\epsilon)e^{-s(T_1+T_2)}\right|}{|2b\lambda + \lambda^2 + b^2 - b^2\epsilon e^{-s(T_1+T_2)} + b\lambda(1-\epsilon)e^{-s(T_1+T_2)}|} \tag{3.50}$$

According to the characteristic of the time delay element $e^{-sT_{1,2}}$

$$|e^{-sT_{1,2}}| = 1 \tag{3.51}$$

Applying (3.51), (3.49) and (3.50) can be simplified as:

$$\|S\| \; for \; scheme1 = \frac{|2b\lambda| + |\lambda^2 b^2 + (\epsilon - 1) + b\lambda(1-\epsilon)|}{|2b\lambda + \lambda^2 b^2 + 1 - \epsilon + b\lambda(1-\epsilon)|} \leq 1 \tag{3.52}$$

$$\|S\| \; for \; scheme2 = \frac{|2b\lambda| + |\lambda^2 - b^2 + b^2\epsilon - b\lambda(1-\epsilon)|}{|2b\lambda + \lambda^2 + b^2 - b^2\epsilon + b\lambda(1-\epsilon)|} \leq 1 \tag{3.53}$$

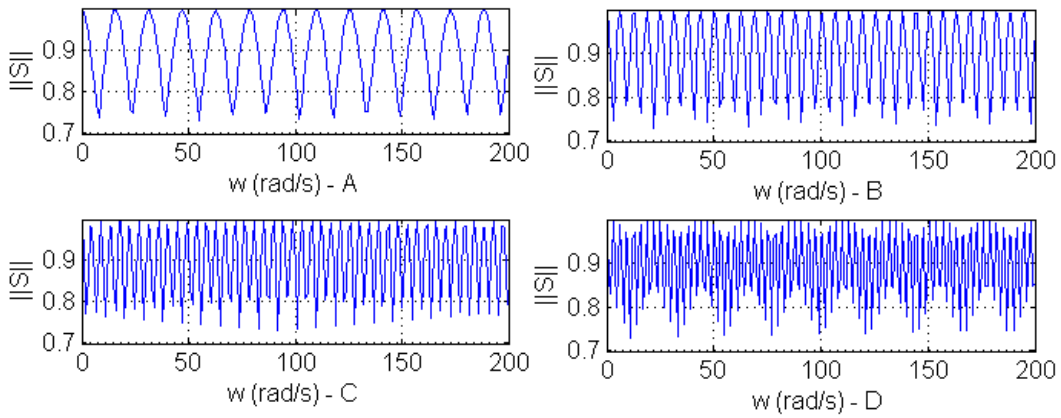

Figure 3.16. Scattering norm of scheme 1 with different time delays: A. 200 ms, B. 500 ms, C. 700 ms, D. 1s. ($b = 2.5\ \lambda = 2.5\ \epsilon = 1$)

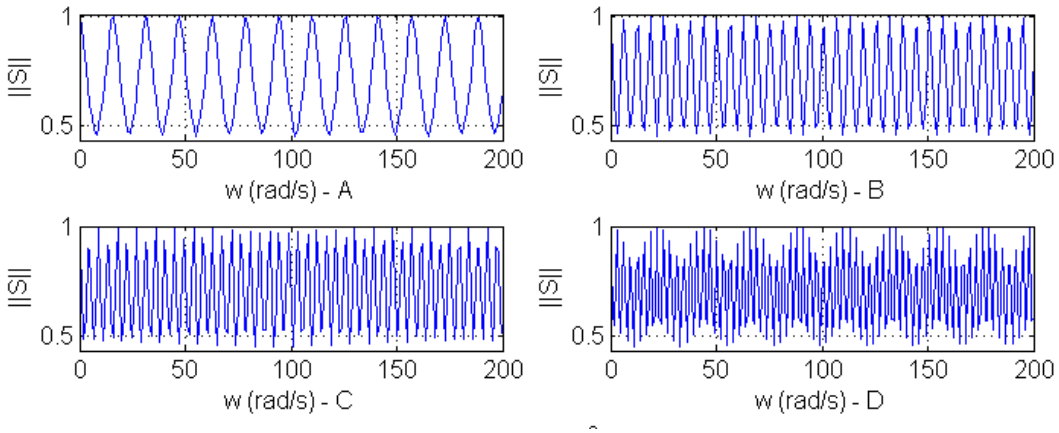

Figure 3.17. Scattering norm of scheme 2 with different time delays: A. 200 ms, B. 500 ms, C. 700 ms, D. 1s. ($b = 2.5\ \lambda = 2.5\ \epsilon = 1$)

Noting b and λ are positive and $0 \leq \epsilon \leq 1$, $\|S\|$ in (3.52) and (3.53) is no larger than 1. From (3.51), the value of $e^{-sT_{1,2}}$ is periodically changing with time delays. Therefore, the periodicity of $e^{-sT_{1,2}}$ determines that the scattering norm $\|S\|$ is also periodic. Since the angular frequency can be considered as a factor of the product of $\omega T_{1,2}$, $T_{1,2}$ can be treated as the gains of the angular frequency to influence the scattering norm by which the scattering norm $\|S\|$ can be extended or compressed periodically. Hence, the changing values of the scattering norm $\|S\|$ with varying ω are shown in Figures 3.16 and 3.17. The values of time delays only affect the waveforms' frequency rather than the magnitude of the scattering norm through setting the impedances b and λ as positive constants. The vertex of the scattering norm remains unchanged which is no more than 1. Therefore, the passivity of the communication channels can be guaranteed.

By applying the proposed wave transformation, the energy information such as torque, position and velocity signals can be transmitted through the communication channels without influencing the channel passivity. The control block diagram is shown as Figure 3.18.

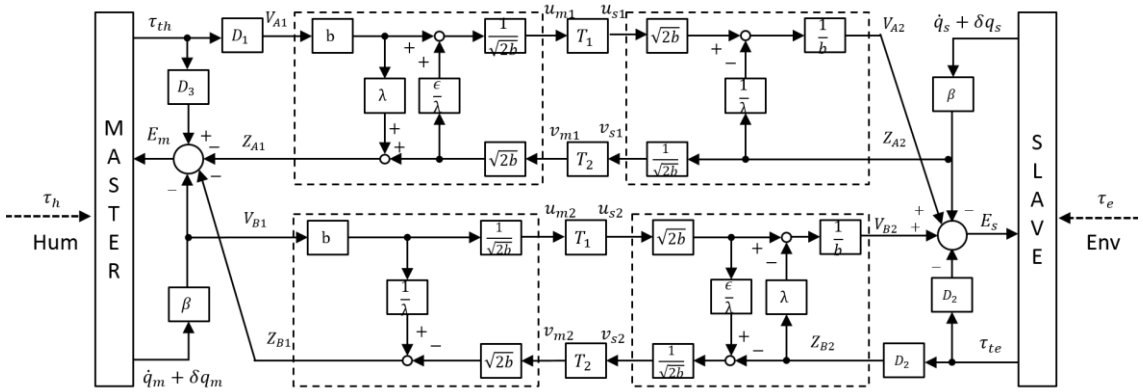

Figure 3.18. Control block diagram of the system applying the modified wave transformation

The control terms E_m and E_s are introduced as follows:

$$
\begin{aligned}
E_m(t) &= D_3\tau_{th}(t) - Z_{A1}(t) - Z_{B1}(t) - \beta\big(\dot{q}_m(t) + \delta q_m(t)\big) \\
&= (D_3 - b\lambda D_1)\tau_{th}(t) - D_2\tau_{te}\big(t - T_2(t)\big) \\
&+ \beta\left(\dot{q}_s\big(t - T_2(t)\big) + \delta q_s\big(t - T_2(t)\big)\right) - \beta\big(\dot{q}_m(t) + \delta q_m(t)\big) \\
&- \Bigg(\frac{b}{\lambda}\beta\big(\dot{q}_m(t) + \delta q_m(t)\big) \\
&- \frac{\epsilon b}{\lambda}\,\beta\left(\dot{q}_m\left(t - T_1(t) - T_2\big(t - T_1(t)\big)\right)\right. \\
&\left. + \delta q_m\left(t - T_1(t) - T_2\big(t - T_1(t)\big)\right)\right)\Bigg)
\end{aligned}
\tag{3.54}
$$

$$E_s(t) = V_{A2}(t) + V_{B2}(t) - D_4\tau_{te}(t) - \beta\big(\dot{q}_s(t) + \delta q_s(t)\big) = D_1\tau_{th}\big(t - T_1(t)\big)$$
$$- \Big(\frac{\lambda D_2}{b} - D_4\Big)\tau_{te}(t) + \beta\Big(\dot{q}_m\big(t - T_1(t)\big) + \delta q_m\big(t - T_1(t)\big)\Big)$$
$$- \beta\big(\dot{q}_s(t) + \delta q_s(t)\big)$$
$$- \Bigg(\frac{\beta}{b\lambda}\big(\dot{q}_s(t) + \delta q_s(t)\big)$$
$$- \frac{\epsilon\beta}{b\lambda}\Big(\dot{q}_s\Big(t - T_2(t) - T_1\big(t - T_2(t)\big)\Big)$$
$$+ \delta q_s\Big(t - T_2(t) - T_1\big(t - T_2(t)\big)\Big)\Big)\Bigg) \tag{3.55}$$

where $D_{3,4}$ are diagonal positive-definite matrices. By defining new variables:

$$r_i(t) = \dot{q}_i(t) + \delta q_i(t) \tag{3.56}$$

(3.54) and (3.55) can be simplified as (3.57) and (3.58).

$$E_m(t) = \beta\Big(r_s\big(t - T_2(t)\big) - r_m(t)\Big) + \Big((D_3 - b\lambda D_1)\tau_{th}(t) - D_2\tau_{te}\big(t - T_2(t)\big)\Big)$$
$$- \frac{b}{\lambda}\beta\big(r_m(t) - \epsilon r_m(t - T_1(t) - T_2(t - T_1(t)))\big) \tag{3.57}$$

$$E_s(t) = \beta\Big(r_m\big(t - T_1(t)\big) - r_s(t)\Big) + \Bigg(D_1\tau_{th}\big(t - T_1(t)\big) - \Big(\frac{\lambda D_2}{b} - D_4\Big)\tau_{te}(t)\Bigg)$$
$$- \frac{\beta}{b\lambda}\Big(r_s(t) - \epsilon r_s\Big(t - T_2(t) - T_1\big(t - T_2(t)\big)\Big)\Big) \tag{3.58}$$

The main aim of the control laws is to provide a stable system with accurate position tracking and to enhance the force tracking during manipulations. The first terms in bracket of (3.57) and (3.58) represent accurate position transmissions. By setting $D_3 - b\lambda D_1 = D_2$ and $D_1 = \frac{\lambda D_2}{b} - D_4$, accurate force tracking can also be achieved. When the rate of the time delay is small, the third terms in bracket of (3.57) and (3.58) can be ignored. When large time-varying delays exist, these two biased terms can adversely influence the tracking accuracy. Properly enhancing the value of λ can

increase the system transparency. However, these two terms are necessary for system stability and cannot be cancelled, which will be analyzed later.

The accurate position tracking is derived if

$$\lim_{t\to\infty}\left\|q_m\left(t-T_1(t)\right)-q_s(t)\right\|=\lim_{t\to\infty}\left\|\dot{q}_m\left(t-T_1(t)\right)-\dot{q}_s(t)\right\|=0 \qquad (3.59)$$

$$\lim_{t\to\infty}\left\|q_s\left(t-T_2(t)\right)-q_m(t)\right\|=\lim_{t\to\infty}\left\|\dot{q}_s\left(t-T_2(t)\right)-\dot{q}_m(t)\right\|=0 \qquad (3.60)$$

We define the coordination position and velocity errors between the master and slave manipulators as follows:

$$e_{pm}(t)=q_m\left(t-T_1(t)\right)-q_s(t), e_{vm}(t)=\dot{q}_m\left(t-T_1(t)\right)-\dot{q}_s(t) \qquad (3.61)$$

$$e_{ps}(t)=q_s\left(t-T_2(t)\right)-q_m(t), e_{vs}(t)=\dot{q}_s\left(t-T_2(t)\right)-\dot{q}_m(t) \qquad (3.62)$$

Combining the control terms (3.57)-(3.58) with the robots' dynamics, the new control laws are designed as follows:

$$\tau_m=E_m-\widehat{M}_m(q_m)\{\delta\dot{q}_m\}-\hat{C}_m(q_m,\dot{q}_m)\{\delta q_m\}+\hat{g}_m(q_m) \qquad (3.63)$$

$$\tau_s=E_s-\widehat{M}_s(q_s)\{\delta\dot{q}_s\}-\hat{C}_s(q_s,\dot{q}_s)\{\delta q_s\}-\hat{g}_s(q_s) \qquad (3.64)$$

where $\widehat{M}_i(q_i)$, $\hat{C}_i(q_i,\dot{q}_i)$, $\hat{g}_i(q_i)$ are the estimates of $M_i(q_i)$, $C_i(q_i,\dot{q}_i)$, $g_i(q_i)$. Substituting (3.63) and (3.64) into (3.37) and (3.38) and considering Property 3 which states that the dynamics are linearly parameterizable, the new system dynamics is expressed as:

$$M_m(q_m)\dot{r}_m+C_m(q_m,\dot{q}_m)r_m=E_m+\tau_h-Y_m\tilde{\theta}_m \qquad (3.65)$$

$$M_s(q_s)\dot{r}_s+C_s(q_s,\dot{q}_s)r_s=E_s-\tau_e-Y_s\tilde{\theta}_s \qquad (3.66)$$

where $\tilde{\theta}_i(t)=\theta_i-\hat{\theta}_i(t)$. $\hat{\theta}_i$ are the estimates of the manipulators' actual constant p-dimensional inertial parameters given by θ_i. $\tilde{\theta}_i$ are the estimation errors. Let the estimates of the uncertain parameters evolve as:

$$\dot{\hat{\theta}}_m(t) = \psi Y_m^T(q_m, r_m) r_m(t), \dot{\hat{\theta}}_s(t) = \Lambda Y_s^T(q_s, r_s) r_s(t) \tag{3.67}$$

where ψ and Λ are constant positive definite matrices.

3.4.3 Stability Analysis on Passive/Non-passive External Force

Passive Human and Environmental forces:

Assumption 1: The human and environment are passive and can be modeled as (3.68) and (3.69) which contain positions, velocities and accelerations.

$$\tau_h(t) = -\alpha_m r_m(t) - \alpha'_m \dot{r}_m(t) \tag{3.68}$$

$$\tau_e(t) = \alpha_s r_s(t) + \alpha'_s \dot{r}_s(t) \tag{3.69}$$

where α_m, α'_m, α_s and α'_s are positive constants. However, since acceleration signals with noises may significantly influence stability. Therefore, we use the extended active observer [137] to measure forces for transmission, which only contain position and velocity signals. That is:

$$\tau_{th}(t) = -\alpha_m r_m(t) \tag{3.70}$$

$$\tau_{te}(t) = \alpha_s r_s(t) \tag{3.71}$$

Theorem 3.1. Consider the teleoperator in (3.65)-(3.66), controlled by (3.57)-(3.58). When the human and environmental forces satisfy (3.68)-(3.71), velocities, positions and the errors of positions and velocities are bounded, i.e. $\{q_i(t),\ r_i(t),\ \dot{q}_i(t),\ r_s(t - T_2(t)) - r_m(t),\ r_s(t - T_2(t)) - r_m(t)\} \in L_\infty \cap L_2$, $\{e_{pm}(t), e_{ps}(t), e_{vm}(t), e_{vs}(t)\} \in L_\infty$ Moreover, during free space movement $\tau_h(t) = \tau_e(t) = 0$, velocities asymptotically converge to zero and position tracking is achieved: $\lim_{t\to\infty} \|q_m(t - T_1(t)) - q_s(t)\| = \lim_{t\to\infty} \|q_s(t - T_2(t)) - q_m(t)\| = 0$.

Proof.

Consider a positive semi-definite function $V(q_i, \dot{q}_i, t)$ for the system as:

$$V = \frac{1}{2}\left[r_m^T(t)M_m(q_m)r_m(t) + r_s^T(t)M_s(q_s)r_s(t) + \tilde{\theta}_m^T\Gamma^{-1}\tilde{\theta}_m + \tilde{\theta}_s^T\Lambda^{-1}\tilde{\theta}_s\right]$$
$$+ \frac{\beta}{2}\frac{1}{1-\dot{T}_1(t)}\int_{t-T_1(t)}^{t} r_m^T(\eta)r_m(\eta)d\eta$$
$$+ \frac{\beta}{2}\frac{1}{1-\dot{T}_2(t)}\int_{t-T_2(t)}^{t} r_s^T(\eta)r_s(\eta)d\eta$$
$$+ \frac{b\beta}{2\lambda}\int_{t-T_1(t)-T_2\left(t-T_1(t)\right)}^{t} r_m^T(\eta)r_m(\eta)d\eta$$
$$+ \frac{\beta}{2b\lambda}\int_{t-T_1(t)-T_2(t-T_1(t))}^{t} r_s^T(\eta)r_s(\eta)d\eta + r_m^T(t)\alpha_m'\delta r_m(t)$$
$$+ r_s^T(t)\alpha_s'r_s(t) + q_m^T(t)\alpha_m\delta q_m(t) + q_s^T(t)\alpha_s\delta q_s(t)$$
$$+ \frac{(D_3 - b\lambda D_1)\alpha_m}{2}\int_{t-T_1}^{t} r_m^T(\eta)\, r_m(\eta)d\eta$$
$$+ \frac{\left(\frac{\lambda D_2}{b} - D_4\right)\alpha_s}{2}\int_{t-T_2}^{t} r_s^T(\eta)\, r_s(\eta)d\eta \qquad (3.72)$$

Applying property 3 and (3.67), the derivative of V can be written as:

$\dot{\mathrm{V}} = ① + ② + ③$, where

$$① = -\frac{\beta}{2}\left(e_{vm}(t) + \delta e_{pm}(t)\right)^T\left(e_{vm}(t) + \delta e_{pm}(t)\right) - \frac{\beta}{2}\Big(e_{vs}(t) +$$
$$\delta e_{ps}(t)\Big)^T\left(e_{vs}(t) + \delta e_{ps}(t)\right) - \left(\dot{q}_m^T(t)\alpha_m\dot{q}_m(t) + q_m^T(t)\alpha_m\delta^2 q_m(t) +\right.$$
$$\left.\dot{q}_s^T(t)\alpha_s\dot{q}_s(t) + q_s^T(t)\alpha_s\delta^2 q_s(t)\right) \qquad (3.73)$$

$$② = -\left(\frac{\beta b}{2\lambda}\Big(r_m(t) - r_m\big(t - T_1(t) - T_2(t)\big)\Big)^T\Big(r_m(t) - r_m\big(t - T_1(t) - T_2(t)\big)\Big) -\right.$$
$$\left.\frac{\beta}{2}\frac{\dot{T}_1(t)}{1-\dot{T}_1(t)}r_m^T(t)r_m(t)\right) - \left(\frac{\beta}{2b\lambda}\Big(r_s(t) - r_s\left(t - T_1(t) - T_2\big(t - T_1(t)\big)\right)\Big)^T\left(r_s(t) -\right.\right.$$
$$\left.\left.r_s\left(t - T_1(t) - T_2\big(t - T_1(t)\big)\right)\right) - \frac{\beta}{2}\frac{\dot{T}_2(t)}{1-\dot{T}_2(t)}r_s^T(t)r_s(t)\right) \qquad (3.74)$$

$$③ = -\left(\frac{(D_3-b\lambda D_1)\alpha_m}{2} r_m^T(t) r_m(t) + D_2\alpha_s r_m(t) r_s\big(t-T_2(t)\big) + \frac{\left(\frac{\lambda D_2}{b}-D_4\right)\alpha_s\left(1-\dot{T}_2(t)\right)}{2} r_s^T\big(t-T_2(t)\big) r_s\big(t-T_2(t)\big)\right) - \left(\frac{\left(\frac{\lambda D_2}{b}-D_4\right)\alpha_s}{2} r_s^T(t) r_s(t) + D_1\alpha_m r_m\big(t-T_1(t)\big) + \frac{(D_3-b\lambda D_1)\alpha_m\left(1-\dot{T}_1(t)\right)}{2} r_m^T\big(t-T_1(t)\big) r_m\big(t-T_1(t)\big)\right) \quad (3.75)$$

The Lyapunov approach requires $\dot{V}$ is negative semi-definite. According to (3.73), ① is absolutely negative. Since $\big(r_m(t) - r_m(t-T_1(t)-T_2(t-T_1(t)))\big)^T \big(r_m(t) - r_m(t-T_1(t)-T_2(t-T_1(t)))\big)$ and $\big(r_s(t) - r_s(t-T_1(t)-T_2(t-T_1(t)))\big)^T \big(r_s(t) - r_s(t-T_1(t)-T_2(t-T_1(t)))\big)$ can be simplified as $\zeta_1 \mathrm{r_m^T(t) r_m(t)}$ and $\zeta_2 \mathrm{r_s^T(t) r_s(t)}$ where $\zeta_{1,2} \geq 0$. ② can be rewritten as: $② = -\left(\frac{\beta b}{2\lambda}\zeta_1 - \frac{\beta}{2}\frac{\dot{T}_1(t)}{1-\dot{T}_1(t)}\right) r_m^T(t) r_m(t) - \left(\frac{\beta}{2b\lambda}\zeta_2 - \frac{\beta}{2}\frac{\dot{T}_2(t)}{1-\dot{T}_2(t)}\right) r_s^T(t) r_s(t)$. The terms $\frac{\beta b}{2\lambda}\zeta_1 - \frac{\beta}{2}\frac{\dot{T}_1(t)}{1-\dot{T}_1(t)}$ and $\frac{\beta}{2b\lambda}\zeta_2 - \frac{\beta}{2}\frac{\dot{T}_2(t)}{1-\dot{T}_2(t)}$ must be positive. That is:

$$\frac{\zeta_1}{\frac{\lambda}{b}+\zeta_1} \geq \dot{T}_1(t), \frac{\zeta_2}{\frac{1}{b\lambda}+\zeta_2} \geq \dot{T}_2(t) \quad (3.76)$$

Since $\left|\dot{\mathrm{T}}_{1,2}\right| < 1$, by setting $0 < \lambda \leq \mathrm{b}, \mathrm{b} > 1$, ② can be guaranteed to be negative. However, as analyzed, enhancing the value of λ can increase transparency. Therefore, when the time delays are not sharply varying ($\dot{\mathrm{T}}_{1,2}$ are not close to 1), setting $\lambda = \mathrm{b}$ can achieve the optimized trade-off between stability and transparency.

In (3.75), the sufficient conditions for a negative ③ are:

$$\frac{D_2^2}{(D_3 - b\lambda D_1)\left(\frac{\lambda D_2}{b} - D_4\right)} \frac{1}{1-\dot{T}_2} \leq \alpha_s^{-1}\alpha_m \quad (3.77)$$

$$\frac{D_1^2}{(D_3 - b\lambda D_1)\left(\frac{\lambda D_2}{b} - D_4\right)} \frac{1}{1-\dot{T}_1} \leq \alpha_m^{-1}\alpha_s \quad (3.78)$$

As analyzed, setting $D_3 - b\lambda D_1 = D_2$ and $D_1 = \frac{\lambda D_2}{b} - D_4$ can achieve accurate force tracking. In the presence of time-varying delays, increasing the value of D_3 and decreasing the value of D_4 can relax the requirement of (3.74). By satisfying (3.76)-(3.78), $\dot{V}$ is negative and the system stability is guaranteed.

Integrating both sides of (3.73), we get:

$$
\begin{aligned}
+\infty > V(0) \geq V(0) - V(t) \\
&\geq \int_0^t \left(\frac{\beta}{2} \left(e_{vm}(t) + \delta e_{pm}(t) \right)^T \left(e_{vm}(t) + \delta e_{pm}(t) \right) \right. \\
&+ \frac{\beta}{2} \left(e_{vs}(t) + \delta e_{ps}(t) \right)^T \left(e_{vs}(t) + \delta e_{ps}(t) \right) + \dot{q}_m^T(t) \alpha_m \dot{q}_m(t) \\
&\left. + q_m^T(t) \alpha_m \delta^2 q_m(t) + \dot{q}_s^T(t) \alpha_s \dot{q}_s(t) + q_s^T(t) \alpha_s \delta^2 q_s(t) \right) dt \quad (3.79)
\end{aligned}
$$

Since V is positive semi-definite and $\dot{V}$ is negative semi-definite, therefore, $\lim_{t \to \infty} V$ exists and is finite. Thus, $\tilde{\theta}_i(t) \in L_\infty$, $\{e_{pi}(t) + e_{vi}(t),\ q_i(t),\ r_i(t), \dot{q}_i(t)\} \in L_\infty \cap L_2$. Therefore, it is easily derived that $\{q_s(t) - q_m(t), q_m(t) - q_s(t)\} \in L_\infty \cap L_2$, Rewriting $q_m\left(t - T_1(t)\right) - q_s(t)$ as $q_m\left(t - T_1(t)\right) - q_s(t) = q_m(t) - q_s(t) + q_m\left(t - T_1(t)\right) - q_m(t)$, and $q_s\left(t - T_2(t)\right) - q_m(t)$ as $q_s\left(t - T_2(t)\right) - q_m(t) = q_s(t) - q_m(t) + q_s\left(t - T_2(t)\right) - q_s(t)$. Factually, $q_m\left(t - T_1(t)\right) - q_m(t) = -\int_{t - T_1(t)}^{t} \dot{q}_m(\eta) d\eta \leq \sqrt{\max(T_1(t))} \|\dot{q}_m(t)\|_2$ and $q_s\left(t - T_2(t)\right) - q_s(t) = -\int_{t - T_2(t)}^{t} \dot{q}_s(\eta) d\eta \leq \sqrt{\max(T_2(t))} \|\dot{q}_s(t)\|_2$ (using Schwartz's inequality), we can conclude that $e_{ps}(t) = q_s\left(t - T_2(t)\right) - q_m(t)$ and $e_{pm}(t) = q_m\left(t - T_1(t)\right) - q_s(t) \in L_\infty$. Since $e_{pi}(t) + e_{vi}(t) \in L_\infty \cap L_2$ and $e_{pi}(t) \in L_\infty$, it can be seen that $e_{vi}(t) \in L_\infty$.

In free motion, the system's dynamic model (3.65) and (3.66) can also be written as:

$$\ddot{q}_i = M_i^{-1}\left[E_i - Y_i \tilde{\theta}_i - C_i r_i \pm \tau_j\right] - \delta \dot{q}_i \quad (3.80)$$

Differentiating both sides of (3.80):

$$\frac{d}{dt}\ddot{q}_i = \frac{d}{dt}(M_i^{-1})\left[E_i - Y_i\tilde{\theta}_i - C_i r_i \pm \tau_j\right] + M_i^{-1}\frac{d}{dt}\left[E_i - Y_i\tilde{\theta}_i - C_i r_i \pm \tau_j\right] - \delta\ddot{q}_i \tag{3.81}$$

For the first term of the right side of (3.81), we have [153]:

$$\frac{d}{dt}(M_i^{-1}) = -M_i^{-1}\dot{M}_i M_i^{-1} = -M_i^{-1}(C_i + C_i^T)M_i^{-1} \tag{3.82}$$

According to Properties 1 and 4, $\frac{d}{dt}(M_i^{-1})$ is bounded. Based on Property 5, the terms in bracket of (61) are also bounded. Therefore, $\frac{d}{dt}\ddot{q}_i(t) \in L_\infty$ and $\ddot{\mathrm{q}}_\mathrm{i}(\mathrm{t})$ are uniformly continuous ($\int_0^t \ddot{q}_i(\eta)d\eta = \dot{q}_i(t) - \dot{q}_i(0)$). Since $\dot{\mathrm{q}}_\mathrm{i}(\mathrm{t}) \to 0$, it can be concluded that $\ddot{\mathrm{q}}_\mathrm{i}(\mathrm{t}) \to 0$ based on Barbălat's Lemma.

Active Human and Environmental Forces:

Assumption 2: In the case of non-passive human forces and environmental forcer, the human and environment can be modeled as:

$$\tau_h(t) = \alpha_0(t) - \alpha_m r_m(t) - \alpha_m'\dot{r}_m(t) \tag{3.83}$$

$$\tau_e(t) = \alpha_1(t) + \alpha_s r_s(t) + \alpha_s'\dot{r}_s(t) \tag{3.84}$$

$$\tau_{th}(t) = \alpha_0(t) - \alpha_m r_m(t) \tag{3.85}$$

$$\tau_{te}(t) = \alpha_1(t) + \alpha_s r_s(t) \tag{3.86}$$

where $\alpha_0(t)$ and $\alpha_1(t)$ are bounded positive variables, which generate energy as an active term.

Theorem 3.2. The proposed system is stable and all signals in this system are ultimately bounded, when the human and environmental forces satisfy (3.83)-(3.86).

Proof. We define $\bar{x}_c = [q_m, q_s, \dot{q}_m, \dot{q}_s]^T$ and $x_c = [q_m, q_s, r_m, r_s]^T$. There is a linear map between the two vectors [25]:

$$\bar{x}_c = \Gamma_c x_c \tag{3.87}$$

where Γ_c is a non-singular constant matrix. By choosing the previous Lyapunov function V, the new derivative $\dot{V}^*$ can be written as:

$$\dot{V}^* = \dot{V} + r_m^T[(D_3 - b\lambda D_1)\alpha_0 + \alpha_0 - D_2\alpha_1] + r_s^T\left[D_1\alpha_0 - \left(\frac{\lambda D_2}{b} - D_4\right)\alpha_1 - \alpha_1\right] \tag{3.88}$$

Note that

$$r_m^T|(D_3 - b\lambda D_1)\alpha_0 + \alpha_0 - D_2\alpha_1| \le n^T\|x_c\||(D_3 - b\lambda D_1)\alpha_0 + \alpha_0 - D_2\alpha_1| \tag{3.89}$$

$$r_s^T\left|D_1\alpha_0 - \left(\frac{\lambda D_2}{b} - D_4\right)\alpha_1 - \alpha_1\right| \le n^T\|x_c\|\left|D_1\alpha_0 - \left(\frac{\lambda D_2}{b} - D_4\right)\alpha_1 - \alpha_1\right| \tag{3.90}$$

Therefore (3.88) can be rewritten as:

$$\dot{V}^* \le \dot{V} + 2\|x_c\|a_c \tag{3.91}$$

where $a_c = n^T\left(|(D_3 - b\lambda D_1)\alpha_0 + \alpha_0 - D_2\alpha_1| + \left|D_1\alpha_0 - \left(\frac{\lambda D_2}{b} - D_4\right)\alpha_1 - \alpha_1\right|\right) > 0$. (3.92) is true:

$$\begin{aligned}\dot{V} &\le -\left(\dot{q}_m^T(t)\alpha_m\dot{q}_m(t) + q_m^T(t)\alpha_m\delta^2 q_m(t) + \dot{q}_s^T(t)\alpha_s\dot{q}_s(t) + q_s^T(t)\alpha_s\delta^2 q_s(t)\right)\\ &\le -\Upsilon_c\|\bar{x}_c\|^2\end{aligned} \tag{3.92}$$

where Υ_c is the smallest eigenvalue of α_m, $\alpha_m\delta^2$, α_s, $\alpha_s\delta^2$. Substituting (3.92) into (3.91) and $0 < \mu_c < 1$:

$$\begin{aligned}\dot{V}^* &\le -\Upsilon_c\|\bar{x}_c\|^2 + 2\|\bar{x}_c\|\\ &= -\Upsilon_c(1-\mu_c)\|\Gamma_c\|^2\|x_c\|^2 - \Upsilon_c\mu_c\|\Gamma_c\|^2\|x_c\|^2 + 2\|x_c\|\alpha_c\end{aligned} \tag{3.93}$$

(3.93) can be simplified as:

$$\dot{\mathrm{V}}^* \le -\Upsilon_c(1-\mu_c)\|\Gamma_c\|^2\|x_c\|^2, \forall\|\mathrm{x}\| \ge \frac{2\alpha_c}{\Upsilon\mu\|\Gamma\|^2} \tag{3.94}$$

If the values of x are set to be large which satisfy $\|x\| \geq \frac{2\alpha}{\Upsilon\mu\|\Gamma\|^2}$, the derivative $\dot{V}^*$ is negative semi-definite. Hence, x and $\bar{x}$ are bounded, which means r_i, q_i, $\dot{q}_i$ are also bounded.

3.4.4 Sliding Mode Control (SMC)

In (3.65) and (3.66), the existence of the uncertain parameters $Y_i\tilde{\theta}_i$ and the immeasurable elements $\pm\alpha_i'\dot{r}_i(t)$ of the external force τ_j may reduce the system transparency. In this study,a sliding mode control algorithm is applied to compensate for these terms. Adding a sliding-mode control term τ_{ci}, the dynamic models (3.65) and (3.66) can be re-written as (3.95). The aim is to use the sliding mode compensation terms τ_{ci} to omit $-Y_i\tilde{\theta}_i - \alpha_i'\dot{r}_i$ in (3.95).

$$M_i(q_i)\dot{r}_i + C_i(q_i,\dot{q}_i)r_i = E_i + \tau_c - \alpha_i r_i - \alpha_i'\dot{r}_i - Y_i\tilde{\theta}_i \tag{3.95}$$

The proposed algorithm sets the sliding surface ϖ as:

$$\varpi = M_i(q_i)r_i(t) - \int_0^t \left(C_i^T(q_i,\dot{q}_i)r_i(\eta) + E_i(\eta) - \alpha_i r_i(\eta)\right)d\eta \tag{3.96}$$

Using property 2, (3.96) can be expressed as:

$$\varpi = \int_0^t \left(M_i(q_i)\dot{r}_i(\eta) + C_i(q_i,\dot{q}_i)r_i(\eta) - E_i(\eta) + \alpha_i r_i(\eta)\right)d\eta \tag{3.97}$$

Based on (3.95), if the sliding surface ϖ converges to zero, the terms $-\alpha_i'\dot{r}_i(t) - Y_i\tilde{\theta}_i$ can be compensated for by τ_{ci}. Building a Lyapunov function for the sliding mode controller:

$$V_1 = \frac{1}{2}\varpi_m^T\varpi_m + \frac{1}{2}\varpi_s^T\varpi_s \tag{3.98}$$

Therefore, the derivative of (3.98) will result in:

$$\dot{V}_1 = (\tau_{cm} + \alpha'_m \dot{r}_m + Y_m \tilde{\theta}_m)^T \varpi_m + (\tau_{cs} + \alpha'_s \dot{r}_s + Y_s \tilde{\theta}_s)^T \varpi_s \quad (3.99)$$

The sliding control input is designed as:

$$\tau_c = -K_{sliding} \varpi_i - B_{sliding} sig(\varpi_i)^{\Theta} \quad (3.100)$$

where

$sig(\vartheta)^{\Theta} = [|\vartheta_1|^{\Theta_1} sign(\vartheta_1)\ |\vartheta_2|^{\Theta_2} sign(\vartheta_2) \dots\ |\vartheta_n|^{\Theta_n} sign(\vartheta_n)]^T$. $\vartheta = [\vartheta_1\ \vartheta_2 \dots\ \vartheta_n]^T \in R^n$, Θ_1 , Θ_2 , …, $\Theta_n > 0$, and sign(.) is the standard signum function. By tuning $K_{sliding}$ and $B_{sliding}$ as large values, $\dot{V}_1$ is negative semi-definite and ϖ will converge to zero. Therefore, the proposed SMC will not influence the system stability.

Moreover, under the condition of passive human and environmental input, the system of (3.95) with the sliding surface ϖ_i can stay stable in finite time.

Lemma 1 [67]: Consider the dynamics model $\dot{x} = f(x), f(0) = 0$ ($x \in R^n$). If there is a positive-definite scalar function V_1 such that (3.101) is satisfied:

$$\dot{V}_1(x) \leq -AV_1(x) - BV_1^{\Xi}(x) \quad (3.101)$$

Where $A, B > 0$, $0 < \Xi < 1$, the system is finit-time stable, and the settling time satisfy (3.102):

$$T_c \leq \frac{1}{A(1-\Xi)} ln \frac{AV_1^{1-\Xi}(x_0) + B}{B} \quad (3.102)$$

Lemma 2 [67]: Note $l_{1,2} > 0$ and $0 < p < 1$, (3.103) is true:

$$(l_1 + l_2)^p \leq l_1^p + l_2^p \quad (3.103)$$

Reconsider the Lyapunov function V_1 in (3.98) and its derivative is given in (3.99). By choosing large values of $K_{sliding}$ and $B_{sliding}$, there definitely exist positive constants $K'_{sliding}$ and $B'_{sliding}$ so that

$$\left|-K'_{sliding}\varpi_i - B'_{sliding}sig(\varpi_i)^{\varTheta}\right|$$
$$\leq \left|-K_{sliding}\varpi_i - B_{sliding}sig(\varpi_i)^{\varTheta} + \alpha'_i\dot{r}_i + Y_i\tilde{\theta}_i\right| \quad (3.104)$$

Therefore, (3.99) can be rewritten as:

$$\dot{V}_1 = (\tau_{cm} + \alpha'_m\dot{r}_m + Y_m\tilde{\theta}_m)^T\varpi_m + (\tau_{cs} + \alpha'_s\dot{r}_s + Y_s\tilde{\theta}_s)^T\varpi_s$$
$$\leq -K'_{sliding}\varpi_m^T\varpi_m - B'_{sliding}\varpi_m^T sig(\varpi_m)^{\varTheta} - K'_{sliding}\varpi_s^T\varpi_s$$
$$- B'_{sliding}\varpi_s^T sig(\varpi_s)^{\varTheta} \quad (3.105)$$

According to Lemma 1 and 2, we get

$$\dot{V}_1 \leq -2K'_{sliding}V_1 - 2B'_{sliding}V_1^{\frac{1+\varTheta}{2}} \quad (3.106)$$

Therefore, the settling time is derived as:

$$T_c \leq \frac{1}{2K'_{sliding}\left(1-\frac{1+\varTheta}{2}\right)} ln\frac{2K'_{sliding}V_1^{1-\frac{1+\varTheta}{2}}(x_0) + 2B'_{sliding}}{2B'_{sliding}} \quad (3.107)$$

When the system uncertainty is fully eliminated, the system dynamics of (3.95) can be written as:

$$\dot{\varpi}_i(t) = -K'_{sliding}\varpi_i - B'_{sliding}sig(\varpi_i)^{\varTheta} \quad (3.108)$$

where $\varpi_{i0} = \varpi_i(0)$ is the terminal attractor of the system (3.108). Based on [158], the finite time T_s that is taken to travel from $\varpi_i(0)$ to $\varpi_i(0 + T_s)$ is given by

$$T_s = -\frac{1}{K'_{sliding}}\int_{\varpi_{i0}}^{0}\frac{d\varpi_i}{\varpi_i} - \frac{1}{B'_{sliding}}\int_{\varpi_{i0}}^{0}\frac{d\varpi_i}{sig(\varpi_i)^{\varTheta}}$$
$$= \frac{1}{K'_{sliding}}\ln(|\varpi_{i0}|) + \frac{1}{B'_{sliding}(1-\varTheta)}|\varpi_{i0}|^{1-\varTheta} \quad (3.109)$$

Therefore, the stability and synchronization performance of the teleoperation system can be achieved in finite time and the exact convergence time is

$$T_{finite} = T_c + T_s \tag{3.110}$$

3.4.5 Experiment Validation

In this sub-section, a series of experimental results are carried out to validate the proposed nonlinear teleoperation system. The experiments are performed on two 3-DOF Phantom manipulators: Phantom Omni and Phantom Desktop (Sensable Technologies, Inc., Wilmington, MA) as shown in Figure 3.19. The control loop is configured as a 1 kHz sampling rate. The controller parameters are given as: $b = 2.5, \lambda = 2.5, \epsilon = 0.9, D_1 = D_2 = 1, D_3 = 3.5, D_4 = 0.4, \delta = 1, \beta = 2.5, K_{sliding} = B_{sliding} = 1, \Theta = \frac{1}{3}$.

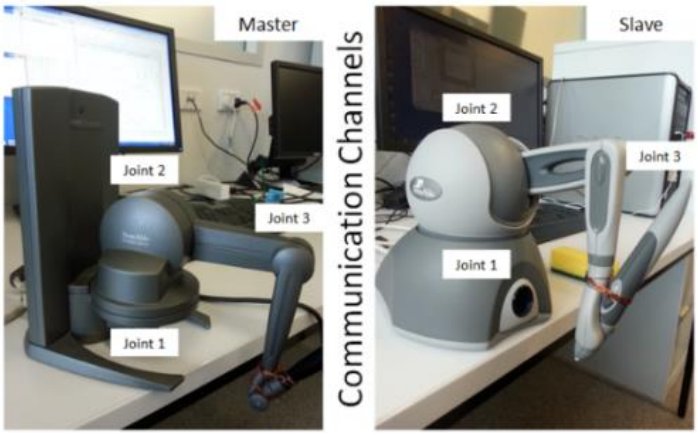

Figure 3.19. Experimental setup

3.4.5.1 Experimental Work using 1-DOF

In this section, the proposed 4-CH wave-based architecture is compared against two linear wave-based systems in the literature, the 4-CH architecture applying the

conventional wave transformation [108] (System A) and the modified wave-based system for reduced

wave reflections [132] (System B). Since the wave-based systems for comparison are stable only under constant delays, this experiment uses a virtual constant time of 300 ms (one way). The experiments are conducted for three scenarios, free space motion, hard contact, and soft contact. The experiments are conducted using joint 1 of the two robots in Figure 3.19. Joint 2 and 3 are fixed which do not influence the experimental results. All gain values for the controllers and dynamics remain unchanged throughout the experiments.

Figure 3.20 shows the velocity and position tracking performances of the three systems in free motion. The position tracking errors in System A is caused by the bias term in (20)

The cut-off frequency of the low-pass filter in System A should be set low to restrict the band-width of the communication channel and suppress the oscillatory behavior caused by wave reflections. By reducing the wave reflections, the signal perturbations are reduced in System B. However, since this system has no direct position information transmission, position drift can slowly occur. Compared with the two systems, the oscillatory behavior caused by wave reflections is eliminated and highly accurate trajectory tracking is achieved in the proposed system.

In the next experiment, the slave robot is controlled by the three wave-based systems to contact with a solid wall from around the 3rd second to the 17th second. In this situation, the speed of the slave robot quickly converges to zero. Figure 3.21 illustrates the torque tracking ($\tau_{th} \leftrightarrow \tau_{te}$) and position tracking performances of the three systems. When contacting the solid wall, even applying low-pass filters, both of position and torque tracking still have small signal variations caused by wave reflections in System A. The biased term in (3.7) also interrupt the system to achieve accurate position tracking even applying the 4-CH architecture. Since the robot has no movement in the steady state, the biased term $b\dot{x}_m(t)$ in (3.5) quickly converges to zero, which does not affect the force tracking of System B. Therefore, accurate force tracking performance can be achieved in System B with little signal variation. Without direct position tracking, large position drift occurs in System B. Unlike the two

systems, the force signals and the trajectory signals of the proposed three-channel system quickly track in the transient state without signals variations and position drift. During the soft environmental contact, the slave robot is controlled by the three wave-based systems in contact with a soft sponge from the 3rd second to the 17th second. In this situation, the slave robot is still moving and its speed slowly converges to zero. Figure 3.22 shows the torque tracking ($\tau_{th} \leftrightarrow \tau_{te}$) and position tracking of the three systems in soft contact. Due to the biased term in (19), System A cannot achieve accurate force tracking and as a result large signal variations still occur. Since the biased term $b\dot{x}_m$ in (3.5) has a large value in this situation, inaccurate force tracking is achieved in System B where the slave robot's force tracks the master robot's force in a very slow speed. The two systems also cannot achieve accurate position tracking during soft contact. Compared with the two systems, in the proposed system, the forces quickly track each other without signal perturbations in the steady state and the high accuracy of position tracking is also achieved.

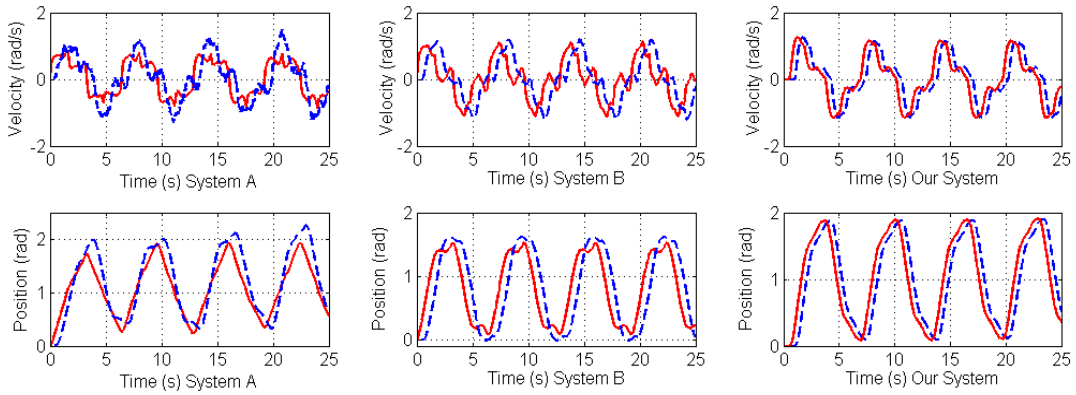

Figure 3.20. Free motion – 1 DOF (red – $\dot{q}_m$ & q_m, blue – $\dot{q}_s$ & q_s)

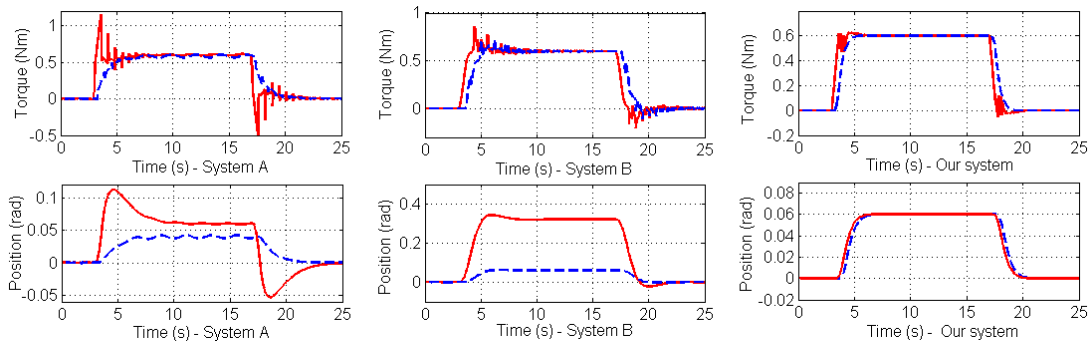

Figure 3.21. Hard contact – 1 DOF (red – τ_{th} & q_m, blue – τ_{te} & q_s)

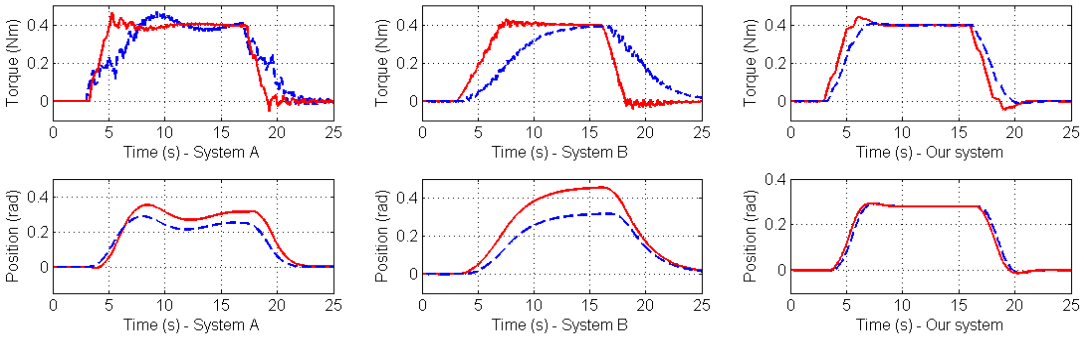

Figure 3.22. Soft contact – 1 DOF (red –τ_{th} & q_m, blue –τ_{te} & q_s)

3.4.5.2 Experimental test using 3-DOF

This Sub-section validates the system's task performance in 3-DOF. Two computers are used to control the two haptic devices and the communication channel is the Internet. The time delay (one way) varies between 440 ms ~ 560 ms. In the first experiment, the performance of our system is compared with the nonlinear wave-based system proposed in [23] (System C) in free motion. System C adds two additional channels for direct position signals transmission to the traditional wave transformation in order to enhance the trajectory tracking in free motion. System C also uses additional velocity dampers to guarantee the system stability under time-varying delays. Figure 3.23 illustrates the torque tracking ($\tau_m \leftrightarrow \tau_{te}$) and position tracking performances of System C, where the control signal τ_m is the feedback torque felt by the operator. Due to the wave reflections, the slave robot's motion varies when

tracking the master robot although the additional direct position signals transmission enhances the accuracy of the trajectory tracking. Moreover, the velocity dampers used to guarantee system stability decrease the system transparency and the operator can still feel feedback torque during free motion. Figure 3.24 shows the torque tracking ($\tau_m \leftrightarrow \tau_{te}$) and position tracking of our system without the proposed SMC. In this system, the wave reflection is eliminated to the extent that the signals do not have the large signals variations. However, due to the parameter uncertainties, the position tracking still has small tracking errors. Moreover, the system using the proposed wave transformation is still damped due to the effect of time delays so that the operator can also feel the feedback torque. By adding the SMC, the control signal fed back to the master robot is no longer τ_m, but the sum of τ_m and the control torque τ_{cm} from the SMC. Figure 3.25 shows the torque tracking ($\tau_m + \tau_{cm} \leftrightarrow \tau_{te}$) and position tracking of our system with the proposed SMC. Since the parameter uncertainties are compensated for by the SMC, highly accurate position tracking can be achieved. The torque felt by the operator is nearly zero as shown in Figure 3.25.

The next experiment demonstrates the ability of the proposed system to deal with the transient environment. Our system is compared with the nonlinear wave-based system [25] (System D). The slave robot is controlled to contact to a "reverse wall" which is like the scenario of a needle puncture as might be experienced in medical applications [154]. Figures 3.26 and 3.27 show the torque tracking ($\tau_{th} - \tau_{te}$) and position tracking of the two systems. The slave start to contact with the remote wall in the 3rd second. After hard contact for several seconds, the wall is suddenly removed in the 8th second allowing the slave end effector to move in free space. System D uses the conventional impedance matching approach to diminish the wave reflections, which works fine in the steady-state environment. However, as analyzed, when the impedance of human and environment suddenly changes, the impedances will mismatch and the wave reflections are reinstated. Therefore, large signals variations and position drift occur as shown in Figure 3.26. Unlike System D, the proposed system with direct position and force transmission is less affected by the unpredictable changes of the human and environmental impedances. Highly accurate force and position tracking are still achieved in the sudden changing environment as shown in Figure 3.27.

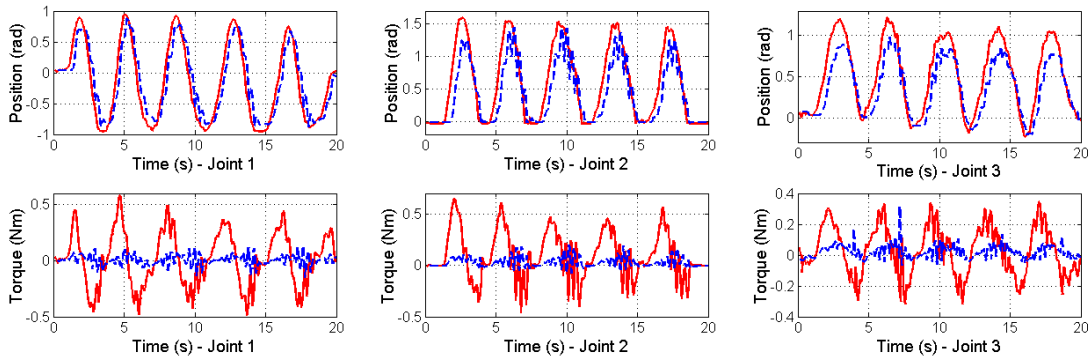

Figure 3.23 Free motion – 3 DOF (System C, red $-q_m$ & τ_m, blue – q_s & τ_{te})

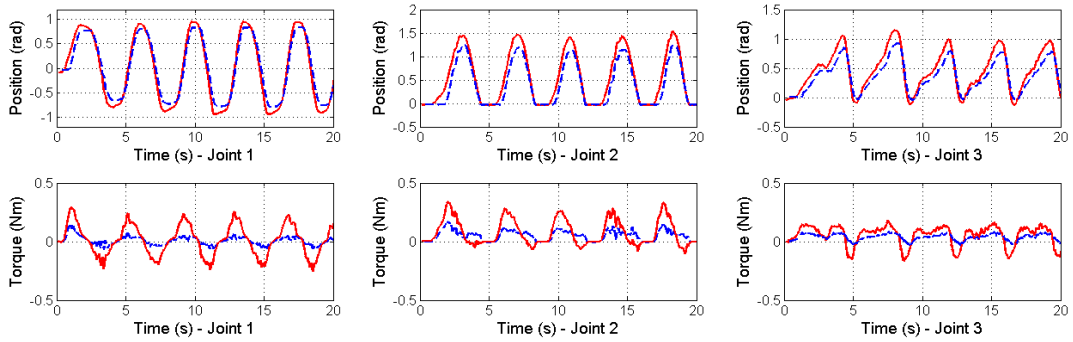

Figure 3.24 Free motion without SMC – 3 DOF (Our system, red $-q_m$ & τ_m, blue – q_s & τ_{te})

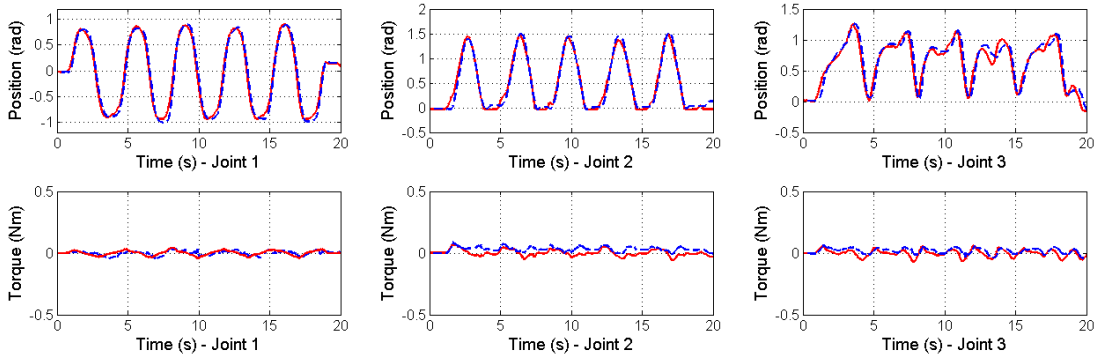

Figure 3.25. Free motion with SMC – 3 DOF (Our system, red $-q_m$ & $(\tau_m + \tau_c)$, blue $-q_s$ & τ_{te})

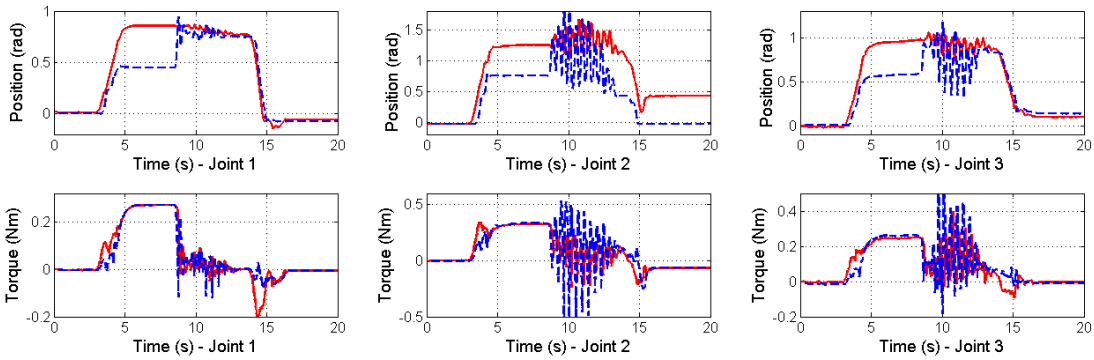

Figure 3.26. Contacting with a reverse wall – 3 DOF (System D, red $-q_m$ & τ_{th}, blue $-q_s$ & τ_{te})

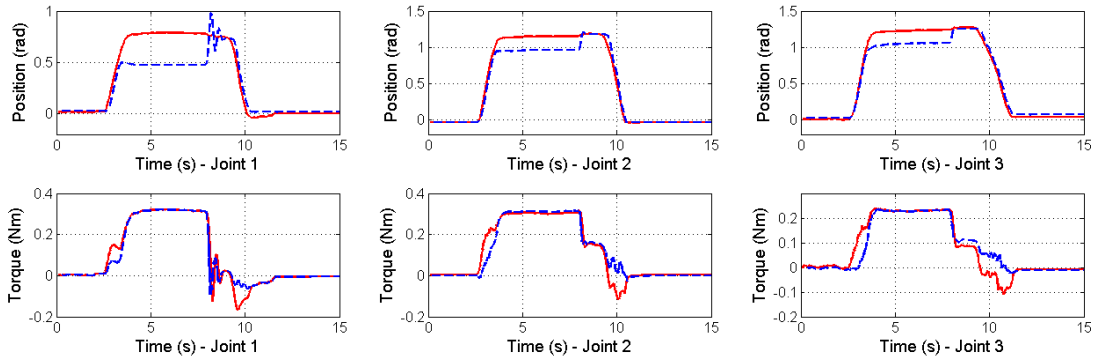

Figure 3.27. Contacting with a reverse wall – 3 DOF (Our system, red $-q_m$ & τ_{th}, blue $-q_s$ & τ_{te})

3.5 Summary

In Chapter 3, a novel wave transformation scheme for reduced wave-based reflections is applied to the 4-CH linear system to achieve high delay-based transparency and simultaneously guarantee system stability at the presence of constant time delays. The proposed wave transformation scheme is also extended to the non-linear teleoperation system to derive high transparency and robust stability in the presence of time-varying delays. A sliding mode control algorithm is also designed to reduce the adverse effect of the internal parameter uncertainties and promote the system synchronization performance in finite time. The delay-based stability and conditions for realizing high

transparency are analytically studied in this chapter. The HILINK microcontroller board with a set of DC motors is applied to conduct the experiment of the linear teleoperation system and the experimental platform consisting of two 3-DOF Phantom manipulators is applied to conduct the experiment of the non-linear teleoperation system. The experimental results for different environment situations confirm that the proposed systems can achieve superior performance over the previous work in achieving the optimal trade-off between transparency and stability in the presence of different time delays.

4 BILATERAL TELEOPREATION SYSTEM WITH WAVE-BASED TDPA

4.1 Introduction

Time Domain Passivity Approach (TDPA) is another passivity-based method for guaranteeing the channel passivity in the presence of time delays. Unlike the conservative wave-based methods [25] that guarantee the time delayed channels' passivity by over-dissipating energy, TDPA, which consists of two main components: a passivity observer and a passivity controller, can adaptively dissipate energy and meanwhile the energy over-dissipation are circumvented [51]. The passivity observer and the passivity controller are used to monitor the system passivity and to dissipate the active energy, respectively. Therefore, higher transparency can be achieved. TDPA was first introduced by Hannaford et al [51] in 2004. This method is extended in [47] to deal with the time-varying delay issues. In [155], this approach is simplified to a power-based TDPA which dissipates energy as soon as any active energy is produced. The power-based TDPA proposed in [155] is extended in [156] to deal with the position drift issues. However, although the above TDPA-based system can guarantee system stability under time-varying delays, transparency degradation is also its main drawback, even in the presence of small constant or no time delay where high transparency can be easily derived by many non-passivity based schemes.

This Chapter introduces an innovative wave-based TDPA applied to a 4-CH nonlinear teleoperation system that can derive higher transparency than previous passivity-based systems in the presence of arbitrary time delays. A PPC system is proposed in combination with an extended wave-based TDPA to restrict the synchronization errors of the position and the velocity of the master and the slave and the measured human and environmental torques, and simultaneously guarantee the passivity of the whole system. Furthermore, a new wave-based TDPA distinct from the original one with new passivity observers and controllers to further improve the whole system's transparency, especially, in the worst cases where large time delays exist and their rate are large than

one. RBF neural network is also applied to deal with the nonlinear system's dynamic uncertainties.

4.2 Review of TDPA

In a conventional TDPA-based control system, the system passivity can be defined as [155], [156]:

$$\begin{aligned} P(t) &= \tau_m(t)\dot{q}_m(t) - \tau_s(t)\dot{q}_s(t) \\ &= \frac{1}{2b}\tau_m^T(t)\tau_m(t) - \frac{1}{2b}\left(\tau_m(t) - b\dot{q}_m(t)\right)^2 + b\dot{q}_s^T(t)\dot{q}_s(t) \\ &\quad - \frac{1}{2b}\left(\tau_s(t) + b\dot{q}_s(t)\right)^2 - \frac{1}{2b}\dot{T}_2(t)\tau_m^T(t)\tau_m(t) - \frac{b}{2}\dot{T}_1(t)\dot{q}_s^T(t)\dot{q}_s(t) \\ &\quad + \frac{dE}{dt} = P_{diss} + \frac{dE}{dt} \end{aligned} \tag{4.1}$$

$$E(t) = \frac{1}{2b}\int_{t-T_2(t)}^{t} \tau_s^T(\eta)\tau_s(\eta)\, d\eta + \frac{b}{2}\int_{t-T_1(t)}^{t} \dot{q}_m^T(\eta)\dot{q}_m(\eta)\, d\eta \tag{4.2}$$

Similar to the wave impedance, b in the TDPA-based system is a positive constant that relates to the unit of torque and velocity.

Since P_{diss} is not observable at any single port of the TDPN, in order to facilitate real-time monitoring of TDPN passivity, P_{diss} can be written as:

$$P_{diss}(t) = P_{diss}^m(t) + P_{diss}^s(t) \tag{4.3}$$

where $P_{diss}^m(t)$ and $P_{diss}^s(t)$ are the power dissipation components which are observable at the master and slave ports, respectively.

$$P_{diss}^m(t) = \frac{1}{b}\tau_m^T(t)\tau_m(t) - \frac{1}{2b}\left(\tau_m(t) - b\dot{q}_m(t)\right)^2 - \frac{1}{2b}\dot{T}_2(t)\tau_m^T(t)\tau_m(t) \tag{4.4}$$

$$P_{diss}^s(t) = b\dot{q}_s^T(t)\dot{q}_s(t) - \frac{1}{2b}\left(\tau_s(t) + b\dot{q}_s(t)\right)^2 - \frac{b}{2}\dot{T}_1(t)\dot{q}_s^T(t)\dot{q}_s(t) \tag{4.5}$$

In this Chapter, the time-varying delays are assumed not to increase or decrease faster than the time itself, i.e. $\left|\dot{\mathrm{T}}_{1,2}(\mathrm{t})\right| < 1$. $\dot{T}_{1,2}$ is replaced by a constant parameter ϵ in [155] and [156]. Its value is set to be the upper bound of $\dot{T}_{1,2}$. The passivity observers on the master and the slave side can be written as:

$$P_{obs}^{m}(t) = \frac{1}{b}\tau_m^T(t)\tau_m(t) - \frac{1}{2b}\left(\tau_m(t) - b\dot{q}_m(t)\right)^2 - \frac{1}{2b}\epsilon\tau_m^T(t)\tau_m(t) \qquad (4.6)$$

$$P_{obs}^{s}(t) = b\dot{q}_s^T(t)\dot{q}_s(t) - \frac{1}{2b}\left(\tau_s(t) + b\dot{q}_s(t)\right)^2 - \frac{b}{2}\epsilon\dot{q}_s^T(t)\dot{q}_s(t) \qquad (4.7)$$

By applying the passivity observers, the power flows can be detected in each port. Two passivity controllers attached at each port are activated when P_{obs}^{m} and P_{obs}^{s} are negative so that $P_{ctr}^{m} = -P_{obs}^{m}$ and $P_{ctr}^{s} = -P_{obs}^{s}$ where P_{ctr}^{m} and $P_{ctr}^{s}$are the dissipated power from the passivity controllers. By using the two passivity controllers, the torque perceived by the operator $\tau_m'(t)$ and the command velocity of slave $\dot{q}_s'(t)$ can be derived as [155]:

$$\tau_m'(t) = \tau_s(t - T_2(t)) + \tau_{PC}(t) \qquad (4.8)$$

$$\dot{q}_s'(t) = \dot{q}_m(t - T_1(t)) - \dot{q}_{PC}(t) \qquad (4.9)$$

where $\tau_{\mathrm{PC}}(\mathrm{t})$ is the output of the master side passivity controller and $\dot{\mathrm{q}}_{\mathrm{PC}}(\mathrm{t})$ is the output of the slave side passivity controller.

Unlike the wave-based system, TDPA using the passivity observers and passivity controllers can robustly guarantee the passivity of the communication channels in the presence of time varying delays. However, as a conservative method for system passivity, this method can largely degrade the system's transparency in the presence of the constant time delays or even no delay ($\epsilon = 0$). During the free space movement ($\tau_{m,s} = 0$), (17) can be simplified as $P_{obs}^{m}(t) = -\frac{b}{2}\dot{q}_m^2(t)$, and during the hard environmental contact ($\dot{\mathrm{q}}_{\mathrm{m,s}} = 0$), (18) can be simplified as $P_{obs}^{s}(t) = -\frac{1}{2b}\tau_m^2(t)$. Under these conditions, $P_{obs}^{m}(t)$ and $P_{obs}^{s}(t)$ are negative to the extent that accurate

torque and trajectory tracking performances cannot be achieved due to the adverse effect of the passivity controllers.

4.3 Proposed Wave-based TDPA System

The wave-based TDPA proposed in this analysis exhibits three novel characteristics compared to the previous work:

(1) Under constant time delays, the proposed wave transformation guarantees the passivity of the communication channels and ensures that the passivity dissipation detected by the proposed observer is positive so that the proposed passivity controllers do not affect the torque and trajectory tracking like (2.37)-(2.38). The proposed system can achieve higher transparency than the conventional TDPA-based system in [155], [156].

(2) In the presence of arbitrary time-varying delays, the proposed wave-based TDPA takes effect by observing the negative power P_{diss} to robustly guarantee the system passivity and is not as over-conservative as the conventional wave-based controllers in [25].

(3) The consistent problems of the wave-based system, i.e. wave-based reflections and position drift are simultaneously solved in the proposed system.

4.3.1 Proposed Wave Variable Transformation

Figure 4.1 shows the modified wave variable transformation proposed in this section. The modified wave variable transformation is applied to encode the feed-forward signals V'_m with the feedback signals I'_s. The wave variables in this controller are defined as follows:

$$u_m(t) = \frac{bV'_m(t) + I_m(t)}{\sqrt{2b}}, u_s(t) = \frac{bV_s(t) + I'_s(t)}{\sqrt{2b}} \tag{4.10}$$

$$v_m(t) = \frac{BI_m(t) - bV'_m(t)}{\sqrt{2b}}, v_s(t) = \frac{BI'_s(t) - bV_s(t)}{\sqrt{2b}} \tag{4.11}$$

where b and B are positive wave characteristic impedances ($\mathrm{b}, \mathrm{B} > 1$). By applying impedance matching to reduce the wave-based reflections, V_m' and I_s' are derived as:

$$V_m'(t) = V_m(t) - \frac{1}{b} I_m(t) \tag{4.12}$$

$$I_s'(t) = I_s(t) + \frac{b}{B} V_s\,(t) \tag{4.13}$$

where

$$V_m(t) = \alpha_1 k_a \tau_h(t) + \beta\big(\dot{q}_m(t) + \delta q_m(t)\big) \tag{4.14}$$

$$I_s(t) = \alpha_2 k_b \tau_e(t) - \beta\big(\dot{q}_s(t) + \delta q_s(t)\big) \tag{4.15}$$

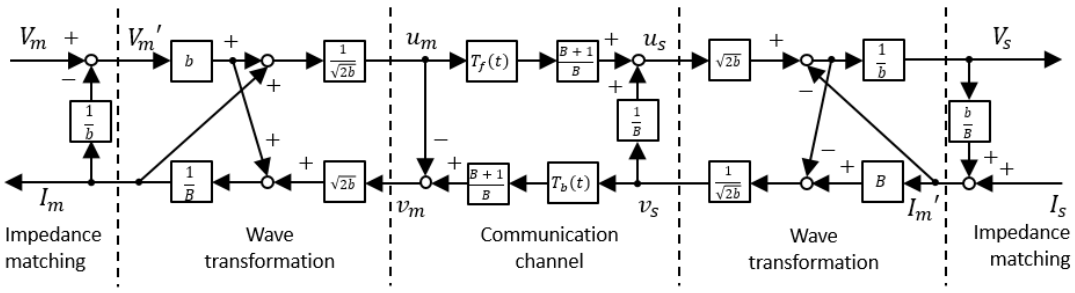

Figure 4.1. Proposed wave-based transformation

τ_h and τ_e are measured human and environmental torques. $q_{m,s}$ are the master and slave's positions. α_1, α_2, k_a, k_b, β and δ are positive constants. According to (4.14) and (4.15), since the four signals of torque and position signals of the master and the slave, are transmitted through the communication channels, the system applying the proposed wave controller is called 4-CH wave-based teleoperation system. Substituting (4.14) and (4.15) into (4.12) and (4.13), the proposed wave variables can be written as:

$$u_m(t) = \frac{b}{\sqrt{2b}} V_m(t), u_s(t) = \frac{(b + \frac{b}{B}) V_s(t) + I_s(t)}{\sqrt{2b}} \tag{4.16}$$

$$v_m(t) = \frac{(B+1)I_m(t) - bV_m(t)}{\sqrt{2b}}, v_s(t) = \frac{B}{\sqrt{2b}} I_s(t) \tag{4.17}$$

As shown in (4.16)-(4.17), since the outgoing wave variable $u_m(t)$ and $v_s(t)$ no longer contain components of the incoming wave variables $u_s(t)$ and $v_m(t)$, the circulating wave-based reflections can be prevented. In addition, based on (4.14)-(4.17), since the sign of $\tau_h(t)$ is opposite to that of $\tau_e(t)$, $V_{m,s}(t)$, $u_{m,s}(t)$ have opposite signs to $\mathrm{I_{m,s}(t)}$, $\mathrm{v_{m,s}(t)}$. In the communication channel, based on Figure 3, the incoming wave variables $u_s(t)$ and $v_m(t)$ are derived as:

$$u_s(t) = \left(\frac{1}{B} + 1\right) u_m\big(t - T_1(t)\big) + \frac{1}{B} v_s(t) \tag{4.18}$$

$$v_m(t) = \left(\frac{1}{B} + 1\right) v_s\big(t - T_2(t)\big) - u_m(t) \tag{4.19}$$

Substituting (4.16) and (4.17) into (4.18) and (4.19), the feed-forward and feedback signals transmission in the modified wave controller can be derived as:

$$V_s(t) = V_m(t - T_1(t)) \tag{4.20}$$

$$I_m(t) = I_s(t - T_2(t)) \tag{4.21}$$

Compared with the conventional wave controller, the biased term in (2.37) and (2.38) are thoroughly compensated for in the proposed wave-based system. Thus, highly accurate tracking performances can be achieved. The following equations can be derived based on (4.16)-(4.19):

$$I_m(t) = \frac{\sqrt{2b}}{1+B}(u_m(t) + v_m(t)), V_m(t) = \sqrt{\frac{2}{b}} u_m(t) \tag{4.22}$$

$$I_s(t) = \frac{\sqrt{2b}}{B} v_s(t), V_s(t) = \frac{B\sqrt{2b}}{Bb+b}\big(Bu_s(t) - v_s(t)\big) \tag{4.23}$$

Hence the power flow into the TDPN using the modified wave controller can be expressed as:

$$P(t) = V_m(t)I_m(t) - V_s(t)I_s(t)$$

$$= \frac{2}{1+B}\big(u_m(t)+v_m(t)\big)u_m(t) - \frac{2}{B(1+B)}\big(Bu_s(t)-v_s(t)\big)v_s(t)$$

$$= \frac{2}{1+B}u_m^T(t)u_m(t) + \frac{2}{M(1+B)}v_m^T(t)v_m(t)$$

$$- \frac{1}{M(1+B)}\big(v_m(t)-Mu_m(t)\big)^T\big(v_m(t)-Mu_m(t)\big)$$

$$- \frac{1}{M(1+B)}\big(v_s^T(t)v_s(t)-v_m^T(t)v_m(t)\big) + \frac{2}{B(1+B)}v_s^T(t)v_s(t)$$

$$+ \frac{2M}{1+B}u_s^T(t)u_s(t)$$

$$- \frac{1}{M(1+B)}\big(v_s(t)+Mu_s(t)\big)^T\big(v_s(t)+Mu_s(t)\big)$$

$$- \frac{M}{1+B}\big(u_m^T(t)u_m(t)-u_s^T(t)u_s(t)\big)$$

$$= \frac{2}{1+B}u_m^T(t)u_m(t) + \frac{2}{M(1+B)}v_m^T(t)v_m(t)$$

$$- \frac{1}{M(1+B)}\big(v_m(t)-Mu_m(t)\big)^T\big(v_m(t)-Mu_m(t)\big)$$

$$- \frac{1}{M(1+B)}\dot{T}_2 v_m^T(t)v_m(t) + \frac{2}{B(1+B)}v_s^T(t)v_s(t)$$

$$+ \frac{2M}{1+B}u_s^T(t)u_s(t)$$

$$- \frac{1}{M(1+B)}\big(v_s(t)+Mu_s(t)\big)^T\big(v_s(t)+Mu_s(t)\big)$$

$$- \frac{M}{1+B}\dot{T}_1 u_s^T(t)u_s(t) + \frac{M}{1+B}\int_{t-T_1(t)}^{t} u_m^T(\eta)u_m(\eta)d\eta$$

$$+ \frac{1}{M(1+B)}\int_{t-T_2(t)}^{t} v_s^T(\eta)v_s(\eta)d\eta$$

$$= P_{diss}(t) + \frac{dE}{dt}(t) \qquad (4.24)$$

$$E(t) = \frac{M}{1+B}\int_{t-T_1(t)}^{t} u_m^T(\eta)u_m(\eta)d\eta + \frac{1}{M(1+B)}\int_{t-T_2(t)}^{t} v_s^T(\eta)v_s(\eta)d\eta \qquad (4.25)$$

$$P_{diss}(t) = \frac{2}{1+B}u_m^T(t)u_m(t) + \frac{2}{M(1+B)}v_m^T(t)v_m(t)$$
$$- \frac{1}{M(1+B)}\big(v_m(t) - Mu_m(t)\big)^T\big(v_m(t) - Mu_m(t)\big)$$
$$- \frac{1}{M(1+B)}\dot{T}_2 v_m^T(t)v_m(t) + \frac{2}{B(1+B)}v_s^T(t)v_s(t)$$
$$+ \frac{2M}{1+B}u_s^T(t)u_s(t)$$
$$- \frac{1}{M(1+B)}\big(v_s(t) + Mu_s(t)\big)^T\big(v_s(t) + Mu_s(t)\big)$$
$$- \frac{M}{1+B}\dot{T}_1 u_s^T(t)u_s(t) \qquad (4.26)$$

where M is a positive constant which relates the unit of $u_{m,s}$ and $v_{m,s}$. According to (4.25), the net energy flow in the TDPN is absolutely positive to guarantee passivity of the TDPN. Based on the definition of passivity and assuming $E(0) = 0$, the energy flow is derived as [156]:

$$E_{flow}(t) = \int_0^t P(\eta)d\eta = \int_0^t (P_{diss}(\eta) + \frac{dE}{dt}(\eta))d\eta = E(t) - E(0) + \int_0^t P_{diss}(\eta)d\eta$$
$$\geq \int_0^t P_{diss}(\eta)d\eta \qquad (4.27)$$

Therefore, under the condition that $P_{diss}(\eta) \geq 0$, based on (4.27), the energy flow $E_{flow}(t)$ is more than zero and the passivity of the TDPN can be achieved. $P_{diss}(t)$ in (4.26) can also be defined as the sum of master power dissipation components $P_{diss}^{m}(t)$ and slave power dissipation components $P_{diss}^{s}(t)$:

$$P_{diss}^m(t) = \frac{2}{1+B}u_m^T(t)u_m(t) + \frac{2}{M(1+B)}v_m^T(t)v_m(t)$$
$$- \frac{1}{M(1+B)}\big(v_m(t) - Mu_m(t)\big)^T\big(v_m(t) - Mu_m(t)\big)$$
$$- \frac{1}{M(1+B)}\dot{T}_2 v_m^T(t)v_m(t) \qquad (4.28)$$

$$P_{diss}^{s}(t) = \frac{2}{B(1+B)} v_s^T(t) v_s(t) + \frac{2M}{1+B} u_s^T(t) u_s(t) - \frac{1}{M(1+B)} \left(v_s(t) + M u_s(t)\right)^T \left(v_s(t) + M u_s(t)\right) - \frac{M}{1+B} \dot{T}_1 u_s^T(t) u_s(t) \quad (4.29)$$

Based on (4.28) and (4.29), since $P_{diss}^{m}(t)$ and $P_{diss}^{s}(t)$ only contain the signals observed at the master and slave ports, respectively, the proposed passivity observer can observe the power dissipation components in real time. The proposed wave-based system aims to guarantee the passivity of the communication channels in the presence of constant delays. Accordingly, $P_{diss}^{m}(t)$ and $P_{diss}^{s}(t)$ are required to be no less than 0 under the condition $\dot{T}_{1,2}$=0. Therefore, (4.28) and (4.29) can be simplified as:

$$P_{diss}^{m}(t) = (2-M) u_m^T(t) u_m(t) + \frac{1}{M} v_m^T(t) v_m(t) + 2 v_m(t) u_m(t) \geq 0 \quad (4.30)$$

$$P_{diss}^{s}(t) = \left(\frac{2}{B} - \frac{1}{M}\right) v_s^T(t) v_s(t) + 2M u_s^T(t) u_s(t) - 2 v_s(t) u_s(t) \geq 0 \quad (4.31)$$

According to (4.20)-(4.31) and noting that $u_{m,s}(t)$ have opposite sign to $v_{m,s}(t)$, the condition for $P_{diss}(t) \geq 0$ in the presence of constant time delays can be derived as:

$$\begin{cases} 2\sqrt{\dfrac{(2-M)}{M}} \geq 2 \Rightarrow 1 \geq M > 0 \\ \dfrac{2}{B} - \dfrac{1}{M} \geq 0 \Rightarrow 2M \geq B > 1 \end{cases} \quad (4.32)$$

Normally, *M* and *B* can be set to be 1 and 2, respectively. When (4.32) is satisfied, the passivity of the communication channels can be robustly guaranteed by the proposed wave variable transformation.

4.3.2 Extended power-based TDPA

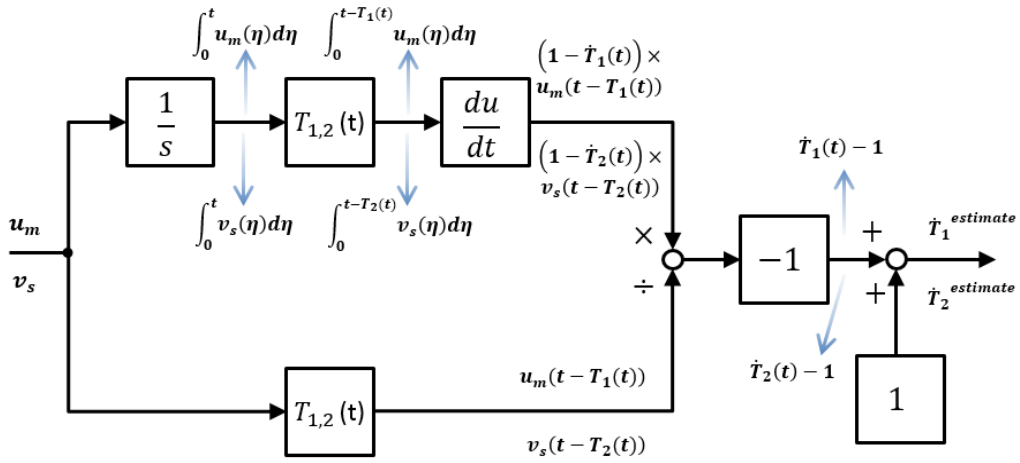

Figure 4.2. Time delay differential estimator

According to (4.28)-(4.29), $\dot{T}_{1,2}$ are hard to measure in real time. One option is like the conventional TDPA [68] that conservatively estimates a parameter ϵ ($\epsilon \leq 1$) which is equal to the upper bound of $\dot{T}_{1,2}$. Additionally, a time delay differential estimator is proposed in this thesis as shown in Fig.4. When this estimator is used, the integral of $u_m(t)$ and $v_s(t)$ should be sent outside the wave transformation. The proposed passivity observer is derived as:

$$P_{obs}^{m}(t) = \frac{2}{1+B}u_m^T(t)u_m(t) + \frac{2}{M(1+B)}v_m^T(t)v_m(t) - \frac{1}{M(1+B)}\big(v_m(t)-Mu_m(t)\big)^T\big(v_m(t)-Mu_m(t)\big) - \frac{1}{M(1+B)}\varepsilon_1 v_m^T(t)v_m(t) \quad (4.33)$$

$$P_{obs}^{s}(t) = \frac{2}{B(1+B)}v_s^T(t)v_s(t) + \frac{2M}{1+B}u_s^T(t)u_s(t) - \frac{1}{M(1+B)}\big(v_s(t)+Mu_s(t)\big)^T\big(v_s(t)+Mu_s(t)\big) - \frac{M}{1+B}\varepsilon_2 u_s^T(t)u_s(t) \quad (4.34)$$

where

$$\varepsilon_{1,2} = \begin{cases} \dot{T}_{1,2}^{estimate}, if\ \dot{T}_{1,2}^{estimate} \leq 1 \\ 1, else, if\ \ \dot{T}_{1,2}^{estimate} > 1 \end{cases} \tag{4.35}$$

By using the passivity observer, we design the passivity controller to be:

$$\hat{I}_m(t) = I_m(t) + \Gamma_1(t)V_m(t) \tag{4.36}$$

$$\hat{V}_s(t) = V_s(t) + \Gamma_2(t)I_s(t) \tag{4.37}$$

where $\hat{I}_m(t)$ and $\hat{V}_s(t)$ are the final control signals to master and slave after modification by the passivity controllers. The Coefficients $\Gamma_1(t)$ and $\Gamma_2(t)$ are derived as:

$$\Gamma_1(t) = \begin{cases} 0, \ \ if\ P_{obs}^m(t) > 0 \\ -P_{obs}^m(t)\left(V_m^T(t)V_m(t)\right)^{-1}, \ \ else, if\ |V_m(t)| > 0 \end{cases} \tag{4.38}$$

$$\Gamma_2(t) = \begin{cases} 0, \ \ if\ P_{obs}^s(t) > 0 \\ P_{obs}^s(t)\left(I_s^T(t)I_s(t)\right)^{-1}, \ \ else, if\ |I_s(t)| > 0 \end{cases} \tag{4.39}$$

Theorem 4.1. The designed passivity controller (4.36)-(4.39) can ensure the passivity of the TDPNs in the presence of arbitrary time delays.

Proof.

$$\begin{aligned} P^*(t) &= V_m(t)\hat{I}_m(t) - \hat{V}_s(t)I_s(t) \\ &= \left(I_m(t) + \Gamma_1(t)V_m(t)\right)V_m(t) - \left(V_s(t) + \Gamma_2(t)I_s(t)\right)I_s(t) \\ &= \left(V_m(t)I_m(t) - V_s(t)I_s(t)\right) + \Gamma_1(t)V_m^T(t)V_m(t) - \Gamma_2(t)I_s^T(t)I_s(t) \\ &= \left(P_{diss}(t) + \frac{dE(t)}{dt}\right) + \Gamma_1(t)V_m^T(t)V_m(t) - \Gamma_2(t)I_s^T(t)I_s(t) \\ &= \left(P_{obs}^m(t) + \Gamma_1(t)V_m^T(t)V_m(t)\right) + \left(P_{obs}^s(t) - \Gamma_2(t)I_s^T(t)I_s(t)\right) \\ &+ \frac{dE(t)}{dt} = P_{diss}(t) + \frac{dE}{dt}(t) \end{aligned} \tag{4.40}$$

Based on the definition of the coefficients $\Gamma_1(t)$ and $\Gamma_2(t)$ in (4.38) and (4.39), P^{*}_{diss} can be ensured to be non-negative. Therefore, in the presence of time-varying delays, the proposed wave-based TDPA takes effect to guarantee the passivity of the communication channels when $P^{m}_{obs}(t)$ and $P^{s}_{obs}(t)$ are negative. Unlike the TDPA-based system in previous work, in the presence of constant and decreasing time delays, highly accurate tracking performances can be achieved in the proposed system. Only when the time delays are increasing, the system passivity is maintained by reducing transparency.

4.3.3 Control Laws

The dynamic models of the master and slave apply (3.37) and (3.38) in Section 3. By applying the modified wave controller, the passivity observer and the passivity controller, the energy information such as torque, position and velocity signals are expected to be transmitted through the communication channels without influencing the system passivity. Two control terms S_m and S_s in the master and slave side are introduced as follows:

$$\begin{aligned} S_m(t) &= \alpha_2\tau_{th}(t) - \beta\big(\dot{q}_m(t) + \delta q_m(t)\big) - \hat{I}_m(t) \\ &= \alpha_2\Big(\tau_{th}(t) - k_b\tau_{te}\big(t - T_2(t)\big)\Big) \\ &\quad + \beta\Big(\dot{q}_s\big(t - T_2(t)\big) + \delta q_s\big(t - T_2(t)\big)\Big) - \beta\big(\dot{q}_m(t) + \delta q_m(t)\big) \\ &\quad - \Gamma_1(t)\Big(\alpha_1 k_a\tau_{th}(t) + \beta\big(\dot{q}_m(t) + \delta q_m(t)\big)\Big) \end{aligned} \tag{4.41}$$

$$\begin{aligned} S_s(t) &= \hat{V}_s(t) - \beta\big(\dot{q}_s(t) + \delta q_s(t)\big) - \alpha_1\tau_e(t) \\ &= \alpha_1\Big(k_a\tau_{th}\big(t - T_1(t)\big) - \tau_{te}(t)\Big) \\ &\quad + \beta\Big(\dot{q}_m\big(t - T_1(t)\big) + \delta q_m\big(t - T_1(t)\big)\Big) - \beta\big(\dot{q}_s(t) + \delta q_s(t)\big) \\ &\quad + \Gamma_2(t)\Big(\alpha_2 k_b\tau_{te}(t) - \beta\big(\dot{q}_s(t) + \delta q_s(t)\big)\Big) \end{aligned} \tag{4.42}$$

By defining new variables $r_i(t) = \dot{q}_i(t) + \delta q_i(t)$, (4.41) and (4.42) can be simplified as (4.43) and (4.44).

$$S_m = \alpha_2\tau_h(t) - \beta r_m(t) - \hat{I}_m(t)$$
$$= \alpha_2\left(\tau_h(t) - k_b\tau_e\left(t - T_2(t)\right)\right) + \beta\left(r_s\left(t - T_2(t)\right) - r_m(t)\right)$$
$$- \Gamma_1(t)\left(\alpha_1 k_a\tau_h(t) + \beta r_m(t)\right) \quad (4.43)$$

$$S_s = \hat{V}_s(t) - \beta r_s(t) - \alpha_1\tau_e(t)$$
$$= \alpha_1\left(k_a\tau_h\left(t - T_1(t)\right) - \tau_e(t)\right) + \beta\left(r_m\left(t - T_1(t)\right) - r_s(t)\right)$$
$$+ \Gamma_2(t)\left(\alpha_2 k_b\tau_e(t) - \beta r_s(t)\right) \quad (4.44)$$

Based on (4.43)-(4.44), the diagram of the proposed 4-CH system can be configured as Figure 4.3.

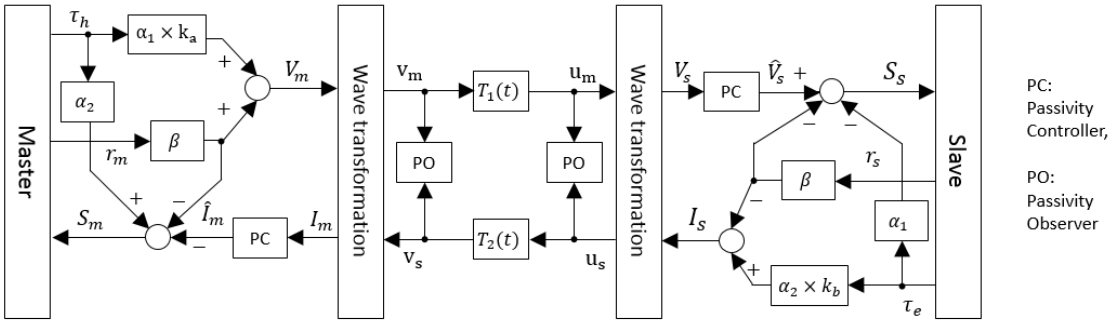

Figure 4.3. Diagram of the proposed 4-CH system

The human operator and the environment are assumed to be passive and are modeled as (3.68) and (3.69). Since acceleration signals with noises may significantly influence stability, we use the force observer to measure torques for transmission which only contain position and velocity signals. The transmitted force signals are modeled as (3.70)-(3.71)

Theorem 4.2. Consider the proposed nonlinear bilateral teleoperation system where the applied and measured operator torque and environmental torque are assumed to be passive as (3.68)-(3.69). During this scenario, for all initial conditions, all signals in this system are bounded and the master and slave manipulators state synchronized in the sense of (3.59) and (3.60).

Proof. Consider a positive semi-definite function $V(q_i, \dot{q}_i, t)$ for the system as:

$$V = \frac{1}{2}\left[r_m^T(t)M_m(q_m)r_m(t) + r_s^T(t)M_s(q_s)r_s(t) + \tilde{\theta}_m^T\psi^{-1}\tilde{\theta}_m + \tilde{\theta}_s^T\Lambda^{-1}\tilde{\theta}_s\right]$$
$$+ \frac{\beta}{2}\frac{1}{1-\dot{T}_1(t)}\int_{t-T_1(t)}^{t} r_m^T(\eta)r_m(\eta)d\eta$$
$$+ \frac{\beta}{2}\frac{1}{1-\dot{T}_2(t)}\int_{t-T_2(t)}^{t} r_s^T(\eta)r_s(\eta)d\eta + \frac{\alpha_2\alpha_m}{2}\int_{t-T_1(t)}^{t} r_m^T(\eta)\, r_m(\eta)d\eta$$
$$+ \frac{\alpha_1\alpha_s}{2}\int_{t-T_2(t)}^{t} r_s^T(\eta)\, r_s(\eta)d\eta + q_m^T(t)\alpha_m\delta q_m(t) + q_s^T(t)\alpha_s\delta q_s(t)$$
$$+ r_m^T(t)\alpha_m'\delta r_m(t) + r_s^T(t)\alpha_s' r_s(t) \qquad (4.45)$$

Since V is the sum of several quadratic terms, V is positive semi-definite. Applying property 3, the derivative of V are derived as:

$$\dot{V} = r_m^T(t)S_m(t) + r_s^T(t)S_s(t) - r_m^T(t)\alpha_m r_m(t) - r_s^T(t)\alpha_s r_s(t)$$
$$+ \frac{1}{1-\dot{T}_1(t)}r_m^T(t)\frac{\beta}{2}r_m(t) - r_m^T\big(t-T_1(t)\big)\frac{\beta}{2}r_m\big(t-T_1(t)\big)$$
$$+ \frac{1}{1-\dot{T}_2(t)}r_s^T(t)\frac{\beta}{2}r_s(t) - r_s^T\big(t-T_2(t)\big)\frac{\beta}{2}r_s\big(t-T_2(t)\big)$$
$$+ r_m^T(t)\frac{\alpha_2\alpha_m}{2}r_m(t)$$
$$- \frac{\alpha_2\alpha_m}{2}\Big(1-\dot{T}_1(t)\Big)r_m^T\big(t-T_1(t)\big)r_m\big(t-T_1(t)\big) + r_s^T(t)\frac{\alpha_1\alpha_s}{2}r_s(t)$$
$$- \frac{\alpha_1\alpha_s}{2}\Big(1-\dot{T}_2(t)\Big)r_s^T(t-T_2)r_s(t-T_2) + \dot{q}_m(t)2\alpha_m\delta q_m(t)$$
$$+ \dot{q}_s(t)2\alpha_s\delta q_s(t)$$

$$
\begin{aligned}
= -\frac{\beta}{2}\left(e_{vm}(t) + \delta e_{pm}(t)\right)^T \left(e_{vm}(t) + \delta e_{pm}(t)\right) \\
-\frac{\beta}{2}\left(e_{vs}(t) + \delta e_{ps}(t)\right)^T \left(e_{vs}(t) + \delta e_{ps}(t)\right) \\
-\left(\dot{q}_m^T(t)\alpha_m \dot{q}_m(t) + q_m^T(t)\alpha_m \delta^2 q_m(t) + \dot{q}_s^T(t)\alpha_s \dot{q}_s(t)\right. \\
\left. + q_s^T(t)\alpha_s \delta^2 q_s(t)\right) \\
-\left(\left(\frac{\alpha_2\alpha_m}{2} + \beta\Gamma_1(t) - \alpha_1\alpha_m k_a \Gamma_1(t) - \frac{\dot{T}_1(t)\beta}{2 - 2\dot{T}_1(t)}\right) r_m^T(t) r_m(t)\right. \\
+ \alpha_2 k_b \alpha_s r_m^T(t) r_s\left(t - T_2(t)\right) \\
\left. + \frac{\alpha_1\alpha_s}{2}\left(1 - \dot{T}_2(t)\right) r_s^T\left(t - T_2(t)\right) r_s\left(t - T_2(t)\right)\right) \\
-\left(\left(\frac{\alpha_1\alpha_s}{2} + \beta\Gamma_2(t) - \alpha_2\alpha_s k_b \Gamma_2(t) - \frac{\dot{T}_2(t)\beta}{2 - 2\dot{T}_2(t)}\right) r_s^T(t) r_s(t)\right. \\
+ \alpha_1 k_a \alpha_m r_s^T(t) r_m\left(t - T_1(t)\right) \\
\left. + \frac{\alpha_2\alpha_m}{2}\left(1 - \dot{T}_1(t)\right) r_m^T\left(t - T_1(t)\right) r_m\left(t - T_1(t)\right)\right) \leq 0 \qquad (4.46)
\end{aligned}
$$

In order to derive a negative semi-definite $\dot{V}$, the last two terms of (4.46) must be no more than zero. A sufficient condition is derived as:

$$
\sqrt{\left(\alpha_2\alpha_m + 2\beta\Gamma_1(t) - 2\alpha_1\alpha_m k_a \Gamma_1(t) - \frac{\dot{T}_1(t)\beta}{1 - \dot{T}_1(t)}\right)\alpha_1\alpha_s\left(1 - \dot{T}_2(t)\right)} \geq \alpha_2\alpha_s\, k_b \qquad (4.47)
$$

$$
\sqrt{\left(\alpha_1\alpha_s + 2\beta\Gamma_2(t) - 2\alpha_2\alpha_s k_b \Gamma_2(t) - \frac{\dot{T}_2(t)\beta}{1 - \dot{T}_2(t)}\right)\alpha_2\alpha_m\left(1 - \dot{T}_1(t)\right)} \geq \alpha_1\alpha_m k_a \qquad (4.48)
$$

To make (4.47) and (4.48) true, $\alpha_2\alpha_m + 2\beta\Gamma_1(t) - 2\alpha_1\alpha_m k_a\Gamma_1(t) - \frac{\dot{T}_1(t)\beta}{1-\dot{T}_1(t)}$ and $\alpha_1\alpha_s + 2\beta\Gamma_2(t) - 2\alpha_2\alpha_s k_b\Gamma_2(t) - \frac{\dot{T}_2(t)\beta}{1-\dot{T}_2(t)}$ must be non-negative. That is:

$$\alpha_2\alpha_m + 2\beta\Gamma_1(t) - 2\alpha_1\alpha_m k_a\Gamma_1(t) - \frac{\dot{T}_1(t)\beta}{1-\dot{T}_1(t)} \geq 0 \tag{4.49}$$

$$\alpha_1\alpha_s + 2\beta\Gamma_2(t) - 2\alpha_2\alpha_s k_b\Gamma_2(t) - \frac{\dot{T}_2(t)\beta}{1-\dot{T}_2(t)} \geq 0 \tag{4.50}$$

In the presence of constant or decreasing time delays ($\dot{T}_{1,2} \leq 0$), the passivity of the communication channels are guaranteed by the proposed wave controller and $\Gamma_{1,2}(t) = 0$. Resulting in (4.47) and (4.48) to be true. When the time delays are increasing, $\Gamma_1(t)$ is positive and $\Gamma_2(t)$ is negative. The terms $\frac{\dot{T}_1(t)}{1-\dot{T}_1(t)}$ and $\frac{\dot{T}_2(t)}{1-\dot{T}_2(t)}$ can be seen as the energy generated by the increasing time delays which can be dissipated by the passivity controllers as analyzed in Section 3. By setting

$$\alpha_2 k_b \alpha_s \geq \beta \geq \alpha_1 k_a \alpha_m \tag{4.51}$$

(4.49) and (4.50) are true. Since the terms $\Gamma_1(t)$ and $\Gamma_2(t)$ can compensate for the effects of time-varying delays, (4.52) and (4.53) can be simplified as:

$$k_b^2 \leq \alpha_1 \alpha_2^{-1} \alpha_m \alpha_s^{-1} \tag{4.52}$$

$$k_a^2 \leq \alpha_2 \alpha_1^{-1} \alpha_s \alpha_m^{-1} \tag{4.53}$$

Therefore, it is derived that $k_{a,b} \leq 1$. With an appropriate selection of α_1 and α_2, choosing k_a and k_b close enough to 1 will result in a nearly perfect torque tracking. Since the value of the position control gain β is not influenced by the former analyzed stability condition, highly accurate position tracking can be achieved in the presence of constant or slow-varying time delays ($\dot{T}_{1,2} \to 0$). In the presence of sharp-varying time delays ($\dot{T}_{1,2} \to 1$), due to the large effect of $\Gamma_{1,2}(t)$, both torque tracking and trajectory tracking will be degraded in order to guarantee the stability of the system.
By satisfying (4.52) and (4.53), $\dot{V}$ is guaranteed to be negative semi-definite. Integrating both sides of (4.46), we get:

$$
\begin{aligned}
+\infty > V(0) &\geq V(0) - V(t) \\
&\geq \int_0^t \frac{\beta}{2}\Big(e_{vm}(t) + \delta e_{pm}(t)\Big)^T \Big(e_{vm}(t) + \delta e_{pm}(t)\Big) \\
&+ \frac{\beta}{2}\Big(e_{vs}(t) + \delta e_{ps}(t)\Big)^T \Big(e_{vs}(t) + \delta e_{ps}(t)\Big) \\
&+ \big(\dot{q}_m^T(t)\alpha_m \dot{q}_m(t) + q_m^T(t)\alpha_m \delta^2 q_m(t) + \dot{q}_s^T(t)\alpha_s \dot{q}_s(t) \\
&+ q_s^T(t)\alpha_s \delta^2 q_s(t)\big) \\
&+ \left(\left(\frac{\alpha_2 \alpha_m}{2} + \beta\Gamma_1(t) - \alpha_1 \alpha_m k_a \Gamma_1(t) - \frac{\dot{T}_1(t)}{2 - 2\dot{T}_1(t)}\right) r_m^T(t) r_m(t)\right. \\
&+ \alpha_2 k_b \alpha_s r_m^T(t) r_s\big(t - T_2(t)\big) \\
&\left. + \frac{\alpha_1 \alpha_s}{2}\Big(1 - \dot{T}_2(t)\Big) r_s^T\big(t - T_2(t)\big) r_s\big(t - T_2(t)\big)\right) \\
&+ \left(\left(\frac{\alpha_1 \alpha_s}{2} + \beta\Gamma_2(t) - \alpha_2 \alpha_s k_b \Gamma_2(t) - \frac{\dot{T}_2(t)}{2 - 2\dot{T}_2(t)}\right) r_s^T(t) r_s(t)\right. \\
&+ \alpha_1 k_a \alpha_m r_s^T(t) r_m\big(t - T_1(t)\big) \\
&\left. + \frac{\alpha_2 \alpha_m}{2}\Big(1 - \dot{T}_1(t)\Big) r_m^T\big(t - T_1(t)\big) r_m\big(t - T_1(t)\big)\right) \qquad (4.54)
\end{aligned}
$$

Due to the positive semi-definite storage functional V and its negative semi-definite differential $\dot{V}$, $\lim_{t\to\infty} V$ exists and is finite. Also, $r_i(t), \tilde{\theta}_i(t) \in L_\infty$, $e_{vi}(t)$, $e_{pi}(t)$, q_i, $\dot{q}_i \in L_\infty \cap L_2$. Since a square integrable signal with a bounded derivative converges to the origin [25], $\lim_{t\to\infty} e_{pm}(t) = \lim_{t\to\infty} e_{vm}(t) = \lim_{t\to\infty} e_{ps}(t) = \lim_{t\to\infty} e_{vs}(t) = 0$. Therefore, the master and slave manipulators state synchronize in the sense of (3.59) and (3.60). The system's dynamic model (3.37) and (3.38) can also be written as:

$$
\ddot{q}_i(t) = M_i^{-1}\big[S_i - Y_i\tilde{\theta}_i \pm \tau_j(t) - C_i r_i(t)\big] - \delta\dot{q}_i(t) \qquad (4.55)
$$

Differentiating both sides of (4.55):

$$\frac{d}{dt}\ddot{q}_i(t) = \frac{d}{dt}(M_i^{-1})\left[S_i - Y_i\tilde{\theta}_i \pm \tau_j(t) - C_i r_i(t)\right] + M_i^{-1}\frac{d}{dt}\left[S_i - Y_i\tilde{\theta}_i \pm \tau_j(t) - C_i r_i(t)\right] - \delta\ddot{q}_i(t) \quad (4.56)$$

For the first term of the right side of (4.56), we have [153]:

$$\frac{d}{dt}(M_i^{-1}) = -M_i^{-1}\dot{M}_i M_i^{-1} = -M_i^{-1}(C_i + C_i^T)M_i^{-1} \quad (4.57)$$

According to Properties 1 and 4, $\frac{d}{dt}(M_i^{-1})$ is bounded. Based on Property 5, the terms in bracket of (4.56) are also bounded. Therefore, $\frac{d}{dt}\ddot{q}_i(t) \in L_\infty$ and $\ddot{q}_i(t)$ are uniformly continuous ($\int_0^t \ddot{q}_i(\eta)d\eta = \dot{q}_i(t) - \dot{q}_i(0)$). Since $\dot{q}_i(t) \to 0$, it can be concluded that $\ddot{q}_i(t) \to 0$ based on Barbălat's Lemma [25].

When manipulating the robots to move through the desired path, the human operator can generate energy as well as damping energy. Therefore, in normal conditions, the human forces are not passive. Considering this situation, the human and environment are modeled as (3.83)-(3.86)

where α_0 is a bounded positive variable, which generates energy as an active term. Define $\bar{x}_d = [q_m, q_s, \dot{q}_m, \dot{q}_s]^T$ and $x_d = [q_m, q_s, r_m, r_s]^T$. There is a linear map between the two vectors $\bar{x}_d(t) = \varsigma_d x_d(t)$, where ς is a non-singular constant matrix.

Theorem 4.3. The proposed system is stable and all signals in this system are ultimately bounded.

Proof. By choosing the previous Lyapunov function V and applying (3.83) and (3.86), the new derivative $\dot{V}^*$ can be written as:

$$\dot{V}^* = \dot{V} + r_m^T[\alpha_2\alpha_0 + \alpha_0 - \Gamma_1\alpha_1 k_a\alpha_0] + r_s^T[\alpha_1 k_a\alpha_0] \quad (4.58)$$

Note that

$$r_m^T[\alpha_2\alpha_0 + \alpha_0 - \Gamma_1\alpha_1 k_a\alpha_0] \le n^T\|x\|\|\alpha_2\alpha_0 + \alpha_0 - \Gamma_1\alpha_1 k_a\alpha_0| \quad (4.59)$$

$$r_s^T[\alpha_1 k_a\alpha_0] \le n^T\|x\|\|\alpha_1 k_a\alpha_0| \quad (4.60)$$

where vector $\mathrm{n} = [1\ 1\ \ldots\ 1]^{\mathrm{T}}$. Therefore (4.81) can be rewritten as:

$$\dot{\mathrm{V}}^{*} \leq \dot{\mathrm{V}} + 2\|\mathrm{x}\|\mu_d \tag{4.61}$$

where $\mu_d = \mathrm{n}^{\mathrm{T}}|\alpha_2\alpha_0 + \alpha_0 - \Gamma_1\alpha_1\mathrm{k_a}\alpha_0 + \alpha_1\mathrm{k_a}\alpha_0| > 0$. (4.62) is true:

$$\begin{aligned}\dot{V} &\leq -\left(\dot{q}_m^T(t)\alpha_m\dot{q}_m(t) + q_m^T(t)\alpha_m\delta^2 q_m(t) + \dot{q}_s^T(t)\alpha_s\dot{q}_s(t) + q_s^T(t)\alpha_s\delta^2 q_s(t)\right) \\ &\leq -\Upsilon_d\|\bar{x}\|^2\end{aligned} \tag{4.62}$$

where Υ_d is the smallest eigenvalue of α_{m}, $\alpha_{\mathrm{m}}\delta^2$, α_{s}, $\alpha_{\mathrm{s}}\delta^2$. Setting $0 < \xi_d < 1$:

$$\begin{aligned}\dot{\mathrm{V}}^{*} &\leq -\Upsilon_d\|\bar{\mathrm{x}}_d\|^2 + 2\|\mathrm{x}_d\|\mu \\ &= -\Upsilon_d(1-\xi_d)\|\varsigma_d\|^2\|\mathrm{x}_d\|^2 - \Upsilon_d\xi_d\|\varsigma_d\|^2\|x_d\|^2 + 2\|x_d\|\mu_d\end{aligned} \tag{4.63}$$

(4.63) can be simplified as:

$$\dot{\mathrm{V}}^{*} \leq -\Upsilon_d(1-\xi_d)\|\varsigma_d\|^2\|\mathrm{x}_d\|^2, \forall\|\mathrm{x}_d\| \geq \frac{2\mu_d}{\Upsilon_d\xi_d\|\varsigma_d\|^2} \tag{4.64}$$

Based on (4.64), for large value of x_d satisfying $\|\mathrm{x}_d\| \geq \frac{2\mu_d}{\Upsilon_d\xi_d\|\varsigma_d\|^2}$, the derivative $\dot{\mathrm{V}}^{*}$ is negative semi-definite. Hence, x and $\bar{\mathrm{x}}$ are bounded, which means r_i, q_i, $\dot{q}_i$ are also bounded.

4.3.4 Experiment results

A series of experiments are carried out to validate the proposed passivity-based teleoperation system. The bilateral teleoperation platform consists of two 3-DOF Phantom haptic devices: Phantom Omni and Phantom Desktop (Sensable Technologies, Inc., Wilmington, MA) as shown in Figure 3.19. During the experimental process, the control loop is configured as a 1 kHz sampling rate. The wave impedance b is set as 2.5. As discussed in Section 3, the impedances B and M are 2 and 1, respectively. δ is set to be 1. Setting large value of the position controller β can achieve accurate position tracking. However, if it is too large, the system can be felt over-damped and large variations may occur. Based on the experimental results,

setting β to be 2 can achieve highly accurate position tracking without large variation. k_a and k_b are set to be 0.9. Thus, α_1 and α_2 are set to be 1.9 and 2.3, respectively.

4.3.4.1 Experimental Validation using 1-DOF

In this sub-section, the performance of the proposed system is compared with the TDPA-based systems proposed in [155] and [156] under different conditions: free motion and hard contact. Three experiments have been done in this subsection, where the first two are done under 200ms constant delays (one way) and the final one is done under 500ms time delays with 200ms variations. The experiments in this sub-section use joint 2 of the master and slave robots as shown in Fig.5 where the gravity takes effect. Gravity compensation is applied in all of the systems. The parameters of the conventional TDPA-based system are set as recommended in [155] and [156].

During free motion, the position tracking between the master and the slave robot, the observed power $P_{obs}^{m}(t)$ and $P_{obs}^{s}(t)$, the human felt torque τ_m and environment torque τ_e of the system in [156], the system in [155] and the proposed system are shown in Figures 4.4, 4.5 and 4.6, respectively. In Figures 4.4 and 4.5, since [155] and [156] apply similar passivity observers, even the upper bound of $\dot{T}_{1,2}$ is 0, $P_{obs}^{m}(t)$ is still negative as analyzed in Section 2 and the passivity controllers are launched to reduce the control signals as (4.8)-(4.9). Therefore, the operator can still feel feedback force and the slave robot cannot accurately track the master robot during free motion. Unlike the systems in [155] and [156], since the passivity of the proposed system is guaranteed by the proposed wave controller, $P_{obs}^{m}(t)$ and $P_{obs}^{s}(t)$ are positive and the passivity controller will not take effect. Accurate position tracking can be derived and the torque felt by the human operator is nearly zero as shown in Figure 4.6.

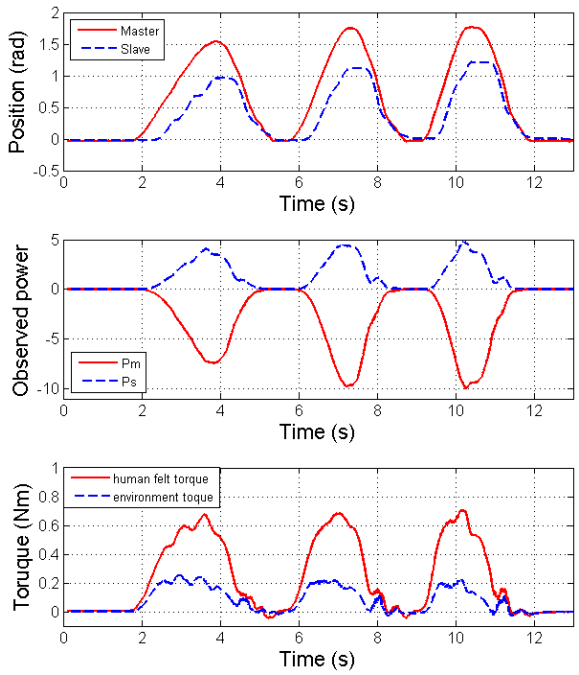

Figure 4.4. Position tracking, observed power, and torque tracking (τ_m and τ_e) of the system in [156] during free motion

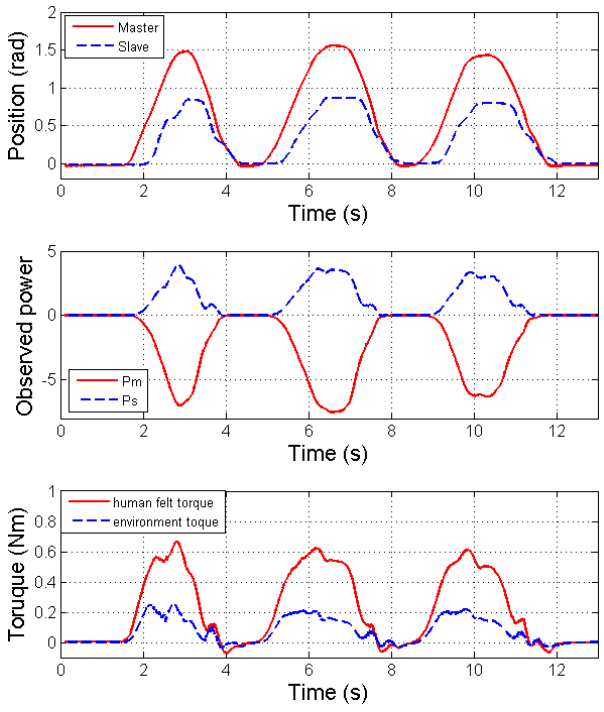

Figure 4.5. Position tracking, observed power, and torque tracking (τ_m and τ_e) of the system in [155] during free motion

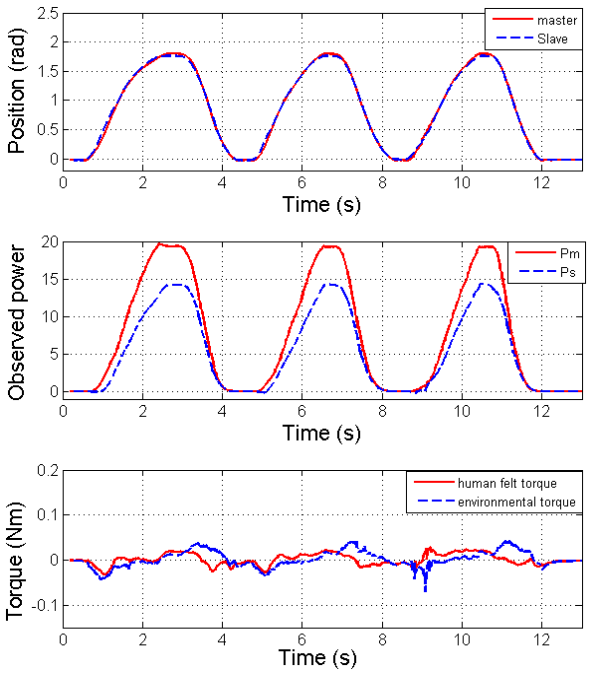

Figure 4.6. Position tracking, observed power, and torque tracking (τ_m and τ_e) of the proposed system during free motion

During hard contact, the slave robot is controlled in contact with a solid wall. As shown in Figures 4.7 and 4.8, both of $P_{obs}^{m}(t)$ and $P_{obs}^{s}(t)$ are negative in the systems in [155] and [156], and the accuracy of the torque tracking between τ_h and τ_e is significantly affected by the conventional TDPA. On the contrary, the observed power in the proposed system is still positive and highly accurate torque tracking is achieved as shown in Figure 4.9. It can be concluded that by applying the proposed wave transformation to guarantee the system passivity, the proposed system has high performance under constant time delays. When the time delay varies, the upper bound ϵ of the differential of the time delay is set to be 0.2 in the three systems. Figures 4.10-4.12 show the torque tracking of the three systems in the hard contact situation. As shown in Figures 4.10 and 4.11, according to (4.6)-(4.7), the upper bound ϵ increases the negative values of the observed powers in the systems [155] and [156]. Therefore, large torque tracking errors caused by the passivity controllers occur during the hard contact. By using the proposed passivity observer which is as not conservative as that in [155] and [156], the amplitude of the observed power in the proposed system

is not reduced as large as that in the systems in [155] and [156]. Hence, the tracking errors are smaller than that in the other two systems.

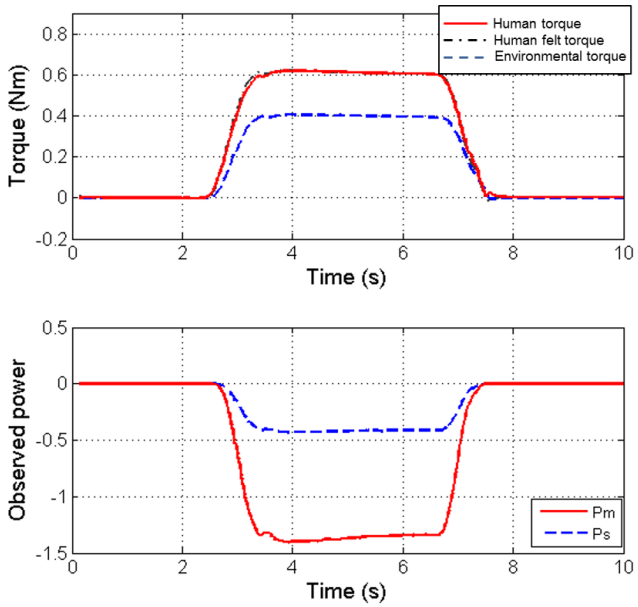

Figure 4.7. Torque tracking (τ_h, τ_m and τ_e) and observed power of the system in [156] during hard contact (constant delay)

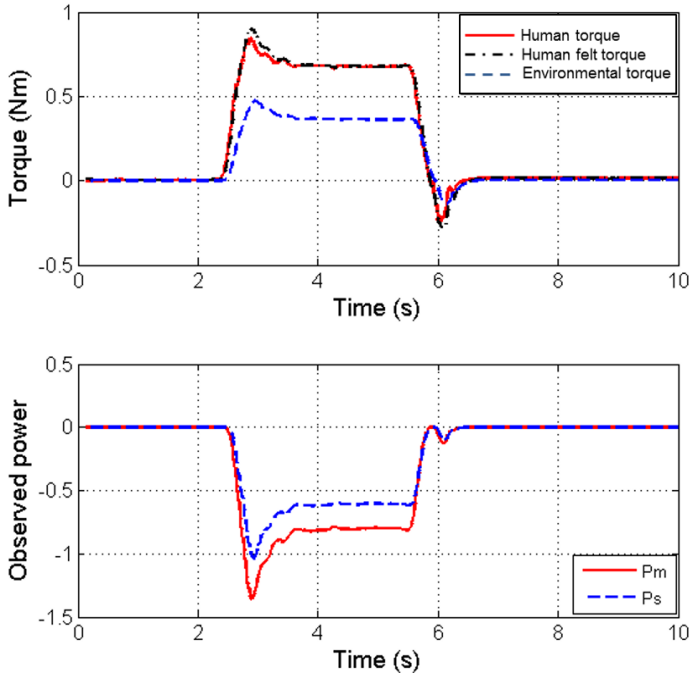

Figure 4.8. Torque tracking (τ_h, τ_m and τ_e) and observed power of the system in [155] during hard contact (constant delay)

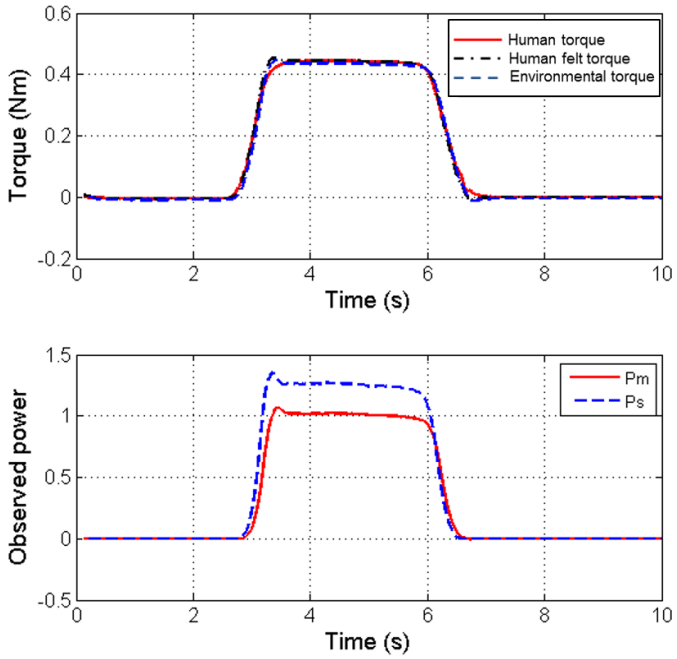

Figure 4.9. Torque tracking (τ_h, τ_m and τ_e) and observed power of the proposed system during hard contact (constant delay)

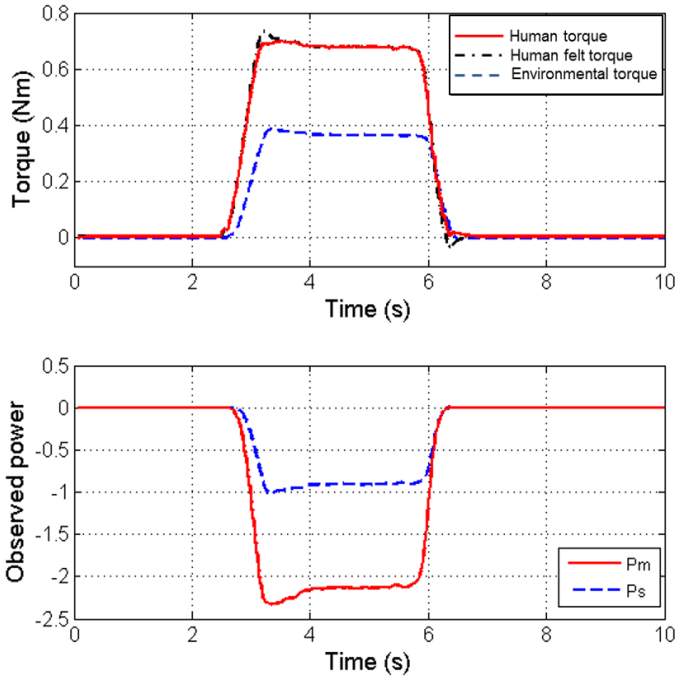

Figure 4.10. Torque tracking (τ_h, τ_m and τ_e) and observed power of the system in [156] during hard contact (time-varying delay)

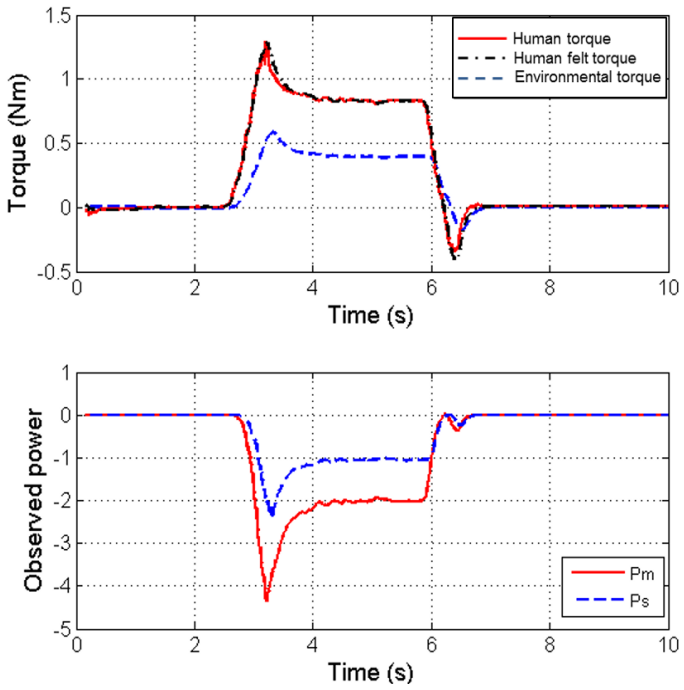

Figure 4.11. Torque tracking (τ_h, τ_m and τ_e) and observed power of the system in [155] during hard contact (time-varying delay)

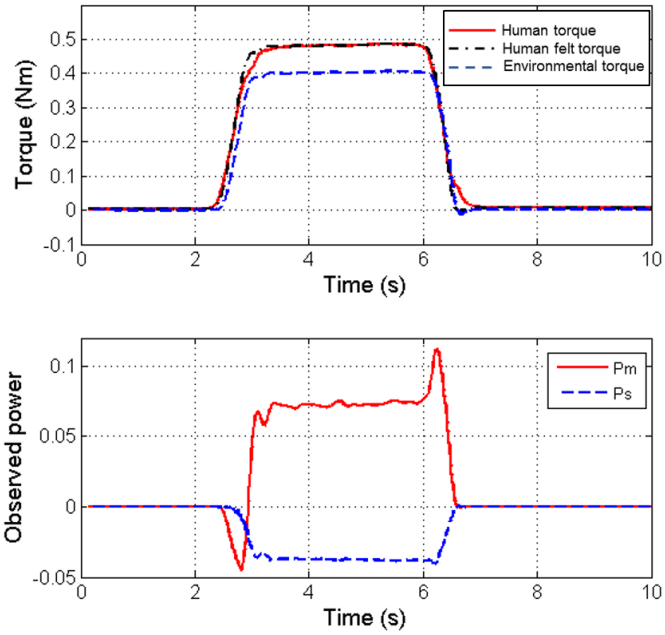

Figure 4.12. Torque tracking (τ_h, τ_m and τ_e) and observed power of the proposed system during hard contact (time-varying delay)

4.3.4.2 Experimental Validation using 2-DOF

In this sub-section, the slave robot is controlled to draw a pentacle "☆" on a table. Joint 1 and joint 3 of the master and slave robots are deployed to validate the experiment. Friction exists between the manipulators and the table. Figure 4.13 shows the pentacle "☆" drawn by our proposed system (A), system in [108] (B), the system in [74] (C), and the system in [132] (D) in the presence of constant time delays. The time delay (one way) is 500ms. As analyzed in Section 2, in spite of using 4-ch architecture, the system in [108], cannot compensate for the biased terms of the conventional wave transformation in spite of the extra control parameters. Hence, the position tracking is seriously influenced by the presence of large time delays. The system in [74] partially compensates for the biased term to enhance the velocity tracking of the wave-based system. However, since the torque reflection is not improved and the wave reflections exist, the operator feels a damped system when driving the master/slave and it is hard to control a slave robot to draw a perfect pentacle "☆". As analyzed before, the torque reflection in the system in [132] is affected by $\mathrm{b}\dot{x}_m(t)$, and the velocity tracking is also affected by $\mathrm{F_s(t-T_1-T_2)-F_s(t)}$, the motion of the slave robot is still influenced although the wave reflections are reduced. Compared with the three systems, the proposed system has the most accurate position tracking. Moreover, by matching impedance, the proposed system is not over-damped and can offer the operator good feelings for the remote environment. Therefore, the proposed system can draw the most standard pentacle "☆". Figure 4.14 shows the pentacle "☆" drawn by A. our proposed system, B. system in [155], C. the system in [156], D. the system in [25] in the presence of time-varying delays. The time delays (one way) are 500ms with approximate 200ms variation. Figure 4.15 shows $\dot{T}_{1,2}$ derived by the time delay differential estimator. In [25], the extra energy caused by time-varying delays is eliminated by applying the scaling gain $\sqrt{1-\epsilon}$ in the forward

and backward communication paths.The upper bound ϵ is set to be 0.2 in the systems in [155], [156] and [25].

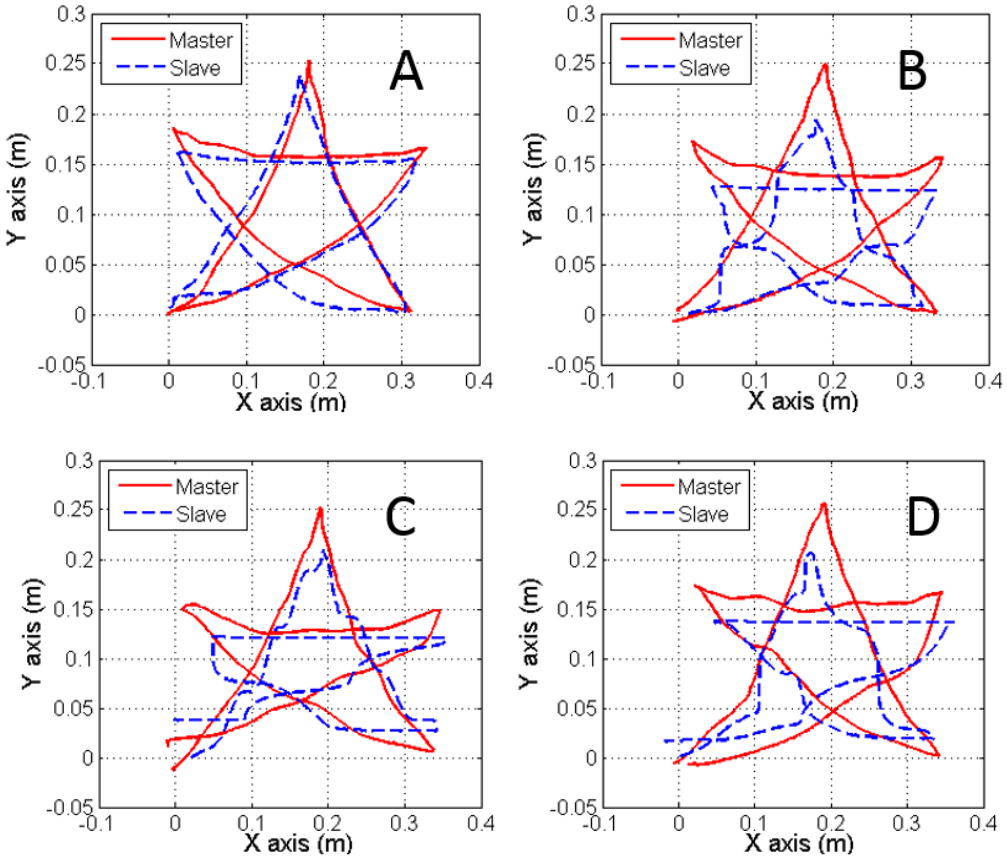

Figure 4.13. Drawing pentacle "☆" under constant time delays, A. our system, B. system in [108], C. system in [74], C. system in [132]

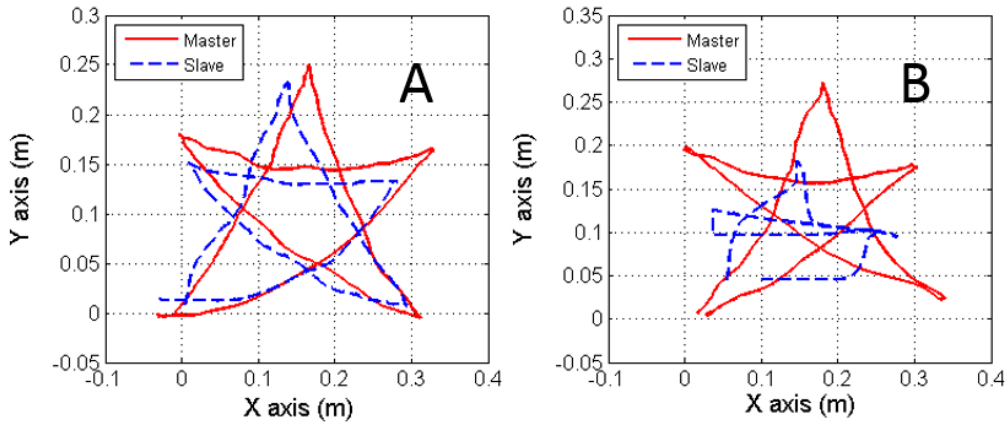

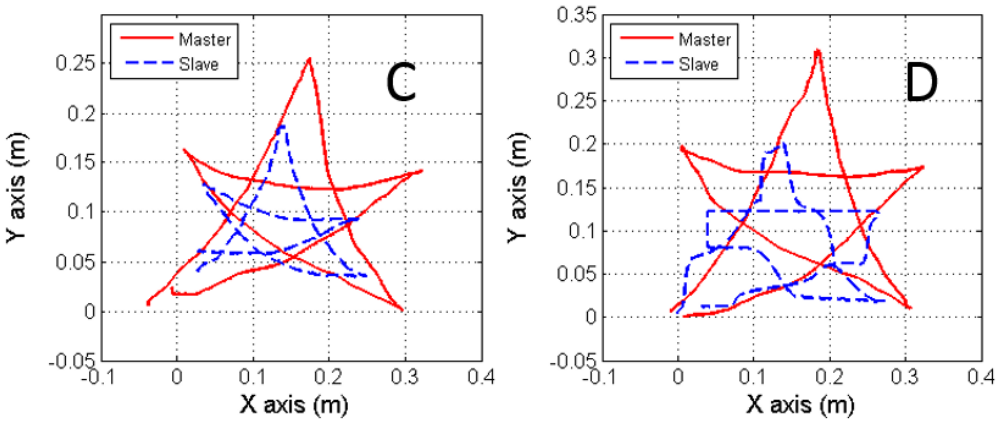

Figure 4.14. Drawing pentacle "☆" under time-varying delays, A. our system, B. system in [155], C. system in [156], D. system in [25]

Under time-varying delays, the pentacle "☆" drawn by the slave robots using the four systems shrink due to the use of the passivity controller and the scaling gain. $P_{obs}^{m}(t)$ and $P_{obs}^{s}(t)$ observed in the proposed system are shown in Figure 4.16, which is still not totally negative. It means the proposed scheme is not as conservative as the conventional TDPA. Therefore, the proposed system can draw the pentacle "☆" with good shape. The system in [155] has the worst performance since the passivity controller seriously affects the work performance and operator's feelings for the remote environment. Moreover, without direct position transmission, this system can be easily affected by position drift. Since [156] is an extension of [155] to deal with position drift, the system in [156] has better trajectory tracking than the system in [155]. However, since its passivity observer is as conservative as [155], its trajectory tracking is also reduced. Although using impedance matching to reduce wave reflections, the slave motion of the wave-based system in [25] is affected by the biased terms of the wave transformation and the scaling gain $\sqrt{1-\epsilon}$.

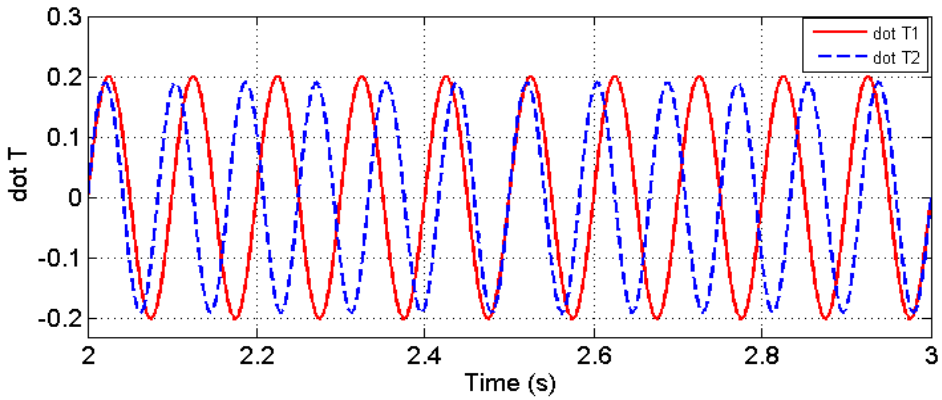

Figure 4.15. Estimated $\dot{T}_{1,2}$

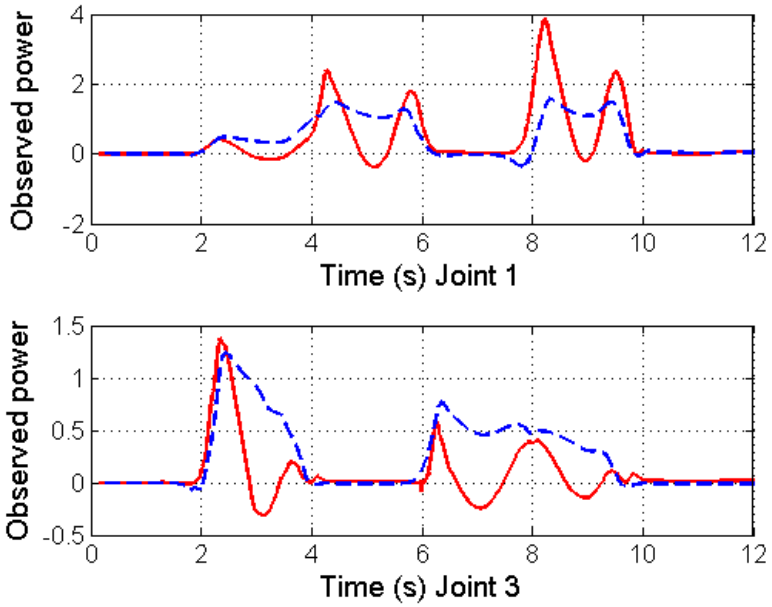

Figure 4.16. Observed power in the proposed system in the presence of time-varying delays

4.3.4.3 Experimental Validation using 3-DOF

The experiment in this section demonstrates the ability of the proposed system in dealing with the transient environment. The slave robot is controlled by two nonlinear systems to make contact with a "reverse wall" which is like the scenario of a needle puncture as might be experienced in medical applications [154]. In this scenario, the

slave end effector freely moves into a solid wall during the first 2 seconds. After hard contact for seconds, the wall is suddenly removed allowing the slave end effector to move in free space. The configuration parameters of the comparison system are set as recommended in [25]. The position and torque tracking of the two systems are shown in Figs.20 and 21. The time delay is set to be 500 ms with 100 ms variation. Figure 4.17 shows the estimated $\dot{T}_{1,2}$.

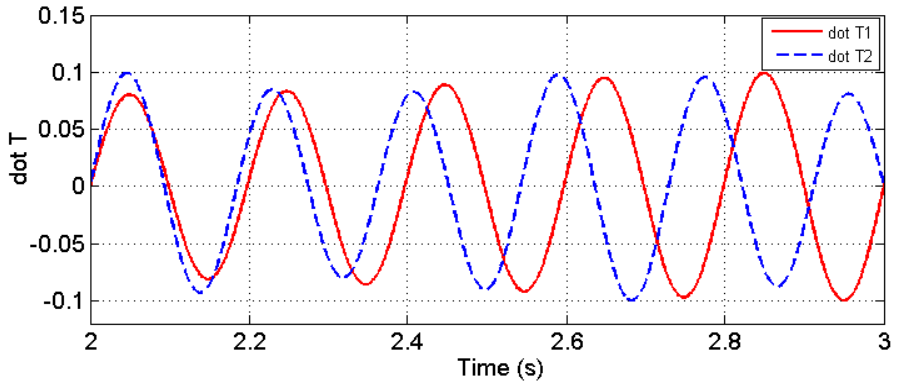

Figure 4.17. Estimated $\dot{T}_{1,2}$

The system in [25] uses the conventional impedance matching approach to diminish the wave reflections. The torque and trajectory tracking in [25] can be written as:

$$r_s(t) = \frac{r_m(t - T_1(t))}{2} - \frac{\tau_s(t)}{2b} \tag{4.65}$$

$$\tau_m(t) = \frac{\tau_s(t - T_2(t))}{2} + \frac{br_m(t)}{2} \tag{4.66}$$

where $\tau_{m,s}(t)$ are closely related to the impedances of human and environment.

Figure 4.18 clearly shows one evident drawback of the conventional impedance matching. That is, if the impedances of human and environment suddenly change, the impedances will mismatch and the wave-based reflections are reinstated. Therefore, large signal variations and position drift will occur as shown in Figure 4.18.

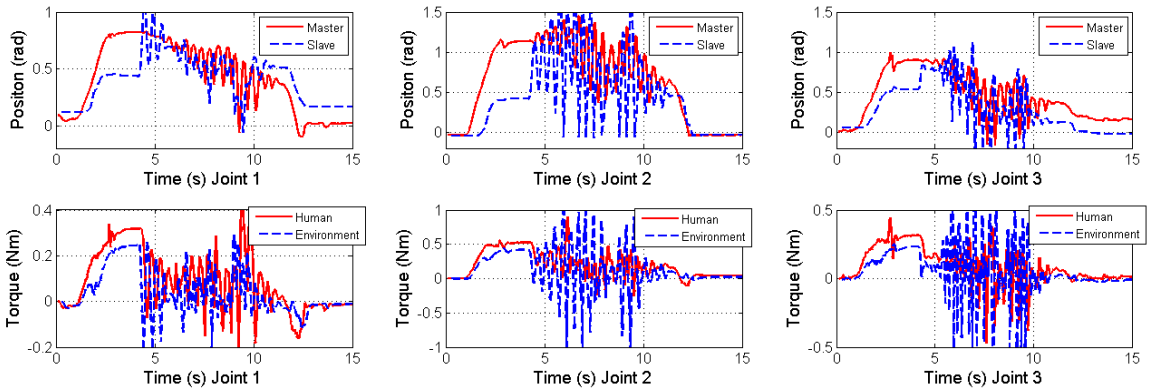

Figure 4.18 Contact with a reverse wall using the system presented in [25]: position tracking and torque tracking (τ_h and τ_e)

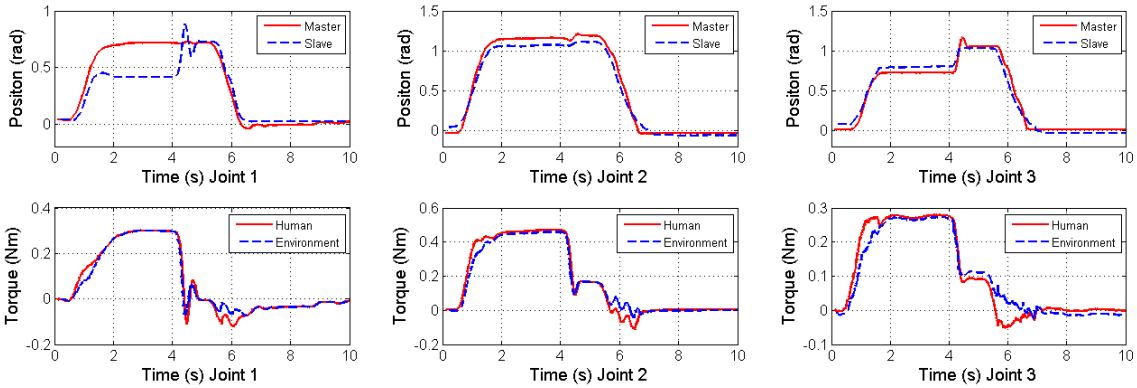

Figure 4.19. Contact with a reverse wall using the proposed system: position tracking and torque tracking (τ_h and τ_e)

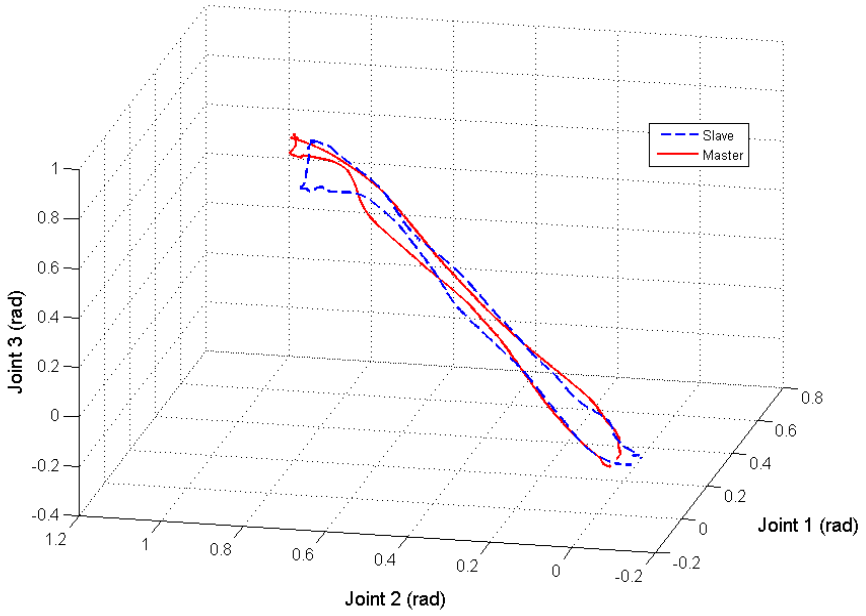

Figure 4.20. Contact with a reverse wall-position tracking

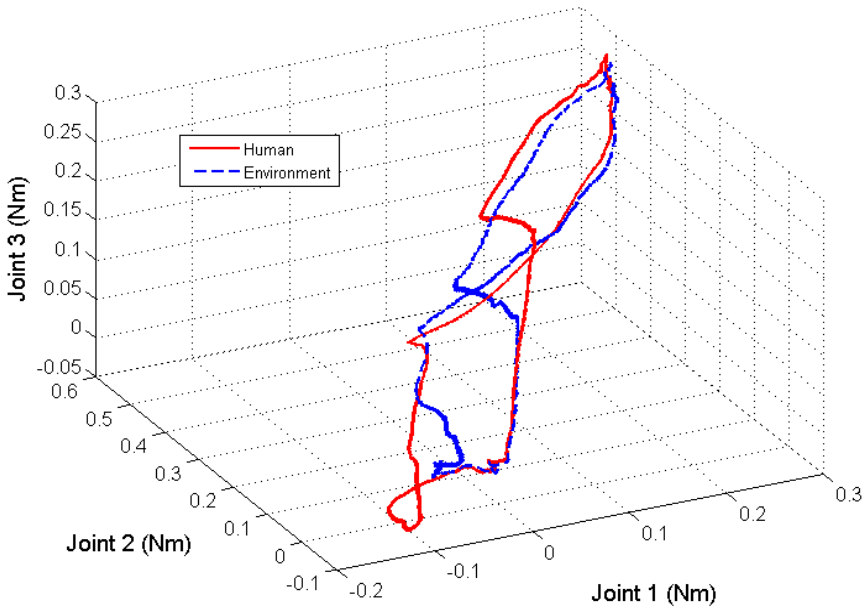

Figure 4.21. Contact with a reverse wall-torque tracking

In the proposed system, by using the modified impedance matching approach, perfect torque and trajectory tracking can be achieved. Moreover, by using the 4-CH transmission, the control signals $I_{m,s}(t)$ and $V_{m,s}(t)$ are less affected by the unpredictable changes of the human and environmental impedances. Therefore, highly accurate torque tracking between τ_h and τ_e and position tracking are still achieved in the sudden changing environment as shown in Figure 4.19. The position tracking and torque tracking in fig.21 are shown in 3D figures as Figures 4.20 and 4.21.

Another advantage of the proposed system is its reasonable performance in the worst case when $\dot{T}_{1,2} \rightarrow 1$ as shown in Figure 4.22. In this experiment, the time delays are set as 2s with 1s variations. Under this condition, the scaling gain $\sqrt{1-\epsilon}$ used in [25] is too conservative which is equal to zero and the slave robot are uncontrollable. In this situation, we use the proposed system to draw a letter "O" in free space as shown in Figure 4.23. The proposed wave-based TDPA guarantee the system's stability by reducing transparency in the presence of sharp-varying time delays. Reasonable performance can still be achieved in the worst scenario, although signals variations are caused by the time-varying delays and the shape of "O" drawn by the slave is shrunk by the passivity controller.

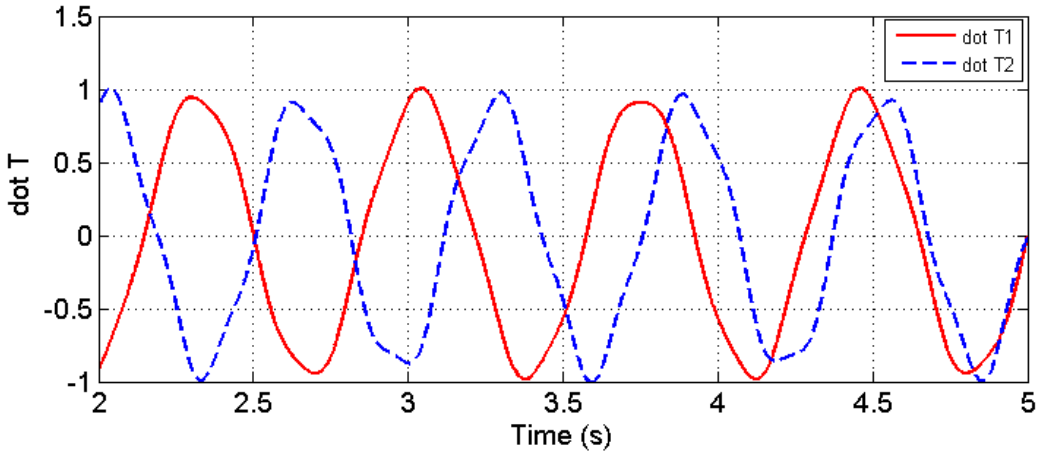

Figure 4.22. Estimated $\dot{T}_{1,2}$

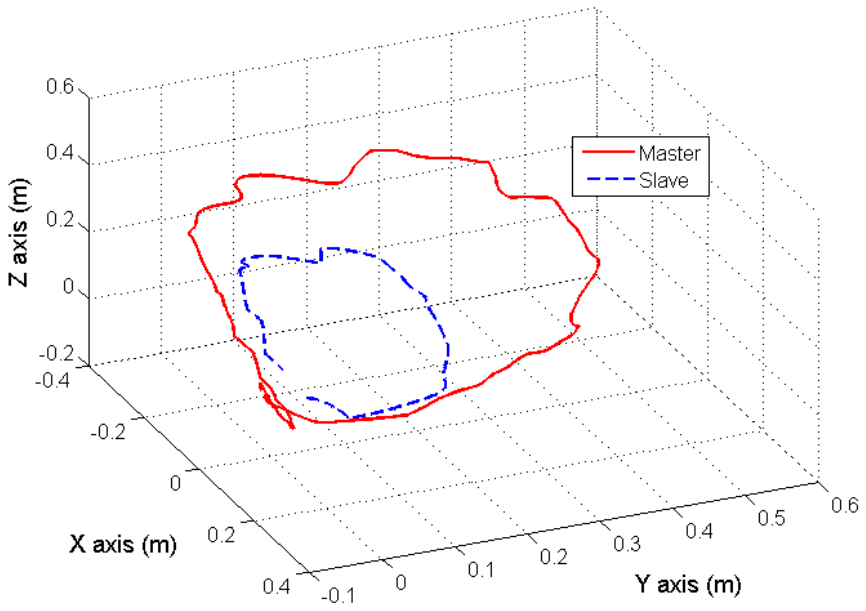

Figure 4.23. Drawing letter “O” using proposed system

4.4 Prescribed performance control with extended wave-based TDPA

Our proposed wave-based TDPA in Section 4.3 can significantly enhance the system transparency compared with the previous approaches in the presence of arbitrary time delays. However, it is only proposed to guarantee the passivity of communication channels. In practice, the control algorithms in the master side and the slave sides can also insert extra energy into the system especially when the measured external force signals are involved, to the extent that the overall system’s passivity may still be easily jeopardized without proper control parameters. Further exploration for of the TDPA based control researches is still needed.

Traditionally, the transient-state control performance is the main criterion in a control system [159]. Ilchmann et al. further analyse the tracking control for the nonlinear system and introduces the prescribed performance control (PPC) to obtain the prescribed desired transient behaviour [160].. The principal purpose of the PPC is to restrict the boundary of the tracking error to a randomly predefined small residual set with a convergence speed below a prescribed value, exhibiting a maximum overshoot less than a prescribed specified constant [161]. Xie et al. propose a new control

algorithm combined with neural network for a robot system to assure the system's tracking error to be restricted by a prescribed decreasing boundary [162]. Bechlioulis et al. propose a new neuro-adaptive force/position control algorithm [163]. The performance of error evolution within prescribed bounds in both problems of regulation and tracking in robotic system is achieved in [164]. Kostarigka et al. analyse the pre-set performance control problem for a flexible joint robot with unknown and possibly variable elasticity [165]. In the bilateral teleoperation research, Yang et al firstly apply the PPC to enhance the position synchronization performance [166]-[167] of the master and the slave robots. However, their approach primitively primarily has two major shortcomings. First, their proposed PPC approaches methods can only guarantee the position synchronization in the presence of constant time delays. Secondly, they only consider the case of free space movement without the effect of human and environmental forces is considered. In [168], they treat the external forces as disturbances that are eliminated by using fuzzy logic controllers, whereas in the real application in the environmental contact, the external forces are non-removal. In fact, force tracking also plays a crucial role in the application of bilateral teleoperation that can largely enhance perception of the operator of the remote environment.

In this section, we have further extended the wave-based TDPA in section 3.3 to guarantee the passivity of the overall system by introducing new passivity observers and controllers to monitor the passivity of the master side and the slave side. Furthermore, we apply the PPC algorithm to achieve prescribed transient tracking behaviour of the position, velocity and external force signals. By combining the extended wave-based TDPA and PPC algorithms, the proposed system can achieve reasonable position, velocity and force tracking performances in the presence of arbitrary time delays.

4.4.1 Problem formulation

We define the new synchronization variables as $r_i(t) = \dot{q}_i(t) + \delta q_i(t)$ where δ is a positive constant. The primitive objective of a bilateral teleoperation is to have the positions of the slave accurately synchronized to the position of the master. In the

presence of time-varying delays, the position and velocity synchronization errors between the master and the slave can be defined as (3.61)-(3.62)

In this section, the unsymmetrical time delays $T_1(t)$ and $T_2(t)$ are assumed not to increase or decrease faster than the time itself. That is, $\left|\dot{T}_{1,2}(t)\right| \leq \bar{\mu}_{1,2} < 1$, where $\bar{\mu}_{1,2}$ are the upper bounds of $\dot{T}_{1,2}(t)$.

A secondary objective of the bilateral teleoperation is that the operator can genuinely feel the remote environment, which is predicated on the accurate force tracking between the two robots. In this section, the measured human and environmental torques are modeled as (15)-(16) which contains position and velocity signals [28]-[29], [157]. The measured external torques are acquired by using the extended active observer [50].

$$\tau_h(t) = -\alpha_m r_m(t) \tag{4.67}$$

$$\tau_e(t) = \alpha_s r_s(t) \tag{4.68}$$

where α_m and α_s are positive constants. Therefore, the torque tracking errors are defined as (17)-(18) where k_{1-2} are positive definite diagonal matrices.

$$e_{tm}(t) = k_1\tau_h(t) + k_2\tau_e\big(t - T_2(t)\big) \tag{4.69}$$

$$e_{ts}(t) = -k_1\tau_h\big(t - T_1(t)\big) - k_2\tau_e(t) \tag{4.70}$$

Based on the position, velocity and torque tracking errors e_{pi}, e_{vi} and e_{ti} on the slave and the master sides, we can define the total errors for tracking of the transmission signals:

$$\begin{aligned} e_m(t) &= e_{vm}(t) + \delta e_{pm}(t) + e_{tm}(t) \\ &= r_s\big(t - T_2(t)\big) - r_m(t) + k_2\alpha_s r_s\big(t - T_2(t)\big) - k_1\alpha_m r_m(t) \end{aligned} \tag{4.71}$$

$$\begin{aligned} e_s(t) &= e_{vs}(t) + \delta e_{ps}(t) + e_{ts}(t) \\ &= r_m\big(t - T_1(t)\big) - r_s(t) + k_1\alpha_m r_m\big(t - T_1(t)\big) - k_2\alpha_s r_s(t) \end{aligned} \tag{4.72}$$

Considering the effect of the time-varying delays, $\dot{e}_i(t)$ can be written as:

$$\dot{e}_m(t) = (1 - \dot{T}_2(t))\dot{r}_s\big(t - T_2(t)\big) - \dot{r}_m(t) + (1 - \dot{T}_2(t))k_2\alpha_s\dot{r}_s\big(t - T_2(t)\big) - k_1\alpha_m\dot{r}_m(t) \tag{4.73}$$

$$\dot{e}_s(t) = \Big(1 - \dot{T}_1(t)\Big)\dot{r}_m\big(t - T_1(t)\big) - \dot{r}_s(t) + \Big(1 - \dot{T}_1(t)\Big)k_1\alpha_m\dot{r}_m\big(t - T_1(t)\big) - k_2\alpha_s\dot{r}_s(t) \tag{4.74}$$

where $\dot{r}_i(t) = \ddot{q}_i(t) + \delta\dot{q}_i(t)$ contains the velocity and acceleration signals.

The prescribed performance consists of the minimum convergence velocity, the maximum steady state error and the maximum allowed overshoot are set to be a priori. Considering the tracking errors e_i in (4.73)-(4.74), the prescribed performance is achieved if e_i are restricted in a predefined region bounded by a decaying function of time. The prescribed performance can be expressed as:

$$\begin{cases} -H_iA_i(t) < e_i(t) < A_i(t), & if\ e_i(0) \geq 0 \\ -A_i(t) < e_i(t) < H_iA_i(t), & if\ e_i(0) \leq 0 \end{cases} \tag{4.75}$$

where $0 < H_i < 1$ and $A_i(t)$ is defined as:

$$A_i(t) = (A_{i0} - A_{i\infty})e^{-L_it} + A_{i\infty} \tag{4.76}$$

where A_{i0} , $A_{i\infty}$ and L_i are positive constants. $A_{i0} = A_i(0)$ and $A_{i\infty} = lim_{t\to\infty}A_i(t)$. A_{i0} is the initial value of $A_i(t)$, L_i is the minimum convergence velocity and $A_{i\infty}$ is the maximum allowed steady state error.

Define

$$\epsilon_i(t) = R_i(\frac{e_i(t)}{A_i(t)}) \tag{4.77}$$

where $\epsilon_i(t)$ is the error vector via transformation. R_i is a smooth, strictly increasing function shown as follows:

$$R_i\left(\frac{e_i(t)}{A_i(t)}\right)=\begin{cases} ln\dfrac{\dfrac{e_i(t)}{A_i(t)}+H_i}{H_i-H_i\dfrac{e_i(t)}{A_i(t)}}, & if\ e_i(0)\geq 0 \\ ln\dfrac{H_i\dfrac{e_i(t)}{A_i(t)}+H_i}{H_i-\dfrac{e_i(t)}{A_i(t)}}, & if\ e_i(0)<0 \end{cases} \tag{4.78}$$

The derivative of $\epsilon_i(t)$ can be written as:

$$\dot{\epsilon}_i(t)=\partial R_i\left(\dot{e}_i(t)-\frac{\dot{A}_i(t)e_i(t)}{A_i(t)}\right) \tag{4.79}$$

where $\partial R_i=\frac{\partial R_i}{\partial e_i/A_i}\frac{1}{A_i}$.

Since R_i is a smooth strictly increasing function and satisfies: $R_i\colon(-H_i,1)\rightarrow(-\infty,+\infty), e_i(0)\geq 0$ and $R_i\colon(-1,H_i)\rightarrow(-\infty,+\infty), e_i(0)<0$ based on (4.75), by guaranteeing the boundedness of $\epsilon_i(t)$, (4.75) can be achieved. When $\epsilon_i(t)$ converges to zero, e_i will also converges to zero to the extent that the accurate position, velocity and torque tracking can be achieved. Based on equation (4.78), the following inequalities are true

$$\begin{cases} -L_i<\dfrac{\dot{A}_i(t)}{A_i(t)}<0 \\ |\epsilon_i(t)|>\dfrac{4}{(H_i+1)A_i(t)}|e_i(t)| \\ \partial R_i>\dfrac{4}{(H_i+1)A_i(t)}>\dfrac{4}{(H_i+1)A_{i0}}>0 \\ e_i^T(t)\partial R_i\epsilon_i(t)\geq\left(\dfrac{4}{(H_i+1)A_{i0}}\right)^2\|e_i\|^2 \end{cases} \tag{4.80}$$

4.4.2 Control algorithm design

The master-slave teleoperation system can be described by the pairs of power-conjugated variables, force, position and velocity at each terminal. Equation (4.81) describes the power flow $P(t)$ to the bilateral teleoperation.

$$\begin{aligned} P(t) &= V_{ou}(t)I_{in}(t) - V_{in}(t)I_{ou}(t) \\ &= \underbrace{\left(V_{ou}(t)I_{in}(t) - V_m(t)I_m(t)\right)}_{P_m-master} + \underbrace{\left(V_m(t)I_m(t) - V_s(t)I_s(t)\right)}_{P_{com}-comm.\ cha.} \\ &+ \underbrace{\left(V_s(t)I_s(t) - V_{in}(t)I_{ou}(t)\right)}_{P_s-slave} \end{aligned} \tag{4.81}$$

where $V_{ou}(t)$, $I_{in}(t)$, $V_{in}(t)$ and $I_{ou}(t)$ are output signal from the master, input signal into the master, input signal into the slave and output signal from the slave. $V_m(t)$, $I_m(t)$, $V_s(t)$ and $I_s(t)$ are the transmission control signals for the communication channels. From (4.81), only when the passivity of the master, the communication channels and the slave are simultaneously maintained, can the overall system's passivity be guaranteed.

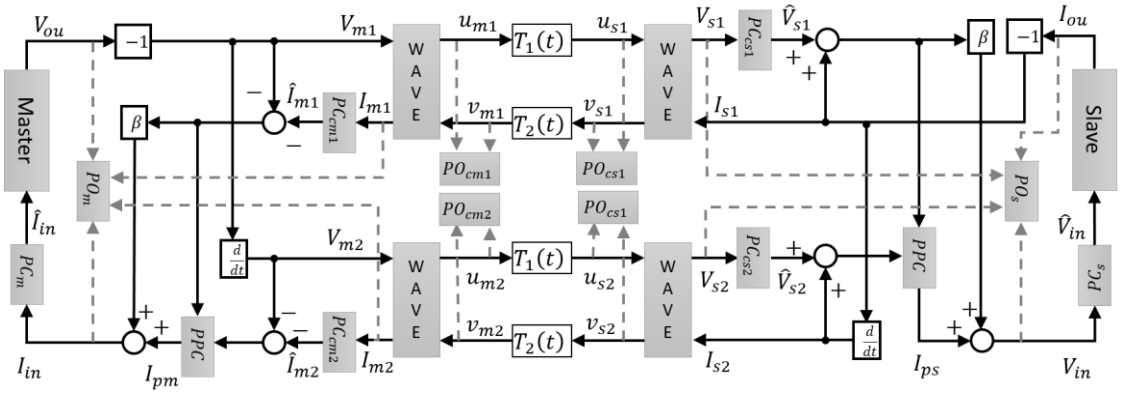

Figure 4.24. Total block diagram

The total block diagram of the proposed system is shown in Fig.3, where

$$V_{ou}(t) = -r_m(t) + k_1\tau_h(t)$$
$$I_{ou}(t) = r_s(t) + k_2\tau_e(t)$$

$$V_{m1}(t) = -V_{ou}(t)$$
$$V_{m2}(t) = -\dot{V}_{ou}(t) = \dot{r}_m(t) - k_1\dot{\tau}_h(t)$$
$$I_{s1}(t) = -I_{ou}(t)$$
$$I_{s2}(t) = -\dot{I}_{ou}(t) = -\dot{r}_s(t) - k_2\dot{\tau}_e(t) \tag{4.82}$$

$V_{m1}(t)$ and $V_{m2}(t)$, $I_{s1}(t)$ and $I_{s2}(t)$ are separately transmitted via the wave transformation in Fig.2 for their further application in PPC controllers. Therefore, the power flow P_{com} in the communication channels can be expressed as: $P_{com}(t) = P_{com1}(t) + P_{com2}(t) = \big(V_{m1}(t)I_{m1}(t) - V_{s1}(t)I_{s1}(t)\big) + \big(V_{m2}(t)I_{m2}(t) - V_{s2}(t)I_{s2}(t)\big)$. we design the passivity observers for the communication channels as ($j = 1,2$):

$$P_{cmj}(t) = \frac{2}{1+B}u_{mj}^T(t)u_{mj}(t) + \frac{2}{M(1+B)}v_{mj}^T(t)v_{mj}(t) - \frac{1}{M(1+B)}\Big(v_{mj}(t) - Mu_{mj}(t)\Big)^T\Big(v_{mj}(t) - Mu_{mj}(t)\Big) - \frac{1}{M(1+B)}\varepsilon_2 v_{mj}^T(t)v_{mj}(t) \tag{4.83}$$

$$P_{csj}(t) = \frac{2}{B(1+B)}v_{sj}^T(t)v_{sj}(t) + \frac{2M}{1+B}u_{sj}^T(t)u_{sj}(t) - \frac{1}{M(1+B)}\Big(v_{sj}(t) + Mu_{sj}(t)\Big)^T\Big(v_{sj}(t) + Mu_{sj}(t)\Big) - \frac{M}{1+B}\varepsilon_1 u_{sj}^T(t)u_{sj}(t) \tag{4.84}$$

Based on (4.83) and (4.84), since $P_{cm}(t)$ and $P_{cs}(t)$ only have the information observed at the master and slave terminals, respectively, $P_{cm}(t)$ and $P_{cs}(t)$ can observe the power dissipation components in real time. The proposed wave transformation aims to guarantee the passivity of the communication channels in the presence of constant delays. When $\dot{T}_{1,2} \geq 0$, $P_{cm}(t)$ and $P_{cs}(t)$ are required to observe non-negative power information so that the passivity controllers will not be launched to affect the system transparency. As analysed in Section 4.3, by setting $2\sqrt{\frac{(2-M)}{M}} \geq$

$2 \Rightarrow 1 \geq M > 0$ and $\frac{2}{B} - \frac{1}{M} \geq 0 \Rightarrow 2M \geq B > 1$, $P_{cmj}(t)$ and $P_{csj}(t)$ can surely observe non-negative power information when $\dot{T}_{1,2} \geq 0$. $\varepsilon_{1,2}$ in (4.82)-(4.83) are the measured differential of time delays using the Time delay differential estimator in Fig.4.2. The measured $\dot{T}_{1,2}$ can be applied to the proposed passivity observers and the PPC controllers.

We design the passivity controllers for the communication channels as:

$$\hat{I}_{mj}(t) = I_{mj}(t) + \Gamma_{cmj}(t)V_{mj}(t) \tag{4.85}$$

$$\hat{V}_{sj}(t) = V_{sj}(t) + \Gamma_{csj}(t)I_{sj}(t) \tag{4.86}$$

where

$$\Gamma_{cmj}(t) = \begin{cases} 0, \ \ if\ P_{cmj}(t) > 0 \\ -P_{cmj}(t)\left(V_{mj}^T(t)V_{mj}(t)\right)^{-1}, \ \ else, if\ \left|V_{mj}(t)\right| > 0 \end{cases} \tag{4.87}$$

$$\Gamma_{csj}(t) = \begin{cases} 0, \ \ if P_{csj}(t) > 0 \\ P_{csj}(t)\left(I_s^T(t)I_s(t)\right)^{-1}, \ \ else, if\ |I_s(t)| > 0 \end{cases} \tag{4.88}$$

Moreover, to observe the power flow on the master and slave sides, we also design the passivity observers to be:

$$P_m(t) = V_{ou}(t)I_{in}(t) - V_{m1}(t)I_{m1}(t) - V_{m2}(t)I_{m2}(t) \tag{4.89}$$

$$P_s(t) = V_{s1}(t)I_{s1}(t) + V_{s2}(t)I_{s2}(t) - V_{in}(t)I_{ou}(t) \tag{4.90}$$

The passivity controllers for the master and the slave side are designed as:

$$\hat{I}_{in}(t) = I_{in}(t) + \Gamma_m(t)V_{ou}(t) \tag{4.91}$$

$$\hat{V}_{in}(t) = V_{in}(t) + \Gamma_s(t)I_{ou}(t) \tag{4.92}$$

where

$$\Gamma_m(t) = \begin{cases} 0, \ \ if\ P_m(t) > 0 \\ \left(-P_m(t) + \sum_{j=1}^{2} \Gamma_{cmj}(t) V_{mj}^T(t) V_{mj}(t)\right)\left(V_{ou}^T(t) V_{ou}(t)\right)^{-1}, \\ else, if\ |V_{ou}(t)| > 0 \end{cases} \tag{4.93}$$

$$\Gamma_s(t) = \begin{cases} 0, \ \ if P_s(t) > 0 \\ \left(P_s(t) + \sum_{j=1}^{2} \Gamma_{csj}(t) I_{sj}^T(t) I_{sj}(t)\right)\left(I_{ou}^T(t) I_{ou}(t)\right)^{-1}, \\ else, if\ |I_{ou}(t)| > 0 \end{cases} \tag{4.94}$$

$\hat{I}_{in}(t)$ and $\hat{V}_{in}(t)$ can be seen as the final inputs to the master and the slave robots. Based on (4.87)-(4.88) and (4.93)-(4.94), it is noticeable that $\Gamma_{cmj}(t) \geq 0$, $\Gamma_{csj}(t) \leq 0$, $\Gamma_m(t) \geq 0$, $\Gamma_s(t) \leq 0$.

Theorem 4.4. The designed passivity controllers (43)-(52) can ensure the passivity of the whole master-slave system in the presence of arbitrary time delays.

Proof.

$$P^*(t) = V_{ou}(t)\hat{I}_{in}(t) - \hat{V}_{in}(t) I_{ou}(t)$$
$$= \left(V_{ou}(t)\hat{I}_{in}(t) - V_{m1}(t)\hat{I}_{m1}(t) - V_{m2}(t)\hat{I}_{m2}(t)\right) + \left(V_{m1}(t)\hat{I}_{m1}(t) - \hat{V}_{s1}(t) I_{s1}(t) + V_{m2}(t)\hat{I}_{m2}(t) - \hat{V}_{s2}(t) I_{s2}(t)\right) + \left(\hat{V}_{s1}(t) I_{s1}(t) + \hat{V}_{s2}(t) I_{s2}(t) - \hat{V}_{in}(t) I_{ou}(t)\right)$$
$$= \left(V_{ou}(t)\left(I_{in}(t) + \Gamma_m(t) V_{ou}(t)\right) - \sum_{j=1}^{2} V_{mj}(t)\left(I_{mj}(t) + \Gamma_{cmj}(t) V_{mj}(t)\right)\right) + \sum_{j=1}^{2}\left(V_{mj}(t)\left(I_{mj}(t) + \Gamma_{cmj}(t) V_{mj}(t)\right) - \left(V_{sj}(t) + \Gamma_{csj}(t) I_{sj}(t)\right) I_{sj}(t)\right) + \left(\sum_{j=1}^{2}\left(V_{sj}(t) + \Gamma_{csj}(t) I_{sj}(t)\right) I_{sj}(t) - \left(V_{in}(t) + \Gamma_s(t) I_{ou}(t)\right) I_{ou}(t)\right)$$

$$= \left(P_m - \sum_{j=1}^{2} \Gamma_{cmj}(t) V_{mj}^T(t) V_{mj}(t) + \Gamma_m(t) V_{ou}^T(t) V_{ou}(t)\right) + \sum_{j=1}^{2} \left(P_{cmj}(t) + P_{csj}(t) + \frac{dE_j(t)}{dt} + \Gamma_{cmj}(t) V_{mj}^T(t) V_{mj}(t) - \Gamma_{csj}(t) I_{sj}^T(t) I_{sj}(t)\right) + \left(P_s + \sum_{j=1}^{2} \Gamma_{csj}(t) I_{sj}^T(t) I_{sj}(t) - \Gamma_s(t) I_{ou}^T(t) I_{ou}(t)\right)$$

$$= P_m^*(t) + P_{diss}^*(t) + \frac{dE}{dt}(t) + P_s^*(t)$$

Based on the definitions of the passivity controllers, $P_m^*(t)$, $P_{diss}^*(t)$ and $P_s^*(t)$ are ensured to be non-negative, which is the sufficient condition for guaranteeing the passivity of the master-slave system.

The outputs of the PPC controllers are given as:

$$I_{pm}(t) = d_m \partial R_m \epsilon_m(t) + \bar{I}_{pm}(t) - \Gamma_{cm2}(t) V_{m2}(t) \tag{4.95}$$

$$I_{ps}(t) = d_s \partial R_s \epsilon_s(t) + \bar{I}_{ps}(t) - \Gamma_{cs2}(t) I_{s2}(t) \tag{4.96}$$

where

$$\bar{I}_{pm}(t) = \begin{cases} \dfrac{\left(I_{m1}(t) - k_1 \tau_h(t) - \dfrac{1}{d_m} \dot{e}_m(t)\right) d_m \partial R_m \epsilon_m(t) r_m(t)}{\|r_m(t)\|^2}, if\ \|r_m(t)\|^2 > 0 \\ 0,\ \ if\ \|r_m(t)\|^2 = 0 \end{cases} \tag{4.97}$$

$$\bar{I}_{ps}(t) = \begin{cases} \dfrac{\left(k_2 \tau_e(t) - V_{s1}(t) - \dfrac{1}{d_s} \dot{e}_s(t)\right) d_s \partial R_s \epsilon_s(t) r_s(t)}{\|r_m(t)\|^2}, if\ \|r_s(t)\|^2 > 0 \\ 0,\ \ if\ \|r_s(t)\|^2 = 0 \end{cases} \tag{4.98}$$

d_m and d_s are positive definite diagonal matrices.

By using the extended TDPA and PPC algorithms, the control terms $S_m(t)$ and $S_s(t)$ can be finally designed as:

$$S_m(t) = \hat{I}_{in}(t) = \beta\left(-V_{m1}(t) - \hat{I}_{m1}(t)\right) + I_{pm}(t) + \Gamma_m(t)V_{ou}(t)$$
$$= \beta\left(r_s\left(t - T_2(t)\right) - r_m(t)\right) + \beta\left(k_1\tau_h(t) + k_2\tau_e\left(t - T_2(t)\right)\right)$$
$$- \Gamma_{cm1}(t)\left(r_m(t) - k_1\tau_h(t)\right) + d_m\partial R_m\epsilon_m(t) + \bar{I}_{pm}(t)$$
$$- \Gamma_{cm2}(t)\left(\dot{r}_m(t) - k_1\dot{\tau}_h(t)\right) - \Gamma_m(t)\left(r_m(t) - k_1\tau_h(t)\right) \quad (4.99)$$

$$S_s(t) = \hat{V}_{in}(t) = \beta\left(\hat{V}_{s1}(t) + I_{s1}(t)\right) + d_s\partial R_s\epsilon_s(t) + \bar{I}_{ps}(t) - \Gamma_{cs2}(t)I_{s2}(t)$$
$$+ \Gamma_s(t)I_{ou}(t)$$
$$= \beta\left(r_m\left(t - T_1(t)\right) - r_s(t)\right) - \beta\left(k_1\tau_h\left(t - T_1(t)\right) + k_2\tau_e(t)\right)$$
$$- \Gamma_{cs1}(t)\left(r_s(t) + k_2\tau_e(t)\right) + d_s\partial R_s\epsilon_s(t) + \bar{I}_{ps}(t)$$
$$+ \Gamma_{cs2}(t)\left(\dot{r}_s(t) + k_2\dot{\tau}_e(t)\right) + \Gamma_s(t)\left(r_s(t) + k_2\tau_e(t)\right) \quad (4.100)$$

4.4.3 Stability analysis

This section analyzes stability and position and torque tracking performances of the system in Section 4.4 using Lyapunov functions.

Theorem 4.5. Considering the bilateral teleoperation described in (3.37)-(3.38) and control laws in (4.99)-(4.100), then with the human and environmental torques modeled as (4.67)-(4.68), the errors of position, velocity and torque are bounded and the prescribed synchronization performance is guaranteed.

Proof. Consider a positive semi-definite function $V = V_1 + V_2 + V_3$ for the system as:

$$V_1 = \frac{1}{2}\left[r_m^T(t)M_m(q_m)r_m(t) + r_s^T(t)M_s(q_s)r_s(t) + \tilde{\theta}_m^T\Gamma^{-1}\tilde{\theta}_m + \tilde{\theta}_s^T\Lambda^{-1}\tilde{\theta}_s\right] \quad (4.101)$$

$$V_2 = \frac{\beta}{2}\frac{1}{1-\dot{T}_1(t)}\int_{t-T_1(t)}^{t} r_m^T(\eta) r_m(\eta) d\eta + \frac{\beta}{2}\frac{1}{1-\dot{T}_2(t)}\int_{t-T_2(t)}^{t} r_s^T(\eta) r_s(\eta) d\eta$$
$$+ \frac{\beta k_1 \alpha_m}{2}\frac{1}{1-\dot{T}_1(t)}\int_{t-T_1(t)}^{t} r_m^T(\eta)\, r_m(\eta) d\eta$$
$$+ \frac{\beta k_2 \alpha_s}{2}\frac{1}{1-\dot{T}_2(t)}\int_{t-T_2(t)}^{t} r_s^T(\eta)\, r_s(\eta) d\eta + q_m^T(t)\alpha_m \delta q_m(t)$$
$$+ q_s^T(t)\alpha_s \delta q_s(t) + \dot{q}_m^T(t)\Gamma_{cm2}(t)\delta\dot{q}_m(t)$$
$$+ \dot{q}_m^T(t) k_1 \alpha_m \Gamma_{cm2}(t)\delta\dot{q}_m(t) + \dot{q}_s^T(t)\big(-\Gamma_{cs2}(t)\big)\delta\dot{q}_s(t)$$
$$+ \dot{q}_s^T(t)\big(-k_2\alpha_s\Gamma_{cs2}(t)\big)\delta\dot{q}_s(t) \qquad (4.102)$$

$$V_3 = \frac{1}{2}\epsilon_m^T\epsilon_m + \frac{1}{2}\epsilon_s^T\epsilon_s \qquad (4.103)$$

The derivative of V_1 with the adaptive tuning laws and the definitions of e_i and $\dot{e}_i$ is given by

$$\dot{V}_1 = r_m^T(t)\Big[\beta\Big(r_s\big(t-T_2(t)\big) - r_m(t)\Big) + \beta\Big(k_1\tau_h(t) + k_2\tau_e\big(t-T_2(t)\big)\Big)$$
$$- \Gamma_{cm1}(t)\big(r_m(t) - k_1\tau_h(t)\big) - \Gamma_{cm2}(t)\big(\dot{r}_m(t) - k_1\dot{\tau}_h(t)\big)$$
$$- \Gamma_m(t)\big(r_m(t) - k_1\tau_h(t)\big) + \tau_h(t)\Big]$$
$$+ r_s^T(t)\Big[\beta\Big(r_m\big(t-T_1(t)\big) - r_s(t)\Big)$$
$$- \beta\Big(k_1\tau_h\big(t-T_1(t)\big) + k_2\tau_e(t)\Big) - \Gamma_{cs1}(t)\big(r_s(t) + k_2\tau_e(t)\big)$$
$$+ \Gamma_{cs2}(t)\big(\dot{r}_s(t) + k_2\dot{\tau}_e(t)\big) + \Gamma_s(t)\big(r_s(t) + k_2\tau_e(t)\big)\Big] - (d_m e_m(t)$$
$$+ \dot{e}_m(t))\partial R_m\epsilon_m(t) - (d_s e_s(t) + \dot{e}_s(t))\partial R_s\epsilon_s(t) \qquad (4.104)$$

The time derivatives of V_2 are given as

$$\dot{V}_2 = \frac{\beta}{2}\left(r_m^T(t) r_m(t) - r_m^T\big(t - T_1(t)\big) r_m\big(t - T_1(t)\big) + \frac{\dot{T}_1(t)}{1 - \dot{T}_1(t)} r_m^T(t) r_m(t) \right)$$
$$+ \frac{\beta}{2}\left(r_s^T(t) r_s(t) - r_s^T\big(t - T_2(t)\big) r_s\big(t - T_2(t)\big) \right.$$
$$\left. + \frac{\dot{T}_2(t)}{1 - \dot{T}_2(t)} r_s^T(t) r_s(t) \right)$$
$$+ \frac{\beta k_1 \alpha_m}{2}\left(r_m^T(t) r_m(t) - r_m^T\big(t - T_1(t)\big) r_m\big(t - T_1(t)\big) \right.$$
$$\left. + \frac{\dot{T}_1(t)}{1 - \dot{T}_1(t)} r_m^T(t) r_m(t) \right)$$
$$+ \frac{\beta k_2 \alpha_s}{2}\left(r_s^T(t) r_s(t) - r_s^T\big(t - T_2(t)\big) r_s\big(t - T_2(t)\big) \right.$$
$$\left. + \frac{\dot{T}_2(t)}{1 - \dot{T}_2(t)} r_s^T(t) r_s(t) \right) + 2 q_m^T(t) \alpha_m \delta \dot{q}_m(t) + 2 q_s^T(t) \alpha_s \delta \dot{q}_s(t)$$
$$+ 2 \dot{q}_m^T(t) \Gamma_{cm2}(t) \delta \ddot{q}_m(t) + 2 \dot{q}_m^T(t) k_1 \alpha_m \Gamma_{cm2}(t) \delta \ddot{q}_m(t)$$
$$+ 2 \dot{q}_s^T(t) \big(-\Gamma_{cs2}(t)\big) \delta \ddot{q}_s(t) + 2 \dot{q}_s^T(t) \big(-k_2 \alpha_s \Gamma_{cs2}(t)\big) \delta \ddot{q}_s(t) \quad (4.105)$$

Applying (4.77) and (4.80), the derivative of V_3 can be expressed as

$$\dot{V}_3 = \epsilon_m^T(t) \dot{\epsilon}_m(t) + \epsilon_s^T(t) \dot{\epsilon}_s(t)$$
$$= \epsilon_m^T(t) \partial R_m \left(\dot{e}_m(t) - \frac{\dot{A}_m(t) e_m(t)}{A_m(t)} \right)$$
$$+ \epsilon_s^T(t) \partial R_s \left(\dot{e}_s(t) - \frac{\dot{A}_s(t) e_s(t)}{A_s(t)} \right)$$
$$\leq \epsilon_m^T(t) \partial R_m \dot{e}_m(t) + \epsilon_m^T(t) \partial R_m L_m e_m(t) + \epsilon_m^T(t) \partial R_m \dot{e}_m(t)$$
$$+ \epsilon_m^T(t) \partial R_m L_m e_m(t) \quad (4.106)$$

With (4.104)-(4.106) and applying (4.80), $\dot{V}$ can be derived as:

$$\dot{V} \leq \left(\left(\frac{\beta k_1 \alpha_m}{2} + \Gamma_{cm1}(t) + k_1 \alpha_m \Gamma_{cm1}(t) + \Gamma_m(t) + k_1 \alpha_m \Gamma_m(t) - \frac{\dot{T}_1(t)\beta}{2 - 2\dot{T}_1(t)} \right.\right.$$
$$\left. - \frac{\dot{T}_1(t)\beta k_1 \alpha_m}{2 - 2\dot{T}_1(t)} \right) r_m^T(t) r_m(t) - \beta k_2 \alpha_s r_m^T(t) r_s\big(t - T_2(t)\big)$$
$$\left. + \frac{\beta k_2 \alpha_s}{2} r_s^T\big(t - T_2(t)\big) r_s\big(t - T_2(t)\big) \right)$$
$$- \left(\left(\frac{\beta k_2 \alpha_s}{2} + \Gamma_{cs1}(t) + k_2 \alpha_s \Gamma_{cs1}(t) - \Gamma_s(t) - k_2 \alpha_s \Gamma_s(t) \right.\right.$$
$$- \frac{\dot{T}_2(t)\beta}{2 - 2\dot{T}_2(t)} - \frac{\dot{T}_2(t)\beta k_2 \alpha_s}{2 - 2\dot{T}_2(t)} \Big) r_s^T(t) r_s(t)$$
$$\left. - \beta k_1 \alpha_m r_s^T(t) r_m\big(t - T_1(t)\big) + \frac{\beta k_1 \alpha_m}{2} r_m^T\big(t - T_1(t)\big) r_m\big(t - T_1(t)\big) \right)$$
$$- \ddot{q}_m^T(t) \Gamma_{cm2}(t) \ddot{q}_m(t) - \dot{q}_m(t) \Gamma_{cm2}(t) \delta^2 \dot{q}_m(t)$$
$$- \ddot{q}_m^T(t) k_1 \alpha_m \Gamma_{cm2}(t) \ddot{q}_m(t) - \dot{q}_m(t) k_1 \alpha_m \Gamma_{cm2}(t) \delta^2 \dot{q}_m(t)$$
$$- \ddot{q}_s^T(t)\big(-\Gamma_{cs2}(t)\big)\ddot{q}_s(t) - \dot{q}_s(t)\big(-\Gamma_{cs2}(t)\big)\delta^2 \dot{q}_s(t)$$
$$- \ddot{q}_s^T(t)\big(-k_2 \alpha_s \Gamma_{cs2}(t)\big)\ddot{q}_s(t) - \dot{q}_s(t)\big(-k_2 \alpha_s \Gamma_{cs2}(t)\big)\delta^2 \dot{q}_s(t)$$
$$- \frac{\beta}{2}\Big(e_{vm}(t) + \delta e_{pm}(t)\Big)^T \Big(e_{vm}(t) + \delta e_{pm}(t)\Big)$$
$$- \frac{\beta}{2}\Big(e_{vs}(t) + \delta e_{ps}(t)\Big)^T \Big(e_{vs}(t) + \delta e_{ps}(t)\Big)$$
$$- \big(\dot{q}_m^T(t) \alpha_m \dot{q}_m(t) + q_m^T(t) \alpha_m \delta^2 q_m(t) + \dot{q}_s^T(t) \alpha_s \dot{q}_s(t)$$
$$+ q_s^T(t) \alpha_s \delta^2 q_s(t)\big) - (d_m - L_m)\left(\frac{4}{(H_m + 1)A_{m0}}\right)^2 \|e_m(t)\|^2$$
$$- (d_s - L_s)\left(\frac{4}{(H_s + 1)A_{s0}}\right)^2 \|e_s(t)\|^2 \qquad (4.107)$$

In order to derive a negative semi-definite $\dot{V}$, the first two terms of (4.107) must be non-positive. A sufficient condition is derived as:

$$\left(\beta k_1\alpha_m + 2\Gamma_{cm1}(t) + 2k_1\alpha_m\Gamma_{cm1}(t) + 2\Gamma_m(t) + 2k_1\alpha_m\Gamma_m(t) - \frac{\dot{T}_1(t)\beta}{1-\dot{T}_1(t)} - \frac{\dot{T}_1(t)\beta k_1\alpha_m}{1-\dot{T}_1(t)}\right) \geq \beta k_2\alpha_s \quad (4.108)$$

$$\left(\beta k_2\alpha_s + 2\Gamma_{cs1}(t) + 2k_2\alpha_s\Gamma_{cs1}(t) - 2\Gamma_s(t) - 2k_2\alpha_s\Gamma_s(t) - \frac{\dot{T}_2(t)\beta}{1-\dot{T}_2(t)} - \frac{\dot{T}_2(t)\beta k_2\alpha_s}{1-\dot{T}_2(t)}\right) \geq \beta k_1\alpha_m \quad (4.109)$$

According to Section 3, when the time delays are varying, the terms $\frac{\dot{T}_1(t)}{1-\dot{T}_1(t)}$ and $\frac{\dot{T}_2(t)}{1-\dot{T}_2(t)}$ can be seen as the energy generated by the increasing time delays which can be dissipated by the passivity controllers as analyzed in Section 3. By treating the terms $\Gamma_{cm1}(t)$, $\Gamma_{cs1}(t)$, $\Gamma_m(t)$, $\Gamma_s(t)$, $\frac{\dot{T}_1(t)}{1-\dot{T}_1(t)}$, $\frac{\dot{T}_2(t)}{1-\dot{T}_2(t)}$ to be zero, (4.108) and (4.109) can be simplified as

$$k_1\alpha_m = k_2\alpha_s \quad (4.110)$$

To guarantee $-(d_m - L_m)\left(\frac{4}{(H_m+1)A_{m0}}\right)^2 \|e_m(t)\|^2 - (d_s - L_s)\left(\frac{4}{(H_s+1)A_{s0}}\right)^2 \|e_s(t)\|^2$ to be negative semi-definite, (4.111)-(4.112) should be satisfied.

$$d_m \geq L_m \quad (4.111)$$

$$d_s \geq L_s \quad (4.112)$$

By satisfying (4.111)-(4.112), $\dot{V}$ is guaranteed to be negative semi-definite. Integrating both sides of (4.107), we get

$$
\begin{aligned}
+\infty > V(0) &\geq V(0) - V(t) \\
&\geq \int_0^t \ddot{q}_m^T(t)\Gamma_{cm2}(t)\ddot{q}_m(t) + \dot{q}_m(t)\Gamma_{cm2}(t)\delta^2\dot{q}_m(t) \\
&+ \ddot{q}_m^T(t)k_1\alpha_m\Gamma_{cm2}(t)\ddot{q}_m(t) + \dot{q}_m(t)k_1\alpha_m\Gamma_{cm2}(t)\delta^2\dot{q}_m(t) \\
&+ \ddot{q}_s^T(t)\big(-\Gamma_{cs2}(t)\big)\ddot{q}_s(t) + \dot{q}_s(t)\big(-\Gamma_{cs2}(t)\big)\delta^2\dot{q}_s(t) \\
&+ \ddot{q}_s^T(t)\big(-k_2\alpha_s\Gamma_{cs2}(t)\big)\ddot{q}_s(t) + \dot{q}_s(t)\big(-k_2\alpha_s\Gamma_{cs2}(t)\big)\delta^2\dot{q}_s(t) \\
&+ \frac{\beta}{2}\Big(e_{vm}(t) + \delta e_{pm}(t)\Big)^T\Big(e_{vm}(t) + \delta e_{pm}(t)\Big) \\
&+ \frac{\beta}{2}\Big(e_{vs}(t) + \delta e_{ps}(t)\Big)^T\Big(e_{vs}(t) + \delta e_{ps}(t)\Big) \\
&+ \big(\dot{q}_m^T(t)\alpha_m\dot{q}_m(t) + q_m^T(t)\alpha_m\delta^2 q_m(t) + \dot{q}_s^T(t)\alpha_s\dot{q}_s(t) \\
&+ q_s^T(t)\alpha_s\delta^2 q_s(t)\big) + (d_m - L_m)\left(\frac{4}{(H_m+1)A_{m0}}\right)^2\|e_m(t)\|^2 \\
&+ (d_s - L_s)\left(\frac{4}{(H_s+1)A_{s0}}\right)^2\|e_s(t)\|^2
\end{aligned} \tag{4.113}
$$

Due to the positive semi-definite storage functional V and its negative semi-definite differential $\dot{V}$, $\lim_{t\to\infty} V$ exists and is finite. Also, $r_i(t), \tilde{\theta}_i(t), \epsilon_i(t) \in L_\infty$. Based on (4.113), $e_i(t)$, $e_{vi}(t) + \delta e_{pi}(t)$, q_i, $\dot{q}_i$, $\ddot{q}_i \in L_\infty \cap L_2$. Therefore, e_{pi}, e_{vi}, $e_{ti} \in L_\infty \cap L_2$. The prescribed synchronization performance is obtained. Moreover, the position, velocity and torque synchronization errors asymptotically converge to zero when time tends to infinity based on the definition of PPC.

In this study, time-varying delays and modeled human and environmental torques are considered. By using the extended wave-based TDPA and prescribed performance control algorithms, the prescribed synchronization control performance of position, velocity and torque can be ensured and the system's passivity is guaranteed in the presence of arbitrary time delays.

4.4.4 Experimental results

This section demonstrate a series of experiments to validate the proposed system. The applied experimental platform consists of two 3-DOF Phantom haptic devices: Phantom Omni and Phantom Desktop (Sensable Technologies, Inc., Wilmington, MA) as shown in Fig.3.19. During the experimental process, the control loop is configured as a 1 kHz sampling rate. The Internet is applied as the communication channels in the experiment, and to tune the values of the time delays, extra Simulink time-delay models are also used. The wave impedance b is set as 2.5 and the impedances B and M are 2 and 1, respectively. $\delta = 0.5$, $k_1 = k_2 = 1$, $\alpha_m = \alpha_s = 1.5$ $\beta = 4$, $d_m = d_s = 1.5$, $L_m = L_s = 0.7$, $A_m(0) = A_s(0) = 2$, $A_m(\infty) = A_s(\infty) = 0.4$.

4.4.4.1 Constant time delays

The initial experiments are conducted under constant time delays. The values of time delay are around 600 ms. The first experiment demonstrates the system's performance during free motion. Figs.4.25-4.27 show the position, velocity and torque of the two robots and their related tracking errors during free motion. Under constant time delays, the system passivity are guaranteed by the wave transformation and the passivity controllers are not launched to affect the system transparency. Moreover, the application of PPC algorithm guarantees the errors of the position, velocity and torque to have small variance (no more than 0.1).

Then, the slave robot is controlled to have contact with a solid wall. The position, velocity and torque of the master and the slave and their tracking errors are shown in Fig. 4.28-4.30. As shown in Fig. 4.30, the proposed algorithm can provide an accurate torque tracking and the torque tracking errors of zero when the slave is in contact with the solid wall from the 3rd second to the 6th second. Moreover, the proposed PPC algorithm also guarantees the convergence of the position tracking errors to a small value during hard contact so that the problem of position drift is largely reduced.

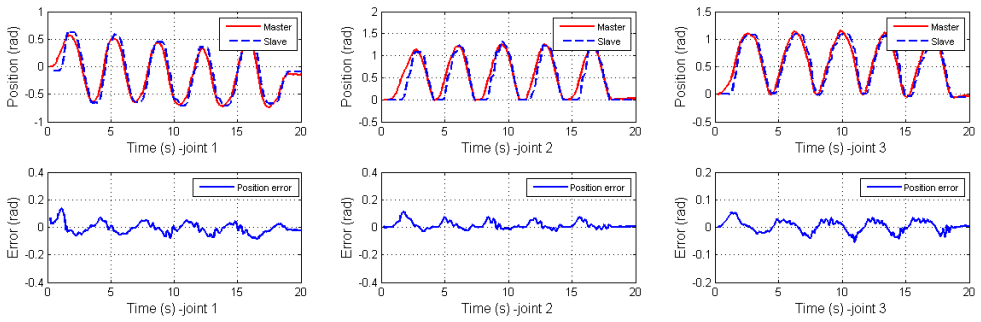

Figure 4.25. Position tracking during free motion (constant time delay)

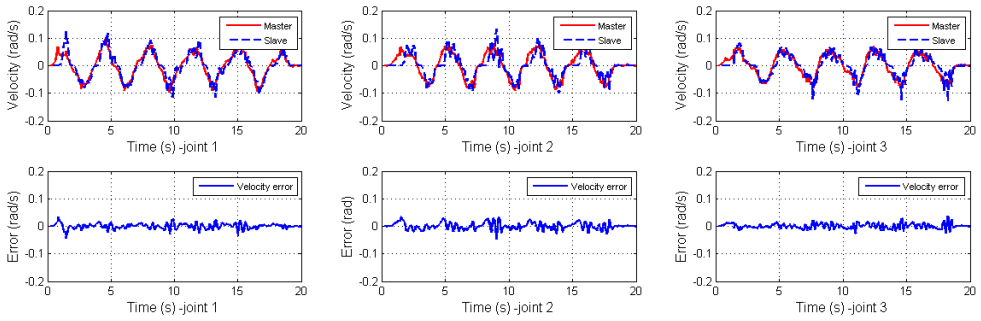

Figure 4.26. Velocity tracking during free motion (constant time delay)

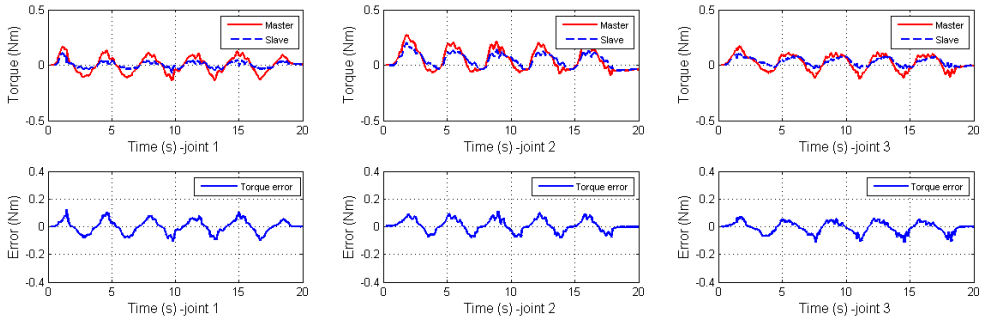

Figure 4.27. Torque tracking during free motion (constant time delay)

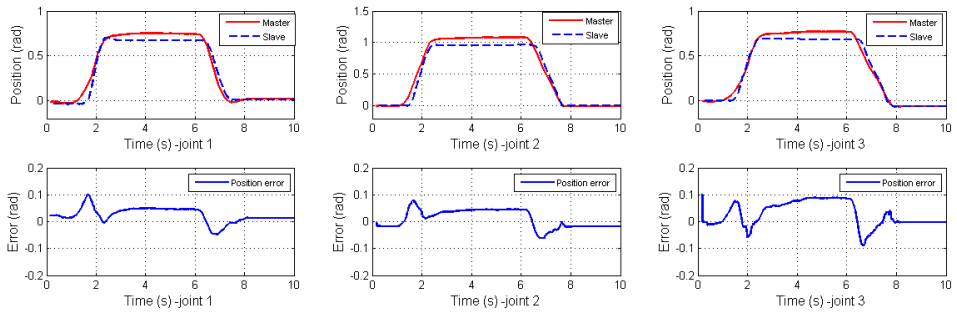

Figure 4.28. Position tracking during hard contact (constant time delay)

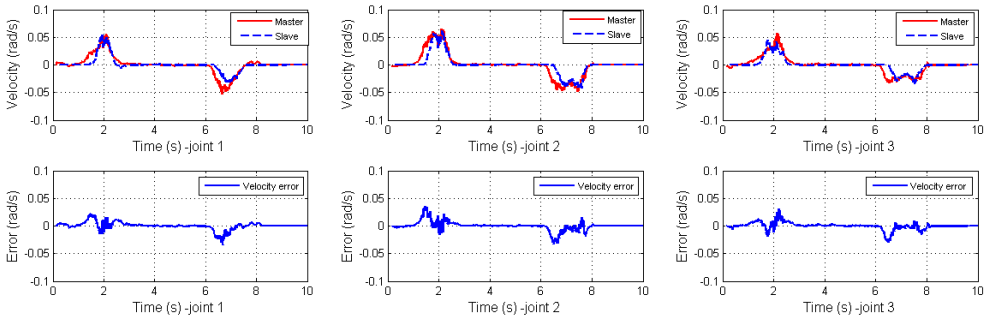

Figure 4.29. Velocity tracking during hard contact (constant time delay)

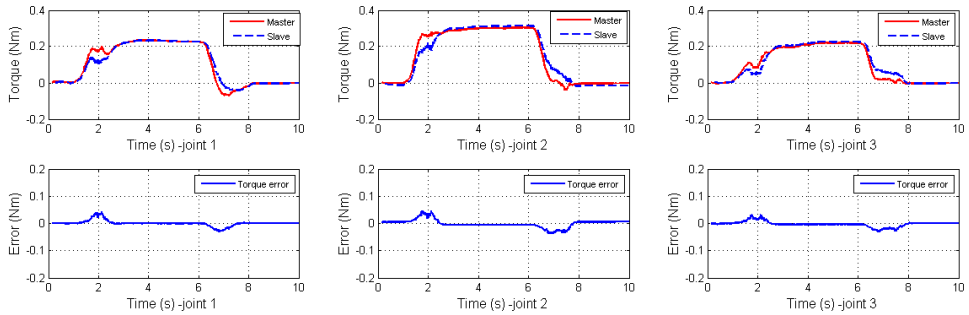

Fig.4.30. Torque tracking during hard contact (constant time delay)

4.4.4.2 Time-varying delays

n this subsection, the system's performance in the presence of large time delays with large variations are demonstrated. The values of time delays are around 1 second with a variation of 500 ms. Figs. 4.31-4.33 show the position, velocity and torque information of the master and the slave and the related tracking errors during free

motion. In the presence of such a large and fast varying time delays, the passivity controllers are directly launched to guarantee the system passivity, activated by the negative powers from the passivity observers. Therefore, the system transparency is reduced and the tracking errors of the position, velocity and torque are enlarged. However, the proposed PPC algorithm restrict these tracking errors within a reasonable range (no more than 0.4). Also, by combining the passivity approaches and PPC, the slave's motion can track the master's motion without any variation even in the presence of large time-varying delays as shown in Fig.4.31.

In the next experiments the tracking performance of the algorithm during hard environmental contact is demonstrated. Figs.4.34-14.36 show the position, velocity and torque information and their tracking errors. From the 3rd second to the 6th second, the slave robot is controlled while in contact with a solid wall. With the PPC algorithm, the position tracking errors are restricted to be no more than 0.4 and the torque tracking errors are no more than 0.1. After the 6th second, the slave robot is controlled by the master robot to lose contact from the solid wall and to return to the origin. All of the signals including position, velocity and torque quickly converge to zero. Reasonable tracking performances are still achieved in the presence of large time varying delays. Based on the results obtained under constant and varying delays, it can be concluded that the proposed control laws with extended wave-based TDPA and PPC can achieve accurate position, velocity and torque tracking and robust system stability.

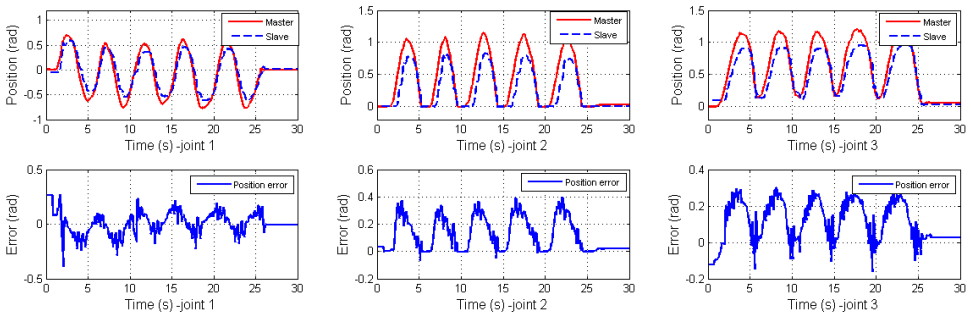

Figure 4.31. Position tracking during free motion (time-varying delay)

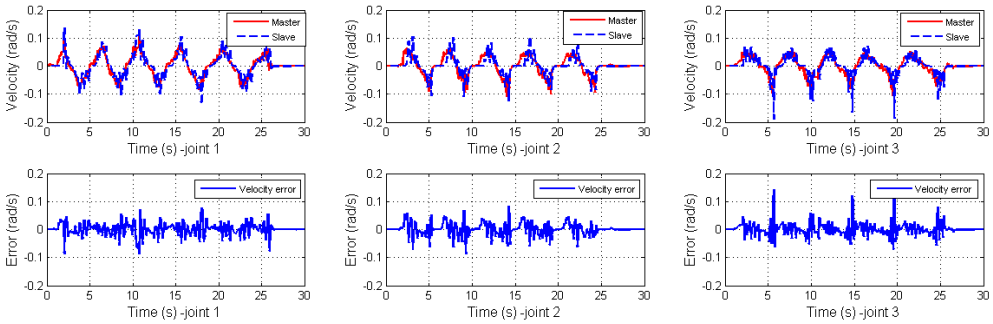

Figure 4.32. Velocity tracking during free motion (time-varying delay)

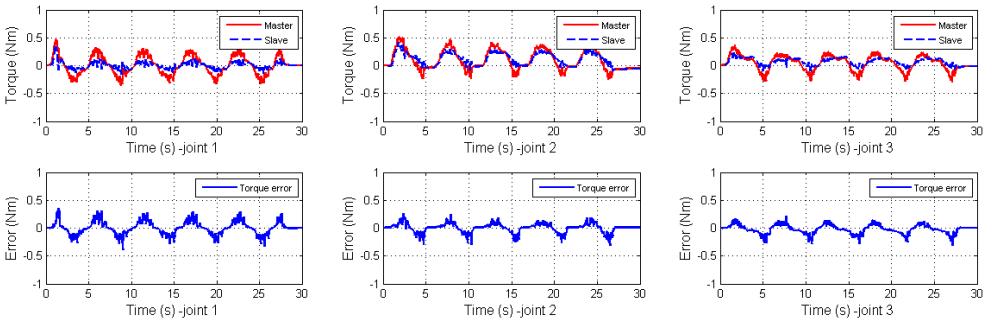

Figure 4.33. Torque tracking during free motion (time-varying delay)

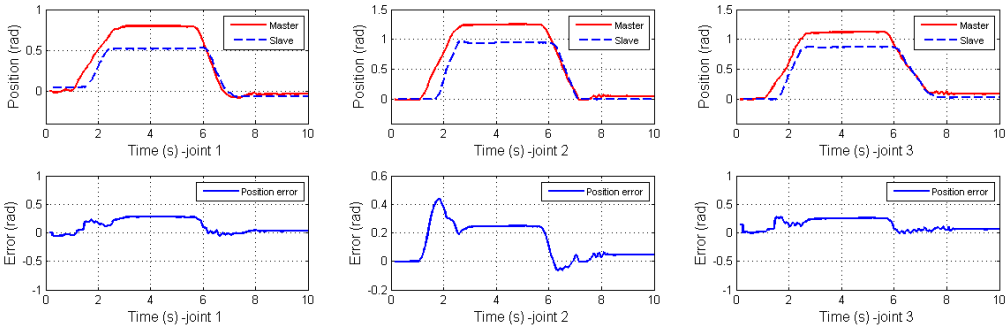

Fig.4.34. Position tracking during hard contact (time-varying delay)

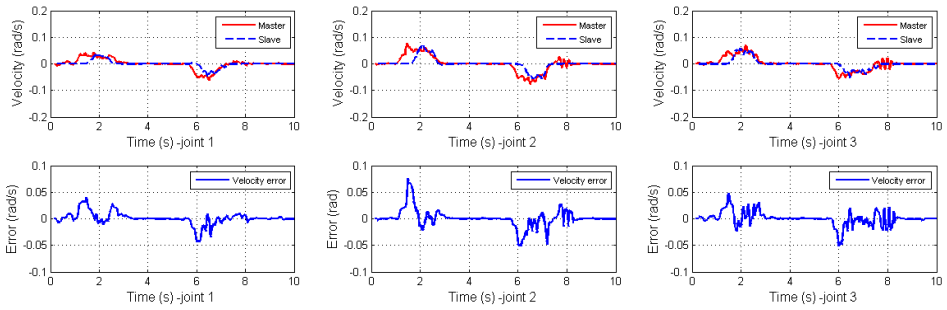

Figure 4.35. Velocity tracking during hard contact (time-varying delay)

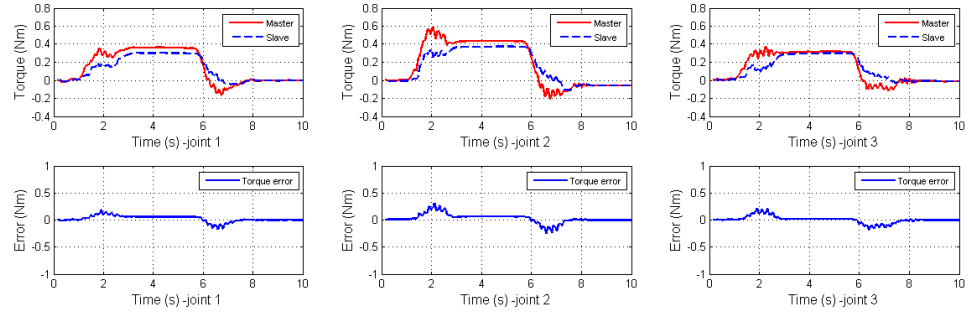

Figure 4.36. Torque tracking during hard contact (time-varying delay)

4.5 Neural network-based teleoperation system applying modified wave-based TDPA

In recent times, the neural networks (NN) have received much attention due to their prominent properties such as learning capability mapping and parallel processing. Deployment of NNs in the control of robot systems has significantly improved their performance [170]-[171]. In bilateral teleoperation research, a control system with acceleration measurement is designed in [169] using NN to estimate nonlinear uncertainties. In [167], the NN is applied in a prescribed performance control system. A terminal sliding mode control system with NN is also designed in [172]. Unfortunately, these systems are extremely restricted by constant time delays and are established under the assumption that the external force is zero, which is against reality. In [173], the neural network based system is applied to a system under time-varying delay. As a drawback, the system should have the precise knowledge of external forces

including the coefficient values of mass and damping. [174] and [175] extend the application of neural networks to multilateral teleoperation. It is assumed that the disturbances should be restricted by large velocity signals, and the rate of time delays should be less than one. [176] surveys the currently state-of-the art in application of NNs in control systems.

In Section 4.3 and 4.4, we proposed the wave-based TDPA system to more accurately observe the power flow during different time delay scenarios. However, the strict restriction of the rate of time delays and degraded position and torque tracking owning to passivity controllers in the presence of sharply-varying delays are its two principal weaknesses of the approach.

In section 4.5, we proposed a new wave-based TDPA system to guarantee the whole system's stability and achieve high tracking performance in the presence of the time-varying delays without rate restrictions. Compared with the previous power-based TDPA, the proposed wave-based TDPA can more efficiently monitor the power flow under the condition of arbitrary time delays. The proposed passivity controllers do not influence position and force tracking. NN is applied to the proposed system to estimate and eliminate the dynamic uncertainties. The proposed control algorithm is deployed in the absence of the knowledge of the upper bound of the neural network approximation error and external disturbance.

4.5.1 System formulation

In this section, more complex dynamic models of the teleoperator are applied, which deployed:

$$M_m(q_m)\ddot{q}_m + C_m(q_m,\dot{q}_m)\dot{q}_m + F_m\dot{q}_m + f_{cm}(\dot{q}_m) + g_m(q_m) - F_m^* = \tau_m + \tau_h \tag{4.114}$$

$$M_s(q_s)\ddot{q}_s + C_s(q_s,\dot{q}_s)\dot{q}_s + F_s\dot{q}_s + f_{cs}(\dot{q}_s) + g_s(q_s) - F_s^* = \tau_s - \tau_e \tag{4.115}$$

where $i = m, s$ for the master and slave. $\ddot{q}_i(t)$, $\dot{q}_i(t)$, $q_i(t) \in R^{n\times 1}$ are the joint acceleration, velocity and position, respectively. $M_i(q_i(t)) \in R^{n\times n}$ are the inertia

matrices, $C_i(q_i(t), \dot{q}_i(t)) \in R^{n\times n}$ are Coriolis/centrifugal effects. $g_i(q_i(t)) \in R^n$ are the vectors of gravitational forces and τ_i are the control signals. $\tau_h(t)$ and $\tau_e(t)$ are the actual human and environmental torques applied to the robots. $F_i\dot{q}_i(t)$ denote the viscous friction and $f_{ci}(\dot{q}_i(t))$ denote the Coulomb friction. $F_i^*(t) \in R^{n\times 1}$ are the bounded unknown disturbances. It is assumed that the Coulomb friction function $f_{ci}(\dot{q}_i(t))$ in the master and slave sides are bounded and piecewise continuous functions.

In this section, the external human and environmental torques are modelled as (5) and (6), where $\tau_{h,e}^*(t)$ stand for, respectively, the positive and bounded human operator and the environment exogenous input. $K_{h,e}$, $B_{h,e}$ and $M_{h,e}$ represent the non-negative constant scalars corresponding to the mass, damping and stiffness of human and environment. $\Delta k_{h,e}$, $\Delta b_{h,e}$, $\Delta m_{h,e}$ are the unknown bounded variables relating to $K_{h,e}$, $B_{h,e}$ and $M_{h,e}$. δ is a positive constant. Moreover, we use the extended active observer (EAOB) to measure the human and environmental torques [70], and simultaneously derive the acceleration signals. Compared with other force observers, EAOB possesses the advantage of external noises suppression by applying Kalman filter, and is fit for application of nonlinear systems.

$$\tau_h(t) = \tau_h^*(t) - (K_h + \Delta k_h)\delta q_m(t) - (B_h + \Delta b_h)\delta\dot{q}_m(t) - (M_h + \Delta m_h)\delta\ddot{q}_m(t) \quad (4.116)$$

$$\tau_e(t) = \tau_e^*(t) + (K_e + \Delta k_e)\delta q_s(t) + (B_e + \Delta b_e)\delta\dot{q}_s(t) + (M_e + \Delta m_e)\delta\ddot{q}_s(t) \quad (4.117)$$

The main advantage of the NNs is that it has the ability to approximate any smooth nonlinear function with arbitrary precision owing to their inherent approximate capabilities. The Radial Basis Function (RBF) NN is applied to approximate a continuous function $f(X)$: $R^q \rightarrow R^p$ expressed as follows:

$$f(X) = W^T\Phi(X) + \xi(X) \quad (4.118)$$

where $X \in \Omega_x \subset R^q$ is the input vector. $W \in R^{n \times p}$ is the weight matrix. n is the number of the neurons. $\xi(X)$ is the approximation errors.

$\Phi(X) = [\Phi_1(X), \Phi_2(X), \ldots, \Phi_k(X), \ldots, \Phi_n(X)]$, where $\Phi_k(X)$ is the RBF Gaussian function:

$$\Phi_k(X) = \exp(-\frac{1}{2\mathrm{H}_k{}^2}\|X - C_k\|^2) \tag{4.119}$$

Where C_k and H_k are the center and the width of the k-th neuron, respectively. According to the universal approximation property of NNs, for any continuous function f(X), there exists an NN such that

$$f(X) = W^{*T}\Phi(X) + \xi^*(X), \|\xi^*(X)\| \leq \xi^*_{up} \tag{4.120}$$

where W^* and $\xi^*(X)$ are the ideal weight and error in the approximation, respectively. ξ^*_{up} is $\xi^*(X)$'s upper bound. The dynamic functions of the manipulaters can be considered to be piecewise continuous functions due to the existing friction and backlash. Assume that $f(X)$ is a piecewise function which can be written as: $f(X) = f_1(X) + f_2(X)$, where $f_1(X)$ is the continuous part and $f_2(X)$ is the bounded piecewise term, respectively. Therefore:

$$f(X) = W^{*T}\Phi(X) + \xi^*(X) + f_2(X) = W^{*T}\Phi(X) + \bar{\xi}^*(X) \tag{4.121}$$

where $\bar{\xi}^*(X) = \xi^*(X) + f_2(X)$, $\bar{\xi}^*(X) \leq \bar{\xi}^*_{up}$. $\bar{\xi}^*_{up}$ is the upper bound of the approximation error.

Remark 1. In this section, the unsymmetrical time delays $T_1(t)$ and $T_2(t)$ are assumed to be bounded by $\bar{\mu}_{1,2}$. That is, $\left|\dot{\mathrm{T}}_{1,2}(\mathrm{t})\right| \leq \bar{\mu}_{1,2}$. Moreover, the time-varying delays $T_{1,2}(t)$ are considered to be the sum of the constant time delays $\bar{T}_{1,2}$ with their bounded perturbations $\Delta T_{1,2}(t)$. That is, $T_{1,2}(t) = \bar{T}_{1,2} + \Delta T_{1,2}(t) \leq \bar{T}_{1,2} + \bar{\varepsilon}_{1,2} = T^{max}_{1,2}$, where $\bar{\varepsilon}_{1,2}$ are the upper bounds of the perturbations and $T^{max}_{1,2}$ are the upper bounds of the $T_{1,2}(t)$.

Fig.4.37 shows the proposed 4-CH wave variable transformation which contains two wave transformation schemes.

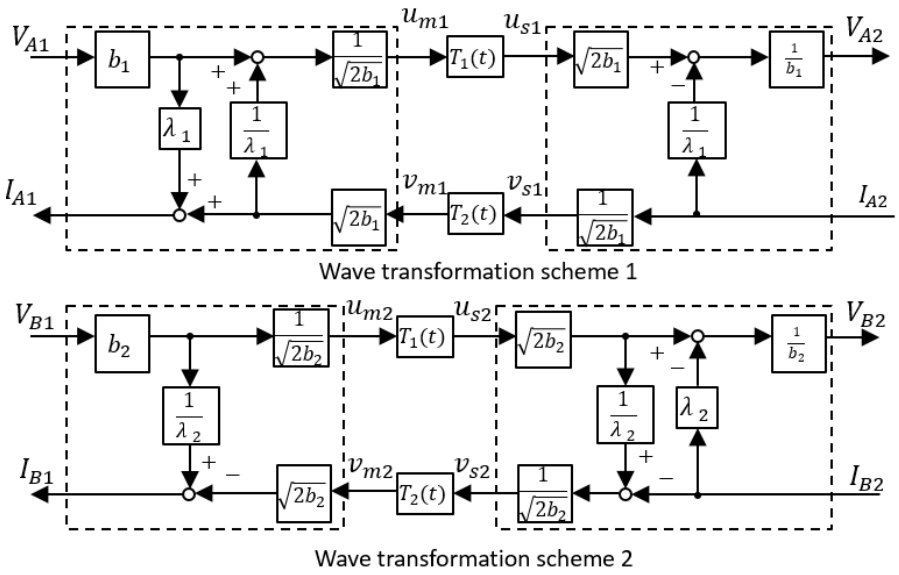

Figure 4.37. 4-CH wave variable transformation

The two wave transformation schemes are applied to encode the feed-forward signals V_{A1} and V_{B1} with the feedback signals I_{A2} and I_{B2}, where $V_{A1}(t) = \beta\delta q_m(t) + \alpha\delta\dot{q}_m(t)$, $V_{B1}(t) = \alpha_1\delta\dot{q}_m(t)$, $I_{A2}(t) = \alpha_1\delta\dot{q}_s(t)$, $I_{B2}(t) = -\beta\delta q_s(t) - \alpha\delta\dot{q}_s(t)$. α, α_1 and β are diagonal positive-definite matrices. δ are positive constants. In this system, position and velocity are transmitted between the two robots.

The wave variables in the two schemes are defined as follows:

$$u_{m1}(t) = \frac{b_1 V_{A1}(t) + \frac{1}{\lambda_1} I_{A2}\big(t - T_2(t)\big)}{\sqrt{2b_1}}, u_{s1}(t) = \frac{b_1 V_{A2}(t) + \frac{1}{\lambda_1} I_{A2}(t)}{\sqrt{2b_1}} \quad (4.122)$$

$$v_{m1}(t) = \frac{I_{A2}\big(t - T_2(t)\big)}{\sqrt{2b_1}}, v_{s1}(t) = \frac{I_{A2}(t)}{\sqrt{2b_1}} \quad (4.123)$$

$$u_{m2}(t) = \frac{b_2 V_{B1}(t)}{\sqrt{2b_2}}, u_{s2}(t) = \frac{b_2 V_{B1}(t - T_1(t))}{\sqrt{2b_2}} \quad (4.124)$$

$$v_{m2}(t) = \frac{\frac{b_2}{\lambda_2} V_{B1}(t) - I_{B1}(t)}{\sqrt{2b_2}}, v_{s2}(t) = \frac{\frac{b_2}{\lambda_2} V_{B1}(t - T_1(t)) - I_{B2}(t)}{\sqrt{2b_2}} \quad (4.125)$$

where $b_{1,2}$ and $\lambda_{1,2}$ are the positive characteristic impedances. After equations transformation, the following equations can be derived based on (4.122)-(4.125):

$$V_{A1}(t) = \sqrt{\frac{2}{b_1}}\left(u_{m1}(t) - \frac{1}{\lambda_1}v_{m1}(t)\right), V_{A2}(t) = \sqrt{\frac{2}{b_1}}\left(u_{s1}(t) - \frac{1}{\lambda_1}v_{s1}(t)\right) \quad (4.126)$$

$$I_{A1} = \lambda_1\sqrt{2b_1}u_{m1}(t), I_{A2}(t) = \sqrt{2b_1}v_{s1}(t) \quad (4.127)$$

$$V_{B1}(t) = \sqrt{\frac{2}{b_2}}u_{m2}(t), V_{B2}(t) = \lambda_2\sqrt{\frac{2}{b_2}}v_{s2}(t) \quad (4.128)$$

$$I_{B1} = \sqrt{2b_2}\left(\frac{1}{\lambda_2}u_{m2}(t) - v_{m2}(t)\right), I_{B2} = \sqrt{2b_2}\left(\frac{1}{\lambda_2}u_{s2}(t) - v_{s2}(t)\right) \quad (4.129)$$

Therefore, the control signals after transmission in Fig.1 can be derived as

$$I_{A1} = \alpha_1\delta\dot{q}_s\big(t - T_2(t)\big) + b_1\lambda_1\big(\beta\delta q_m(t) + \alpha\delta\dot{q}_m(t)\big) \quad (4.130)$$

$$\begin{aligned} I_{B1} = &-\beta\delta q_s\big(t - T_2(t)\big) - \alpha\delta\dot{q}_s\big(t - T_2(t)\big) \\ &+ \frac{b_2\alpha_1}{\lambda_2}\Big(\delta\dot{q}_m(t) - \delta\dot{q}_m\Big(t - T_1(t) - T_2\big(t - T_1(t)\big)\Big)\Big) \end{aligned} \quad (4.131)$$

$$\begin{aligned} V_{A2}(t) = V_{A2}(t) \\ &= \beta\delta q_m\big(t - T_1(t)\big) + \alpha\delta\dot{q}_m\big(t - T_1(t)\big) \\ &- \frac{\alpha_1}{b_1\lambda_1}\Big(\delta\dot{q}_s(t) - \delta\dot{q}_s\Big(t - T_2(t) - T_1\big(t - T_2(t)\big)\Big)\Big) \end{aligned} \quad (4.132)$$

$$V_{B2}(t) = \alpha_1\delta\dot{q}_m\big(t - T_1(t)\big) + \frac{\lambda_2}{b_2}\big(\beta\delta q_s(t) + \alpha\delta\dot{q}_s(t)\big) \quad (4.133)$$

Define $T_{l1}(t) = T_2(t) + T_1\big(t - T_2(t)\big)$ and $T_{l2}(t) = T_1(t) + T_2\big(t - T_1(t)\big)$. Also, $\dot{T}_{l1}(t) \le \bar{\mu}_1, \dot{T}_{l2}(t) \le \bar{\mu}_2$.

The proposed 4-CH wave variable transformation can actually be seen as the combination of two 2-port network. Therefore, the power flow in the 4-CH wave variable transformation can be defined as:

$$P_{4CH}(t) = P_1(t)[scheme1] + P_2(t)[scheme2]$$

$$P_1(t) = V_{A1}(t)I_{A1}(t) - V_{A2}(t)I_{A2}(t)$$
$$= 2\lambda_1 u_{m1}^T(t)u_{m1}(t) + \frac{2}{\lambda_1}v_{s1}^T(t)v_{s1}(t) - 2\big(u_{m1}^T(t)v_{m1}(t) + u_{s1}^T(t)v_{s1}(t)\big)$$
$$= \lambda_1\big(u_{m1}^T(t)u_{m1}(t) - u_{s1}^T(t)u_{s1}(t)\big) + \frac{1}{\lambda_1}\big(v_{s1}^T(t)v_{s1}(t) - v_{m1}^T(t)v_{m1}(t)\big) +$$
$$\frac{1}{\lambda_1}\big(v_{m1}(t) - \lambda_1 u_{m1}(t)\big)^T\big(v_{m1}(t) - \lambda_1 u_{m1}(t)\big) + \frac{1}{\lambda_1}\big(v_{s1}(t) - \lambda_1 u_{s1}(t)\big)^T\big(v_{s1}(t) -$$
$$\lambda_1 u_{s1}(t)\big)$$
$$= \frac{d}{dt}\int_{t-T_1(t)}^{t}\lambda_1\, u_{m1}^T(\eta)u_{m1}(\eta)d\eta + \frac{d}{dt}\int_{t-T_2(t)}^{t}\frac{1}{\lambda_1}v_{s1}^T(\eta)v_{s1}(\eta)d\eta + \frac{1}{\lambda_1}\big(v_{m1}(t) -$$
$$\lambda_1 u_{m1}(t)\big)^T\big(v_{m1}(t) - \lambda_1 u_{m1}(t)\big) + \frac{1}{\lambda_1}\big(v_{s1}(t) - \lambda_1 u_{s1}(t)\big)^T\big(v_{s1}(t) - \lambda_1 u_{s1}(t)\big) -$$
$$\lambda_1\dot{T}_1(t)u_{s1}^T(t)u_{s1}(t) - \frac{1}{\lambda_1}\dot{T}_2(t)v_{m1}^T(t)v_{m1}(t)$$
$$= \frac{dE_1(t)}{dt} + P_1^{diss}(t) \tag{4.134}$$

$$E_1(t) = \int_{t-T_1(t)}^{t}\lambda_1\, u_{m1}^T(\eta)u_{m1}(\eta)dt + \int_{t-T_2(t)}^{t}\frac{1}{\lambda_1}v_{s1}^T(\eta)v_{s1}(\eta)dt \tag{4.135}$$

$$P_1^{diss}(t) = \frac{1}{\lambda_1}\big(v_{m1}(t) - \lambda_1 u_{m1}(t)\big)^T\big(v_{m1}(t) - \lambda_1 u_{m1}(t)\big)$$
$$+ \frac{1}{\lambda_1}\big(v_{s1}(t) - \lambda_1 u_{s1}(t)\big)^T\big(v_{s1}(t) - \lambda_1 u_{s1}(t)\big)$$
$$- \lambda_1\dot{T}_1(t)u_{s1}^T(t)u_{s1}(t) - \frac{1}{\lambda_1}\dot{T}_2(t)v_{m1}^T(t)v_{m1}(t) \tag{4.136}$$

and

$$P_2(t) = V_{B1}(t)I_{B1}(t) - V_{B2}(t)I_{B2}(t)$$
$$= \frac{2}{\lambda_2}u_{m2}^T(t)u_{m2}(t) + 2\lambda_2 v_{s2}^T(t)v_{s2}(t) - 2\big(u_{m2}^T(t)v_{m2}(t) + u_{s2}^T(t)v_{s2}(t)\big)$$

$$= \frac{1}{\lambda_2}\left(u_{m2}^T(t)u_{m2}(t) - u_{s2}^T(t)u_{s2}(t)\right) + \lambda_2\left(v_{s2}^T(t)v_{s2}(t) - v_{m2}^T(t)v_{m2}(t)\right) +$$

$$\lambda_2\left(v_{m2}(t) - \frac{1}{\lambda_2}u_{m2}(t)\right)^T\left(v_{m2}(t) - \frac{1}{\lambda_2}u_{m2}(t)\right) + \lambda_2\left(v_{s2}(t) -$$

$$\frac{1}{\lambda_2}u_{s2}(t)\right)^T\left(v_{s2}(t) - \frac{1}{\lambda_2}u_{s2}(t)\right)$$

$$= \frac{d}{dt}\int_{t-T_1(t)}^{t}\frac{1}{\lambda_2}u_{m2}^T(\eta)u_{m2}(\eta)d\eta + \frac{d}{dt}\int_{t-T_2(t)}^{t}\lambda_2\, v_{s2}^T(\eta)v_{s2}(\eta)d\eta + \lambda_2\left(v_{m2}(t) -$$

$$\frac{1}{\lambda_2}u_{m2}(t)\right)^T\left(v_{m2}(t) - \frac{1}{\lambda_2}u_{m2}(t)\right) + \lambda_2\left(v_{s2}(t) - \frac{1}{\lambda_2}u_{s2}(t)\right)^T\left(v_{s2}(t) -$$

$$\frac{1}{\lambda_2}u_{s2}(t)\right) - \frac{1}{\lambda_2}\dot{T}_1(t)u_{s2}^T(t)u_{s2}(t) - \lambda_2\dot{T}_2(t)v_{m2}^T(t)v_{m2}(t)$$

$$= \frac{dE_2(t)}{dt} + P_2^{diss}(t) \tag{4.137}$$

$$E_2(t) = \int_{t-T_1(t)}^{t}\frac{1}{\lambda_2}u_{m2}^T(\eta)u_{m2}(\eta)d\eta + \int_{t-T_2(t)}^{t}\lambda_2\, v_{s2}^T(\eta)v_{s2}(\eta)d\eta \tag{4.138}$$

$$\begin{aligned} P_2^{diss}(t) = {} & \lambda_2\left(v_{m2}(t) - \frac{1}{\lambda_2}u_{m2}(t)\right)^T\left(v_{m2}(t) - \frac{1}{\lambda_2}u_{m2}(t)\right) \\ & + \lambda_2\left(v_{s2}(t) - \frac{1}{\lambda_2}u_{s2}(t)\right)^T\left(v_{s2}(t) - \frac{1}{\lambda_2}u_{s2}(t)\right) \\ & - \frac{1}{\lambda_2}\dot{T}_1(t)u_{s2}^T(t)u_{s2}(t) - \lambda_2\dot{T}_2(t)v_{m2}^T(t)v_{m2}(t) \end{aligned} \tag{4.139}$$

According to (4.135) and (4.138), the net energy flows are absolutely positive to guarantee passivity of the communication network. Based on the definition of passivity and assuming $E_1(0) = E_2(0) = 0$, the energy flow is derived as:

$$E_{flow}(t) = \int_0^t P_{4CH}(\eta)d\eta = \int_0^t (P_1^{diss}(\eta) + P_2^{diss}(\eta) + \frac{dE_1}{dt}(\eta) + \frac{dE_2}{dt}(\eta))d\eta$$
$$= E_1(t) + E_2(t) - E_1(0) - E_2(0) + \int_0^t P_1^{diss}(\eta) + P_2^{diss}(\eta)d\eta$$
$$\geq \int_0^t P_1^{diss}(\eta) + P_2^{diss}(\eta)d\eta \quad (4.140)$$

Therefore, in the situation that $P_1^{diss}(\mathrm{t}) + P_2^{diss}(\mathrm{t}) \geq 0$, according to (4.140), the energy flow $E_{flow}(t)$ is no less than zero and the passivity of the time delayed network can be guaranteed.

$P_1^{diss}(\mathrm{t}) + P_2^{diss}(\mathrm{t})$ can also be defined as the sum of master power dissipation components $P_{diss}^m(t)$ and slave power dissipation components $P_{diss}^s(t)$ based on (4.134) and (4.137).

$$\mathrm{P}_{\mathrm{diss}}^{\mathrm{m}}(\mathrm{t}) = \frac{1}{\lambda_1}\left(v_{m1}(t) - \lambda_1 u_{m1}(t)\right)^T\left(v_{m1}(t) - \lambda_1 u_{m1}(t)\right)$$
$$+ \lambda_2\left(v_{m2}(t) - \frac{1}{\lambda_2}u_{m2}(t)\right)^T\left(v_{m2}(t) - \frac{1}{\lambda_2}u_{m2}(t)\right)$$
$$- \frac{1}{\lambda_1}\dot{T}_2(t)v_{m1}^T(t)v_{m1}(t) - \lambda_2\dot{T}_2(t)v_{m2}^T(t)v_{m2}(t) \quad (4.141)$$

$$\mathrm{P}_{\mathrm{diss}}^{\mathrm{s}}(\mathrm{t}) = \frac{1}{\lambda_1}\left(v_{s1}(t) - \lambda_1 u_{s1}(t)\right)^T\left(v_{s1}(t) - \lambda_1 u_{s1}(t)\right)$$
$$+ \lambda_2\left(v_{s2}(t) - \frac{1}{\lambda_2}u_{s2}(t)\right)^T\left(v_{s2}(t) - \frac{1}{\lambda_2}u_{s2}(t)\right)$$
$$- \lambda_1\dot{T}_1(t)u_{s1}^T(t)u_{s1}(t) - \frac{1}{\lambda_2}\dot{T}_1(t)u_{s2}^T(t)u_{s2}(t) \quad (4.142)$$

According to (4.141) and (4.142), the proposed passivity observers can observe the power dissipation components in real time, as $\mathrm{P}_{\mathrm{diss}}^{\mathrm{m}}(\mathrm{t})$ and $\mathrm{P}_{\mathrm{diss}}^{\mathrm{s}}(\mathrm{t})$ only contain the signals observed at the master and slave ports, respectively. The proposed 4-CH wave transformation is proposed to guarantee the passivity of the communication channels in the presence of constant delays so that the $\mathrm{P}_{\mathrm{diss}}^{\mathrm{m}}(\mathrm{t})$ and $\mathrm{P}_{\mathrm{diss}}^{\mathrm{s}}(\mathrm{t})$ are required to be

positive when $\dot{T}_1(t) = \dot{T}_2(t) = 0$. Therefore, in the constant time delay situation, (4.141) and (4.142) can be simplified as:

$$P_{diss}^{m}(t) = \frac{1}{\lambda_1}\left(v_{m1}(t) - \lambda_1 u_{m1}(t)\right)^T \left(v_{m1}(t) - \lambda_1 u_{m1}(t)\right) + \lambda_2 \left(v_{m2}(t) - \frac{1}{\lambda_2} u_{m2}(t)\right)^T \left(v_{m2}(t) - \frac{1}{\lambda_2} u_{m2}(t)\right) \quad (4.143)$$

$$P_{diss}^{s}(t) = \frac{1}{\lambda_1}\left(v_{s1}(t) - \lambda_1 u_{s1}(t)\right)^T \left(v_{s1}(t) - \lambda_1 u_{s1}(t)\right) + \lambda_2 \left(v_{s2}(t) - \frac{1}{\lambda_2} u_{s2}(t)\right)^T \left(v_{s2}(t) - \frac{1}{\lambda_2} u_{s2}(t)\right) \quad (4.144)$$

(4.143) and (1.143) are definitely non-negative. Therefore, the communication channels' passivity can be guaranteed by the proposed 4-CH wave transformation and the passivity controllers will not be launched to degrade the system transparency.

The value of $\dot{T}_{1,2}$ can be measured by using the time delay differential estimator in Fig.4.2. When this estimator is used, the integral of $u_{m1}(t)$ and $v_{s1}(t)$ should be sent outside the wave transformation. The passivity observers are designed as:

$$P_{obs}^{m}(t) = \frac{1}{\lambda_1}\left(v_{m1}(t) - \lambda_1 u_{m1}(t)\right)^T \left(v_{m1}(t) - \lambda_1 u_{m1}(t)\right) + \lambda_2 \left(v_{m2}(t) - \frac{1}{\lambda_2} u_{m2}(t)\right)^T \left(v_{m2}(t) - \frac{1}{\lambda_2} u_{m2}(t)\right) - \frac{\hat{\dot{T}}_2}{\lambda_1} v_{m1}^T(t) v_{m1}(t) - \lambda_2 \hat{\dot{T}}_2 v_{m2}^T(t) v_{m2}(t) \quad (4.145)$$

$$P_{obs}^{s}(t) = \frac{1}{\lambda_1}\left(v_{s1}(t) - \lambda_1 u_{s1}(t)\right)^T \left(v_{s1}(t) - \lambda_1 u_{s1}(t)\right) + \lambda_2 \left(v_{s2}(t) - \frac{1}{\lambda_2} u_{s2}(t)\right)^T \left(v_{s2}(t) - \frac{1}{\lambda_2} u_{s2}(t)\right) - \lambda_1 \hat{\dot{T}}_1 u_{s1}^T(t) u_{s1}(t) - \frac{\hat{\dot{T}}_1}{\lambda_2} u_{s2}^T(t) u_{s2}(t) \quad (4.146)$$

$$\hat{T}_{1,2} = \begin{cases} \dot{T}_{1,2}^{estimate}, if\ \dot{T}_{1,2}^{estimate} < \bar{\mathrm{M}}_{1,2} \\ \bar{M}_{1,2}, else, if\ \ \dot{T}_{1,2}^{estimate} \geq \bar{M}_{1,2} \end{cases} \tag{4.147}$$

where $\bar{M}_{1,2}$ are constants and satisfies $\bar{M}_{1,2} > \dot{T}_{1,2}$. In this section, we set $\bar{M}_1 = \bar{M}_2 = 2$.

By using the passivity observer, we design the passivity controller to be:

$$\hat{V}_s(t) = V_{A2}(t) - V_{B2}(t) - \Gamma_2(t) \tag{4.148}$$

$$\hat{I}_m(t) = -I_{A1} - I_{B1} - \Gamma_1(t) \tag{4.149}$$

where $\hat{\mathrm{V}}_\mathrm{s}(\mathrm{t})$ and $\hat{\mathrm{I}}_\mathrm{m}(\mathrm{t})$ are the output control signals from the passivity controllers in the slave side and master side, respectively. $\Gamma_1(t)$ and $\Gamma_2(t)$ are designed as (4.150)-(4.152), where $\sigma_{1,2}$ are positive constants.

$$\Gamma_1(t) = \begin{cases} 0, \ \ if\ P_{obs}^m(t) \geq 0\ or\ \dot{q}_m(t) = 0 \\ \frac{\alpha\bar{\mu}_2 \delta\dot{q}_s^T(t-T_2(t))\dot{q}_s(t-T_2(t))}{2\dot{q}_m(t)} + \left(\frac{\beta\lambda_2(\bar{\varepsilon}_1+\bar{\varepsilon}_2)+b_2\alpha\bar{\mu}_2\sigma_1}{2\lambda_2}\right)\delta\dot{q}_m(t), else \end{cases} \tag{4.150}$$

$$\Gamma_2(t) = \begin{cases} 0, \ \ if\ P_{obs}^s(t) \geq 0\ or\ \dot{q}_s(t) = 0 \\ \frac{\alpha\bar{\mu}_1 \delta\dot{q}_m^T(t-T_1(t))\dot{q}_m(t-T_1(t))}{2\dot{q}_s(t)} + \left(\frac{\beta(\bar{\varepsilon}_1+\bar{\varepsilon}_2)}{2} + \frac{\alpha\bar{\mu}_1\sigma_2}{2b_1\lambda_1}\right)\delta\dot{q}_s(t), else \end{cases} \tag{4.151}$$

4.5.2 Design and analysis of the proposed teleoperation system

Based on the external force models (4.116)-(4.117), the teleoperation dynamics can be rewritten as the following form:

$$\begin{aligned} &M_m(q_m)\delta\ddot{q}_m + C_m(q_m,\dot{q}_m)\delta\dot{q}_m \\ &\qquad = \tau_m + \tau_h^*(t) - B_h\delta\dot{q}_m(t) - M_h\delta\ddot{q}_m(t) + F_m^* - f_m(X_m) \end{aligned} \tag{4.152}$$

$$\begin{aligned} &M_s(q_s)\delta\ddot{q}_s + C_s(q_s,\dot{q}_s)\delta\dot{q}_s \\ &\qquad = \tau_s - \tau_e^*(t) - B_e\delta\dot{q}_s(t) - M_e\delta\ddot{q}_s(t) + F_s^* - f_s(X_s) \end{aligned} \tag{4.153}$$

where $X_i(t) = [\ddot{q}_i^T(t), \dot{q}_i^T(t), q_i^T(t)]^T$. $f_i(X_i)$ are defined as:

$$f_i(X_i) = F_i\dot{q}_i + f_{ci}(\dot{q}_i) + \tilde{g}_i(q_i) + M_i(q_i)(1-\delta)\ddot{q}_i + C_i(q_i,\dot{q}_i)(1-\delta)\dot{q}_i + (K_{h,e} + \Delta k_{h,e})\delta q_i + \Delta b_{h,e}\delta\dot{q}_i + \Delta m_{h,e}\delta\ddot{q}_i \quad (4.154)$$

where $\tilde{g}_i(q_i) = g_i(q_i) - \hat{g}_i(q_i)$. $\hat{g}_i(q_i)$ are the estimated model of $g_i(q_i)$.

According to NNs approximation property, the functions $\hat{f}_i(X_i)$ are applied in this section to approximate $f_i(X_i)$ with

$$\hat{f}_i(X_i) = \widehat{W}_i^T \Phi_i(X_i) \quad (4.155)$$

where $\widehat{W}_i$ are the NN adaption parameters and $\Phi_i(X_i)$ are the NN basis functions. Define

$$\tilde{f}_i(X_i) = \hat{f}_i(X_i) - f_i(X_i) = \left(\widehat{W}_i^T - W_i^{*T}\right)\Phi_i(X_i) = \widetilde{W}_i^T \Phi_i(X_i) + \bar{\xi}_i^*(X) \quad (4.156)$$

Due to the piecewise continuous function $f_{ci}(\dot{q}_i)$, we assume that $\bar{\xi}_i^*(X)$ are made up of ξ_i^* and $f_{ci}(\dot{q}_i)$.

Combine the proposed wave-based TDPA control method and the neural network control method, the control laws of the overall teleoperation systems are given as follows:

$$\tau_m(t) = \hat{f}_m(X_m) + \hat{I}_m(t) - (\alpha-\alpha_1)\delta\dot{q}_m(t) - (1-b_1\lambda_1)\beta\delta q_m(t) - Y_m(t) =$$
$$\hat{f}_m(X_m) - I_{A1} - I_{B1} - \Gamma_1(t) - (\alpha-\alpha_1)\delta\dot{q}_m(t) - (1-b_1\lambda_1)\beta\delta q_m(t) - Y_m(t)$$

$$= \hat{f}_m(X_m) + \beta\left(\delta q_s\left(t-T_2(t)\right) - \delta q_m(t)\right) + (\alpha-\alpha_1)\left(\delta\dot{q}_s\left(t-T_2(t)\right) - \delta\dot{q}_m(t)\right)$$
$$-\frac{b_2\alpha_1}{\lambda_2}\left(\delta\dot{q}_m(t) - \delta\dot{q}_m\left(t-T_{l2}(t)\right)\right) - b_1\lambda_1\alpha\delta\dot{q}_m(t) - \Gamma_1(t)$$
$$- Y_m(t) \quad (4.157)$$

$$\tau_s(t) = \tau_s(t) = \hat{f}_s(X_s) + \hat{V}_s(t) - (\alpha-\alpha_1)\delta\dot{q}_s(t) - (1-\frac{\lambda_2}{b_2})\beta\delta q_s(t) - Y_s(t) =$$
$$\hat{f}_s(X_s) + V_{A2}(t) - V_{B2}(t) - \Gamma_2(t) - (\alpha-\alpha_1)\delta\dot{q}_s(t) - (1-\frac{\lambda_2}{b_2})\beta\delta q_m(t) - Y_s(t)$$

$$= \hat{f}_s(X_s) + \beta\left(\delta q_m\left(t - T_1(t)\right) - \delta q_s(t)\right) + (\alpha - \alpha_1)\left(\delta \dot{q}_m\left(t - T_1(t)\right) - \delta \dot{q}_s(t)\right)$$
$$- \frac{\alpha}{b_1\lambda_1}\left(\delta \dot{q}_s(t) - \delta \dot{q}_s\left(t - T_{l1}(t)\right)\right) - \frac{\lambda_2\alpha}{b_2}\,\delta \dot{q}_s(t) - \Gamma_2(t)$$
$$- Y_s(t) \tag{4.158}$$

where σ, $\sigma_{1,2}$ are positive constants. $Y_m(t)$ and $Y_s(t)$ are the designed adaptive control laws as:

$$Y_i(t) = \begin{cases} \dfrac{\delta \dot{q}_i(t)}{\|\delta \dot{q}_i(t)\|}\widehat{\Theta}_i(t), & if \|\dot{q}_i(t)\| \neq 0 \\ 0, & if \|\dot{q}_i(t)\| = 0 \end{cases} \tag{4.159}$$

$$\dot{\widehat{\Theta}}_i(t) = \|\dot{q}_i(t)\| \tag{4.160}$$

Remark 2. The adaptive control laws $Y_i(t)$ are mainly used to deal with the approximation error, external positive input and unknown disturbance. $\widehat{\Theta}_i$(t) are applied to estimate the upper bounds Θ_i the sum of NN approximate error, the bounded external disturbance F_i^* and the exogenous input $\tau_{h,e}^*(t)$. That is, $\Theta_i \geq \left\|\bar{\xi}_i^*(X) + F_i^* \pm \tau_{h,e}^*\right\|$.

In the ideal situation where $\tilde{f}_i(X_i) = 0$, the adaptive controllers can be considered as damping terms which may influence transparency. However, by setting $0 < \delta < 1$, the adverse influence can be effectively reduced.

Based on the control laws (4.157)-(4.158), $\hat{f}_i(X_i)$ and $Y_i(t)$ are used to diminish the side effects of system uncertainties as well as external disturbance and input. We now analyze the remaining parts of the control laws $-b_1\lambda_1\alpha\delta\dot{q}_m(t)$ and $-\frac{\lambda_2\alpha}{b_2}\,\delta\dot{q}_s(t)$ applied to guarantee the system's stability. The two terms $-\frac{b_2\alpha_1}{\lambda_2}\left(\delta\dot{q}_m(t) - \delta\dot{q}_m\left(t - T_{l1}(t)\right)\right)$ and $-\frac{\alpha_1}{b_1\lambda_1}\left(\delta\dot{q}_s(t) - \delta\dot{q}_s\left(t - T_{l2}(t)\right)\right)$ can strengthen tracking performances and system stability. Under small time delays, these two terms are close to zero. When large time delays exist, these two terms can be treated as dampers that can enhance stability. Also setting small value for α_1 can efficiently reduce the values of the two terms. The remaining parts are to derive accurate position and velocity

signals tracking. When large and sharply varying delays occur, $\Gamma_{1,2}(t)$ will be immediately launched to guarantee the whole system's stability. More details on setting control parameters will be introduced later. The total block diagram of the proposed teleoperation system is shown in Fig.4.38.

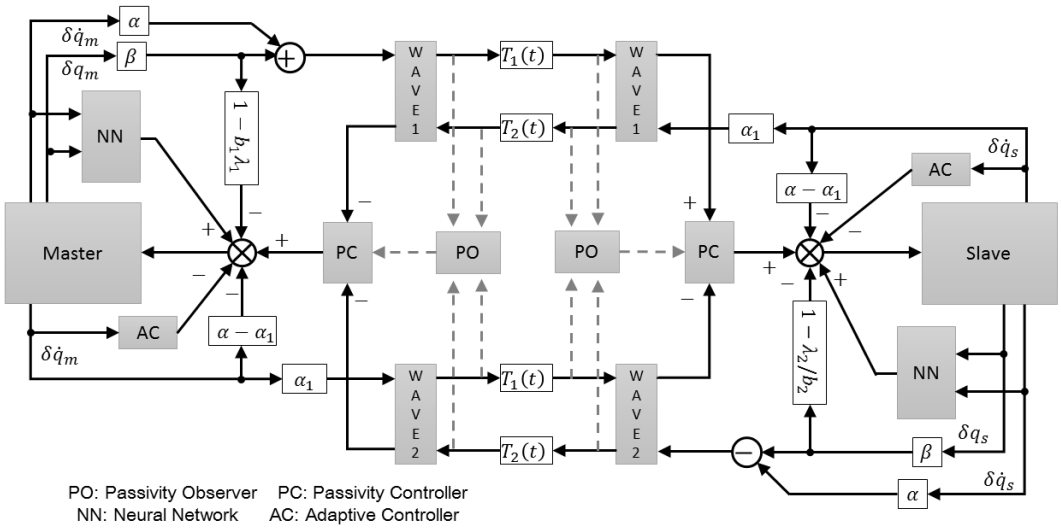

Figure 4.38. Total block diagram

Theorem 4.6. Consider the teleoperation system (1)-(2). If the control laws are constructed by (4.157) and (4.158), the NN adaptive laws are

$$\dot{\hat{W}}_i = \Omega_i \Phi_i(X_i)\delta\dot{q}_i \tag{4.161}$$

where Ω_i are the positive definite matrices. The position and velocity tracking errors will asymmetrically converge to zero in the presence of arbitrary time delays.

Proof. Consider a positive semi-definite function $\mathrm{V(t)}$ for the system as:

$$\mathrm{V(t)} = V_1(t) + V_2(t) + V_3(t) + V_4(t) + V_5(t)$$

where

$$V_1(t) = \frac{1}{2}\delta\dot{q}_m^T(t)M_m(q_m(t))\delta\dot{q}_m(t) + \frac{1}{2}\delta\dot{q}_s^T(t)M_s(q_s(t))\delta\dot{q}_s(t) + \frac{1}{2}tr\left(\widetilde{W}_m^T\Omega_m^{-1}\widetilde{W}_m\right) + \frac{1}{2}tr\left(\widetilde{W}_s^T\Omega_s^{-1}\widetilde{W}_s\right) \quad (4.162)$$

$$V_2(t) = \frac{\beta}{2}\left(\delta q_m(t) - \delta q_s(t)\right)^T\left(\delta q_m(t) - \delta q_s(t)\right) + \frac{1}{2}\left(\Theta_m - \hat{\Theta}_m(t)\right)^2 + \frac{1}{2}\left(\Theta_s - \hat{\Theta}_s(t)\right)^2 \quad (4.163)$$

$$V_3(t) = \frac{\beta}{2}\int_{-T_1(t)}^{0}\int_{t+\gamma}^{t}\delta^2\dot{q}_m^T(\eta)\dot{q}_m(\eta)d\eta d\gamma + \frac{\beta}{2}\int_{-T_2(t)}^{0}\int_{t+\gamma}^{t}\delta^2\dot{q}_s^T(\eta)\dot{q}_s(\eta)d\eta d\gamma \quad (4.164)$$

$$V_4(t) = \frac{\alpha-\alpha_1}{2}\int_{t-T_1(t)}^{t}\delta^2\dot{q}_m^T(\eta)\dot{q}_m(\eta)d\eta + \frac{\alpha-\alpha_1}{2}\int_{t-T_2(t)}^{t}\delta^2\dot{q}_s^T(\eta)\dot{q}_s(\eta)d\eta + \frac{b_2\alpha_1}{2\lambda_2}\int_{t-T_1(t)-T_2\left(t-T_1(t)\right)}^{t}\delta^2\dot{q}_m^T(\eta)\dot{q}_m(\eta)d\eta + \frac{\alpha_1}{2b_1\lambda_1}\int_{t-T_2(t)-T_1\left(t-T_2(t)\right)}^{t}\delta^2\dot{q}_s^T(\eta)\dot{q}_s(\eta)d\eta \quad (4.165)$$

$$V_5(t) = \delta^2\dot{q}_m^T(t)\frac{M_h}{2}\dot{q}_m(t) + \delta^2\dot{q}_s^T(t)\frac{M_e}{2}\dot{q}_s(t) \quad (4.166)$$

Using property 2 in Section 2, the control laws (4.157) and (4.158), the modelled human and environmental torques (4.116) and (4.117), and the NNs adaptive laws (4.161), the time derivative of $V_1(t)$ can be written as:

$$\dot{V}_1(t) = \delta\dot{q}_m^T(t)\Big(\hat{f}_m(X_m) - f_m(X_m) - B_h\delta\dot{q}_m(t) - M_h\delta\ddot{q}_m(t) + \tau_h^*(t) + F_m^*$$
$$+ \beta\left(\delta q_s\big(t - T_2(t)\big) - \delta q_m(t)\right)$$
$$+ (\alpha - \alpha_1)\left(\delta\dot{q}_s\big(t - T_2(t)\big) - \delta\dot{q}_m(t)\right) - 2b_1\lambda_1\alpha\delta\dot{q}_m(t)$$
$$- \frac{b_2\alpha_1}{\lambda_2}\left(\delta\dot{q}_m(t) - \delta\dot{q}_m\big(t - T_{l2}(t)\big)\right) - \Gamma_1(t) - \frac{\delta\dot{q}_m(t)}{\|\delta\dot{q}_m(t)\|}\hat{\Theta}_m(t)\Big)$$
$$+ \delta\dot{q}_s^T(t)\Big(\hat{f}_s(X_s) - f_s(X_s) - B_e\delta\dot{q}_s(t) - M_e\delta\ddot{q}_s(t) + F_s^* - \tau_e^*(t)$$
$$+ \beta\left(\delta q_m\big(t - T_1(t)\big) - \delta q_s(t)\right)$$
$$+ (\alpha - \alpha_1)\left(\delta\dot{q}_m\big(t - T_1(t)\big) - \delta\dot{q}_s(t)\right) - \frac{2\lambda_2\alpha}{b_2}\delta\dot{q}_s(t)$$
$$- \frac{\alpha_1}{b_1\lambda_1}\left(\delta\dot{q}_s(t) - \delta\dot{q}_s\big(t - T_{l1}(t)\big)\right) - \Gamma_2(t) - \frac{\delta\dot{q}_s(t)}{\|\delta\dot{q}_s(t)\|}\hat{\Theta}_s(t)\Big)$$
$$- tr(\widetilde{W}_m^T\Phi_m(X_m)\delta\dot{q}_m(t)) - tr(\widetilde{W}_s^T\Phi_s(X_s)\delta\dot{q}_s(t)) \qquad (4.162)$$

Also, the time derivative of $V_2(t)$ is given by

$$\dot{V}_2(t) = \beta\delta\dot{q}_m^T(t)\left(\delta q_m(t) - \delta q_s\big(t - T_2(t)\big)\right)$$
$$+ \beta\delta\dot{q}_s^T(t)\left(\delta q_s(t) - \delta q_m\big(t - T_1(t)\big)\right) - \beta\delta\dot{q}_m^T(t)\int_{t-T_2(t)}^{t}\delta\dot{q}_s(\eta)d\eta$$
$$- \beta\delta\dot{q}_s^T(t)\int_{t-T_1(t)}^{t}\dot{q}_m(\eta)d\eta + \big(\hat{\Theta}_m(t) - \Theta_m\big)\dot{\hat{\Theta}}_m(t)$$
$$+ \big(\hat{\Theta}_s(t) - \Theta_s\big)\dot{\hat{\Theta}}_s(t) \qquad (4.163)$$

After algebraic manipulations, time derivative of $V_3(t)$ is found to satisfy

$$\dot{V}_3(t) \le T_1^{max}\dot{q}_m^T(t)\frac{\beta\delta^2}{2}\dot{q}_m(t) - \frac{\beta}{2}\int_{t-T_1(t)}^{t}\delta^2\dot{q}_m^T(\eta)\dot{q}_m(\eta)d\eta$$
$$+ T_2^{max}\dot{q}_s^T(t)\frac{\beta\delta^2}{2}\dot{q}_s(t) - \frac{\beta}{2}\int_{t-T_2(t)}^{t}\delta^2\dot{q}_s^T(\eta)\dot{q}_s(\eta)d\eta \qquad (4.164)$$

The time derivative of $V_4(t)$ can also be written as

$$\dot{V}_4(t) = \frac{\alpha - \alpha_1}{2}\Big(\delta^2 \dot{q}_m^T(t)\dot{q}_m(t) - \delta^2 \dot{q}_m^T\big(t - T_1(t)\big)\dot{q}_m\big(t - T_1(t)\big) + \dot{T}_1(t)\delta^2 \dot{q}_m^T\big(t - T_1(t)\big)\dot{q}_m\big(t - T_1(t)\big)\Big) + \frac{\alpha - \alpha_1}{2}\Big(\delta^2 \dot{q}_s^T(t)\dot{q}_s(t) - \delta^2 \dot{q}_s^T\big(t - T_2(t)\big)\dot{q}_s\big(t - T_2(t)\big) + \dot{T}_2(t)\delta^2 \dot{q}_s^T\big(t - T_2(t)\big)\dot{q}_s\big(t - T_2(t)\big)\Big) + \frac{b_2\alpha_1}{2\lambda_2}\Big(\delta^2 \dot{q}_m^T(t)\dot{q}_m(t) - \delta^2 \dot{q}_m^T\big(t - T_{l2}(t)\big)\dot{q}_m\big(t - T_{l2}(t)\big) + \dot{T}_{l2}(t)\delta^2 \dot{q}_m^T\big(t - T_{l2}(t)\big)\dot{q}_m\big(t - T_{l2}(t)\big)\Big) + \frac{\alpha_1}{2b_1\lambda_1}\Big(\delta^2 \dot{q}_s^T(t)\dot{q}_s(t) - \delta^2 \dot{q}_s^T\big(t - T_{l1}(t)\big)\dot{q}_s\big(t - T_{l1}(t)\big) + \dot{T}_{l1}(t)\delta^2 \dot{q}_s^T\big(t - T_{l1}(t)\big)\dot{q}_s\big(t - T_{l1}(t)\big)\Big) \quad (4.165)$$

The differential of $V_5(t)$ is

$$\dot{V}_5(t) = \dot{q}_m^T(t)\delta^2 M_h \ddot{q}_m(t) + \dot{q}_s^T(t)\delta^2 M_e \ddot{q}_s(t) \quad (4.166)$$

By setting σ_{1-2} to make sure

$$\sigma_1 \dot{q}_m^T(t)\dot{q}_m(t) > \dot{q}_m^T\big(t - T_{l2}(t)\big)\dot{q}_m\big(t - T_{l2}(t)\big) \quad (4.169)$$

$$\sigma_2 \dot{q}_s^T(t)\dot{q}_s(t) > \dot{q}_s^T\big(t - T_{l1}(t)\big)\dot{q}_s\big(t - T_{l1}(t)\big) \quad (4.170)$$

using the following inequalities from Lemma 1 in [177]

$$-2\dot{q}_m^T(t)\int_{t-T_2(t)}^{t}\dot{q}_s(\eta)d\eta - \int_{t-T_2(t)}^{t}\dot{q}_s^T(\eta)\dot{q}_s(\eta)d\eta \le T_2^{max}\dot{q}_m^T(t)\dot{q}_m(t)$$

$$-2\dot{q}_s^T(t)\int_{t-T_1(t)}^{t}\dot{q}_m(\eta)d\eta - \int_{t-T_1(t)}^{t}\dot{q}_m^T(\eta)\dot{q}_m(\eta)d\eta \le T_1^{max}\dot{q}_s^T(t)\dot{q}_s(t)$$

and with the adaptive law (4.160), it can be derived that

$$
\begin{aligned}
\dot{\mathrm{V}}(\mathrm{t}) < & -\delta\dot{q}_m^T(t)\left(b_1\lambda_1\alpha - \frac{\beta}{2}(\bar{T}_1 + \bar{T}_2 + \bar{\varepsilon}_1 + \bar{\varepsilon}_2)\right)\delta\dot{q}_m(t) \\
& - \delta\dot{q}_s^T(t)\left(\frac{\lambda_2\alpha}{b_2} - \frac{\beta}{2}(\bar{T}_1 + \bar{T}_2 + \bar{\varepsilon}_1 + \bar{\varepsilon}_2)\right)\delta\dot{q}_s(t) \\
& - \frac{\alpha - \alpha_1}{2}\left(\delta\dot{q}_m(t) - \delta\dot{q}_s\left(t - T_2(t)\right)\right)^T\left(\delta\dot{q}_m(t) - \delta\dot{q}_s\left(t - T_2(t)\right)\right) \\
& - \frac{\alpha - \alpha_1}{2}\left(\delta\dot{q}_s(t) - \delta\dot{q}_m\left(t - T_1(t)\right)\right)^T\left(\delta\dot{q}_s(t) - \delta\dot{q}_m\left(t - T_2(t)\right)\right) \\
& - \frac{b_2\alpha_1}{2\lambda_2}\left(\delta\dot{q}_m(t) - \delta\dot{q}_m\left(t - T_{l2}(t)\right)\right)^T\left(\delta\dot{q}_m(t) - \delta\dot{q}_m\left(t - T_{l2}(t)\right)\right) \\
& - \frac{\alpha_1}{2b_1\lambda_1}\left(\delta\dot{q}_s(t) - \delta\dot{q}_s\left(t - T_{l1}(t)\right)\right)^T\left(\delta\dot{q}_s(t) - \delta\dot{q}_s\left(t - T_{l1}(t)\right)\right) \\
& + \frac{(\alpha - \alpha_1)\dot{T}_1(t)\delta^2}{2}\dot{q}_m^T\left(t - T_1(t)\right)\dot{q}_m\left(t - T_1(t)\right) \\
& + \frac{(\alpha - \alpha_1)\dot{T}_2(t)\delta^2}{2}\dot{q}_s^T\left(t - T_2(t)\right)\dot{q}_s\left(t - T_2(t)\right) \\
& + \frac{\alpha_1\sigma_1\dot{T}_1(t)\delta^2}{2}\dot{q}_m^T(t)\dot{q}_m(t) + \frac{\alpha_1\sigma_2\dot{T}_2(t)\delta^2}{2}\dot{q}_s^T(t)\dot{q}_s(t) \\
& - \delta\dot{q}_m^T(t)\Gamma_1(t) - \delta\dot{q}_s^T(t)\Gamma_2(t) - \delta\dot{q}_m^T(t)B_h\delta\dot{q}_m(t) \\
& - \delta\dot{q}_s^T(t)B_e\delta\dot{q}_s(t) \\
& + \delta\dot{q}_m^T(t)\left(\bar{\xi}_m^*(X) + \tau_h^*(t) + F_m^* - \frac{\dot{q}_m(t)}{\|\dot{q}_m(t)\|}\hat{\Theta}_m(t)\right) \\
& + \delta\dot{q}_s^T(t)\left(\bar{\xi}_s^*(X) - \tau_e^*(t) + F_s^* - \frac{\delta\dot{q}_s(t)}{\|\delta\dot{q}_s(t)\|}\hat{\Theta}_s(t)\right) \\
& + \left(\hat{\Theta}_m(t) - \Theta_m\right)\|\delta\dot{q}_m(t)\| + \left(\hat{\Theta}_s(t) - \Theta_s\right)\|\delta\dot{q}_m(t)\| \qquad (4.171)
\end{aligned}
$$

Substituting the upper bounds Θ_i of $\left\|\bar{\xi}_i^*(X) + F_i^* \pm \tau_{h,e}^*\right\|$ into (4.171)

$$
\begin{aligned}
\dot{\mathrm{V}}(\mathrm{t}) < & -\delta\dot{q}_m^T(t)\left(b_1\lambda_1\alpha - \frac{\beta}{2}(\bar{T}_1 + \bar{T}_2 + \bar{\varepsilon}_1 + \bar{\varepsilon}_2)\right)\delta\dot{q}_m(t) \\
& - \delta\dot{q}_s^T(t)\left(\frac{\lambda_2\alpha}{b_2} - \frac{\beta}{2}(\bar{T}_1 + \bar{T}_2 + \bar{\varepsilon}_1 + \bar{\varepsilon}_2)\right)\delta\dot{q}_s(t) \\
& - \frac{\alpha - \alpha_1}{2}\left(\delta\dot{q}_m(t) - \delta\dot{q}_s\big(t - T_2(t)\big)\right)^T\left(\delta\dot{q}_m(t) - \delta\dot{q}_s\big(t - T_2(t)\big)\right) \\
& - \frac{\alpha - \alpha_1}{2}\left(\delta\dot{q}_s(t) - \delta\dot{q}_m\big(t - T_1(t)\big)\right)^T\left(\delta\dot{q}_s(t) - \delta\dot{q}_m\big(t - T_2(t)\big)\right) \\
& - \frac{b_2\alpha_1}{2\lambda_2}\left(\delta\dot{q}_m(t) - \delta\dot{q}_m\big(t - T_{l2}(t)\big)\right)^T\left(\delta\dot{q}_m(t) - \delta\dot{q}_m\big(t - T_{l2}(t)\big)\right) \\
& - \frac{\alpha_1}{2b_1\lambda_1}\left(\delta\dot{q}_s(t) - \delta\dot{q}_s\big(t - T_{l1}(t)\big)\right)^T\left(\delta\dot{q}_s(t) - \delta\dot{q}_s\big(t - T_{l1}(t)\big)\right) \\
& + \frac{(\alpha - \alpha_1)\dot{T}_1(t)\delta^2}{2}\dot{q}_m^T\big(t - T_1(t)\big)\dot{q}_m\big(t - T_1(t)\big) \\
& + \frac{(\alpha - \alpha_1)\dot{T}_2(t)\delta^2}{2}\dot{q}_s^T\big(t - T_2(t)\big)\dot{q}_s\big(t - T_2(t)\big) \\
& + \frac{\alpha_1\sigma_1\dot{T}_1(t)\delta^2}{2}\dot{q}_m^T(t)\dot{q}_m(t) + \frac{\alpha_1\sigma_2\dot{T}_2(t)\delta^2}{2}\dot{q}_s^T(t)\dot{q}_s(t) \\
& - \delta\dot{q}_m^T(t)\Gamma_1(t) - \delta\dot{q}_s^T(t)\Gamma_2(t) - \delta\dot{q}_m^T(t)B_h\delta\dot{q}_m(t) \\
& - \delta\dot{q}_s^T(t)B_e\delta\dot{q}_s(t) \qquad (4.172)
\end{aligned}
$$

The Lyapunov approach requires $\dot{V}(t)$ to be negative semi-definite. In the presence of constant time delays, $\dot{T}_{1,2}(t)$ and $\bar{\varepsilon}_{1,2}$ are zero. Also, the passivity controllers do not take effect so that $\Gamma_1(t)$ and $\Gamma_2(t)$ are zero, $\dot{V}(t)$ can be guaranteed to be negative semi-definite by properly tuning $b_{1,2}$, $\lambda_{1,2}$, α and β to make sure

$$
b_1\lambda_1\alpha + \frac{b_2\alpha_1}{2\lambda_2}\zeta_a \geq \frac{\beta}{2}(\bar{T}_1 + \bar{T}_2) \qquad (4.173)
$$

$$
\frac{\lambda_2\alpha}{b_2} + \frac{\alpha_1}{2b_1\lambda_1}\zeta_b \geq \frac{\beta}{2}(\bar{T}_1 + \bar{T}_2) \qquad (4.174)
$$

When the time delay is varying, the passivity controllers are launched by the passivity observers, the biased terms $\frac{\beta}{2}(\bar{\varepsilon}_1 + \bar{\varepsilon}_2)\delta^2\dot{q}_m^T(t)\dot{q}_m(t) + \frac{\beta}{2}(\bar{\varepsilon}_1 + \bar{\varepsilon}_2)\delta^2\dot{q}_s^T(t)\dot{q}_s(t) +$

$\frac{(\alpha-\alpha_1)\dot{T}_1(t)\delta^2}{2}\dot{q}_m^T\big(t-T_1(t)\big)\dot{q}_m\big(t-T_1(t)\big)+\frac{(\alpha-\alpha_1)\dot{T}_2(t)\delta^2}{2}\dot{q}_s^T\big(t-T_2(t)\big)\dot{q}_s\big(t-T_2(t)\big)+\frac{\alpha_1\sigma_3\dot{T}_1(t)\delta^2}{2}\dot{q}_m^T(t)\dot{q}_m(t)+\frac{\alpha_1\sigma_4\dot{T}_2(t)\delta^2}{2}\dot{q}_s^T(t)\dot{q}_s(t)$ caused by the time varying delays in (4.174) are directly compensated by $-\delta\dot{q}_m^T(t)\Gamma_1(t)-\delta\dot{q}_s^T(t)\Gamma_2(t)$. No extra parameters need to be tuned when the time delays vary and $\dot{\mathrm{V}}(t)$ is still negative semi-definite.

Integrating both sides of (4.172), we get:

$$
\begin{aligned}
+\infty > V(0) \geq V(0)-V(t) \\
&> \int_0^t \Bigg(\frac{\alpha}{2}\Big(\delta\dot{q}_m(t)-\delta\dot{q}_s\big(t-T_2(t)\big)\Big)^T\Big(\delta\dot{q}_m(t)-\delta\dot{q}_s\big(t-T_2(t)\big)\Big) \\
&+\frac{\alpha}{2}\Big(\delta\dot{q}_s(t)-\delta\dot{q}_m\big(t-T_1(t)\big)\Big)^T\Big(\delta\dot{q}_s(t)-\delta\dot{q}_m\big(t-T_2(t)\big)\Big) \\
&+\frac{b_2\alpha_1}{2\lambda_2}\Big(\delta\dot{q}_m(t)-\delta\dot{q}_m\big(t-T_{l2}(t)\big)\Big)^T\Big(\delta\dot{q}_m(t)-\delta\dot{q}_m\big(t-T_{l2}(t)\big)\Big) \\
&+\frac{\alpha_1}{2b_1\lambda_1}\Big(\delta\dot{q}_s(t)-\delta\dot{q}_s\big(t-T_{l1}(t)\big)\Big)^T\Big(\delta\dot{q}_s(t)-\delta\dot{q}_s\big(t-T_{l1}(t)\big)\Big) \\
&+\delta\dot{q}_m^T(t)B_h\delta\dot{q}_m(t)+\delta\dot{q}_s^T(t)B_e\delta\dot{q}_s(t)\Bigg)dt
\end{aligned}
\tag{4.175}
$$

Therefore, from $V(t)\geq 0$ and $\dot{\mathrm{V}}(t)\leq 0$, it is true that $\widetilde{W}_m$ and $\widetilde{W}_s \in L_\infty$, $\dot{q}_m(t)$ and $\dot{q}_s(t)\in L_2$. $\Big(\dot{q}_m(t)-\dot{q}_s\big(t-T_2(t)\big)\Big)$, $\Big(\dot{q}_s(t)-\dot{q}_m\big(t-T_2(t)\big)\Big)$, $\Big(\dot{q}_m(t)-\dot{q}_m\big(t-T_{l2}(t)\big)\Big)$,$\Big(\dot{q}_s(t)-\dot{q}_s\big(t-T_{l1}(t)\big)\Big)\in L_2$. Using the fact that $q_m(t)-q_s\big(t-T_2(t)\big)=q_m(t)-q_s(t)+\int_{t-T_2(t)}^t\dot{q}_s(t)dt$, $q_s(t)-q_m\big(t-T_1(t)\big)=q_s(t)-q_m(t)+\int_{t-T_1(t)}^t\dot{q}_1(t)dt$ and using Cauchy-Schwarz inequality $\int_{t-T_2(t)}^t\dot{q}_s(t)dt\leq\sqrt{T_2(t)}\dot{q}_s(t)$ and $\int_{t-T_1(t)}^t\dot{q}_m(t)dt\leq\sqrt{T_1(t)}\dot{q}_m(t)$, we can get $q_m(t)-q_s\big(t-T_2(t)\big), q_s(t)-q_m\big(t-T_1(t)\big)\in L_\infty$.

The system's dynamic model in (4.116)-(4.117) can also be written as:

$$
\begin{aligned}
\delta\ddot{q}_i = M_i^{-1}(q_i)\big[\tau_i \pm \tau_{h,e}^*(t)-B_{h,e}\delta\dot{q}_i(t)-M_{h,e}\delta\ddot{q}_i(t)+F_i^*-f_i(X_i) \\
-C_i(q_i,\dot{q}_i)\delta\dot{q}_i\big]
\end{aligned}
\tag{4.176}
$$

Differentiating both sides of (4.176):

$$\frac{d}{dt}\delta\ddot{q}_i = \frac{d}{dt}\left(M_i^{-1}(q_i)\right)\left[\tau_i \pm \tau_{h,e}^*(t) - B_{h,e}\delta\dot{q}_i(t) - M_{h,e}\delta\ddot{q}_i(t) + F_i^* - f_i(X_i) - C_i(q_i,\dot{q}_i)\delta\dot{q}_i\right] + M_i^{-1}(q_i)\frac{d}{dt}\left[\tau_i \pm \tau_{h,e}^*(t) - B_{h,e}\delta\dot{q}_i(t) - M_{h,e}\delta\ddot{q}_i(t) + F_i^* - f_i(X_i) - C_i(q_i,\dot{q}_i)\delta\dot{q}_i\right] \quad (4.177)$$

For the first term of the right side of (4.177), we have $\frac{d}{dt}(M_i^{-1}) = -M_i^{-1}\dot{M}_i M_i^{-1} = -M_i^{-1}(C_i + C_i^T)M_i^{-1}$. According to Properties 1 and 3, $\frac{d}{dt}(M_i^{-1})$ is bounded. Based on Property 4, the terms in bracket of (4.181) are also bounded. Therefore, $\frac{d}{dt}\ddot{q}_i(t) \in L_\infty$ and $\ddot{\mathrm{q}}_\mathrm{i}(\mathrm{t})$ are uniformly continuous ($\int_0^t \ddot{q}_i(\eta)d\eta = \dot{q}_i(t) - \dot{q}_i(0)$). Since $\dot{q}_i(t) \to 0$, it can be concluded that $\ddot{q}_i(t) \to 0$ based on Barbălat's Lemma.

4.5.3 Experimental results

The teleoperation system for the experiments consist of two 3-DOF Phantom manipulators: Phantom Omni and Phantom Desktop (Sensable Technologies, Inc., Wilmington, MA) as shown in Fig.3.19 The two haptic devices are connected by two computers which are directly connected via a network cable and network cards. The Matlab software is applied to establish the proposed control system. To further enlarge and tune the value of the time delays, Simulink time delay blocks are also applied. During the experimental process, the control loop is configured as a 1 kHz sampling rate. The general control parameters are configured as: $b_1 = b_2 = 2$, $\alpha = [15,15,15]^T$, $\beta = [15,15,15]^T$, $\gamma = [10,10,10]^T$ $\delta = 0.2$, $\Omega_s = \Omega_m = [25,25,25]^T$. $\sigma_1 = \sigma_2 = 2$. The neurons of the neural network in the experiment are seven. Since the experimental platform is 3-DOF experiment and $X_i(t) = [\ddot{q}_i^T(t), \dot{q}_i^T(t), q_i^T(t)]^T$, the centre of the RBF is set as $C = 0.5 \times ones(9,7)$ and the width of the RBF is set as $H = 0.1 \times ones(7,1)$. The parameters relating to the time delays will be introduced in each experiment.

4.5.3.1 Innovative passivity observers

The intention of the experiments in this sub-section is to display the novelty of the proposed passivity observers. The proposed system is compared with a novel TDPA-based system in [156]. The time delays are constant and T_1 is 200 ms, T_2 is 100 ms. We set $\lambda_1 = 0.075$, $\lambda_2 = 0.3$, $\bar{\mu}_1 = \bar{\mu}_2 = \bar{\varepsilon}_1 = \bar{\varepsilon}_2 = 0$. In the system in [156], the slave PD controllers are chosen as $K_p = 10$ and $K_d = 5$. b in their passivity observers is 2.5.

Fig.4.39 shows the position tracking, tracking errors and observed power of the two systems. Even under small constant time delays whilst the rate of the time delays are zero, the power observed on the master side is still non-positive so that the passivity controllers are still launched to reduce tracking performance. As shown in Fig.4.39, the slave cannot quickly and closely track the master in the presence of such small delays in the system in [156]. Unlike [156], the power signals observed on the master and the slave sides of the proposed system are positive owning to the designed wave-based passivity observer, and the passivity controllers are not launched. Therefore, the tracking error is close to zero.

On the other hand, Fig.4.40 displays the torque tracking, tracking errors and observed power signals of the two systems. The power observed on the slave side in the system in [156]

is definitely non-positive. Therefore, large torque tracking errors are caused by the passivity controllers. By contrast, the power signals observed in the proposed system are non-negative so that the torque tracking error is guaranteed at the range of ± 0.05. From these two figures, we can see that the proposed wave-based passivity observers facilitate our system to be not as conservative as the conventional power-based system and guarantee the system high tracking performance in the presence of constant time delays.

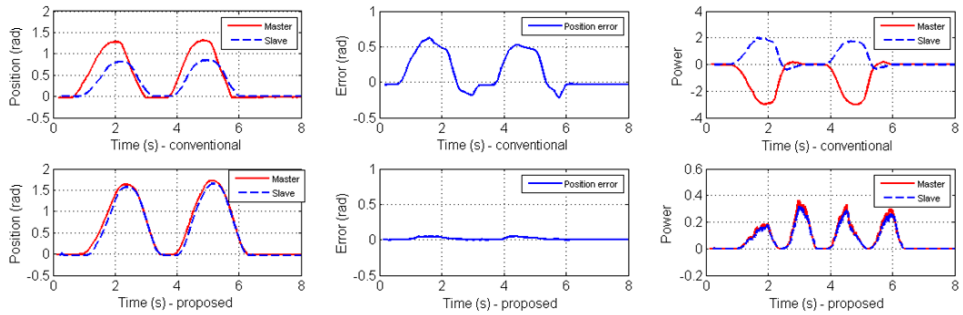

Figure 4.39. Free motion under constant time delays (Comparison between [156] and our system)

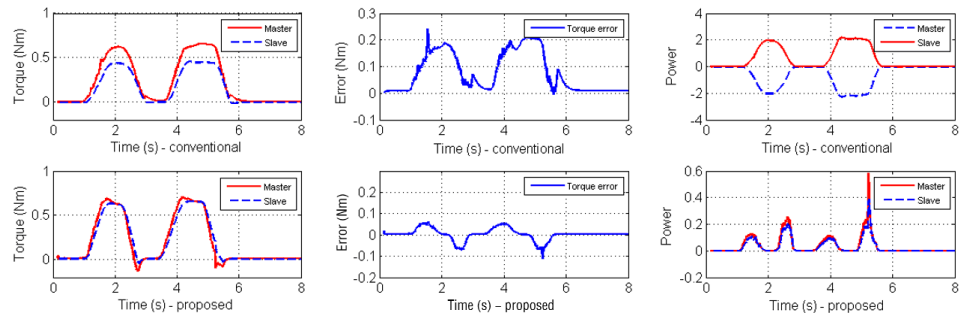

Figure 4.40. Hard contact under constant time delays (Comparison between [156] and our system)

4.5.3.2 Eliminating wave reflection

In this sub-section, we compare our system with the wave-based system proposed in [25] in order to show the novelty of wave reflections elimination in the proposed system.Fig.4.41 and 4.42 show the position and torque tracking and their relating tracking errors in contacting a reverse wall. The time delays in this experiment are around 900 ms with 100 variations, and its rate is around 0.2. Fig.4.43 shows the values of the forward and backward time delays. we set $\lambda_1 = 0.45, \lambda_2 = 1.8$, $\bar{\mu}_1 = \bar{\mu}_2 = 0.2$, $\bar{\varepsilon}_1 = \bar{\varepsilon}_2 = 0.2$. The wave-based system in [25] uses a traditional wave transformation with impedance matching to encode the velocity and position signals. Based on their recommendation, we set $K_m = K_s = b = 4$. The extra energy caused

by time-varying delays in their system is eliminated by applying the scaling gain $\sqrt{1-\bar{\mu}_{1,2}}$.

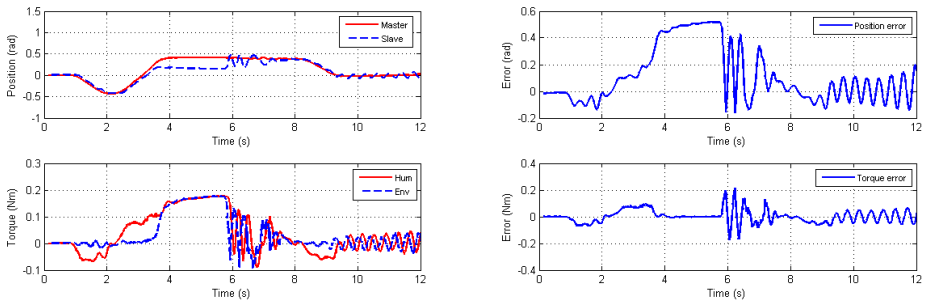

Figure 4.41. Contact to a reverse wall under slowly varying delays (wave-based system in [25])

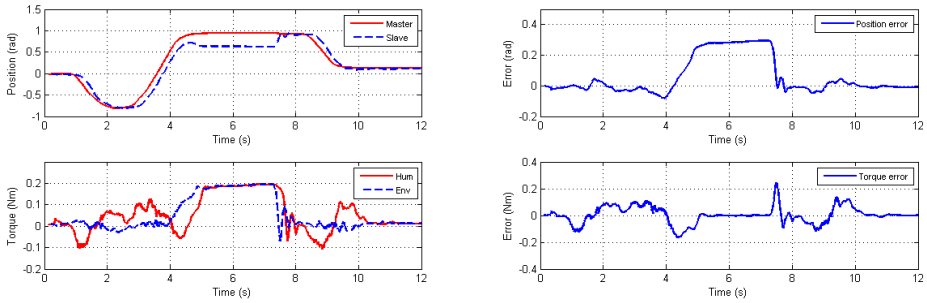

Figure 4.42. Contact to a reverse wall under slowly varying delays (our system)

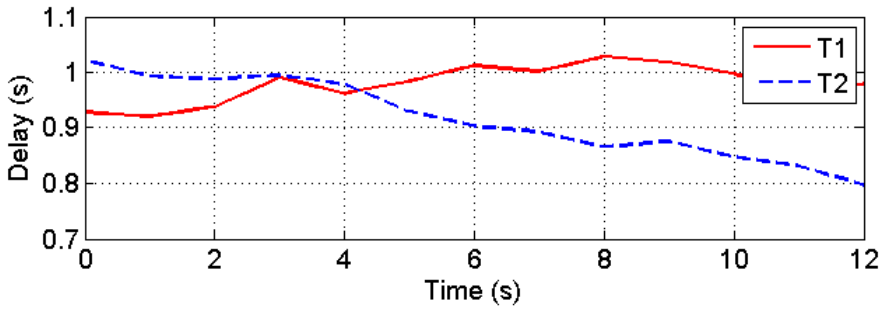

Figure 4.43. Time delays

Before the 4th second, the slave robot in the two systems are controlled to conduct a free motion at first, and we can see that both of the two systems have accurate position

tracking. Then the slave robot contacts to reverse wall and accurate torque tracking is also achieved in this two systems. Therefore, both of the two system have good performance on steady state. However, after hard contact for less than 2 seconds, the wall is suddenly removed thereby transiently changing the environment. Even the system in [25] has impedance matching approaches, due to the sudden changing environment, the impedances of the system is mismatched and the wave-reflections reinstate so that large perturbations occur and the system's position and torque tracking performances are adversely influenced. By contrast, based on the designed wave variables, the outgoing signals do not contain necessary signals and the wave reflections are eliminated. Therefore, the proposed system has better performance on the transient state and the position error directly returned to zero after removing the wall.

4.5.3.3 Performance in the presence of time-varying delays

Since velocity and position signals are the main control elements, our proposed system has similarity to a PD+d system. Therefore, in this subsection, we compare our system with the classical PD+d system proposed in [24] in order to show the novelty for dealing with the time-varying delays in the proposed system. The time delays in this experiment are approximately 1 s with 500 ms variations, and the rate is around 0.5. The time delays' pattern in this experiment is shown in Fig.4.44. We set $\lambda_1 = 0.5$, $\lambda_2 = 2$, $\bar{\mu}_1 = \bar{\mu}_2 = 0.5$, $\bar{\varepsilon}_1 = \bar{\varepsilon}_2 = 0.5$.

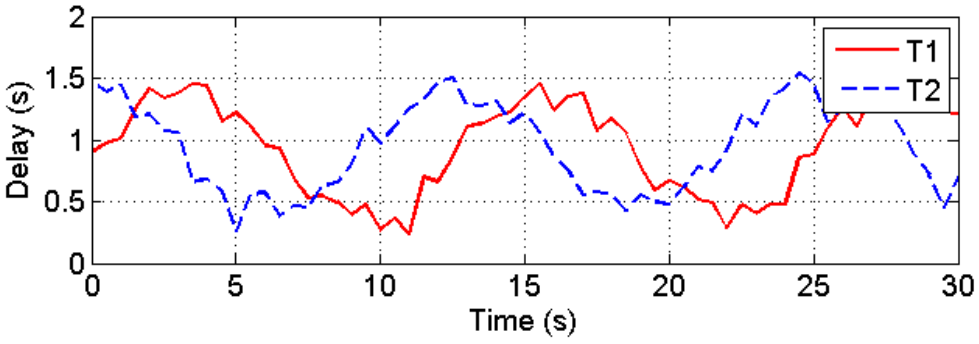

Figure 4.44. Time delays

In order to guarantee stability, the parameters in the system in [24] are required to satisfy $4B_rB_l > (T_1^{max2} + T_2^{max2})K_lK_r$, $B_r \geq B_l$ and $K_r \geq K_l$. Therefore, we set the differential gain $K_d = 3$, the proportional gains $K_r = K_l = 3$. Hence, $B_r = B_l = 3.5$. The PD+d system in [24] also uses the scaling gain $\sqrt{1-\bar{\mu}_{1,2}}$ for the velocities transmission. It is noticeable that when $\bar{\mu}_{1,2} \geq 1$, this approach is too conservative and velocities are not possible to be transmitted. Figs.4.45 and 4.46 demonstrate position tracking, position errors and torque tracking of the two systems. The key element in a PD+d system is the velocity damper which can guarantee the system's stability but, instead, degrade the system's transparency.

As shown in Fig.4.45, in such a large time delays, the velocity damper B_r and B_l in the system in [24] have to be set large enough to guarantee stability, and $\sqrt{1-\bar{\mu}_{1,2}}$ also affect the velocity transmission in a certain degree to the extent that the position tracking is affected and large position errors occur. Also, the operator feels the system over-damped and achieves large feedback forces even under free motion.

By contrast, the velocity dampers in our system are varying predicated on the observed power signals at each port. Based on Fig.4.46, the observed power signals are not definitely negative, so that the passivity controllers keep varying between activation and deactivation modes. Therefore, the proposed system is not as conservative as the classical PD+d system in [24] and can achieve more accurate position tracking performance under large time-varying delays. In addition, since the proposed system is not over-damped, the feedback force felt by the operator is not as large as that in the system in [24].

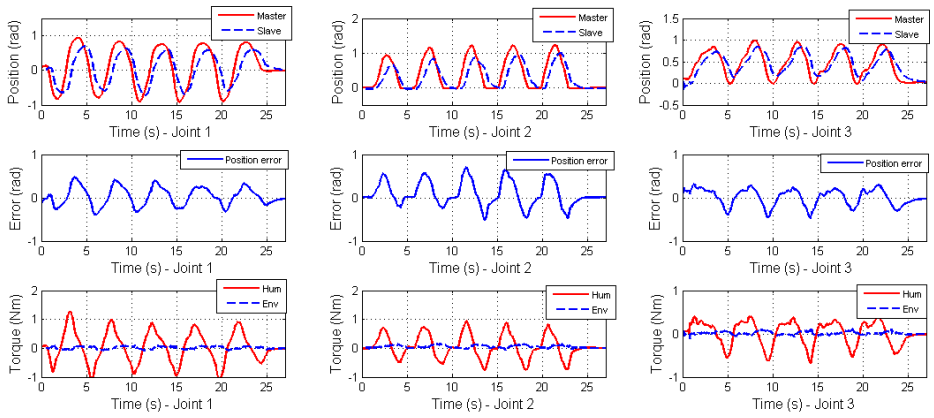

Figure 4.45. Free motion under time varying delays (PD+d system in [24])

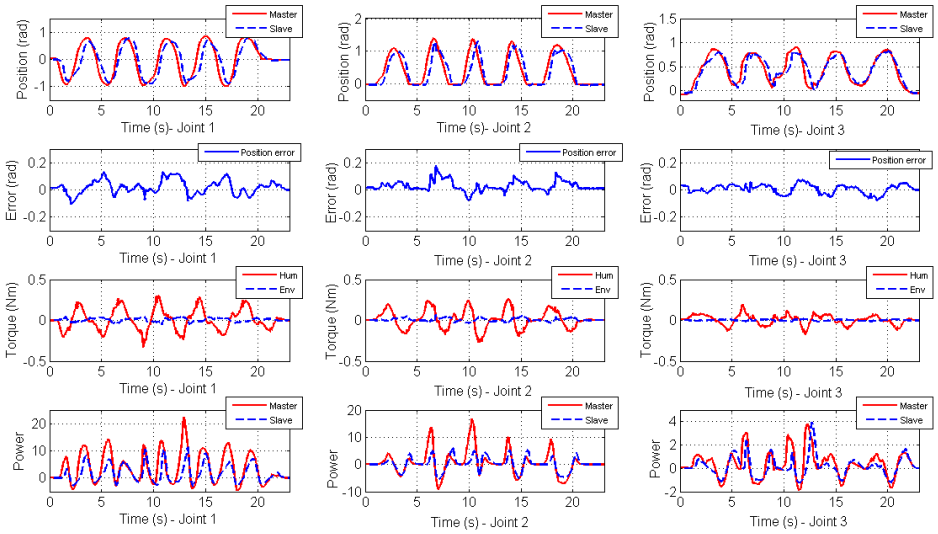

Figure 4.46. Free motion under time varying delays (our system)

4.5.3.4 Performance in the presence of fast-varying delays

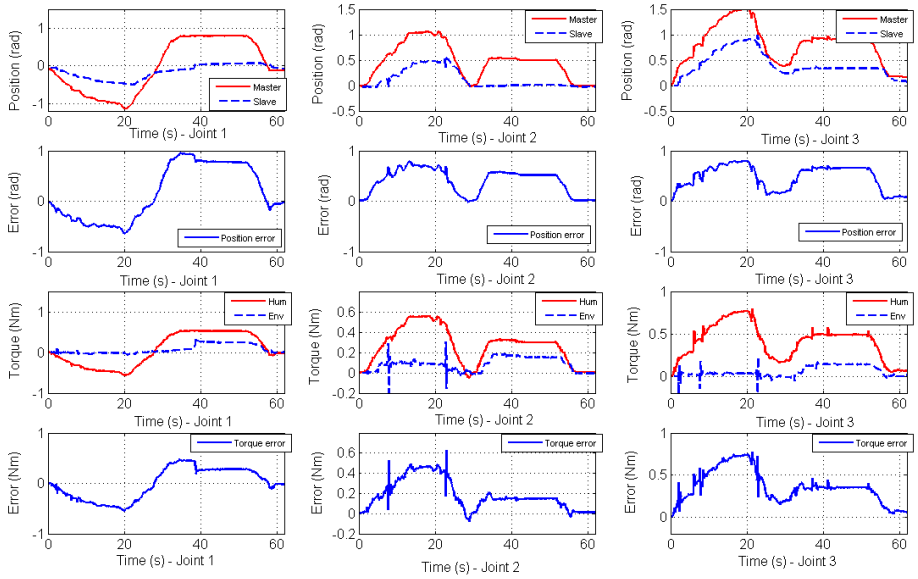

Figure 4.47. Free motion and hard contact under sharply-varying delays (system in Section 4.3)

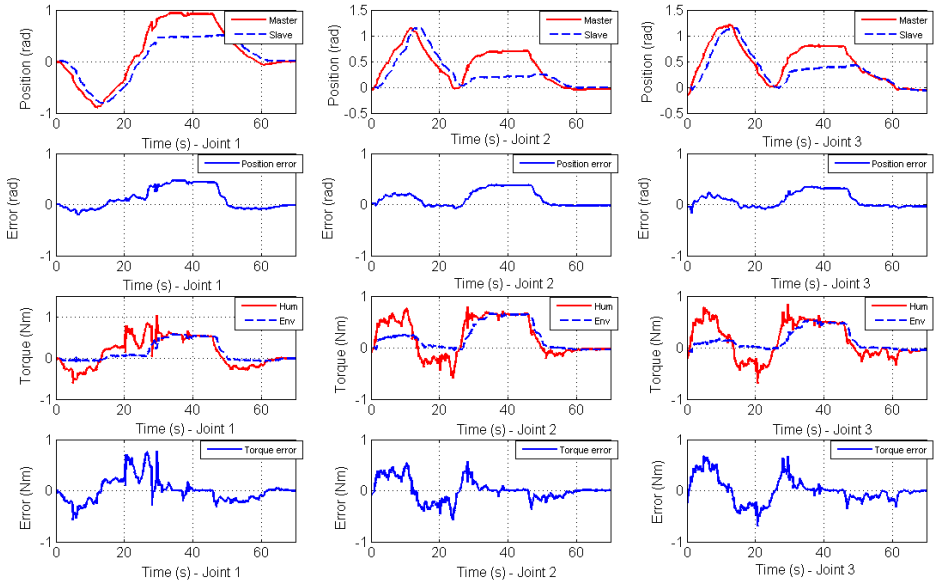

Figure 4.48. Free motion and hard contact under sharply-varying delays (proposed system)

The Novelty of the proposed system is also reflected in dealing with the sharply-varying delays. In this subsection, we compare the new system with the system previously designed in Section 4.3. The time delays for the experiment of the new system are set to be a very large value (around 2s with 1s variations) and with a large rate (around 1.5). We set $\lambda_1 = 1, \lambda_2 = 4$, $\bar{\mu}_1 = \bar{\mu}_2 = 1.5, \bar{\varepsilon}_1 = \bar{\varepsilon}_2 = 1$. The slave robot in these two systems is controlled to conduct a free motion at first and then come in contact with a solid wall in the reverse direction. Figs.4.47 and 4.48 show the position and torque tracking as well as the related tracking errors of the two systems. The pattern of the time delays for the new system are shown in Fig.4.49.

The system we proposed in Section 4.3 suffered from two deficiencies . Firstly, the parameters configuration in Section 4.3 are seriously restricted by the assumption that $\dot{T}_{1,2}(t) \leq 1$. If $\dot{T}_{1,2}(t) > 1$, the stability of the whole system cannot be guaranteed. The time delays of the system in [19] are set as 2s with 1s variations but with a rate of 0.9. The pattern of the time delays for the system in Section 4.3 are shown in Fig.4.50 and the related parameters are set as recommended in Section 4.3.

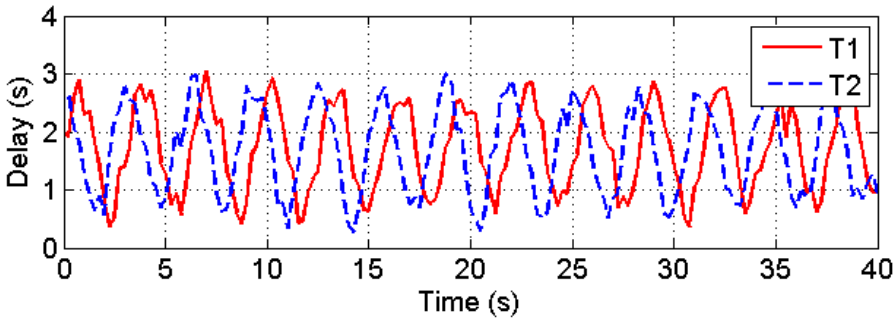

Figure 4.49. Time delays for our new system

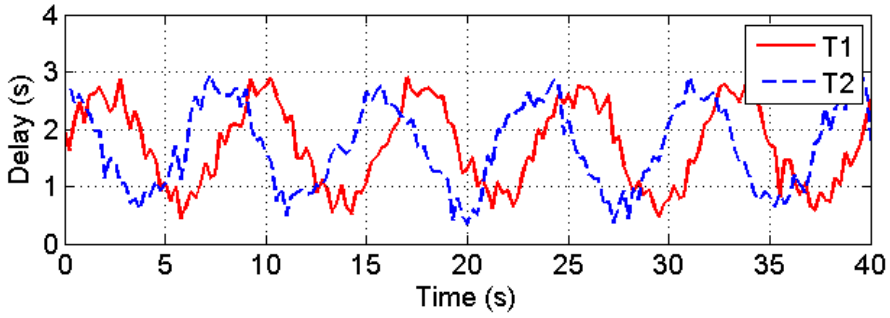

Figure 4.50. Time delays for system in Section 4.3

In addition, the second drawback mainly epitomizes the passivity controllers of the system in Section 4.3, where the passivity controllers guarantee system's stability by largely reducing the position and torque signals. As shown in Fig.4.47, the slave robot cannot closely and rapidly track the master robot during free motion, and large torque tracking errors exist during hard environmental contact.

In contrast, the passivity controllers in our new system are actually velocity dampers with the value varying according to the observed powers. Therefore, according to Fig.4.48, even with the higher rate of time delays, the position tracking in free motion and torque tracking in hard contact are still better that those of the system in Section 4.3. The experiment illustrates that our new system is more practical than system proposed in Section 4.3 in the worst-case scenario.

4.6 Summary

In Chapter 4, new wave-based TDPA systems are proposed to achieve high transparency and stability in the presence of random. Compared with the passivity-based systems of previous work, the proposed systems can achieve higher transparency and simultaneously maintain stability under random time delays. Neural networks are applied to eliminate the system uncertainties. The system stability in different environment is proved. The performance of the proposed algorithm was validated using 3-DOF teleoperation system.

5 MULTILATERAL TELEOPERATION SYSTEMS

5.1 Introduction

The main advantage of the passivity-based systems introduced in Chapters 3 and 4 is simultaneously achieving high transparency and robust stability in the presence of random time delays. With this advantage, the systems introduced in Chapters 3 and 4 are suitable to be deployed in the multilateral teleoperation. In this Chapter, the reduced wave reflections nonlinear system introduced in Chapter 3 is extended to a Single-Master-Multi-Slave teleoperation system to guarantee accurate position synchronization and force reflection of all the robots in the presence of time-varying delays. The wave-based TDPA architecture in Chapter 4.3 is also extended to a flexible dual-user-dual-slave teleoperation system with variable dominance factors. An innovative multi-user shared control teleoperation system is developed to allow the mentor to guide multiple trainees in order to collaboratively drive the slave robot and perform the remote task. The stability of the proposed nonlinear teleoperation systems is analyzed using Lyapunov functions. The experimental results based on a teleoperation platform consisting of multiple haptic devices show that the proposed systems can effectively perform different tasks.

5.2 SMMS System applying Reduced Wave Reflections Architecture

5.2.1 Modeling the n-DOF Multi-lateral Teleoperation System

In Chapter 5.2, the master robot and the n-slave robots are modeled as a pair of multi-DOF serial links with revolute joints. The nonlinear dynamics of such a system can be modeled as:

$$M_m(q_m)\ddot{q}_m + C_m(q_m,)\dot{q}_m + g_m(q_m) = \tau_m + \tau_h \tag{5.1}$$

$$\begin{cases} M_{s1}(q_{s1})\ddot{q}_{s1} + C_{s1}(q_{s1},\dot{q}_{s1})\dot{q}_{s1} + g_{s1}(q_{s1}) = \tau_{s1} - \tau_{e1} \\ M_{s2}(q_{s2})\ddot{q}_{s2} + C_{s2}(q_{s2},\dot{q}_{s2})\dot{q}_{s2} + g_{s2}(q_{s2}) = \tau_{s2} - \tau_{e2} \\ \cdots\cdots \\ M_{sn}(q_{sn})\ddot{q}_{sn} + C_{sn}(q_{sn},\dot{q}_{sn})\dot{q}_{sn} + g_{sn}(q_{sn}) = \tau_{sn} - \tau_{en} \end{cases} \quad (5.2)$$

where $i = m, s$, m – master, s – slave. $\ddot{q}_{ij}$, $\dot{q}_{ij}$, $q_{ij} \in R^n$ are the joint acceleration, velocity and position, respectively and m denots the master and sj denotes the j-th slave. $j \in 1,2,\ldots n$ denotes the number of slave robots. $M_{ij}(q_{ij}) \in R^{n\times n}$ are the inertia matrices, $C_i(q_i,\dot{q}_i) \in R^{n\times n}$ are Coriolis/centrifugal effects. $g_{ij}(q_{ij}) \in R^n$ are the vectors of gravitational forces and τ_{ij} are the control signals. The forces applied on the end-effector of the master and slave robots are related to equivalent torques in their joints by:

$$F_h = J_m^T \tau_h, F_{en} = J_{sn}^T \tau_{en} \quad (5.3)$$

where J_m , J_{sn} are the Jacobean of the master robot and the n-th slave robot, respectively. F_h and F_{en} stand for the human and environment forces, respectively.

Important properties of the above nonlinear dynamic model, which will be used in this section, are as follows:

P1: The inertia matrix $M_{ij}(q_{ij})$ for a manipulator is symmetric positive-definite which verifies:$0 < \sigma_{min}\left(M_{ij}\left(q_{ij}(t)\right)\right) I \le M_{ij}\left(q_{ij}(t)\right) \le \sigma_{max}\left(M_{ij}\left(q_{ij}(t)\right)\right) I \le \infty$, where $I \in R^{n\times n}$ is the identity matrix. σ_{min} and σ_{max} denote the strictly positive minimum (maximum) eigenvalue of M_ij for all configurations q_{ij}.

P2: Under an appropriate definition of the Coriolis/centrifugal matrix, the matrix $\dot{M}_{ij} - 2C_{ij}$ is skew symmetric, which can also be expressed as:

$$\dot{M}_{ij}(q_{ij}(t)) = C_{ij}(q_{ij}(t),\dot{q}_{ij}(t)) + C_{ij}^T(q_{ij}(t),\dot{q}_{ij}(t)) \quad (5.4)$$

P3: The Lagrangian dynamics are linearly parameterizable:

$$M_{ij}(q_{ij})\ddot{q}_{ij} + C_{ij}(q_{ij},\dot{q}_{ij})\dot{q}_{ij} + g_{ij}(q_{ij}) = Y(q_{ij},\dot{q}_{ij},\ddot{q}_{ij}) \quad (5.5)$$

where θ is a constant p-dimensional vector of inertia parameters and $Y(q_{m,s}, \dot{q}_{m,s}, \ddot{q}_{m,s}) \in R^{n \times p}$ is the matrix of known functions of the generalized coordinates and their higher derivatives.

P4: For a manipulator with revolute joints, there exists a positive Z bounding the Coriolis/centrifugal matrix as:

$$\left\| C_{ij}\left(q_{ij}(t), x(t)\right) y(t) \right\|_2 \leq Z \|x(t)\|_2 \|y(t)\|_2 \tag{5.6}$$

P5: The time derivative of $C_{ij}\left(q_{ij}(t), x(t)\right)$ is bounded if $q_{ij}(t)$ and $\dot{q}_{ij}(t)$ are bounded.

5.2.2 Control Laws

In order to guarantee the passivity of the time delayed communication channels between the master robot and each slave robot, the modified wave variable transformation introduced in Chapter 3 is applied in this section as shown in Figure 5.1. The main advantage of the modified wave controllers is the efficient reduction in the wave-based reflections while simultaneously guaranteeing channels' passivity.

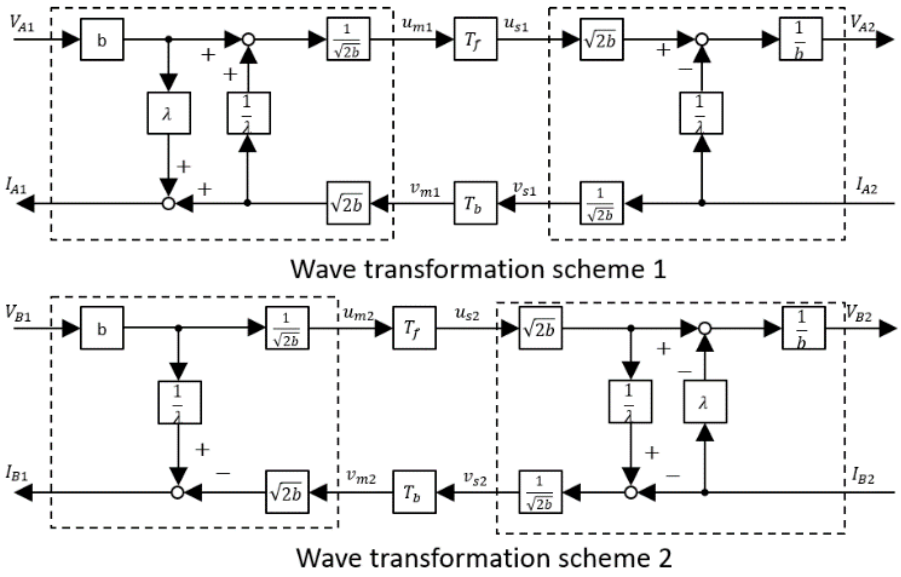

Figure 5.1. Modified wave-variable controllers

The wave variables in the two controllers are defined as follows:

$$u_{m1}(t) = \frac{bV_{A1}(t) + \frac{1}{\lambda} I_{A2}\left(t - T_f(t)\right)}{\sqrt{2b}}, u_{s1}(t) = \frac{bV_{A2}(t) + \frac{1}{\lambda} I_{A2}(t)}{\sqrt{2b}} \tag{5.7}$$

$$v_{m1}(t) = \frac{I_{A2}(t - T_b(t))}{\sqrt{2b}}, v_{s1}(t) = \frac{I_{A2}(t)}{\sqrt{2b}} \tag{5.8}$$

$$u_{m2}(t) = \frac{bV_{B1}(t)}{\sqrt{2b}}, u_{s2}(t) = \frac{bV_{B1}\left(t - T_f(t)\right)}{\sqrt{2b}} \tag{5.9}$$

$$v_{m2}(t) = \frac{\frac{b}{\lambda} V_{B1}(t) - I_{B1}(t)}{\sqrt{2b}}, v_{s2}(t) = \frac{\frac{b}{\lambda} V_{B1}\left(t - T_f(t)\right) - I_{B2}(t)}{\sqrt{2b}} \tag{5.10}$$

where b and λ are the characteristic impedances.

In the proposed SMMS teleoperation system in which one master robot is used to control multiple slave robots, the main objective is to have the positions of all the slave robots accurately synchronized to the position of the master robot. A secondary objective is that all the robots should have accurate force tracking with each other, which means when one slave robot comes in contact with the remote environmental object during free motion, it will immediately feedback the force information to all of other robots to signal them to stop. Via reaching the two targets, all the slave robots will precisely follow the human operator in different environmental scenarios. By applying the two wave controllers, the energy information such as torque, position and velocity signals can be transmitted through the communication channels without influencing the system passivity. By setting $\mathrm{V_{A1}(t) = C_1\tau_h(t)}$, $\mathrm{I_{B1}(t) = \beta\left(\dot{q}_m(t) + \delta q_m(t)\right)}$, $\mathrm{I_{A2}(t) = -\beta(\dot{q}_s(t) + \delta q_s(t))}$, $\mathrm{V_{B2}(t) = C_2\tau_e(t)}$, a new state variables E_m for the master robot is introduced as follows:

$$E_m = \sum_{j=1}^{n} \Big\{ (C_{3j} - b_j \lambda_j C_{1j}) \tau_h(t) - C_{2j} \tau_{ej} \left(t - T_{bj}(t) \right) + \beta_j \left(\dot{q}_{sj} \left(t - T_{bj}(t) \right) + \delta q_{sj} \left(t - T_{bj}(t) \right) \right) - \beta_j \left(\dot{q}_m(t) + \delta q_m(t) \right) - \left(\frac{b_j}{\lambda_j} \beta_j \left(\dot{q}_m(t) + \delta q_m(t) \right) - \frac{b_j}{\lambda_j} \beta_j \left(\dot{q}_m \left(t - T_{fj}(t) - T_{bj}(t) \right) + \delta q_m \left(t - T_{fj}(t) - T_{bj}(t) \right) \right) \right) \Big\} \quad (5.11)$$

where C_{1-4}, β, δ are diagonal positive-definite matrices. In the slave sides, each slave robot receives control signals from the master robot and the other slave robots. The new master-control state variable E_{sn}^* for the n-th slave robot is written as follows:

$$E_{sn}^* = C_{1n} \tau_h \left(t - T_{fn}(t) \right) - \left(\frac{\lambda_n C_{2n}}{b_n} - C_{4n} \right) \tau_{en}(t) + \beta_n \left(\dot{q}_m \left(t - T_{fn}(t) \right) + \delta q_m \left(t - T_{fn}(t) \right) \right) - \beta_n \left(\dot{q}_{sn}(t) + \delta q_{sn}(t) \right) - \left[\frac{\beta_n}{b_n \lambda_n} \left(\dot{q}_{sn}(t) + \delta q_{sn}(t) \right) - \frac{\beta_n}{b_n \lambda_n} \left(\dot{q}_{sn} \left(t - T_{fn}(t) - T_{bn}(t) \right) + \delta q_{sn} \left(t - T_{fn}(t) - T_{bn}(t) \right) \right) \right] \quad (5.12)$$

$$
\begin{aligned}
E_{sn} = {} & C_{1n}\tau_h\left(t - T_{fn}(t)\right) - \left(\frac{\lambda_n C_{2n}}{b_n} - C_{4n}\right)\tau_{en}(t) \\
& + \beta_n\left(\dot{q}_m\left(t - T_{fn}(t)\right) + \delta q_m\left(t - T_{fn}(t)\right)\right) \\
& - \beta_n\left(\dot{q}_{sn}(t) + \delta q_{sn}(t)\right) \\
& - \left[\frac{\beta_n}{b_n\lambda_n}\left(\dot{q}_{sn}(t) + \delta q_{sn}(t)\right)\right. \\
& \left. - \frac{\beta_n}{b_n\lambda_n}\left(\dot{q}_{sn}\left(t - T_{fn}(t) - T_{bn}(t)\right) + \delta q_{sn}\left(t - T_{fn}(t) - T_{bn}(t)\right)\right)\right] \\
& + \sum_{j=1}^{n-1}\left\{\sqrt{1 - \dot{T}_{sj}(t)}\left(\beta_{sj}\left(\dot{q}_{sj}\left(t - T_{sj}(t)\right) + \delta q_{sj}\left(t - T_{sj}(t)\right)\right)\right.\right. \\
& \left.\left. - \beta_{sj}\left(\dot{q}_{sn}(t) + \delta q_{sn}(t)\right)\right)\right\} \\
& - \sum_{j=1}^{n-1}\left\{\sqrt{1 - \dot{T}_{sj}(t)}k_{cj}\tau_{ej}\left(t - T_{sj}(t)\right)\right\}
\end{aligned}
\tag{5.13}
$$

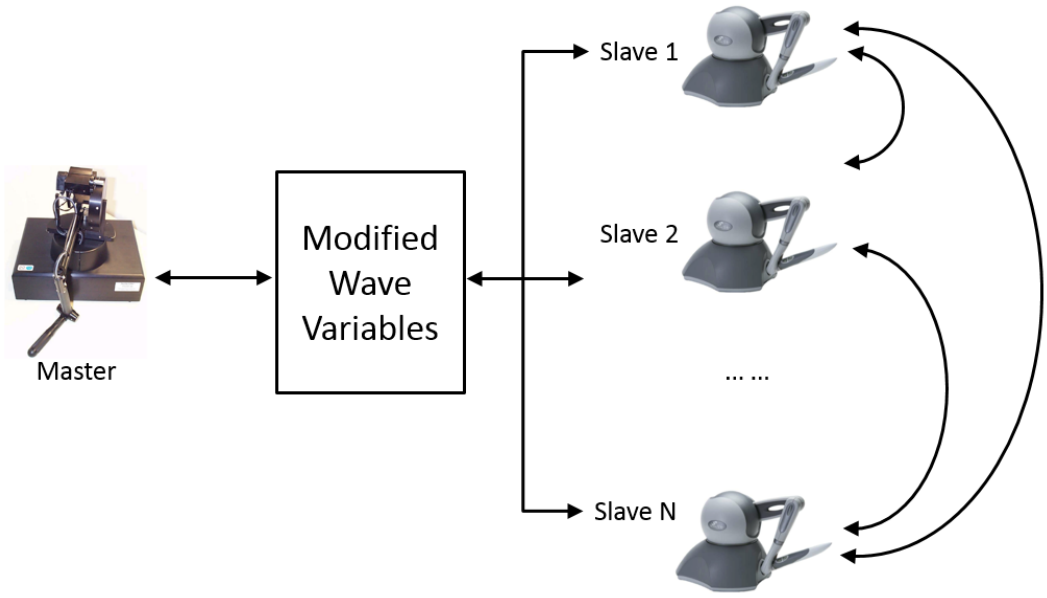

Figure 5.2 Network of the proposed teleoperation system

In order to prevent the position drift between the slave robots, each slave robot should also transmit its position information to the other slave robots. Furthermore, In order

to achieve the secondary objective which is the accurate force tracking, each slave robot's environmental force information is also transmitted via slave-slave communication channels to the other slave robots. The channels' passivity is guaranteed when the wave variable transformation is applied to encode the y-th slave robot's position signals with the transmitted z-th slave robot's control environmental force (y and z denote the arbitrary two slave robots in the n slave robots). Therefore, the final control variable E_{sn} of the n-th slave robot is expressed as (5.13)
where T_{sj} (j ∈ (1,2 ... n)) denote the time-varying delays in the forward slave-slave communication channels, and k_{cj} are diagonal positive-definite matrices. The second last term provides the position control between every two slave robots and the last terms provide force control between every two slave robots. By defining new variables $r_{ij}(t) = \dot{q}_{ij}(t) + \delta q_{ij}(t)$) (5.11) and (5.13) can be simplified as (5.14) and (5.15).

$$E_m = \sum_{j=1}^{n} \Big\{ \big(C_{3j} - b_j \lambda_j C_{1j}\big)\tau_h(t) - C_{2j}\tau_{ej}\Big(t - T_{bj}(t)\Big) + \beta_j \Big(r_{sj}\Big(t - T_{bj}(t)\Big) - r_m(t)\Big) - \frac{b_j}{\lambda_j}\beta_j \Big(r_m(t) - r_m\Big(t - T_{fj}(t) - T_{bj}(t)\Big)\Big)\Big\} \tag{5.14}$$

$$E_{sn} = \Big(C_{1n}\tau_h\Big(t - T_{fn}(t)\Big) - \Big(\frac{\lambda_n C_{2n}}{b_n} - C_{4n}\Big)\tau_{en}(t)\Big) + \beta_n\Big(r_m\Big(t - T_{fn}(t)\Big) - r_{sn}(t)\Big) - \frac{\beta_n}{b_n\lambda_n}\Big[r_{sn}(t) - r_{sn}\Big(t - T_{fn}(t) - T_{bn}(t)\Big)\Big] + \sum_{j=1}^{n-1}\Big\{\beta_{sj}\Big(\sqrt{1 - \dot{T}_{sj}(t)}r_{sj}\Big(t - T_{sj}(t)\Big) - r_{sn}(t)\Big)\Big\} - \sum_{j=1}^{n-1}\Big\{\sqrt{1 - \dot{T}_{sj}(t)}k_{cj}\tau_{ej}\Big(t - T_{sj}(t)\Big)\Big\} \tag{5.15}$$

The main aim of the controller design is to provide a stable multilateral system with accurate position tracking and to enhance the force tracking during manipulations. The position synchronization is derived if

$$\lim_{t\to\infty}\sum_{j=1}^{n}\left\|q_m\left(t-T_{fj}(t)\right)-q_{sj}(t)\right\|=\lim_{t\to\infty}\sum_{j=1}^{n}\left\|\dot{q}_m\left(t-T_{fn}(t)\right)-\dot{q}_{sj}(t)\right\|=0 \quad (5.16)$$

$$\lim_{t\to\infty}\sum_{j=1}^{n}\left\|q_{sj}\left(t-T_{bj}(t)\right)-q_m(t)\right\|=\lim_{t\to\infty}\sum_{j=1}^{n}\left\|\dot{q}_{sj}\left(t-T_{bj}(t)\right)-\dot{q}_m(t)\right\|=0 \quad (5.17)$$

$$\lim_{t\to\infty}\sum_{j=1}^{n}\left\|q_{sj}\left(t-T_{sj}(t)\right)-q_{sn}(t)\right\|=\lim_{t\to\infty}\sum_{j=1}^{n}\left\|\dot{q}_{sj}\left(t-T_{sj}(t)\right)-\dot{q}_{sn}(t)\right\|=0 \quad (5.18)$$

where $\|\cdot\|$ is the Euclidean norm of the enclosed signal. We define the position errors e_{pmn}, e_{psn} and velocity errors e_{vmn}, e_{vsn} between the master and the n-th slave manipulators as follows:

$$e_{pmn}(t)=q_m\left(t-T_{fn}(t)\right)-q_{sn}(t) \quad (5.19)$$

$$e_{vmn}(t)=\dot{q}_m\left(t-T_{fn}(t)\right)-\dot{q}_{sn}(t) \quad (5.20)$$

$$e_{psn}(t)=q_{sn}\left(t-T_{bn}(t)\right)-q_m(t) \quad (5.21)$$

$$e_{vsn}(t)=\dot{q}_{sn}\left(t-T_{bn}(t)\right)-\dot{q}_m(t) \quad (5.22)$$

$$e_{pssn}(t)=q_{sj}\left(t-T_{sj}(t)\right)-q_{sn}(t) \quad (5.23)$$

$$e_{vssn}(t)=\dot{q}_{sj}\left(t-T_{sj}(t)\right)-\dot{q}_{sn}(t) \quad (5.24)$$

The new control laws for the single master robot and the n-th slave robot are designed as follows:

$$\tau_m = E_m - \widehat{M}_m(q_m)\{\delta\dot{q}_m\} - \hat{C}_m(q_m, \dot{q}_m)\{\delta q_m\} + \hat{g}_m(q_m) \tag{5.25}$$

$$\tau_{sn} = E_{sn} - \widehat{M}_{sn}(q_{sn})\{\delta\dot{q}_{sn}\} - \hat{C}_{sn}(q_{ns}, \dot{q}_{sn})\{\delta q_{sn}\} + \hat{g}_{sn}(q_{sn}) \tag{5.26}$$

where $\widehat{M}_i(q_i)$, $\hat{C}_i(q_i, \dot{q}_i)$, $\hat{g}_i(q_i)$ are the estimates of $M_i(q_i)$, $C_i(q_i, \dot{q}_i)$, $g_i(q_i)$. ($i \in (m, s_1, s_2, \dots s_n)$) Substituting (5.25) and (5.26) into (5.1) and (5.2) and considering Property 3 which states that the dynamics are linearly parameterizable, the new system dynamics can be expressed as:

$$M_i(q_i)\dot{r}_i + C_i(q_i, \dot{q}_i)r_i = E_i - Y_i\tilde{\theta}_i \tag{5.27}$$

Where

$$\tilde{\theta}_i(t) = \theta_i(t) - \hat{\theta}_i(t) \tag{5.28}$$

$\hat{\theta}_i$ are the time-varying estimates of the master's and the n-th slave's actual constant p-dimensional inertial parameters given by θ_i. $\tilde{\theta}_i$ are the estimation errors. The time-varying estimates of the uncertain parameters satisfy the following conditions:

$$\dot{\hat{\theta}}_m = \psi Y_m^T(q_m, r_m)r_m, \dot{\hat{\theta}}_{sn} = \Lambda_n Y_{sn}^T(q_{sn}, r_{sn})r_{sn} \tag{5.29}$$

5.2.3 Stability Analysis

5.2.3.1 Free Motion Strategy

Theorem 5.1. Consider the proposed nonlinear multi-lateral teleoperation system in free motion where the human-operator force τ_h and the environmental force τ_e can be assumed to be zero ($\tau_h \equiv \tau_e \equiv 0$). For all initial conditions, all signals in this system are bounded and the master and all of the slave manipulators state are synchronized in the sense of (5.16)-(5.17).

Proof.

Based on (5.14) and (5.15), E_m and E_{sn} have the terms $\sum_{j=1}^{n} -\frac{b_j}{\lambda_j}\beta_j\left(r_m(t) - r_m\left(t - T_{fj}(t) - T_{bj}(t)\right)\right)$ and $-\frac{\beta_n}{b_n\lambda_n}\left[r_{sn}(t) - r_{sn}\left(t - T_{fn}(t) - T_{bn}(t)\right)\right]$, respectively. These two terms can be expressed as $\sum_{j=1}^{n} -\frac{b_j}{\lambda_j}\beta_j r_m(s)(1 - e^{-s(T_{fj}(s)+T_{bj}(s))})$ and $-\frac{\beta_n}{b_n\lambda_n} r_{sn}(s)\left(1 - e^{-s(T_{fn}(s)+T_{bn}(s))}\right)$ in frequency domain. According to the well-known characteristic of the time delay element $|e^{-sT_{f,b}}| = 1$. It is true that $\left(1 - e^{-s\left(T_{fj}(s)+T_{bj}(s)\right)}\right) \in [0,2]$ in the presence of large time-varying delays. It means $r_m(t) - r_m\left(t - T_{fj}(t) - T_{bj}(t)\right) \in [0,2r_m(t)]$ and $r_{sn}(t) - r_{sn}\left(t - T_{fn}(t) - T_{bn}(t)\right) \in [0,2r_{sn}(t)]$ which are varying according to the time delays. Therefore, $\left(r_m(t) - r_m\left(t - T_{fj}(t) - T_{bj}(t)\right)\right)$ and $\left(r_{sn}(t) - r_{sn}\left(t - T_{fn}(t) - T_{bn}(t)\right)\right)$ can be expressed as the varying dampings $\zeta r_m(t)$ and $\zeta r_{sn}(t)$ where ζ varies between 0 and 2. The values of $\zeta r_m(t)$ and $\zeta r_{sn}(t)$ are scaled by the characteristic impedances b and λ of the applied modified wave controllers. Therefore, (5.14) and (5.15) can be expressed as:

$$E_m = \sum_{j=1}^{n}\left\{\left(C_{3j} - b_j\lambda_j C_{1j}\right)\tau_h(t) - C_{2j}\tau_{ej}\left(t - T_{bj}(t)\right) + \beta_j\left(r_{sj}\left(t - T_{bj}(t)\right) - r_m(t)\right) - \frac{b_j}{\lambda_j}\beta_j\zeta r_m(t)\right\} \tag{5.30}$$

$$E_{sn} = \left(C_{1n}\tau_h\left(t - T_{fn}(t)\right) - \left(\frac{\lambda_n C_{2n}}{b_n} - C_{4n}\right)\tau_{en}(t)\right) + \beta_n\left(r_m\left(t - T_{fn}(t)\right) - r_{sn}(t)\right) - \frac{\beta_n}{b_n\lambda_n}\zeta r_{sn}(t) + \sum_{j=1}^{n-1}\left\{\beta_{sj}\left(\sqrt{1 - \dot{T}_{sj}(t)}\, r_{sj}\left(t - T_{sj}(t)\right) - r_{sn}(t)\right)\right\} - \sum_{j=1}^{n-1}\left\{\sqrt{1 - \dot{T}_{sj}(t)}\, k_{cj}\tau_{ej}\left(t - T_{sj}(t)\right)\right\} \tag{5.31}$$

Define a storage functional V, where

$$V = \frac{1}{2}\left[r_m^T(t) M_m(q_m) r_m(t) + \sum_{j=1}^{n} r_{sj}^T(t) M_{sj}(q_{sj}) r_{sj}(t) + \tilde{\theta}_m^T \psi^{-1} \tilde{\theta}_m + \sum_{j=1}^{n} \tilde{\theta}_{sj}^T \Lambda_j^{-1} \tilde{\theta}_{sj} \right]$$
$$+ \sum_{j=1}^{n} \left\{ \frac{\beta_j}{2} \frac{1}{1 - \dot{T}_{fj}} \int_{t-T_{fj}}^{t} r_m^T(\eta) r_m(\eta) d\eta \right\}$$
$$+ \sum_{j=1}^{n} \left\{ \frac{\beta_j}{2} \frac{1}{1 - \dot{T}_{bj}} \int_{t-T_{bj}}^{t} r_{sj}^T(\eta) r_{sj}(\eta) d\eta \right\}$$
$$+ n \sum_{j=1}^{n-1} \left\{ \frac{\beta_{sj}}{2} \int_{t-T_{fj}}^{t} r_{sj}^T(\eta) r_{sj}(\eta) d\eta \right\}$$
$$+ \sum_{j=1}^{n} \left\{ q_m^T(t) \left(\frac{b_j \zeta \beta_j}{\lambda_j} - \frac{\dot{T}_{fj} \beta_j}{2 - 2\dot{T}_{fj}} \right) \delta q_m(t) \right\}$$
$$+ \sum_{j=1}^{n} \left\{ q_{sj}^T(t) \left(\frac{\beta_j \zeta}{b_j \lambda_j} - \frac{\dot{T}_{bj} \beta_j}{2 - 2\dot{T}_{bj}} \right) \delta q_{sj}(t) \right\} \tag{5.32}$$

In order to make V positive semi-definite, $\frac{b_j \zeta \beta_j}{\lambda_j} - \frac{\dot{T}_{fj} \beta_j}{2 - 2\dot{T}_{fj}} \geq 0$ and $\frac{\beta_j \zeta}{b_j \lambda_j} - \frac{\dot{T}_{bj} \beta_j}{2 - 2\dot{T}_{bj}} \geq 0$ ($j \in 1, 2, \ldots n$) should be satisfied, which can be simplified as:

$$\dot{T}_{fj} \leq \frac{2\zeta}{\frac{\lambda_j}{b_j} + 2\zeta} \tag{5.33}$$

$$\dot{T}_{bj} \leq \frac{2\zeta}{b_j \lambda_j + 2\zeta} \tag{5.34}$$

Due to the assumption that $\left|\dot{T}_{f,b}\right| < 1$, by setting a small value of λ_j, (43) and (44) can be easily satisfied. By using the dynamic equations and Property 3, the derivative of V can be written as:

$$
\begin{aligned}
\dot{V} = r_m^T(t)E_m(t) + \sum_{j=1}^{n} r_{sj}^T(t)E_{sj}(t) \\
&+ \sum_{j=1}^{n}\left\{\frac{\beta_j}{2}r_m^T(t)r_m(t) - \frac{\beta_j}{2}r_m^T\left(t - T_{fj}(t)\right)r_m\left(t - T_{fj}(t)\right)\right. \\
&\left.+ \frac{\beta_j \dot{T}_{fj}}{2 - 2\dot{T}_{fj}}r_m^T(t)r_m(t)\right\} \\
&+ \sum_{j=1}^{n}\left\{\frac{\beta_j}{2}r_{sj}^T(t)r_{sj}(t) - \frac{\beta_j}{2}r_{sj}^T\left(t - T_{bj}(t)\right)r_{sj}\left(t - T_{bj}(t)\right)\right. \\
&\left.+ \frac{\beta_j \dot{T}_{bj}}{2 - 2\dot{T}_{bj}}r_{sj}^T(t)r_{sj}(t)\right\} \\
&+ n\sum_{j=1}^{n-1}\left\{\frac{\beta_{sj}}{2}r_{sj}^T(t)r_{sj}(t)\right. \\
&\left.- \left(1 - \dot{T}_{sj}(t)\right)\frac{\beta_{sj}}{2}r_{sj}^T\left(t - T_{sj}(t)\right)r_{sj}\left(t - T_{sj}(t)\right)\right\} \\
&+ \sum_{j=1}^{n}\left\{\dot{q}_m^T(t)2\left(\frac{b_j\zeta\beta_j}{\lambda_j} - \frac{\dot{T}_{fj}\beta_j}{2 - 2\dot{T}_{fj}}\right)\delta q_m(t)\right\} \\
&+ \sum_{j=1}^{n}\left\{\dot{q}_{sj}^T(t)2\left(\frac{\beta_j\zeta}{b_j\lambda_j} - \frac{\dot{T}_{bj}\beta_j}{2 - 2\dot{T}_{bj}}\right)\delta q_{sj}(t)\right\} \\
&= -\sum_{j=1}^{n}\left\{\frac{\beta_j}{2}\left(e_{vmj}(t) + \delta e_{pmj}(t)\right)^T\left(e_{vmj}(t) + \delta e_{pmj}(t)\right)\right\} \\
&- \sum_{j=1}^{n}\left\{\frac{\beta_j}{2}\left(e_{vsj}(t) + \delta e_{psj}(t)\right)^T\left(e_{vsj}(t) + \delta e_{psj}(t)\right)\right\} \\
&- n\sum_{j=1}^{n-1}\left\{\frac{\beta_j}{2}\left(e_{vssj}(t) + \delta e_{pssj}(t)\right)^T\left(e_{vssj}(t) + \delta e_{pssj}(t)\right)\right\} \\
&- \sum_{j=1}^{n}\left\{\dot{q}_m^T(t)\left(\frac{b_j\zeta\beta_j}{\lambda_j} - \frac{\dot{T}_{fj}\beta_j}{2 - 2\dot{T}_{fj}}\right)\dot{q}_m(t)\right.
\end{aligned}
$$

$$+ q_m^T(t)\left(\frac{b_j\zeta\beta_j}{\lambda_j} - \frac{\dot{T}_{fj}\beta_j}{2-2\dot{T}_{fj}}\right)\delta^2 q_m(t)$$
$$+ \dot{q}_{sj}^T(t)\left(\frac{\beta_j\zeta}{b_j\lambda_j} - \frac{\dot{T}_{bj}\beta_j}{2-2\dot{T}_{bj}}\right)\dot{q}_{sj}(t)$$
$$+ q_{sj}^T(t)\left(\frac{\beta_j\zeta}{b_j\lambda_j} - \frac{\dot{T}_{bj}\beta_j}{2-2\dot{T}_{bj}}\right)\delta^2 q_{sj}(t)\Bigg\} \le 0 \qquad (5.35)$$

Based on (5.35), the differential of the functional V is negative semi-definite. Integrating both sides of (5.35), we get:

$$+\infty > V(0) \ge V(0) - V(t)$$
$$\ge \int_0^t \Bigg\{ \sum_{j=1}^{n} \left\{ \frac{\beta_j}{2}\left(e_{vmj}(t) + \delta e_{pmj}(t)\right)^T \left(e_{vmj}(t) + \delta e_{pmj}(t)\right)\right\}$$
$$+ \sum_{j=1}^{n} \left\{ \frac{\beta_j}{2}\left(e_{vsj}(t) + \delta e_{psj}(t)\right)^T \left(e_{vsj}(t) + \delta e_{psj}(t)\right)\right\}$$
$$+ n\sum_{j=1}^{n-1} \left\{ \frac{\beta_j}{2}\left(e_{vssj}(t) + \delta e_{pssj}(t)\right)^T \left(e_{vssj}(t) + \delta e_{pssj}(t)\right)\right\}$$
$$+ \sum_{j=1}^{n} \Bigg\{ \dot{q}_m^T(t)\left(\frac{b_j\zeta\beta_j}{\lambda_j} - \frac{\dot{T}_{fj}\beta_j}{2-2\dot{T}_{fj}}\right)\dot{q}_m(t)$$
$$+ q_m^T(t)\left(\frac{b_j\zeta\beta_j}{\lambda_j} - \frac{\dot{T}_{fj}\beta_j}{2-2\dot{T}_{fj}}\right)\delta^2 q_m(t)$$
$$+ \dot{q}_{sj}^T(t)\left(\frac{\beta_j\zeta}{b_j\lambda_j} - \frac{\dot{T}_{bj}\beta_j}{2-2\dot{T}_{bj}}\right)\dot{q}_{sj}(t)$$
$$+ q_{sj}^T(t)\left(\frac{\beta_j\zeta}{b_j\lambda_j} - \frac{\dot{T}_{bj}\beta_j}{2-2\dot{T}_{bj}}\right)\delta^2 q_{sj}(t)\Bigg\}\Bigg\} dt \qquad (5.36)$$

Since V is positive semi-definite and $\dot{V}$ is negative semi-definite, $\lim_{t\to\infty} V$ exists and is finite. Also, based on (42)-(46), $r_m(t), r_{sj}(t), \tilde{\theta}_m(t), \tilde{\theta}_{sj}(t) \in L_\infty$, $e_{vmj}(t)$, $e_{pmj}(t)$, $e_{vsj}(t)$, $e_{psj}(t)$, $q_m(t)$, $q_{sj}(t)$, $e_{vssj}(t)$, $e_{pssj}(t)$, $\dot{q}_m(t)$, $\dot{q}_{sj}(t) \in L_\infty \cap L_2$. Since a square integrable signal with a bounded derivative converges to the origin, $\lim_{t\to\infty} e_{pmj}(t) = \lim_{t\to\infty} e_{vmj}(t) = \lim_{t\to\infty} e_{psj}(t) = \lim_{t\to\infty} e_{vsj}(t) = \lim_{t\to\infty} e_{pssj}(t) = \lim_{t\to\infty} e_{vssj}(t) =$

0. Therefore, the master and slave manipulators state synchronize in the sense of (5.16)-(5.18).

In free motion, the system's dynamic model (5.27) can also be written as:

$$\ddot{q}_i(t) = M_i^{-1}\left[E_i(t) - Y_i\tilde{\theta}_i - C_i r_m(t)\right] - \delta\dot{q}_i(t) \tag{5.37}$$

Differentiating both sides of (5.37):

$$\frac{d}{dt}\ddot{q}_i(t) = \frac{d}{dt}(M_i^{-1})\left[E_i(t) - Y_i\tilde{\theta}_i - C_i r_i(t)\right] + M_i^{-1}\frac{d}{dt}\left[E_i(t) - Y_i\tilde{\theta}_i - C_i r_i(t)\right] - \delta\ddot{q}_i(t) \tag{5.38}$$

For the first terms of the right sides of (5.38), we have:

$$\frac{d}{dt}(M_i^{-1}) = -M_i^{-1}\dot{M}_i M_i^{-1} = -M_i^{-1}\left(C_i + C_i^T\right)M_i^{-1} \tag{5.39}$$

According to Properties 1 and 4, $\frac{d}{dt}(M_i^{-1})$ are bounded. Based on Property 5, the terms in bracket of (5.38) are also bounded. Therefore, $\frac{d}{dt}\ddot{q}_i(t) \in L_\infty$ and $\ddot{q}_i(t)$ are uniformly continuous ($\int_0^t \ddot{q}_i(\eta)d\eta = \dot{q}_i(t) - \dot{q}_i(0)$). Since $\dot{q}_i(t) \to 0$, it can be concluded that $\ddot{q}_i(t) \to 0$ based on Barbălat's Lemma.

5.2.3.2 Environmental Contact with Passive Human Force

Assume the human and environmental force are passive and can be modeled as:

$$\tau_h(t) = -\alpha_m r_m(t) \tag{5.40}$$

$$\tau_{ej}(t) = \alpha_{sj} r_{sj}(t) \tag{5.41}$$

where α_m and α_{sj} are positive constant matrices and are the properties of the human and the environment, respectively.

Theorem 5.2. The multi-lateral nonlinear teleoperation system is stable and all signals in this system are ultimately bounded, when the human and environmental forces satisfy (5.40) and (5.41).

Proof. Consider a positive semi-definite function V' for the system as:

$$V' = V + \sum_{j=1}^{n}\left\{\frac{(C_{3j} - b_j\lambda_j C_{1j})\alpha_m}{2}\int_{t-T_{fj}}^{t} r_m^T(\eta)r_m(\eta)d\eta\right\} + \sum_{j=1}^{n}\left\{\frac{\left(\frac{\lambda_j C_{2j}}{b_j} - C_{4j}\right)\alpha_{sj}}{2}\int_{t-T_{bj}}^{t} r_{sj}^T(\eta)r_{sj}(\eta)d\eta\right\} + n\sum_{j=1}^{n-1}\left\{\frac{\alpha_{sj}}{2n}\int_{t-T_{sj}}^{t} r_{sj}^T(\eta)r_{sj}(\eta)d\eta\right\} \quad (5.42)$$

The derivative of V' can be written as:

$$\dot{V}' = \sum_{j=1}^{n}\left\{-\left(\frac{(C_{3j} - b_j\lambda_j C_{1j})\alpha_m}{2} r_m^T(t)r_m(t) + C_{2j}\alpha_{sj} r_m^T(t)r_s(t - T_{bj}) + \frac{\left(\frac{\lambda_j C_{2j}}{b_j} - C_{4j}\right)\alpha_{sj}}{2}(1 - \dot{T}_{bj})r_{sj}^T(t - T_{bj})r_{sj}(t - T_{bj})\right)\right\} + \sum_{j=1}^{n}\left\{-\left(\frac{\left(\frac{\lambda_j C_{2j}}{b_j} - C_{4j}\right)\alpha_{sj}}{2} r_s^T(t)r_s(t) + C_{1j}\alpha_m r_s^T(t)r_m(t - T_{fj}) + \frac{(C_{3j} - b_j\lambda_j C_{1j})\alpha_m}{2}(1 - \dot{T}_{fj})r_m^T(t - T_{fj})r_m(t - T_{fj})\right)\right\}$$

$$+n\sum_{j=1}^{n-1}\left\{-\left(\frac{\alpha_{sn}}{2n}r_{sn}^{T}(t)r_{sn}(t)+\sqrt{1-\dot{T}_{sj}(t)}k_{cj}\alpha_{sj}r_{sn}^{T}(t)r_{sj}(t-T_{fj})+\frac{\alpha_{sj}}{2n}(1\right.\right.$$

$$\left.\left.-\dot{T}_{sj})r_{sj}^{T}(t-T_{sj})r_{sj}(t-T_{sj})\right)\right\}-\alpha_{m}r_{m}^{T}(t)r_{m}(t)+\dot{V} \quad (5.43)$$

The Lyapunov approach requires $\dot{V}'$ to be negative semi-definite. Based on the first three terms of the right side of (5.43), the sufficient conditions to satisfy this requirement are that:

$$\frac{1}{1-\dot{T}_{bj}}\frac{C_{2j}^{2}}{(\frac{\lambda_j C_{2j}}{b_j}-C_{4j})(C_{3j}-b_j\lambda_j C_{1j})}I\leq\left(\alpha_m\alpha_{sj}^{-1}\right)^{T} \quad (5.44)$$

$$\frac{1}{1-\dot{T}_{fj}}\frac{C_{1j}^{2}}{(\frac{\lambda_j C_{2j}}{b_j}-C_{4j})(C_{3j}-b_j\lambda_j C_{1j})}I\leq\left(\alpha_{sj}\alpha_m^{-1}\right)^{T} \quad (5.45)$$

$$k_{cj}^{T}k_{cj}\leq\frac{1}{n^{2}}\left(\alpha_{sn}\alpha_{sj}^{-1}\right)^{T} \quad (5.46)$$

By enlarging the values of C_{3j} and decreasing the values of k_{cj}, (5.44)-(5.46) can be satisfied. Hence, $\dot{V}'$ will be negative semi-definite and $\lim_{t\to\infty}V'$ exists and is finite.

5.2.3.3 Environmental Contact with Non-passive Human Force

The human operator can not only dampen energy but also generate energy in order to manipulate the robots to move through the desired path. Therefore, in the common case, the human forces are not passive. In this situation, the human and environment can be modeled as:

$$\tau_h=\alpha_0-\alpha_m r_m \quad (5.47)$$

$$\tau_{ej}=\alpha_{sj}r_{sj} \quad (5.48)$$

where α_0 is a bounded positive constant vector, which generates energy as an active term. We define $\bar{x}_j = \left[q_m, q_{sj}, \dot{q}_m, \dot{q}_{sj}\right]^T$ and $x_j = \left[q_m, q_{sj}, r_m, r_{sj}\right]^T$. There is a linear map between $\bar{x}_j$ and x_j: $\bar{x}_j(t) = \Gamma_j x_j(t)$, where Γ_j are non-singular constant matrices.

Theorem 5.3. The proposed system is stable and all signals in this system are ultimately bounded, when the human and environmental forces satisfy (5.47)-(5.48).

Proof.

By choosing the previous Lyapunov function V', the new derivative $\dot{V}^*$ can be written as:

$$\dot{V}^* = \dot{V}' + \sum_{j=1}^{n} r_m^T\left[\left(C_{3j} - b_j\lambda_j C_{1j}\right)\alpha_0 + \alpha_0\right] + \sum_{j=1}^{n} r_{sj}^T\left[\left(\frac{\lambda_j C_{2j}}{b_j} - C_{4j}\right)\alpha_0\right] \quad (5.49)$$

Note that

$$\sum_{j=1}^{n} r_m^T\left[\left(C_{3j} - b_j\lambda_j C_{1j}\right)\alpha_0 + \alpha_0\right] \le \sum_{j=1}^{n} h^T\|x_j\|\left[\left(C_{3j} - b_j\lambda_j C_{1j}\right)\alpha_0 + \alpha_0\right] \quad (5.50)$$

$$\sum_{j=1}^{n} r_{sj}^T \sum_{j=1}^{n} r_{sj}^T\left[\left(\frac{\lambda_j C_{2j}}{b_j} - C_{4j}\right)\alpha_0\right] \le \sum_{j=1}^{n} h^T\|x_j\| \sum_{j=1}^{n} r_{sj}^T\left[\left(\frac{\lambda_j C_{2j}}{b_j} - C_{4j}\right)\alpha_0\right] \quad (5.51)$$

where vector $h^T = [1,1, \ldots 1]$ has the same ranks as r_m, r_{sj}. Therefore, it is true that:

$$\dot{V}^* \le \dot{V}' + \sum_{j=1}^{n} 2\|x_j\|\alpha_j \quad (5.52)$$

where $\alpha_j = \left(C_{3j} - b_j\lambda_j C_{1j}\right)\alpha_0 + \alpha_0 + \left(\frac{\lambda_j C_{2j}}{b_j} - C_{4j}\right)\alpha_0 > 0$. When the system satisfies (5.44)-(5.46):

$$\dot{V}^* \le -\sum_{j=1}^{n}\left\{\dot{q}_m^T(t)\left(\frac{b_j\zeta\beta_j}{\lambda_j}-\frac{\dot{T}_{fj}\beta_j}{2-2\dot{T}_{fj}}\right)\dot{q}_m(t)+q_m^T(t)\left(\frac{b_j\zeta\beta_j}{\lambda_j}-\frac{\dot{T}_{fj}\beta_j}{2-2\dot{T}_{fj}}\right)\delta^2 q_m(t)\right.$$
$$+\dot{q}_{sj}^T(t)\left(\frac{\beta_j\zeta}{b_j\lambda_j}-\frac{\dot{T}_{bj}\beta_j}{2-2\dot{T}_{bj}}\right)\dot{q}_{sj}(t)$$
$$\left.+q_{sj}^T(t)\left(\frac{\beta_j\zeta}{b_j\lambda_j}-\frac{\dot{T}_{bj}\beta_j}{2-2\dot{T}_{bj}}\right)\delta^2 q_{sj}(t)\right\} \le \sum_{j=1}^{n}-\Upsilon_j\left\|\bar{x}_j\right\|^2 \qquad (5.53)$$

where Υ_j is the smallest eigenvalue of $\left(\frac{\beta_j\zeta}{b_j\lambda_j}-\frac{\dot{T}_{bj}\beta_j}{2-2\dot{T}_{bj}}\right)$, $\left(\frac{\beta_j\zeta}{b_j\lambda_j}-\frac{\dot{T}_{bj}\beta_j}{2-2\dot{T}_{bj}}\right)\delta^2$, $\left(\frac{b_j\zeta\beta_j}{\lambda_j}-\frac{\dot{T}_{fj}\beta_j}{2-2\dot{T}_{fj}}\right)$, $\left(\frac{b_j\zeta\beta_j}{\lambda_j}-\frac{\dot{T}_{fj}\beta_j}{2-2\dot{T}_{fj}}\right)\delta^2$. Substituting (5.53) into (5.52) and setting $0<\mu<1$:

$$\dot{V}^* \le \sum_{j=1}^{n}\left\{-\Upsilon_j\left\|\bar{x}_j\right\|^2+2\left\|x_j\right\|\alpha_j\right\}$$
$$=\sum_{j=1}^{n}\left\{-\Upsilon_j(1-\mu)\left\|\Gamma_j\right\|^2\left\|x_j\right\|^2-\Upsilon_j\mu\left\|\Gamma_j\right\|^2\left\|x_j\right\|^2+2\left\|x_j\right\|\alpha_j\right\} \qquad (5.54)$$

(5.54) can be simplified as:

$$\dot{V}^* \le \sum_{j=1}^{n}\left\{-\Upsilon_j(1-\mu)\left\|\Gamma_j\right\|^2\left\|x_j\right\|^2\right\}, \forall\left\|x_j\right\| \ge \frac{2\alpha_j}{\Upsilon_j\mu\left\|\Gamma_j\right\|^2} \qquad (5.55)$$

Based on (5.55), for large values of x_j, the Lyapunov functions is decreasing. Therefore, x_j and $\bar{x}_j$ are bounded, which means r_m, r_{sj} q_m, q_{sj}, $\dot{q}_m$, $\dot{q}_{sj}$ are also bounded.

5.2.4 Experimental Validation

In this section, the performance of the proposed nonlinear multilateral teleoperation system is validated by a series of experiments. The algorithm is applied to three Phantom manipulators. The 6-DOF PHANToM (TM)* model 1.5 manipulator

(Sensable Technologies, Inc., Wilmington, MA) is chosen to be the master robot which remotely controls a 3-DOF Phantom Omni (Slave 1) and a 3-DOF Phantom Desktop (Slave 2) via the Internet as shown in Figure 5.3. The three haptic devices have different dynamics and initial parameters.

The control loop is configured as a 1 kHZ sampling rate. Based on the controllers analysis in Section 4, the controller parameters are given as: $b_1 = b_2 = 2.5$, $\lambda_1 = \lambda_2 = 0.5, C_1 = C_2 = 1, C_3 = 2\ C_4 = 1.2, \delta = 1.2, \beta_1 = 5, \beta_2 = 3$, $\beta_s = 2$, k_c=1. The communication channel of the experimental platform is the Internet. In order to test the performance of the proposed system in the presence of large time-varying delays, the time delay blocks in the Simulink library are applied to introduce the overall system time delays. The one-way delay between the master and the slave sides is from 650 ms to 750 ms. Theoretically, in the real applications, the slave robots are close to each other, so the time delays between two slave robots are not large and not significantly different. The one-way delay between the two slave robots is set as around 100 ms in this experiment.

Figure 5.3. Experimental setup

In the first experiment, the system performance in free motion is demonstrated. During free motion, the master manipulator is guided by the human operator in the task space and the two slave robots are coupled to the master robot using the proposed system. Figure 5.4 demonstrate the position synchronization performances of the proposed

teleoperation system. Since the wave reflections are eliminated, the slave robots can closely track the master robot without large vibration and signals distortion. The remaining slight signal perturbations in Figure 5.4 are caused by the time-varying delays. The two slave robots can perform exactly the same actions during free motion. In the presence of large time-varying delays, although the dynamic models of the master and slaves are quite different and affected by uncertain parameters, both of the slave robots can reasonably track the master robot's trajectory with little errors. The root mean square errors (RMSE) for position tracking between every two robots in Figure 5.4 are shown in Table 5.1. Therefore, it can be concluded that the main objective: accurate position tracking of the proposed teleoperation system is achieved.

Free motion	Master & Slave 1	Master & Slave 2	Slave 1 & Slave 2
Position joint 1	0.0353	0.0429	0.0465
Position joint 2	0.0434	0.0444	0.035
Position joint 3	0.0453	0.038	0.0431

Table 5.1. RMSE (free motion)

In the next experiment, the two slave robots are driven by the master robot to draw a letter "O" and a triangle "△" on a table as shown in Fig.8. Friction exists between the manipulators and the table. The RMSEs for position tracking between every two robots in Figure 5.5 are shown in Table 5.2. Due to the effect of the friction, the RMSE are larger than that of free motion. The proposed algorithm still makes all of the robots have reasonable trajectory tracking without large signals distortion.

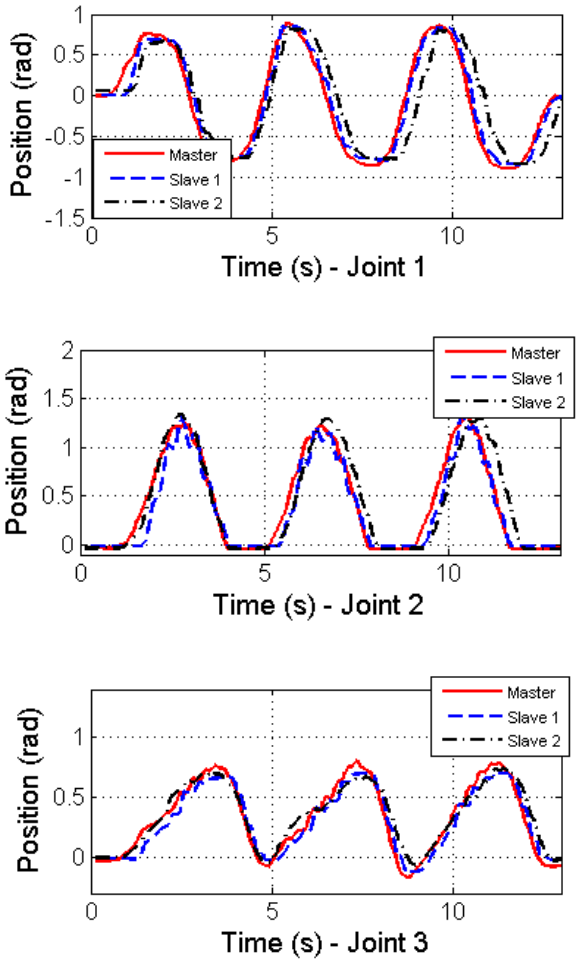

Figure 5.4. Free motion

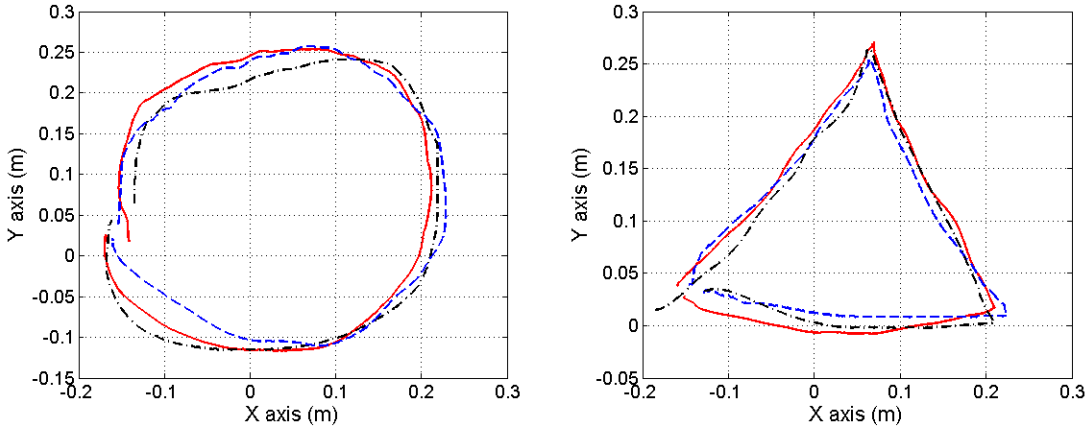

Figure 5.5. Drawing a letter “O” and a triangle “△”

Drawing a letter “O”	Master & Slave 1	Master & Slave 2	Slave 1 & Slave 2
X axis	0.1351	0.1587	0.1265
Y axis	0.1739	0.1704	0.2302
Drawing a triangle “△”	Master & Slave 1	Master & Slave 2	Slave 1 & Slave 2
X axis	0.1043	0.0996	0.112
Y axis	0.1539	0.1425	0.1053

Table 5.2. RMSE (drawing)

In the next experiment, slave manipulators 1 and 2 are guided by the master manipulator to come in contact with different the remote environment as shown in Figure 5.6. The master robot firstly drives the two slave robots to perform the free motion in the first 2 seconds. Then, from the 2^{nd} to the 5^{th} second, Slave 1 starts to contact with a solid wall while Slave 2 is still in free motion. Slave 1 immediately feeds the contact force back to the master robots and Slave 2. The master robot keeps applying force to the two slave robots, but Slave 2 also stops moving to make the motion synchronized with Slave 1 even no environmental force is applied to its manipulator. In the 5^{th} second, the solid wall is suddenly removed. It can be observed that both of the two slave robots quickly track the master robot’s position with little variation, which proves that the proposed algorithm can deal with the sudden changing environment and the wave reflections will not reinstate. The RMSEs for position tracking between every two robots and the RMSEs for force tracking between the master robot and Slave 1 in Figure 5.6 are shown in Tables 5.3 and 5.4.

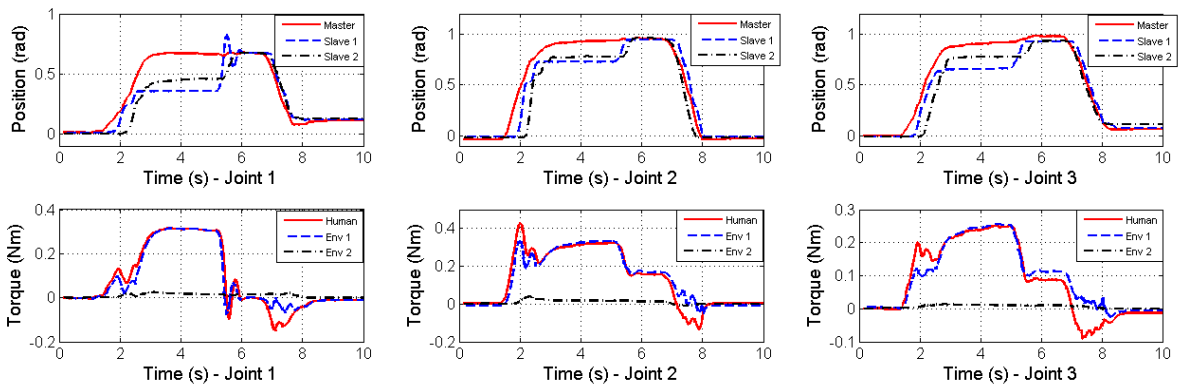

Figure 5.6. Slave 1 contacting to a reverse wall

Contacting with a reverse wall	Master & Slave 1	Master & Slave 2	Slave 1 & Slave 2
Position joint 1	0.308	0.2709	0.0856
Position joint 2	0.2507	0.2444	0.0379
Position joint 3	0.2442	0.2378	0.0801

Table 5.3. RMSE - position (Slave 1contacting with a reverse wall)

Contacting with a reverse wall	Master & Slave 1
Force joint 1	0.0639
Force joint 2	0.0962
Force joint 3	0.0852

Table 5.4. RMSE – force (Slave 1contacting with a reverse wall)

In the final experiment, the two slave robots are driven by the master robot to simultaneously contact with a solid wall. The position and force tracking are shown in Figure 5.7. Under the condition of hard contact, both of the two slave robot feed the environmental forces back to the master robots and the human operator can feel the mixed forces from the two slave robots. Figure 5.7 demonstrate that accurate force

tracking between all of the three robots are achieved. The RMSEs of position and force tracking between every two robots are shown in Table 5.5.

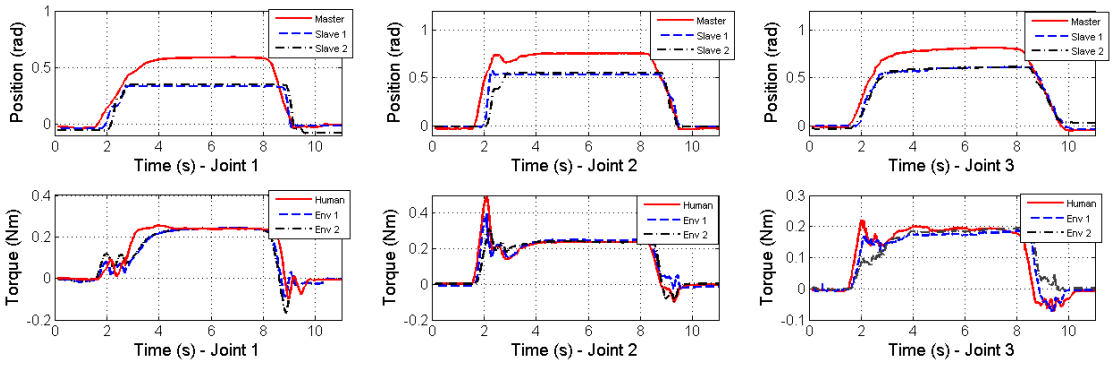

Figure 5.7. Both of the two slave robots contacting to a solid wall

Hard contact	Master & Slave 1	Master & Slave 2	Slave 1 & Slave 2
Position joint 1	0.2501	0.2510	0.0229
Position joint 2	0.2545	0.2587	0.0342
Position joint 3	0.2533	0.2549	0.0247
Force joint 1	0.0678	0.0706	0.025
Froce joint 2	0.0712	0.0698	0.0496
Force joint 3	0.0831	0.0845	0.0737

Table 5.5. RMSE (hard contact of the two slave robots)

5.3 Enhancing Flexibility of the Dual-Master-Dual-Slave Multilateral Teleoperation System

In a good multilateral system, control relationships are built between any two robots so that cooperation of different robots can be enforced and the operators can have different feelings of the dynamics of different slave robots and the other operators. However, the control relationship may also become an interruption that hinder the slave robots to follow the desired motion or disturb the feelings of the operators for

the experiment. Dealing with the control relationships effectively is also a challenge. A multilateral teleoperation system is assessed by the following four criteria:

Stability: The proposed system must maintain stability in the presence of random time delays in different scenarios (e.g. free motion, contacting with different environments), which is a major confronting problems for many multilateral systems.

Transparency: In an ideal transparent condition, the motion trajectory of the slave robots can accurately follow that of the master robots, and the environmental contact forces also highly match with the operators' applied force. When one operator is performing the task alone, the operator can fully feel the dynamics of the remote environment. When muliple operators perform the task together, they should feel the mix dynamics of different environments.

Flexibility: The system must offer each operator large freedom to the extent that the slave robots can be separated to do different tasks, or they can cooperate to perform the same task. Either of the master robots can pointedly control either of the slave robots or both of them. Proper control laws must be deployed to make sure the robots can collaboratively perform the specified task rather than causing interruption to each other.

Correctiveness: When one operator performs the task alone, the other operator has the ability to correct the motion of the slave robots motion when necessary.

In this section, an innovative dual-master-dual-slave (DMDS) system with variable dominance factor is designed to enhance the system flexibility. An innovative wave-based TDPA (Time Delay Passivity Approach) is proposed to guarantee the communication channels' passivity under random delays. The approach will be validated based on a 3-DOF teleoperation system consisting of four haptic devices performing different complex tasks.

5.3.1 Proposed DMDS architecture

In a DMDS teleoperation system, two master robots driven by two operators cooperate to remotely control the two slave robots to collaboratively perform the remote tasks. Fig.5.8 shows the proposed DMDS teleoperation system. The most significant property of the proposed system is using variable dominance factors $E_{1-16}(t)$ to

determine the control relationships between every two robots. In Fig.5.8 the hybrid signals $r_{ij}(t)$ are encoded by the velocities $\dot{q}_{ij}(t)$ and the positions $\delta q_{ij}(t)$.

$$r_{ij}(t) = \dot{q}_{ij}(t) + \delta q_{ij}(t) \tag{5.56}$$

where δ is the positive constant gain. $(i = m, s, j = 1, 2)$. τ_{hsj} and r_{hsj} are the slave feedback signals to the master robots. τ_{emj} and r_{emj} are the master feed-forward signals to the slave robots. In the proposed DMDS teleoperation system, the operator are in the same work space where time delays do not exist between the two master robots. The two slave robots are in different work spaces from the master side so that asymmetric time-varying delays exist between the master and the slave sides and between the two slave robots. $T_{fj}(t)$ and $T_{bj}(t)$ are the forward and backward time delays between the master side and the slave j, and $T_{sj}(t)$ are the time delays between the two slave robots. The control strategy illustrate in can be formulated as follows

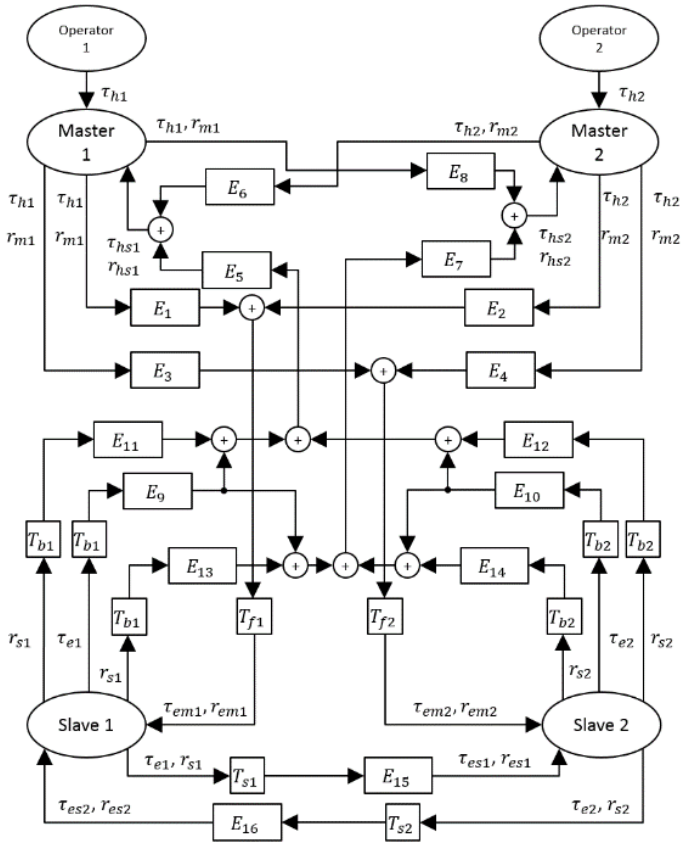

Figure 5.8 Proposed dual-master-dual-slave system

$$\tau_{em1}(t) = E_1\left(t - T_{f1}(t)\right)\tau_{h1}\left(t - T_{f1}(t)\right) + E_2\left(t - T_{f1}(t)\right)\tau_{h2}\left(t - T_{f1}(t)\right) \quad (5.57)$$

$$r_{em1}(t) = E_1\left(t - T_{f1}(t)\right)r_{m1}\left(t - T_{f1}(t)\right) + E_2\left(t - T_{f1}(t)\right)r_{m2}\left(t - T_{f1}(t)\right) \quad (5.58)$$

$$\tau_{em2}(t) = E_3\left(t - T_{f2}(t)\right)\tau_{h1}\left(t - T_{f1}(t)\right) + E_4\left(t - T_{f2}(t)\right)\tau_{h2}\left(t - T_{f2}(t)\right) \quad (5.59)$$

$$r_{em2}(t) = E_3\left(t - T_{f2}(t)\right)r_{m2}\left(t - T_{f2}(t)\right) + E_4\left(t - T_{f2}(t)\right)r_{m2}\left(t - T_{f2}(t)\right) \quad (5.60)$$

$$\tau_{hs1}(t) = E_5(t)E_9(t)\tau_{e1}\left(t - T_{b1}(t)\right) + E_5(t)E_{10}(t)\tau_{e2}\left(t - T_{b2}(t)\right) + E_6(t)\tau_{h2}(t) \quad (5.61)$$

$$r_{hs1}(t) = E_5(t)E_{11}(t)r_{s1}\left(t - T_{b1}(t)\right) + E_5(t)E_{12}(t)r_{s2}\left(t - T_{b2}(t)\right) + E_6(t)r_{h2}(t) \quad (5.62)$$

$$\tau_{hs2}(t) = E_7(t)E_9(t)\tau_{e1}\left(t - T_{b1}(t)\right) + E_8(t)E_{10}(t)\tau_{e2}\left(t - T_{b2}(t)\right) + E_8(t)\tau_{h1}(t) \quad (5.63)$$

$$r_{hs2}(t) = E_7(t)E_{13}(t)r_{s1}\left(t - T_{b1}(t)\right) + E_7(t)E_{14}(t)r_{s2}\left(t - T_{b2}(t)\right) + E_8(t)r_{h2}(t) \quad (5.64)$$

$$\tau_{es1}(t) = E_{15}(t)\tau_{e1}\left(t - T_{s1}(t)\right) \quad (5.65)$$

$$r_{es1}(t) = E_{15}(t)r_{s1}\left(t - T_{s1}(t)\right) \quad (5.66)$$

$$\tau_{es2}(t) = E_{16}(t)\tau_{e2}\left(t - T_{s2}(t)\right) \quad (5.67)$$

$$r_{es2}(t) = E_{16}(t)r_{s2}\left(t - T_{s2}(t)\right) \quad (5.68)$$

In the proposed system, the dominance factors $E_{1-14}(t)$, $E_{15}(t)$ and $E_{16}(t)$ are deployed respectively on the master side, slave 2 side and slave 1 side. The positive dominance factors $E_{1-16}(t)$ varying between 0 and 1 are defined as follows:

$$E_1(t) = E_3(t) = E_5(t) = E_8(t) = E_{11}(t) = E_{13}(t) = \frac{\frac{1}{2}\alpha\tau_{h1}^2(t) + \frac{1}{2}|\alpha\tau_{h1}(t)\tau_{h2}(t)|}{\frac{1}{2}\alpha\tau_{h1}^2(t) + |\alpha\tau_{h1}(t)\tau_{h2}(t)| + \frac{1}{2}\tau_{h2}^2(t)} \tag{5.69}$$

$$E_2(t) = E_4(t) = E_6(t) = E_7(t) = E_{12}(t) = E_{14}(t) = \frac{\frac{1}{2}\tau_{h2}^2(t) + \frac{1}{2}|\alpha\tau_{h1}(t)\tau_{h2}(t)|}{\frac{1}{2}\alpha\tau_{h1}^2(t) + |\alpha\tau_{h1}(t)\tau_{h2}(t)| + \frac{1}{2}\tau_{h2}^2(t)} \tag{5.70}$$

$$E_9(t) = \frac{\tau_{e1}^2\big(t - T_{b1}(t)\big)}{\tau_{e1}^2\big(t - T_{b1}(t)\big) + \tau_{e2}^2\big(t - T_{b2}(t)\big)} \tag{5.71}$$

$$E_{10}(t) = \frac{\tau_{e2}^2\big(t - T_{b2}(t)\big)}{\tau_{e1}^2\big(t - T_{b1}(t)\big) + \tau_{e2}^2\big(t - T_{b2}(t)\big)} \tag{5.72}$$

$$\mathrm{E}_{15}(\mathrm{t}) = \mathrm{E}_{16}(\mathrm{t}) = 1 \tag{5.73}$$

where α is a positive constant tuning gain. The purpose of this system is to allow the trainer to train the trainee to simultaneously control the two slave robots so that the trainee can follow the desired motion and perform the task. The proposed system contains the following three modes:

Training mode: The trainee does not apply force to master 2 ($\tau_{h2} = 0$), and master 1 driven by the trainer leads the slaves and master 2 to perform the desired motion. The dominance factor $E_1(t) = E_3(t) = E_5(t) = E_8(t) = E_{11}(t) = E_{13}(t) = 1$. Therefore, the trainer can fully control the slave robot and feel the dynamics of the environment. When setting $\alpha \gg 1$, the trainee has little influence on the slave robots, which can guarantee the training mode not to be disturbed by the trainee's accidentally applied force.

Guidance mode: Both of the two users apply forces to the master robots. Each of the users feels the mixed dynamics of environment and the other user in this mode.

Evaluation mode: The trainer does not apply force to master 1 ($\tau_{h1} = 0$). The dominance factor $E_1(t) = E_3(t) = E_5(t) = E_8(t) = E_{11}(t) = E_{13}(t) = 0$. Hence, the trainee can fully feel the environmental dynamics and can perform the whole task alone. If the trainee does not follow the required motion and has the risk of failing the task, the trainer can immediately apply force to correct the motion of the slaves.

In this section, the corresponding nonlinear dynamics of the dual-user-multi-slave teleoperation system are modeled as:

$$M_{mj}(q_{mj})\ddot{q}_{mj} + C_{mj}(q_{mj}, \dot{q}_{mj})\dot{q}_{mj} + g_{mj}(q_{mj}) = \tau_{mj} + \tau_{hlj} \quad (5.74)$$

$$M_{sj}(q_{sj})\ddot{q}_{sj} + C_{sj}(q_{sj}, \dot{q}_{sj})\dot{q}_{sj} + g_{sj}(q_{sj}) = \tau_{sj} - \tau_{elj} \quad (5.75)$$

where $M_i(q_i) \in R^{n\times n}$ are the inertia matrices, $C_i(q_i, \dot{q}_i) \in R^{n\times n}$ are Coriolis/centrifugal effects. $g_i(q_i) \in R^n$ are the vectors of gravitational forces, τ_i are the control signals. τ_{hlj}, τ_{elj} denotes the local human and environmental torques applied to the manipulators. New control terms $S_{m1,2}$ for master robots are introduced as:

$$\begin{aligned} S_{m1} = \tau_{h1}(t) &+ E_6(t)\tau_{h2}(t) - E_5(t)E_9(t)\tau_{e1}\big(t - T_{b1}(t)\big) \\ &- E_5(t)E_{10}(t)\tau_{e2}\big(t - T_{b2}(t)\big) + E_6(t)\beta r_{m2}(t) - \beta r_{m1}(t) \\ &+ E_5(t)E_{11}(t)\beta r_{s1}\big(t - T_{b1}(t)\big) \\ &+ E_5(t)E_{12}(t)\beta r_{s2}\big(t - T_{b2}(t)\big) \end{aligned} \quad (5.76)$$

$$\begin{aligned} S_{m2} = \tau_{h2}(t) &+ E_8(t)\tau_{h1}(t) - E_7(t)E_9(t)\tau_{e1}\big(t - T_{b1}(t)\big) \\ &- E_7(t)E_{10}(t)\tau_{e2}\big(t - T_{b2}(t)\big) + E_8(t)\beta r_{m1}(t) - \beta r_{m2}(t) \\ &+ E_7(t)E_{13}(t)\beta r_{s1}\big(t - T_{b1}(t)\big) \\ &+ E_7(t)E_{14}(t)\beta r_{s2}\big(t - T_{b2}(t)\big) \end{aligned} \quad (5.77)$$

In the slave sides, the new control terms $S_{s1,2}$ for the slave robots are written as follows:

$$S_{s1} = \Big(E_1\big(t - T_{f1}(t)\big)\tau_{h1}\big(t - T_{f1}(t)\big) + E_2\big(t - T_{f1}(t)\big)\tau_{h2}\big(t - T_{f1}(t)\big) - \tau_{e1}(t)\Big) + \beta\Big(E_1\big(t - T_{f1}(t)\big)r_{m1}\big(t - T_{f1}(t)\big) + E_2\big(t - T_{f1}(t)\big)r_{m2}\big(t - T_{f1}(t)\big) - r_{s1}(t)\Big) + \beta E_{16}(t)\Big(r_{s2}\big(t - T_{s2}(t)\big) - r_{s1}(t)\Big) - E_{16}(t)(\tau_{e1}(t) + \tau_{e2}\big(t - T_{s2}(t)\big)) \quad (5.78)$$

$$S_{s2} = \Big(E_3\big(t - T_{f2}(t)\big)\tau_{h1}\big(t - T_{f2}(t)\big) + E_4\big(t - T_{f2}(t)\big)\tau_{h2}\big(t - T_{f2}(t)\big) - \tau_{e1}(t)\Big) + \beta\Big(E_3\big(t - T_{f2}(t)\big)r_{m1}\big(t - T_{f2}(t)\big) + E_4\big(t - T_{f2}(t)\big)r_{m2}\big(t - T_{f2}(t)\big) - r_{s1}(t)\Big) + \beta E_{15}(t)\Big(r_{s1}\big(t - T_{s1}(t)\big) - r_{s2}(t)\Big) - E_{15}(t)(\tau_{e2}(t) + \tau_{e1}\big(t - T_{s2}(t)\big)) \quad (5.79)$$

The new control laws for the proposed multilateral teleoperation system are designed as follows:

$$\tau_{ij} = S_{ij} - \widehat{M}_{ij}(q_{ij})\{\delta\dot{q}_{ij}\} - \hat{C}_{ij}(q_{ij}, \dot{q}_{ij})\{\delta q_{ij}\} + \hat{g}_{ij}(q_{ij}) \quad (5.80)$$

where $\widehat{M}_{ij}(q_{ij})$, $\hat{C}_{ij}(q_{ij}, \dot{q}_{ij})$, $\hat{g}_{ij}(q_{ij})$ are the estimates of $M_{ij}(q_{ij})$, $C_{ij}(q_{ij}, \dot{q}_{ij})$, $g_{ij}(q_{ij})$.

Therefore, the new system dynamics can be expressed as:

$$M_{mj}(q_{mj})\dot{r}_{mj} + C_{mj}(q_{mj}, \dot{q}_{mj})r_{mj} = S_{mj} + \tau_{hlj} \quad (5.81)$$

$$M_{sj}(q_{sj})\dot{r}_{sj} + C_{sj}(q_{sj}, \dot{q}_{sj})r_{sj} = S_{sj} - \tau_{elj} \quad (5.82)$$

5.3.2 Experimental results

In this section, a series of experiments are carried out to validate the proposed dual-user-dual-slave teleoperation system. Two computers are applied to control the two masters and the two slaves. The communication channel between the two computers is the Internet. During the experimental process, the control loop is configured as a 1k Hz sampling rate. The wave impedance b, B and M are set as 2.5, 2, 1, respectively. δ is set to be 1. The position controller β is set to 2. Time delay modules of Simulink are also used to enlarge the time delay between the robots. The time delays between the two computers are around 500 ms (one way) with 200 ms variation. Virtual time delay between the two slave robots is set to be 100 ms constant delay. In all of the figures of the experimental results, the colors representing the robots are blue – Master 1 (trainer), red – Master 2 (trainee), green – Slave 1, black – Slave 2.

In the first experiment, the four robots are controlled to draw a circle "○" on a table as show in Fig.5.9, where the three figures represent training, guidance and evaluation modes. In the training mode, the trainee does not apply force and the trainer drives the master 1 to control the other three robot to draw the circle. In the guidance mode, the two users cooperate to drive the four robot to draw the circles. Since time-varying delays exist, the letters drawn by the slave robots have small variations, but the trajectories closely track the master robots.

In the evaluation mode, the trainee drives the master 2 to control the three robots and the trainer does not apply any force at first. Then, the trainee loosens his grip on the manipulator of the master 1 after finishing half of the circle "○". Meanwhile, the trainer immediately holds the master 2's manipulator to finish the remaining task. The trainer can correct the slave robots' motion at any time when the trainee is working alone.

The next experiment proves that the proposed system can directly finish the whole training procedure online without the need for changing any parameters. In this experiment, the two slave robots are controlled to lift a soft sponge three times as shown in Fig.6. The two slave robots apply forces to each other via the soft sponge in the middle. The three times' lifting motions represent the three modes, training mode,

guidance mode and evaluation mode. The trainer uses the master 1 to perform the task alone in the first lifting motion, and then cooperates with the trainee in the second lifting motion. Finally, the trainee performs the task alone using master 2 in the third lifting motion. Fig.5.10 shows the position and torque tracking. The reason of the steady-state errors of position is that the users keep applying force to the master robots while the two slave robots are applying force to restrict the motion of each other. After finishing the task, the force and position signals of all the robots converge to zero and the errors disappear.

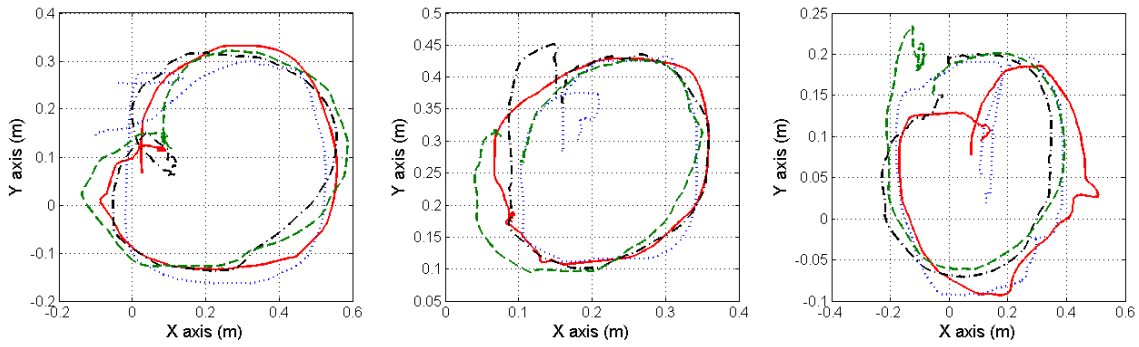

Figure 5.9 Drawing a circle "○" (blue – Master 1 (trainer), red – Master 2 (trainee), green – Slave 1, black – Slave 2)

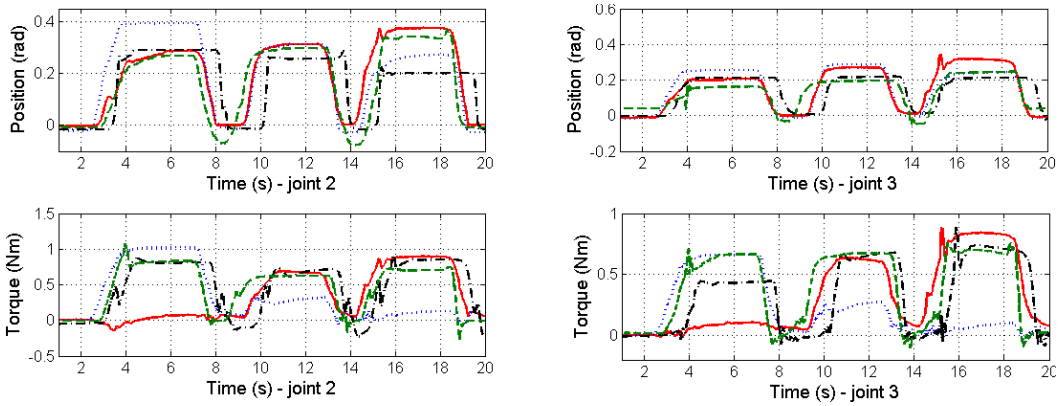

Figure 5.10 Lifting a soft sponge (blue – Master 1 (trainer), red – Master 2 (trainee), green – Slave 1, black – Slave 2)

5.4 Nonlinear multi-user shared control of teleoperation system

Along with the development of the teleoperation application, the multi-user teleoperation control has also been as new direction to investigate. In some application such as rehabilitation and tele-surgery, the main doctor drives the main master robot to remotely conduct the operation while the multiple assistants in different places are required to drive the other master robots to provide necessary assistance. Consider this scenario, multi-user teleoperation becomes significant to be investigated and developed. In this section, a novel multi-user shared control teleoperation control system is proposed that allows the mentor to guide multiple trainees to collaboratively control the remote slave robot. Time-varying delays between every two robots are considered. A new 4-CH wave-based time delay passivity approach is applied to guarantee the time delayed system's stability. The FLs are applied to compensate for the nonlinear dynamic uncertainties. New adaptive controllers are designed to deal with the input saturation problem.

5.4.1 System formulation

In this section, the Multi-master/Single-slave system includes multiple operators that collaboratively control the remote slave robot by means of the corresponding master robots. The authority of the master robots over the slave robot is regulated by pre-setting dominance factors. Each robot is connected with other robots through time delayed communication networks. The time delays among the channels between the master and the slave and the channels between every two masters can influence the system's stability. The master robots and the slave robot are modeled as a pair of n-DOF serial links with revolute joints. Their corresponding nonlinear dynamics are modeled as:

$$M_{mj}(q_{mj})\ddot{q}_{mj} + C_{mj}(q_{mj}, \dot{q}_{mj})\dot{q}_{mj} + F_{mj}\dot{q}_{mj} + f_{cmj}(\dot{q}_{mj}) + g_{mj}(q_{mj}) - F_{mj}^{*} = \tau_{mj} + \tau_{hj} \tag{5.83}$$

$$M_s(q_s)\ddot{q}_s + C_s(q_s, \dot{q}_s)\dot{q}_s + F_s\dot{q}_s + f_{cs}(\dot{q}_s) + g_s(q_s) - F_s^{*} = \tau_s - \tau_e \tag{5.84}$$

where $i = m, s$ for the master and slave. $\ddot{q}_i(t)$, $\dot{q}_i(t)$, $q_i(t) \in R^{n\times 1}$ are the joint acceleration, velocity and position, respectively. $M_i(q_i(t)) \in R^{n\times n}$ are the inertia matrices, $C_i(q_i(t), \dot{q}_i(t)) \in R^{n\times n}$ are Coriolis/centrifugal effects. $g_i(q_i(t)) \in R^n$ are the vectors of gravitational forces and τ_i are the control signals. $\tau_h(t)$ and $\tau_e(t)$ are the actual human and environmental torques applied to the robots. $F_i\dot{q}_i(t)$ denote the viscous friction coefficients and $f_{ci}(\dot{q}_i(t))$ denote the Coulomb friction coefficients. $F_i^*(t) \in R^{n\times 1}$ are the bounded unknown disturbances. In the section, the Coulomb friction function $f_{ci}(\dot{q}_i(t))$ in the master and slave sides are bounded and piecewise continuous functions.

Fuzzy logic control algorithms can be applied to universally approximate the model uncertainties of the dynamics systems. A fuzzy system is a collection of fuzzy IF-THEN rules of the form

$$R^k: IF\ z_1\ is\ A_1^k\ and\ \ldots and\ z_n\ is\ A_n^k, THEN\ y\ is\ B^k$$

where $z = [z_1, z_2, \ldots, z_n]^T \in \Omega_z$ and $y \in \Omega_y$ are the linguistic variables associated with the input and output of FLS, respectively. R^k is the k-th rule. Fuzzy sets $A_1^k \ldots A_n^k$ and B^k are associated with the membership functions $\mu_{A_l^k}(z_l)$ and μ_{B^k}. The FLS applies the strategy of singleton fuzzification, product inference and center-average defuzzification while the output is expressed as:

$$y\big(z(t)\big) = \frac{\sum_{k=1}^{m} y^k \left(\prod_{l=1}^{n} \mu_{A_l^k}\big(z_l(t)\big)\right)}{\sum_{k=1}^{m} \prod_{l=1}^{n} \mu_{A_l^k}\big(z_l(t)\big)} \tag{5.85}$$

where y^k is the point in R at with μ_{B^k} can achieve its maximum value (assuming $\mu_{B^k}(y^k) = 1$). The FLS can be represented as (5.86) by introducing the concept of the fuzzy basic function vector $\varsigma(z(t))$:

$$y\big(z(t)\big) = \theta^T(t)\varsigma(z(t)) \tag{5.86}$$

where the weight factor $\theta(t) = [y^1(t), y^2(t), \ldots, y^m(t)]^T$ and the fuzzy basic function vector $\varsigma\big(z(t)\big) = [\varsigma_1\big(z(t)\big), \varsigma_2\big(z(t)\big), \ldots, \varsigma_m\big(z(t)\big)]$, where

$$\varsigma\big(z(t)\big) = \frac{\prod_{l=1}^{n} \mu_{A_l^k}(z_l(t))}{\sum_{k=1}^{m} \prod_{l=1}^{n} \mu_{A_l^k}(z_l(t))} \tag{5.87}$$

According to the universal approximation theorem, the optimal approximation parameter θ^* exist and $\theta^{*T}(t)\varsigma(z(t))$ can estimate a nonlinear function $G(z(t))$ over a compact set to any degree of accuracy where θ^* can be defined as:

$$\theta^* = arg \min_{\theta \in \Omega_\theta} \big(sup_{z \in \Omega_z} \big| \theta^T(t)\varsigma\big(z(t)\big) - G(z(t)) \big| \big) \tag{5.88}$$

where Ω_θ and Ω_z are the sets of suitable bounds on $\theta(t)$ and $z(t)$, respectively. The minimum approximation error satisfies

$$G\big(z(t)\big) = \theta^{*T}\varsigma\big(z(t)\big) + \epsilon\big(z(t)\big) \tag{5.89}$$

and the positive constants ϵ^* exists such that $\big\|\epsilon\big(z(t)\big)\big\| \leq \epsilon^*$ over the compact set Ω_z. Due to the existing friction and backlash, the robots' dynamic functions can be seen as piecewise continuous functions. Supposing $G'(z(t))$ is also a piecewise function where

$$G'\big(z(t)\big) = G_1\big(z(t)\big)(continuous\ part) + G_2\big(z(t)\big)(bounded\ piecewise\ term)$$

Therefore,

$$G'\big(z(t)\big) = \theta^{*T}\varsigma\big(z(t)\big) + \epsilon\big(z(t)\big) + G_2\big(z(t)\big) = \theta^{*T}\varsigma\big(z(t)\big) + \bar{\epsilon}\big(z(t)\big) \tag{5.90}$$

where $\bar{\epsilon}\big(z(t)\big) = \epsilon\big(z(t)\big) + G_2\big(z(t)\big)$. $\bar{\epsilon}^*$ is defined as an upper bound of the piecewise function approximation error $\bar{\epsilon}^* \geq \big\|\bar{\epsilon}\big(z(t)\big)\big\|$.

To guarantee the communication channels passivity in the presence of constant time delays, we extend the wave variable transformation in Fig.4.37 to the multi-user shared-control architecture under time-varying delays shown as Fig.5.11. Master 1 driven by the mentor leads the other master robots (Master 2…N) that are driven by the trainees to cooperatively control the remote slave robot. We define the dominance factors $F_{1\ldots N}$ and $E_{1\ldots N}$ such that $0 \leq F_{1\ldots N}, E_{1\ldots N} \leq 1$. The E_1 factor determines the

authority of trainer over the other trainees and $E_{2\ldots N}$ imply the supremacy of trainees over the trainer. $F_{1\ldots N}$ illustrate the supremacy of all the users over the slave robot. The dominance factors $E_{1\ldots N}$ and $F_{1\ldots N}$ satisfy the following conditions:

$$\sum_{j=1}^{N} E_j = 1, \sum_{j=1}^{N} F_j = 1 \tag{5.91}$$

$$F_1 = \frac{E_1^2}{E_1^2 + \sum_{j=2}^{N} E_j(1 - E_1)}, F_{j,j\neq 1} = \frac{E_j(1 - E_1)}{E_1^2 + \sum_{j=2}^{N} E_j(1 - E_1)} \tag{5.92}$$

This system can be separated into three mode: the training mode, the guidance mode and the evaluation mode. In the training mode ($E_1 = 1, F_1 = 1$), the master-1 fully controls the slave robot as well as other masters. The trainees can only feel the dynamics of the master 1. In the guidance mode ($0 < E_1, F_1 < 1$), all of the users cooperate to perform the remote task. Master 1 receives the mixed dynamics of the slave and the other masters while Master-j ($j \neq 1$) receives the mixed dynamics of the slave and the master 1. In the evaluation mode ($E_1 = 0, F_1 = 0$), Master 1 cannot control other robots. The mentor evaluates the other users' performances based on the received mixed dynamics of the other masters.

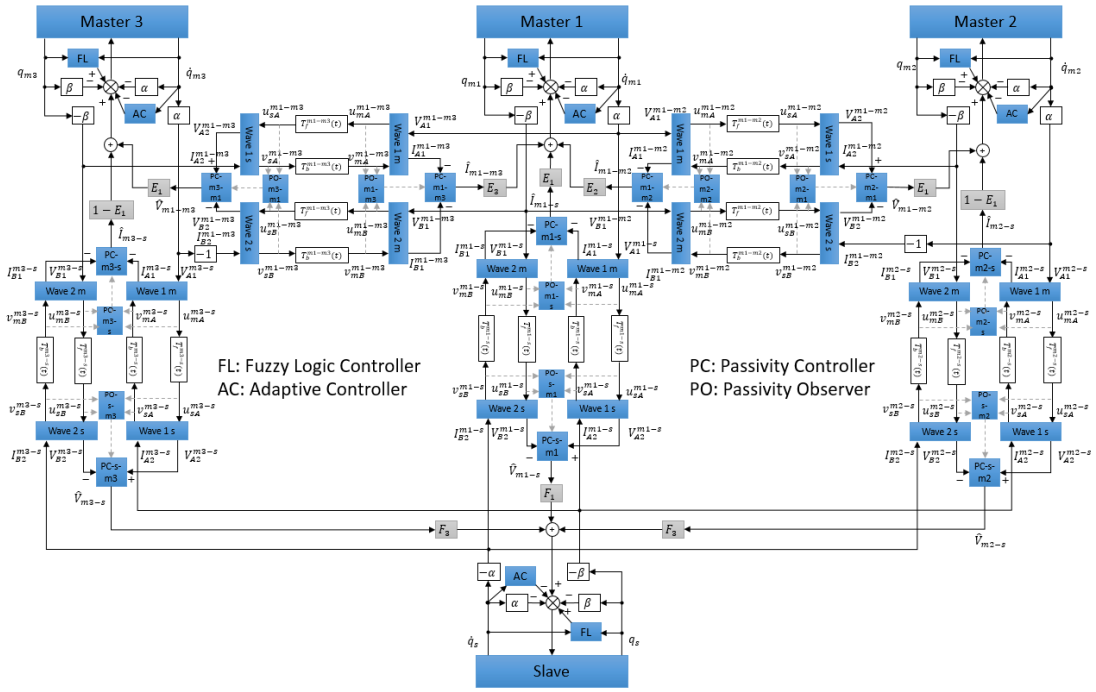

Figure 5.11 Total block diagram of the proposed multi-user architecture

Remark 1. In this section, the unsymmetrical time delays $T_f^{mj-s}(t)$, $T_b^{mj-s}(t)$, $T_f^{m1-mj}(t)$, $T_b^{m1-mj}(t)$ are assumed not to increase or decrease faster than the time itself. That is, $\left|\dot{T}_{f,b}^{mj-s}(t)\right| \le \bar{\mu}_{f,b}^{mj-s} < 1$ and $\left|\dot{T}_{f,b}^{m1-mj}(t)\right| \le \bar{\mu}_{f,b}^{m1-mj} < 1$ where $\bar{\mu}_{f,b}^{mj-s}$ and $\bar{\mu}_{f,b}^{m1-mj}$ are the upper bounds of the differentials of the time delays. Moreover, the time-varying delays $T_{f,b}^{mj-s}(t)$, $T_{f,b}^{m1-mj}(t)$ are considered to be the sum of the constant time delays $\bar{T}_{f,b}^{mj-s}$, $\bar{T}_{f,b}^{m1-mj}$ with their bounded perturbations $\Delta T_{f,b}^{mj-s}(t)$, $\Delta T_{f,b}^{m1-mj}(t)$. That is, $T_{f,b}^{mj-s}(t) = \bar{T}_{f,b}^{mj-s} + \Delta T_{f,b}^{mj-s}(t) \le \bar{T}_{f,b}^{mj-s} + \bar{\varepsilon}_{f,b}^{mj-s} = \bar{\bar{T}}_{f,b}^{mj-s}$, $T_{f,b}^{m1-mj}(t) = \bar{T}_{f,b}^{m1-mj} + \Delta T_{f,b}^{m1-mj}(t) \le \bar{T}_{f,b}^{m1-mj} + \bar{\varepsilon}_{f,b}^{m1-mj} = \bar{\bar{T}}_{f,b}^{m1-mj}$,where $\bar{\varepsilon}_{f,b}^{mj-s}$, $\bar{\varepsilon}_{f,b}^{m1-mj}$ are the upper bounds of the perturbations and $\bar{\bar{T}}_{f,b}^{mj-s}$, $\bar{\bar{T}}_{f,b}^{m1-mj}$ are the upper bounds of the time delays.

The feed-forward control signals from the robots are set as: $V_{A1}^{m1-s}(t) = V_{A1}^{m1-mj}(t) = \alpha\dot{q}_{m1}(t)$, $V_{B1}^{m1-s}(t) = V_{B1}^{m1-mj}(t) = -\beta q_{m1}(t)$, $V_{A1}^{mj-s}(t) =$

$\alpha\dot{q}_{mj}(t)$, $I_{B2}^{m1-mj}(t) = -\alpha\dot{q}_{mj}(t)$, $V_{B1}^{mj-s}(t) = I_{A2}^{m1-mj}(t) = -\beta q_{mj}(t)$, $I_{A2}^{mj-s}(t) = -\beta q_s, I_{B2}^{mj-s}(t) = -\alpha\dot{q}_s$.

The power flow $P(t)$ in the whole network can be expressed as:

$$\begin{aligned} P(t) = \sum_{j=1}^{N} \Big(& V_{A1}^{mj-s}(t) I_{A1}^{mj-s}(t) + V_{B1}^{mj-s}(t) I_{B1}^{mj-s}(t) - V_{A2}^{mj-s}(t) I_{A2}^{mj-s}(t) \\ & - V_{B2}^{mj-s}(t) I_{B2}^{mj-s}(t) \Big) \\ & + \sum_{j=2}^{N} \Big(V_{A1}^{m1-mj}(t) I_{A1}^{m1-mj}(t) + V_{B1}^{m1-mj}(t) I_{B1}^{m1-mj}(t) \\ & - V_{A2}^{mj}(t) I_{A2}^{mj}(t) + V_{B2}^{mj}(t) I_{B2}^{mj}(t) \Big) \end{aligned} \tag{5.93}$$

(5.93) can be further written as:

$$P(t) = \frac{dE(t)}{dt} + P^{diss}(t)$$

where

$$\frac{dE(t)}{dt} = \sum_{j=1}^{N} \left\{ \frac{d}{dt} \int_{t-T_f^{mj-s}(t)}^{t} \lambda_1 u_{mA}^{mj-s^T}(\eta) u_{mA}^{mj-s}(\eta) d\eta \right.$$
$$\left. + \frac{d}{dt} \int_{t-T_f^{mj-s}(t)}^{t} \frac{1}{\lambda_2} u_{mB}^{mj-s^T}(\eta) u_{mB}^{mj-s}(\eta) d\eta \right\}$$
$$+ \sum_{j=2}^{N} \left\{ \frac{d}{dt} \int_{t-T_f^{m1-mj}(t)}^{t} \lambda_1 u_{mA}^{m1-mj^T}(\eta) u_{mA}^{m1-mj}(\eta) d\eta \right.$$
$$\left. + \frac{d}{dt} \int_{t-T_f^{m1-mj}(t)}^{t} \frac{1}{\lambda_2} u_{mB}^{m1-mj^T}(\eta) u_{mB}^{m1-mj}(\eta) d\eta \right\}$$
$$+ \sum_{j=1}^{N} \left\{ \frac{d}{dt} \int_{t-T_b^{mj-s}(t)}^{t} \frac{1}{\lambda_1} v_{sA}^{mj-s^T}(\eta) v_{sA}^{mj-s}(\eta) d\eta \right.$$
$$\left. + \frac{d}{dt} \int_{t-T_b^{mj-s}(t)}^{t} \lambda_2 v_{sB}^{mj-s^T}(\eta) v_{sB}^{mj-s}(\eta) d\eta \right\}$$
$$+ \sum_{j=2}^{N} \left\{ \frac{d}{dt} \int_{t-T_b^{m1-mj}(t)}^{t} \frac{1}{\lambda_1} v_{sA}^{m1-mj^T}(\eta) v_{sA}^{m1-mj}(\eta) d\eta \right.$$
$$\left. + \frac{d}{dt} \int_{t-T_b^{m1-mj}(t)}^{t} \lambda_2 v_{sB}^{m1-mj^T}(\eta) v_{sB}^{m1-mj}(\eta) d\eta \right\} \qquad (5.94)$$

$$P^{diss}(t) = \sum_{j=1}^{N} \left\{ \frac{1}{\lambda_1} \left(v_{mA}^{mj-s}(t) - \lambda_1 u_{mA}^{mj-s}(t) \right)^T \left(v_{mA}^{mj-s}(t) - \lambda_1 u_{mA}^{mj-s}(t) \right) \right.$$
$$\left. + \lambda_2 \left(v_{mB}^{mj-s}(t) - \frac{1}{\lambda_2} u_{mB}^{mj-s}(t) \right)^T \left(v_{mB}^{mj-s}(t) - \frac{1}{\lambda_2} u_{mB}^{mj-s}(t) \right) \right\}$$
$$+ \sum_{j=1}^{N} \left\{ \frac{1}{\lambda_1} \left(v_{sA}^{mj-s}(t) - \lambda_1 u_{sA}^{mj-s}(t) \right)^T \left(v_{sA}^{mj-s}(t) - \lambda_1 u_{sA}^{mj-s}(t) \right) \right.$$
$$\left. + \lambda_2 \left(v_{sB}^{mj-s}(t) - \frac{1}{\lambda_2} u_{sB}^{mj-s}(t) \right)^T \left(v_{sB}^{mj-s}(t) - \frac{1}{\lambda_2} u_{sB}^{mj-s}(t) \right) \right\}$$

$$+\sum_{j=2}^{N}\left\{\frac{1}{\lambda_1}\left(v_{mA}^{m1-mj}(t)-\lambda_1 u_{mA}^{m1-mj}(t)\right)^T\left(v_{mA}^{m1-mj}(t)-\lambda_1 u_{mA}^{m1-mj}(t)\right)\right.$$
$$\left.+\lambda_2\left(v_{mB}^{m1-mj}(t)-\frac{1}{\lambda_2}u_{mB}^{m1-mj}(t)\right)^T\left(v_{mB}^{m1-mj}(t)-\frac{1}{\lambda_2}u_{mB}^{m1-mj}(t)\right)\right\}$$
$$+\sum_{j=2}^{N}\left\{\frac{1}{\lambda_1}\left(v_{sA}^{m1-mj}(t)-\lambda_1 u_{sA}^{m1-mj}(t)\right)^T\left(v_{sA}^{m1-mj}(t)\right.\right.$$
$$\left.-\lambda_1 u_{sA}^{m1-mj}(t)\right)$$
$$\left.+\lambda_2\left(v_{sB}^{m1-mj}(t)-\frac{1}{\lambda_2}u_{sB}^{m1-mj}(t)\right)^T\left(v_{sB}^{m1-mj}(t)-\frac{1}{\lambda_2}u_{sB}^{m1-mj}(t)\right)\right\}$$
$$-\sum_{j=1}^{N}\left\{\lambda_1\dot{T}_f^{mj-s}(t)u_{sA}^{mj-s^T}(t)u_{sA}^{mj-s}(t)\right.$$
$$\left.+\frac{1}{\lambda_2}\dot{T}_f^{mj-s}(t)u_{sB}^{mj-s^T}(t)u_{sB}^{mj-s}(t)\right\}$$
$$-\sum_{j=2}^{N}\left\{\lambda_1\dot{T}_f^{m1-mj}(t)u_{sA}^{m1-mj^T}(t)u_{sA}^{m1-mj}(t)\right.$$
$$\left.+\frac{1}{\lambda_2}\dot{T}_f^{m1-mj}(t)u_{sB}^{m1-mj^T}(t)u_{sB}^{m1-mj}(t)\right\}$$
$$-\sum_{j=1}^{N}\left\{\frac{1}{\lambda_1}\dot{T}_b^{mj-s}(t)v_{mA}^{mj-s^T}(t)v_{mA}^{mj-s}(t)\right.$$
$$\left.+\lambda_2\dot{T}_b^{mj-s}(t)v_{mB}^{mj-s^T}(t)v_{mB}^{mj-s}(t)\right\}$$
$$-\sum_{j=2}^{N}\left\{\frac{1}{\lambda_1}\dot{T}_b^{m1-mj}(t)v_{mA}^{m1-mj^T}(t)v_{mA}^{m1-mj}(t)\right.$$
$$\left.+\lambda_2\dot{T}_b^{m1-mj}(t)v_{mB}^{m1-mj^T}(t)v_{mB}^{m1-mj}(t)\right\} \qquad (5.95)$$

Since P_{diss} is not observable at any terminal of the network, in order to facilitate real-time monitoring of the network's passivity, P_{diss} can be written as:

$$P_{diss}(t)=\sum_{j=1}^{N}P_{diss}^{mj-s}(t)+\sum_{j=2}^{N}P_{diss}^{m1-mj}(t)+\sum_{j=2}^{N}P_{diss}^{mj-m1}(t)$$
$$+\sum_{j=1}^{N}P_{diss}^{s-mj}(t) \qquad (5.96)$$

where

$$P_{diss}^{mj-s}(t) = \frac{1}{\lambda_1}\left(v_{mA}^{mj-s}(t) - \lambda_1 u_{mA}^{mj-s}(t)\right)^T \left(v_{mA}^{mj-s}(t) - \lambda_1 u_{mA}^{mj-s}(t)\right) + \lambda_2 \left(v_{mB}^{mj-s}(t) - \frac{1}{\lambda_2} u_{mB}^{mj-s}(t)\right)^T \left(v_{mB}^{mj-s}(t) - \frac{1}{\lambda_2} u_{mB}^{mj-s}(t)\right) - \frac{1}{\lambda_1} \dot{T}_b^{mj-s}(t) v_{mA}^{mj-s^T}(t) v_{mA}^{mj-s}(t) - \lambda_2 \dot{T}_b^{mj-s}(t) v_{mB}^{mj-s^T}(t) v_{mB}^{mj-s}(t) \quad (5.97)$$

$$P_{diss}^{m1-mj}(t) = \frac{1}{\lambda_1}\left(v_{mA}^{m1-mj}(t) - \lambda_1 u_{mA}^{m1-mj}(t)\right)^T \left(v_{mA}^{m1-mj}(t) - \lambda_1 u_{mA}^{m1-mj}(t)\right) + \lambda_2 \left(v_{mB}^{m1-mj}(t) - \frac{1}{\lambda_2} u_{mB}^{m1-mj}(t)\right)^T \left(v_{mB}^{m1-mj}(t) - \frac{1}{\lambda_2} u_{mB}^{m1-mj}(t)\right) - \frac{1}{\lambda_1} \dot{T}_b^{m1-mj}(t) v_{mA}^{m1-mj^T}(t) v_{mA}^{m1-mj}(t) - \lambda_2 \dot{T}_b^{m1-mj}(t) v_{mB}^{m1-mj^T}(t) v_{mB}^{m1-mj}(t) \quad (5.98)$$

$$P_{diss}^{mj-m1} = \frac{1}{\lambda_1}\left(v_{sA}^{m1-mj}(t) - \lambda_1 u_{sA}^{m1-mj}(t)\right)^T \left(v_{sA}^{m1-mj}(t) - \lambda_1 u_{sA}^{m1-mj}(t)\right) + \lambda_2 \left(v_{sB}^{m1-mj}(t) - \frac{1}{\lambda_2} u_{sB}^{m1-mj}(t)\right)^T \left(v_{sB}^{m1-mj}(t) - \frac{1}{\lambda_2} u_{sB}^{m1-mj}(t)\right) - \lambda_1 \dot{T}_f^{m1-mj}(t) u_{sA}^{m1-mj^T}(t) u_{sA}^{m1-mj}(t) - \frac{1}{\lambda_2} \dot{T}_f^{m1-mj}(t) u_{sB}^{m1-mj^T}(t) u_{sB}^{m1-mj}(t) \quad (5.99)$$

$$P_{diss}^{s-mj}(t) = \frac{1}{\lambda_1}\left(v_{sA}^{mj-s}(t) - \lambda_1 u_{sA}^{mj-s}(t)\right)^T \left(v_{sA}^{mj-s}(t) - \lambda_1 u_{sA}^{mj-s}(t)\right) + \lambda_2 \left(v_{sB}^{mj-s}(t) - \frac{1}{\lambda_2} u_{sB}^{mj-s}(t)\right)^T \left(v_{sB}^{mj-s}(t) - \frac{1}{\lambda_2} u_{sB}^{mj-s}(t)\right) - \lambda_1 \dot{T}_f^{mj-s}(t) u_{sA}^{mj-s^T}(t) u_{sA}^{mj-s}(t) - \frac{1}{\lambda_2} \dot{T}_f^{mj-s}(t) u_{sB}^{mj-s^T}(t) u_{sB}^{mj-s}(t) \quad (5.100)$$

Since the differentials of the time delays are hard to measure in real time, they can be replaced by their upper bounds defined in **Remark 1**. The POs are designed as:

$$\text{PO-mj-s:}\quad P_{obs}^{mj-s}(t)=\frac{1}{\lambda_1}\left(v_{mA}^{mj-s}(t)-\lambda_1 u_{mA}^{mj-s}(t)\right)^T\left(v_{mA}^{mj-s}(t)-\lambda_1 u_{mA}^{mj-s}(t)\right)+$$
$$\lambda_2\left(v_{mB}^{mj-s}(t)-\frac{1}{\lambda_2}u_{mB}^{mj-s}(t)\right)^T\left(v_{mB}^{mj-s}(t)-\frac{1}{\lambda_2}u_{mB}^{mj-s}(t)\right)-$$
$$\frac{1}{\lambda_1}\bar{\mu}_b^{mj-s}v_{mA}^{mj-s^T}(t)v_{mA}^{mj-s}(t)-\lambda_2\bar{\mu}_b^{mj-s}v_{mB}^{mj-s^T}(t)v_{mB}^{mj-s}(t) \tag{5.101}$$

$$\text{PO-m1-mj:}\quad P_{obs}^{m1-mj}(t)=\frac{1}{\lambda_1}\left(v_{mA}^{m1-mj}(t)-\lambda_1 u_{mA}^{m1-mj}(t)\right)^T\left(v_{mA}^{m1-mj}(t)-\right.$$
$$\left.\lambda_1 u_{mA}^{m1-mj}(t)\right)+\lambda_2\left(v_{mB}^{m1-mj}(t)-\frac{1}{\lambda_2}u_{mB}^{m1-mj}(t)\right)^T\left(v_{mB}^{m1-mj}(t)-\right.$$
$$\left.\frac{1}{\lambda_2}u_{mB}^{m1-mj}(t)\right)-\frac{1}{\lambda_1}\bar{\mu}_b^{m1-mj}v_{mA}^{m1-mj^T}(t)v_{mA}^{m1-mj}(t)-$$
$$\lambda_2\bar{\mu}_b^{m1-mj}(t)v_{mB}^{m1-mj^T}(t)v_{mB}^{m1-mj}(t) \tag{5.102}$$

$$\text{PO-mj-m1:}\quad P_{obs}^{mj-m1}(t)=\frac{1}{\lambda_1}\left(v_{sA}^{m1-mj}(t)-\lambda_1 u_{sA}^{m1-mj}(t)\right)^T\left(v_{sA}^{m1-mj}(t)-\right.$$
$$\left.\lambda_1 u_{sA}^{m1-mj}(t)\right)+\lambda_2\left(v_{sB}^{m1-mj}(t)-\frac{1}{\lambda_2}u_{sB}^{m1-mj}(t)\right)^T\left(v_{sB}^{m1-mj}(t)-\right.$$
$$\left.\frac{1}{\lambda_2}u_{sB}^{m1-mj}(t)\right)-\lambda_1\bar{\mu}_f^{m1-mj}u_{sA}^{m1-mj^T}(t)u_{sA}^{m1-mj}(t)-$$
$$\frac{1}{\lambda_2}\bar{\mu}_f^{m1-mj}u_{sB}^{m1-mj^T}(t)u_{sB}^{m1-mj}(t) \tag{5.103}$$

$$\text{PO-s-mj:}\quad P_{obs}^{s-mj}(t)=\frac{1}{\lambda_1}\left(v_{sA}^{mj-s}(t)-\lambda_1 u_{sA}^{mj-s}(t)\right)^T\left(v_{sA}^{mj-s}(t)-\lambda_1 u_{sA}^{mj-s}(t)\right)+$$
$$\lambda_2\left(v_{sB}^{mj-s}(t)-\frac{1}{\lambda_2}u_{sB}^{mj-s}(t)\right)^T\left(v_{sB}^{mj-s}(t)-\frac{1}{\lambda_2}u_{sB}^{mj-s}(t)\right)-$$
$$\lambda_1\bar{\mu}_f^{mj-s}u_{sA}^{mj-s^T}(t)u_{sA}^{mj-s}(t)-\frac{1}{\lambda_2}\bar{\mu}_f^{mj-s}u_{sB}^{mj-s^T}(t)u_{sB}^{mj-s}(t) \tag{5.104}$$

Then, we set the output of the PCs to be:

PC-mj-s: $\hat{I}_{m1-s}(t) = -I_{A1}^{mj-s} - I_{B1}^{mj-s} - \Gamma_{mj-s}(t)$ (5.105)

PC-m1-mj: $\hat{I}_{m1-mj}(t) = -I_{A1}^{m1-mj} - I_{B1}^{m1-mj} - \Gamma_{m1-mj}(t)$ (5.106)

PC-mj-m1: $\hat{V}_{m1-mj}(t) = V_{A2}^{m1-mj} - V_{B2}^{m1-mj} - \Gamma_{mj-m1}(t)$ (5.107)

PC-s-mj: $\hat{V}_{mj-s}(t) = V_{A2}^{mj-s}(t) - V_{B2}^{mj-s}(t) - \Gamma_{s-mj}(t)$ (5.108)

where

$$\Gamma_{mj-s}(t) = \begin{cases} 0, \ \ if\ P_{obs}^{mj-s}(t) \geq 0 \\ \left(\dfrac{\bar{\mu}_f^{mj-s}\alpha}{2 - 2\bar{\mu}_f^{mj-s}} + \bar{\varepsilon}_f^{mj-s}\dfrac{\beta}{2} + \bar{\varepsilon}_b^{mj-s}\dfrac{\beta}{2}\right)\dot{q}_{mj}, \ \ if\ P_{obs}^{mj-s}(t) < 0 \end{cases} \quad (5.109)$$

$$\Gamma_{m1-mj}(t) = \begin{cases} 0, \ \ if\ P_{obs}^{m1-mj}(t) \geq 0 \\ \left(\dfrac{\bar{\mu}_f^{m1-mj}\alpha}{2 - 2\bar{\mu}_f^{m1-mj}} + \bar{\varepsilon}_f^{m1-mj}\dfrac{\beta}{2} + \bar{\varepsilon}_b^{m1-mj}\dfrac{\beta}{2}\right)\dot{q}_{m1}, \ \ if\ P_{obs}^{m1-mj}(t) < 0 \end{cases} \quad (5.110)$$

$$\Gamma_{mj-m1}(t) = \begin{cases} 0, \ \ if\ P_{obs}^{mj-m1}(t) \geq 0 \\ \left(\dfrac{\bar{\mu}_b^{m1-mj}\alpha}{2 - 2\bar{\mu}_b^{m1-mj}} + \bar{\varepsilon}_f^{m1-mj}\dfrac{\beta}{2} + \bar{\varepsilon}_b^{m1-mj}\dfrac{\beta}{2}\right)\dot{q}_{mj}, \ \ if\ P_{obs}^{mj-m1}(t) < 0 \end{cases} \quad (5.111)$$

$$\Gamma_{s-mj}(t) = \begin{cases} 0, \ \ if\ P_{obs}^{s-mj}(t) \geq 0 \\ \left(\dfrac{\bar{\mu}_b^{mj-s}\alpha}{2 - 2\bar{\mu}_b^{mj-s}} + \bar{\varepsilon}_f^{mj-s}\dfrac{\beta}{2} + \bar{\varepsilon}_b^{mj-s}\dfrac{\beta}{2}\right)\dot{q}_{s}, \ \ if\ P_{obs}^{s-mj}(t) < 0 \end{cases} \quad (5.112)$$

Practically, the problem, input saturation, usually appears in an industrial control system, which can be presented as follows:

$$\tau_{ij}(t) = \begin{cases} \bar{\tau}_{ij}(t), if\ \left|\tau_{ij}\right| \leq \mathrm{A}_{ij} \\ A_{ij}, if \left|\tau_{ij}\right| > A_{ij} \end{cases} \quad (5.113)$$

where A_{ij} are the allowable maximum controller output. $\bar{\tau}_{ij}(t)$ are the output of the proposed new control laws.

To compensate for the input errors $\Delta\tau_{ij}(t) = \tau_{ij}(t) - \bar{\tau}_{ij}(t)$ caused by the input saturation problem, the following adaptive controllers are introduced:

$$U_{ij}(t) = c_{ij}h_{ij}(t) + c_{ij}\dot{q}_{ij}(t) \tag{5.114}$$

$$\dot{h}_{ij}(t) = -c_{ij}h_{ij}(t) - \frac{\left\|\Delta\tau_{ij}(t)\right\|^2}{c_{ij}\left\|h_{ij}(t)\right\|^2}h_{ij}(t) - \Delta\tau_{ij}(t) \tag{5.115}$$

where $0 < c_{ij} < 1$.

The control laws of the overall teleoperation system are given as follows:

$$\begin{aligned}
\bar{\tau}_{m1}(t) = {} & \hat{G}_{m1}(Z_{m1}) + E_1\hat{I}_{m1-s}(t) + \sum_{j=2}^{N} E_j\hat{I}_{m1-mj}(t) - \alpha\dot{q}_{m1}(t) - \beta q_{m1}(t) \\
& - Y_{m1}(t) \\
& = \hat{G}_{m1}(Z_{m1}) + \beta E_1\left(q_s\left(t - T_b^{m1-s}(t)\right) - q_{m1}(t)\right) \\
& + \sum_{j=2}^{N}\beta E_j\left(q_{mj}\left(t - T_b^{m1-mj}(t)\right) - q_{m1}(t)\right) \\
& + \alpha E_1\left(\dot{q}_s\left(t - T_b^{m1-s}(t)\right) - \dot{q}_{m1}(t)\right) \\
& + \sum_{j=2}^{N}\alpha E_j\left(\dot{q}_{mj}\left(t - T_b^{m1-mj}(t)\right) - \dot{q}_{m1}(t)\right) - b_1\lambda_1\alpha\dot{q}_{m1}(t) \\
& + \frac{b_2\beta E_1}{\lambda_2}\left(q_{m1}(t) - q_{m1}\left(t - T_f^{m1-s}(t) - T_b^{m1-s}\left(t - T_f^{m1-s}(t)\right)\right)\right) \\
& + \sum_{j=2}^{N}\frac{b_2\beta E_j}{\lambda_2}\Bigg(q_{m1}(t) \\
& - q_{m1}\left(t - T_f^{m1-mj}(t) - T_b^{m1-mj}\left(t - T_f^{m1-mj}(t)\right)\right)\Bigg) - E_1\Gamma_{m1-s}(t) \\
& - \sum_{j=2}^{N} E_j\Gamma_{m1-mj}(t) - U_{m1}(t) - Y_{m1}(t)
\end{aligned} \tag{5.116}$$

$$\bar{\tau}_{mj}(t) = \hat{G}_{mj}(Z_{mj}) + (1-E_1)\hat{I}_{mj-s}(t) + E_1\hat{V}_{m1-mj}(t) - \alpha\dot{q}_{mj}(t) - \beta q_{mj}(t) - Y_{m1}(t)$$
$$= \hat{G}_{mj}(Z_{mj}) + (1-E_1)\beta\left(q_s\left(t - T_b^{mj-s}(t)\right) - q_{mj}(t)\right)$$
$$+ \beta E_1\left(q_{m1}\left(t - T_f^{m1-mj}(t)\right) - q_{mj}(t)\right)$$
$$+ (1-E_1)\alpha\left(\dot{q}_s\left(t - T_b^{mj-s}(t)\right) - \dot{q}_{mj}(t)\right)$$
$$+ \alpha E_1\left(\dot{q}_{m1}\left(t - T_f^{m1-mj}(t)\right) - \dot{q}_{mj}(t)\right) - (1-E_1)b_1\lambda_1\alpha\dot{q}_{mj}(t)$$
$$- \frac{E_1\lambda_2\alpha}{b_2}\dot{q}_{mj}(t)$$
$$+ \frac{(1-E_1)b_2\beta}{\lambda_2}\left(q_{mj}(t)\right.$$
$$\left. - q_{mj}\left(t - T_f^{mj-s}(t) - T_b^{mj-s}\left(t - T_f^{mj-s}(t)\right)\right)\right)$$
$$- \frac{E_1\beta}{b_1\lambda_1}\left(q_{mj}(t)\right.$$
$$\left. - q_{mj}\left(t - T_b^{m1-mj}(t) - T_f^{m1-mj}\left(t - T_b^{m1-mj}(t)\right)\right)\right)$$
$$- (1-E_1)\Gamma_{mj-s}(t) - E_1\Gamma_{mj-m1}(t) - U_{mj}(t) - Y_{mj}(t) \qquad (5.117)$$

$$\bar{\tau}_s(t) = \hat{G}_s(Z_s) + \hat{V}_{mj-s}(t) - \alpha\dot{q}_s(t) - \beta q_s(t) - Y_s(t)$$
$$= \hat{G}_s(Z_s) + \sum_{j=1}^{N} F_j\beta\left(q_{mj}\left(t - T_f^{mj-s}(t)\right) - q_s(t)\right)$$
$$+ \sum_{j=1}^{N} F_j\alpha\left(\dot{q}_{mj}\left(t - T_f^{mj-s}(t)\right) - \dot{q}_s(t)\right) - \frac{\lambda_2\alpha}{b_2}\dot{q}_s(t)$$
$$- \sum_{j=1}^{N}\frac{F_j\beta}{b_1\lambda_1}\left(q_s(t) - q_s\left(t - T_b^{mj-s}(t) - T_f^{mj-s}\left(t - T_b^{mj-s}(t)\right)\right)\right)$$
$$- \sum_{j=1}^{N}\Gamma_{s-mj}(t) - U_s(t) - Y_s(t) \qquad (5.118)$$

where $Y_{mj}(t)$ and $Y_s(t)$ are the designed adaptive control laws as:

$$Y_{ij}(t) = \begin{cases} \dfrac{\dot{q}_{ij}(t)}{\left\|\dot{q}_{ij}(t)\right\|}\widehat{\Theta}_{ij}(t), \ \ if\left\|\dot{q}_{ij}(t)\right\| \neq 0 \\ 0, \ \ if\left\|\dot{q}_{ij}(t)\right\| = 0 \end{cases} \tag{5.119}$$

$$\dot{\widehat{\Theta}}_{ij}(t) = \frac{\left\|\dot{q}_{ij}(t)\right\|^2}{\left\|\dot{q}_{ij}(t)\right\|}, \left\|\dot{q}_{ij}(t)\right\| \neq 0 \tag{5.120}$$

where $\widehat{\Theta}_{ij}$(t) are applied to estimate the upper bounds Θ_{ij} the sum of FLs approximate error and the bounded external disturbance F_{ij}^{*}. That is, $\Theta_{ij} \geq \left\|\bar{\epsilon}_{ij}(Z_{ij}) + F_{ij}^{*}\right\|$.

5.4.2 Stability analysis

Theorem 1. Consider the multi-user teleoperation system (5.83)-(5.84) with the passive human and environment torques modeled as (5.121)-(5.122) which contain position, velocity and acceleration information.

$$\tau_{hj}(t) = -K_{hj}q_{mj}(t) - B_{hj}\dot{q}_{mj}(t) - M_{hj}\ddot{q}_{mj}(t) \tag{5.121}$$

$$\tau_{e}(t) = K_{e}q_{s}(t) + B_{e}\dot{q}_{s}(t) + M_{e}\ddot{q}_{s}(t) \tag{5.122}$$

where $K_{hj,e}$, $B_{hj,e}$, $M_{hj,e}$ are positive constants corresponding to mass, damping and stiffness of human operator and external environment. If the control laws are constructed by (5.116)-(5.118), and FLs adaptive laws are

$$\dot{\hat{\theta}}_{ij} = \Lambda_{ij}\varsigma_{ij}(Z_{ij})\dot{q}_{ij} \tag{5.123}$$

where Λ_{ij} are the positive definite matrices. The position and velocity tracking errors will asymmetrically converge to zero in the presence of arbitrary time delays.

Proof. Consider a positive semi-definite function $V(t)$ for the system as:

$$\mathrm{V(t)} = V_1(t) + V_2(t) + V_3(t) + V_4(t) + V_5(t)$$

where

$$V_1(t) = \frac{1}{2}\left(E_1^2 + \sum_{j=2}^{N} E_j(1-E_1)\right)\dot{q}_s^T(t)M_s(q_s)r_s(t)$$
$$+\frac{1}{2}\sum_{j=1}^{N} E_j r_{mj}^T(t)M_{mj}(q_{mj})r_{mj}(t) + \frac{1}{2}\sum_{j=1}^{N} E_j tr\left(\tilde{\theta}_{mj}^T \Lambda_{mj}^{-1}\tilde{\theta}_{mj}\right)$$
$$+\frac{1}{2}\left(E_1^2 + \sum_{j=2}^{N} E_j(1-E_1)\right)tr\left(\tilde{\theta}_s^T \Lambda_s^{-1}\tilde{\theta}_s\right) \quad (5.124)$$

$$V_2(t) = \frac{\beta E_1^2}{2}\left(q_{m1}(t) - q_s(t)\right)^T\left(q_{m1}(t) - q_s(t)\right)$$
$$+\sum_{j=2}^{N}\frac{\beta E_j(1-E_1)}{2}\left(q_{mj}(t) - q_s(t)\right)^T\left(q_{mj}(t) - q_s(t)\right)$$
$$+\sum_{j=2}^{N}\frac{\beta E_1 E_j}{2}\left(q_{m1}(t) - q_{mj}(t)\right)^T\left(q_{m1}(t) - q_{mj}(t)\right)$$
$$+\sum_{j=1}^{N}\frac{1}{2}E_j\left(\Theta_{mj} - \hat{\Theta}_{mj}(t)\right)^2$$
$$+\frac{1}{2}\left(E_1^2 + \sum_{j=2}^{N} E_j(1-E_1)\right)\left(\Theta_s - \hat{\Theta}_s(t)\right)^2$$
$$+\sum_{j=1}^{N}\frac{1}{2}E_j h_{mj}^T(t)h_{mj}(t)$$
$$+\frac{1}{2}\left(E_1^2 + \sum_{j=2}^{N} E_j(1-E_1)\right)h_s^T(t)h_s(t) \quad (5.125)$$

$$
\begin{aligned}
&V_3(t)\\
&=\frac{\beta E_1^2}{2}\int_{-T_f^{m1-s}(t)}^{0}\int_{t+\gamma}^{t}\dot{q}_{m1}^T(\eta)\dot{q}_{m1}(\eta)d\eta d\gamma+\frac{\beta E_1^2}{2}\int_{-T_b^{m1-s}(t)}^{0}\int_{t+\gamma}^{t}\dot{q}_s^T(\eta)\dot{q}_s(\eta)d\eta d\gamma\\
&+\sum_{j=2}^{N}\left\{\frac{\beta E_j(1-E_1)}{2}\int_{-T_f^{mj-s}(t)}^{0}\int_{t+\gamma}^{t}\dot{q}_{mj}^T(\eta)\dot{q}_{mj}(\eta)d\eta d\gamma\right.\\
&\left.+\frac{\beta E_j(1-E_1)}{2}\int_{-T_b^{mj-s}(t)}^{0}\int_{t+\gamma}^{t}\dot{q}_s^T(\eta)\dot{q}_s(\eta)d\eta d\gamma\right\}\\
&+\sum_{j=2}^{N}\left\{\frac{\beta E_1E_j}{2}\int_{-T_f^{m1-mj}(t)}^{0}\int_{t+\gamma}^{t}\dot{q}_{m1}^T(\eta)\dot{q}_{m1}(\eta)d\eta d\gamma\right.\\
&\left.+\frac{\beta E_1E_j}{2}\int_{-T_b^{m1-mj}(t)}^{0}\int_{t+\gamma}^{t}\dot{q}_{mj}^T(\eta)\dot{q}_{mj}(\eta)d\eta d\gamma\right\}\\
&+\frac{b_2\beta E_1^2}{2\lambda_2}\int_{-T_f^{m1-s}(t)-T_b^{m1-s}\left(t-T_f^{m1-s}(t)\right)}^{0}\int_{t+\gamma}^{t}\dot{q}_{m1}^T(\eta)\dot{q}_{m1}(\eta)d\eta d\gamma\\
&+\sum_{j=2}^{N}\frac{b_2\beta E_1E_j}{2\lambda_2}\int_{-T_f^{m1-mj}(t)-T_b^{m1-mj}\left(t-T_f^{m1-mj}(t)\right)}^{0}\int_{t+\gamma}^{t}\dot{q}_{m1}^T(\eta)\dot{q}_{m1}(\eta)d\eta d\gamma\\
&+\sum_{j=2}^{N}\frac{b_2\beta(1-E_1)E_j}{2\lambda_2}\int_{-T_f^{mj-s}(t)-T_b^{mj-s}\left(t-T_f^{mj-s}(t)\right)}^{0}\int_{t+\gamma}^{t}\dot{q}_{mj}^T(\eta)\dot{q}_{mj}(\eta)d\eta d\gamma\\
&+\sum_{j=2}^{N}\frac{\beta E_1E_j}{2b_1\lambda_1}\int_{-T_b^{m1-mj}(t)-T_f^{m1-mj}\left(t-T_b^{m1-mj}(t)\right)}^{0}\int_{t+\gamma}^{t}\dot{q}_{mj}^T(\eta)\dot{q}_{mj}(\eta)d\eta d\gamma\\
&+\frac{\beta E_1^2}{2b_1\lambda_1}\int_{-T_b^{mj-s}(t)-T_f^{mj-s}\left(t-T_b^{mj-s}(t)\right)}^{0}\int_{t+\gamma}^{t}\dot{q}_s^T(\eta)\dot{q}_s(\eta)d\eta d\gamma\\
&+\sum_{j=2}^{N}\frac{\beta E_j(1-E_1)}{2b_1\lambda_1}\int_{-T_b^{mj-s}(t)-T_f^{mj-s}\left(t-T_b^{mj-s}(t)\right)}^{0}\int_{t+\gamma}^{t}\dot{q}_s^T(\eta)\dot{q}_s(\eta)d\eta d\gamma \quad (5.126)
\end{aligned}
$$

$$
\begin{aligned}
&V_4(t)\\
&=\frac{\alpha E_1^2}{2}\frac{1}{1-\dot{T}_f^{m1-s}(t)}\int_{t-T_f^{m1-s}(t)}^{t}\dot{q}_{m1}^T(\eta)\dot{q}_{m1}(\eta)d\eta\\
&+\frac{\alpha E_1^2}{2}\frac{1}{1-\dot{T}_b^{m1-s}(t)}\int_{t-T_b^{m1-s}(t)}^{t}\dot{q}_s^T(\eta)\dot{q}_s(\eta)d\eta\\
&+\sum_{j=2}^{N}\left\{\frac{\alpha E_1 E_j}{2}\frac{1}{1-\dot{T}_f^{m1-mj}(t)}\int_{t-T_f^{m1-mj}(t)}^{t}\dot{q}_{m1}^T(\eta)\dot{q}_{m1}(\eta)d\eta\right.\\
&\left.+\frac{\alpha E_1 E_j}{2}\frac{1}{1-\dot{T}_b^{m1-mj}(t)}\int_{t-T_b^{m1-mj}(t)}^{t}\dot{q}_{mj}^T(\eta)\dot{q}_{mj}(\eta)d\eta\right\}\\
&+\sum_{j=2}^{N}\left\{\frac{\alpha E_j(1-E_1)}{2}\frac{1}{1-\dot{T}_f^{mj-s}(t)}\int_{t-T_f^{mj-s}(t)}^{t}\dot{q}_{mj}^T(\eta)\dot{q}_{mj}(\eta)d\eta\right.\\
&\left.+\frac{\alpha E_j(1-E_1)}{2}\frac{1}{1-\dot{T}_b^{mj-s}(t)}\int_{t-T_b^{mj-s}(t)}^{t}\dot{q}_s^T(\eta)\dot{q}_s(\eta)d\eta\right\} \qquad (5.127)
\end{aligned}
$$

$$
\begin{aligned}
V_5(t)=\sum_{j=1}^{N}q_{mj}^T(t)\frac{K_{hj}}{2}q_{mj}(t)+q_s^T(t)\frac{K_e}{2}q_s(t)+\sum_{j=1}^{N}\dot{q}_{mj}^T(t)\frac{M_{hj}}{2}\dot{q}_{mj}(t)\\
+\dot{q}_s^T(t)\frac{M_e}{2}\dot{q}_s(t) \qquad (5.128)
\end{aligned}
$$

Using the control laws, the modeled human and environmental torques, the FLs adaptive laws defined in this section, and considering the following inequalities,

$$
-2q_m^T(t)\int_{t-T_2(t)}^{t}\dot{q}_s(\eta)d\eta-\int_{t-T_2(t)}^{t}\dot{q}_s^T(\eta)\dot{q}_s(\eta)d\eta\le T_2^{max}q_m^T(t)q_m(t)
$$

$$
-2q_s^T(t)\int_{t-T_1(t)}^{t}\dot{q}_m(\eta)d\eta-\int_{t-T_1(t)}^{t}\dot{q}_m^T(\eta)\dot{q}_m(\eta)d\eta\le T_1^{max}q_s^T(t)q_s(t)
$$

the time derivative of $V(t)$ can be written as:

$$
\dot{\mathrm{V}}(\mathrm{t})\le-\dot{q}_{m1}^T(t)\left(E_1^2b_1\lambda_1\alpha-\frac{\beta E_1^2}{2}\left(\bar{T}_f^{m1-s}+\bar{T}_b^{m1-s}+\bar{\varepsilon}_f^{m1-s}+\bar{\varepsilon}_b^{m1-s}\right)I\right)\dot{q}_{m1}(t)-
$$

$$
\sum_{j=2}^{N}\dot{q}_{m1}^T(t)\left(E_1E_jb_1\lambda_1\alpha-\frac{\beta E_1E_j}{2}\left(\bar{T}_f^{m1-mj}+\bar{T}_b^{m1-mj}+\bar{\varepsilon}_f^{m1-mj}+\right.\right.
$$

$$\bar{\varepsilon}_b^{m1-mj})I\Big)\dot{q}_{m1}(t) - \sum_{j=2}^{N}\dot{q}_{mj}^T(t)\Bigg((1-E_1)E_j b_1\lambda_1\alpha - \frac{\beta(1-E_1)E_j}{2}\big(\bar{T}_f^{mj-s} + \bar{T}_b^{mj-s} +$$

$$\bar{\varepsilon}_f^{mj-s} + \bar{\varepsilon}_b^{mj-s}\big)I\Bigg)\dot{q}_{mj}(t) - \sum_{j=2}^{N}\dot{q}_{mj}^T(t)\Big(\frac{\lambda_2\alpha E_1E_j}{b_2} - \frac{\beta E_1E_j}{2}\big(\bar{T}_f^{m1-mj} + \bar{T}_b^{m1-mj} +$$

$$\bar{\varepsilon}_f^{m1-mj} + \bar{\varepsilon}_b^{m1-mj}\big)I\Big)\dot{q}_{mj}(t) - \dot{q}_s^T(t)\Big(\frac{\lambda_2\alpha E_1^2}{b_2} - \frac{\beta E_1^2}{2}\big(\bar{T}_f^{m1-s} + \bar{T}_b^{m1-s} + \bar{\varepsilon}_f^{m1-s} +$$

$$\bar{\varepsilon}_b^{m1-s}\big)I\Big)\dot{q}_s(t) - \sum_{j=2}^{N}\dot{q}_s^T(t)\Big(\frac{\lambda_2\alpha(1-E_1)E_j}{b_2} - \frac{\beta(1-E_1)E_j}{2}\big(\bar{T}_f^{mj-s} + \bar{T}_b^{mj-s} + \bar{\varepsilon}_f^{mj-s} +$$

$$\bar{\varepsilon}_b^{mj-s}\big)I\Big)\dot{q}_s(t) - \frac{\alpha E_1^2}{2}\Big(\dot{q}_{m1}(t) - \dot{q}_s\Big(t - T_b^{m1-s}(t)\Big)\Big)^T\Big(\dot{q}_{m1}(t) - \dot{q}_s\Big(t -$$

$$T_b^{m1-s}(t)\Big)\Big) - \frac{\alpha E_1^2}{2}\Big(\dot{q}_s(t) - \dot{q}_{m1}\Big(t - T_f^{m1-s}(t)\Big)\Big)^T\Big(\dot{q}_s(t) - \dot{q}_{m1}\Big(t -$$

$$T_f^{m1-s}(t)\Big)\Big) - \sum_{j=2}^{N}\frac{\alpha E_1E_j}{2}\Big(\dot{q}_{m1}(t) - \dot{q}_{mj}\Big(t - T_b^{m1-mj}(t)\Big)\Big)^T\Big(\dot{q}_{m1}(t) - \dot{q}_{mj}\Big(t -$$

$$T_b^{m1-mj}(t)\Big)\Big) - \sum_{j=2}^{N}\frac{\alpha E_1E_j}{2}\Big(\dot{q}_{mj}(t) - \dot{q}_{m1}\Big(t - T_f^{m1-mj}(t)\Big)\Big)^T\Big(\dot{q}_{mj}(t) - \dot{q}_{m1}\Big(t -$$

$$T_f^{m1-mj}(t)\Big)\Big) - \sum_{j=2}^{N}\frac{\alpha(1-E_1)E_j}{2}\Big(\dot{q}_{mj}(t) - \dot{q}_s\Big(t - T_b^{mj-s}(t)\Big)\Big)^T\Big(\dot{q}_{mj}(t) - \dot{q}_s\Big(t -$$

$$T_b^{mj-s}(t)\Big)\Big) - \sum_{j=2}^{N}\frac{\alpha(1-E_1)E_j}{2}\Big(\dot{q}_s(t) - \dot{q}_{mj}\Big(t - T_f^{mj-s}(t)\Big)\Big)^T\Big(\dot{q}_s(t) - \dot{q}_{mj}\Big(t -$$

$$T_f^{mj-s}(t)\Big)\Big) + \frac{E_1^2\dot{T}_f^{m1-s}(t)\alpha}{2-2\dot{T}_f^{m1-s}(t)}\dot{q}_{m1}^T(t)\dot{q}_{m1}(t) + \sum_{j=2}^{N}\frac{E_1E_j\dot{T}_f^{m1-mj}(t)\alpha}{2-2\dot{T}_f^{m1-mj}(t)}\dot{q}_{m1}^T(t)\dot{q}_{m1}(t) +$$

$$\sum_{j=2}^{N}\frac{(1-E_1)E_j\dot{T}_f^{m1-s}(t)\alpha}{2-2\dot{T}_f^{m1-s}(t)}\dot{q}_{mj}^T(t)\dot{q}_{mj}(t) + \sum_{j=2}^{N}\frac{E_1E_j\dot{T}_b^{m1-mj}(t)\alpha}{2-2\dot{T}_b^{m1-mj}(t)}\dot{q}_{mj}^T(t)\dot{q}_{mj}(t) +$$

$$\frac{E_1^2\dot{T}_b^{m1-s}(t)\alpha}{2-2\dot{T}_b^{m1-s}(t)}\dot{q}_s^T(t)\dot{q}_s(t) + \sum_{j=2}^{N}\frac{(1-E_1)E_j\dot{T}_b^{mj-s}(t)\alpha}{2-2\dot{T}_b^{mj-s}(t)}\dot{q}_s^T(t)\dot{q}_s(t) - E_1^2\dot{q}_{m1}^T(t)\Gamma_{m1-s}(t) -$$

$$\sum_{j=2}^{N}E_1E_j\dot{q}_{m1}^T(t)\Gamma_{m1-mj}(t) - \sum_{j=2}^{N}(1-E_1)E_j\dot{q}_{mj}^T(t)\Gamma_{mj-s}(t) -$$

$$\sum_{j=2}^{N}E_1E_j\dot{q}_{mj}^T(t)\Gamma_{mj-m1}(t) - E_1^2\dot{q}_s^T(t)\Gamma_{s-m1}(t) - \sum_{j=2}^{N}(1-E_1)E_j\dot{q}_s^T(t)\Gamma_{s-mj}(t) -$$

$$\sum_{j=1}^{N}\dot{q}_{mj}^T(t)\Big(B_{hj} - \frac{b_2\beta}{2\lambda_2}\Big)\dot{q}_{mj}(t) - \dot{q}_s^T(t)\Big(B_e - \frac{\beta}{2b_1\lambda_1}\Big)\dot{q}_s(t) - \sum_{j=1}^{N}E_j\Bigg(\frac{\|\Delta\tau_{mj}(t)\|^2}{2c_{mj}} -$$

$$\dot{q}_{mj}^T(t)\Delta\tau_{mj}(t) + \frac{c_{mj}\dot{q}_{mj}^T(t)\dot{q}_{mj}(t)}{2}\Bigg) - \sum_{j=1}^{N}E_j\Bigg(\frac{c_{mj}h_{mj}^T(t)h_{mj}(t)}{2} + c_{mj}\dot{q}_{mj}^T(t)h_{mj}(t) +$$

$$\frac{c_{mj}\dot{q}_{mj}^T(t)\dot{q}_{mj}(t)}{2}\Bigg) - \Big(E_1^2 + \sum_{j=2}^{N}E_j(1-E_1)\Big)\Big(\frac{\|\Delta\tau_s(t)\|^2}{2c_s} - \dot{q}_s^T(t)\Delta\tau_s(t) + \frac{c_s\dot{q}_s^T(t)\dot{q}_s(t)}{2}\Big) -$$

$$\Big(E_1^2 + \sum_{j=2}^{N}E_j(1-E_1)\Big)\Big(\frac{c_sh_s^T(t)h_s(t)}{2} + c_s\dot{q}_s^T(t)h_s(t) + \frac{c_s\dot{q}_s^T(t)\dot{q}_s(t)}{2}\Big) +$$

$$\sum_{j=1}^{N} E_j \dot{q}_{mj}^T(t)\left(\bar{\epsilon}_{mj}(Z_{mj}) + F_{mj}^* - \frac{\dot{q}_{mj}(t)}{\|\dot{q}_{mj}(t)\|}\hat{\Theta}_{mj}(t)\right) + \left(E_1^2 + \sum_{j=2}^{N} E_j(1 - E_1)\right)\dot{q}_s^T(t)\left(\bar{\epsilon}_s(Z_s) + F_s^* - \frac{\dot{q}_s(t)}{\|\dot{q}_s(t)\|}\hat{\Theta}_s(t)\right) + \sum_{j=1}^{N} E_j\left(\hat{\Theta}_{mj}(t) - \Theta_{mj}\right)\frac{\|\dot{q}_{mj}(t)\|^2}{\|\dot{q}_{mj}(t)\|} + \left(E_1^2 + \sum_{j=2}^{N} E_j(1 - E_1)\right)\left(\hat{\Theta}_s(t) - \Theta_s\right)\frac{\|\dot{q}_s(t)\|^2}{\|\dot{q}_s(t)\|} \quad (5.129)$$

Substituting the upper bounds Θ_i of $\|\bar{\epsilon}_s(Z_s) + F_i^*\|$ into (5.129), the final four terms are zero. The Lyapunov approach requires $\dot{V}(t)$ to be negative semi-definite. In the presence of constant time delays, $\dot{T}_{f,b}^{mj-s}(t)$, $\dot{T}_{f,b}^{m1-mj}(t)$, $\bar{\varepsilon}_{f,b}^{mj-s}$, $\bar{\varepsilon}_{f,b}^{m1-mj}$ are zero. Also, the passivity controllers do not take effect so that $\Gamma_{mj-s}(t)$, $\Gamma_{m1-mj}(t)$, $\Gamma_{mj-m1}(t)$, $\Gamma_{s-mj}(t)$ are zero, $\dot{V}(t)$ can be guaranteed to be negative semi-definite by properly tuning $b_{1,2}$, $\lambda_{1,2}$, α and β to make sure

$$b_1\lambda_1\alpha \geq \frac{\beta}{2}\left(\bar{T}_f^{mj-s} + \bar{T}_b^{mj-s}\right) \quad (5.130)$$

$$b_1\lambda_1\alpha \geq \frac{\beta}{2}\left(\bar{T}_f^{m1-mj} + \bar{T}_b^{m1-mj}\right) \quad (5.131)$$

$$\frac{\lambda_2\alpha}{b_2} \geq \frac{\beta}{2}\left(\bar{T}_f^{m1-mj} + \bar{T}_b^{m1-mj}\right) \quad (5.132)$$

$$\frac{\lambda_2\alpha}{b_2} \geq \frac{\beta}{2}\left(\bar{T}_f^{mj-s} + \bar{T}_b^{mj-s}\right) \quad (5.133)$$

$$B_{hj} \geq \frac{b_2\beta}{2\lambda_2} \quad (5.134)$$

$$B_{ej} \geq \frac{\beta}{2b_1\lambda_1} \quad (5.135)$$

When the time delay is varying and the channels passivity is not guaranteed by the wave variable transformation, the PCs are launched by the POs, the positive biased terms caused by the time varying delays in (5.129) are directly compensated by the PCs. No extra parameters need to be tune when the time delays vary and $\dot{V}(t)$ is still negative semi-definite.

Integrating both sides of (5.129), we get:

$$+\infty > V(0) \geq V(0) - V(t)$$

$$\geq \int_0^t \left(\frac{\alpha E_1^2}{2} \left(\dot{q}_{m1}(t) - \dot{q}_s\left(t - T_b^{m1-s}(t)\right) \right)^T \left(\dot{q}_{m1}(t) \right.\right.$$

$$\left. - \dot{q}_s\left(t - T_b^{m1-s}(t)\right) \right)$$

$$+ \frac{\alpha E_1^2}{2} \left(\dot{q}_s(t) - \dot{q}_{m1}\left(t - T_f^{m1-s}(t)\right) \right)^T \left(\dot{q}_s(t) \right.$$

$$\left. - \dot{q}_{m1}\left(t - T_f^{m1-s}(t)\right) \right)$$

$$+ \sum_{j=2}^{N} \frac{\alpha E_1 E_j}{2} \left(\dot{q}_{m1}(t) - \dot{q}_{mj}\left(t - T_b^{m1-mj}(t)\right) \right)^T \left(\dot{q}_{m1}(t) \right.$$

$$\left. - \dot{q}_{mj}\left(t - T_b^{m1-mj}(t)\right) \right)$$

$$+ \sum_{j=2}^{N} \frac{\alpha E_1 E_j}{2} \left(\dot{q}_{mj}(t) - \dot{q}_{m1}\left(t - T_f^{m1-mj}(t)\right) \right)^T \left(\dot{q}_{mj}(t) \right.$$

$$\left. - \dot{q}_{m1}\left(t - T_f^{m1-mj}(t)\right) \right)$$

$$+ \sum_{j=2}^{N} \frac{\alpha (1 - E_1) E_j}{2} \left(\dot{q}_{mj}(t) - \dot{q}_s\left(t - T_b^{mj-s}(t)\right) \right)^T \left(\dot{q}_{mj}(t) \right.$$

$$\left. - \dot{q}_s\left(t - T_b^{mj-s}(t)\right) \right)$$

$$+ \sum_{j=2}^{N} \frac{\alpha (1 - E_1) E_j}{2} \left(\dot{q}_s(t) - \dot{q}_{mj}\left(t - T_f^{mj-s}(t)\right) \right)^T \left(\dot{q}_s(t) \right.$$

$$\left. - \dot{q}_{mj}\left(t - T_f^{mj-s}(t)\right) \right) + \sum_{j=1}^{N} \dot{q}_{mj}^T(t) \left(B_{hj} - \frac{b_2 \beta}{2\lambda_2} \right) \dot{q}_{mj}(t)$$

$$\left. + \dot{q}_s^T(t) \left(B_e - \frac{\beta}{2 b_1 \lambda_1} \right) \dot{q}_s(t) \right) dt \qquad (5.136)$$

Therefore, from $V(t) \geq 0$ and $\dot{\mathrm{V}}(t) \leq 0$, it is true that $\tilde{\theta}_{ij} \in L_\infty$, $\dot{q}_{ij}(t) \in L_2$. $\dot{q}_{mj}(t) - \dot{q}_s\left(t - T_b^{mj-s}(t)\right)$, $\dot{q}_s(t) - \dot{q}_{mj}\left(t - T_f^{mj-s}(t)\right)$, $\dot{q}_{mj}(t) - \dot{q}_{m1}\left(t - T_f^{m1-mj}(t)\right)$, $\dot{q}_{m1}(t) - \dot{q}_{mj}\left(t - T_b^{m1-mj}(t)\right) \in L_2$. Using the fact that $q_m(t) - q_s\left(t - T_2(t)\right) = q_m(t) - q_s(t) + \int_{t-T_2(t)}^{t} \dot{q}_s(t)dt$, $q_s(t) - q_m\left(t - T_1(t)\right) =$

$q_s(t) - q_m(t) + \int_{t-T_1(t)}^{t} \dot{q}_1(t)dt$ and using Cauchy-Schwarz inequality $\int_{t-T_2(t)}^{t} \dot{q}_s(t)dt \le \sqrt{T_2(t)}\dot{q}_s(t)$ and $\int_{t-T_1(t)}^{t} \dot{q}_m(t)dt \le \sqrt{T_1(t)}\dot{q}_m(t)$, we can get $q_{mj}(t) - q_s\left(t - T_b^{mj-s}(t)\right)$, $q_s(t) - q_{mj}\left(t - T_f^{mj-s}(t)\right)$, $q_{mj}(t) - q_{m1}\left(t - T_f^{m1-mj}(t)\right)$, $q_{m1}(t) - \dot{q}_{mj}\left(t - T_b^{m1-mj}(t)\right) \in L_\infty$.

This system's dynamic model can also be written as:

$$\ddot{q}_{ij} = M_{ij}^{-1}(q_{ij})\left[\tau_{ij} \pm \tau_{hj,e} + F_{ij}^{*} - G_{ij}'(Z_{ij}) - C_{ij}(q_{ij}, \dot{q}_{ij})\dot{q}_{ij}\right] \quad (5.137)$$

Differentiating both sides of (5.137):

$$\frac{d}{dt}\ddot{q}_{ij} = \frac{d}{dt}\left(M_{ij}^{-1}(q_{ij})\right)\left[\tau_{ij} \pm \tau_{hj,e} + F_{ij}^{*} - G_{ij}'(Z_{ij}) - C_{ij}(q_{ij}, \dot{q}_{ij})\dot{q}_{ij}\right] + M_i^{-1}(q_i)\frac{d}{dt}\left[\tau_{ij} \pm \tau_{hj,e} + F_{ij}^{*} - G_{ij}'(Z_{ij}) - C_{ij}(q_{ij}, \dot{q}_{ij})\dot{q}_{ij}\right] \quad (5.138)$$

For the first term of the right side of (5.138), we have $\frac{d}{dt}\left(M_{ij}^{-1}\right) = -M_{ij}^{-1}\dot{M}_{ij}M_{ij}^{-1} = -M_{ij}^{-1}\left(C_{ij} + C_{ij}^{T}\right)M_{ij}^{-1}$. According to Properties 1 and 3, $\frac{d}{dt}\left(M_{ij}^{-1}\right)$ is bounded. Based on Property 4, the terms in bracket of (5.138) are also bounded. Therefore, $\frac{d}{dt}\ddot{q}_{ij}(t) \in L_\infty$ and $\ddot{q}_{ij}(t)$ are uniformly continuous ($\int_0^t \ddot{q}_{ij}(\eta)d\eta = \dot{q}_{ij}(t) - \dot{q}_{ij}(0)$). Since $\dot{q}_{ij}(t) \to 0$, it can be concluded that $\ddot{q}_{ij}(t) \to 0$ based on Barbălat's Lemma.

5.4.3 Experimental results

In this section, a series of experiments are carried out to validate the proposed multilateral teleoperation systems. The teleoperation platform consists of four Phantom haptic devices as shown in Figure 5.12 The four devices are connected by two computers that are connected via the Internet. The network environment can be set in the network-simulation block. The Matlab software is applied to establish the proposed control system.

Figure 5.12 Experimental setup for the multi-user system

The first experiment test the training mode of the proposed multi-user teleoperation system, where Master 1 operated by the mentor fully controls the other three robots to conduct a free motion. The dominance factor E_1 is 1, E_2 and E_3 are 0, $F_1 = \frac{E_1^2}{E_1^2+\sum_{j=2}^{N} E_j(1-E_1)} = 1$, $F_2 = F_3 = 0$. In this experiment, the time delays between every two robots are set to be 400 ms with 10 ms slight variations. The position tracking (q_{m1}, q_{m2}, q_{m3}, q_s) and the torque tracking (τ_{m1}, τ_{m2}, τ_{m3}, τ_e) of the three joints of each robot are shown in Fig.5.13. τ_{mj} is the control input of the j-th master which represents the torque felt by the operator. After the 2 seconds, Master 1 starts to freely move, and the other robot closely tracks its motion. During free motion, the environmental torque is zero so that torque felt by the users are also close to zero.

Then, we did the same experiment without the FL controllers. The position tracking (q_{m1}, q_{m2}, q_{m3}, q_s) and the torque tracking (τ_{m1}, τ_{m2}, τ_{m3}, τ_e) of the three joints of each robot are shown in Fig.5.14 Due to the non-ignorable system uncertainty and model errors, the system is damped and the position tracking has larger tracking errors than that in Fig.4, especially in joints 2 and 3 where the gravity model errors take adverse effects. The un-eliminated system uncertainties also affect torque tracking so that the operators can still feel large feedback forces during free motion.

The following experiment tested the guidance mode of the proposed multi-user teleoperation system. In this mode, Master 1 leads the other two robots to collaboratively control the slave robot. In this experiment, the time delays between every two every two robots are enhanced to 500 ms with 200 ms variations. The

dominance factor E_1 is 0.5, E_2 and E_3 are set to be 0.25, $F_1 = \frac{E_1^2}{E_1^2+\sum_{j=2}^{N} E_j(1-E_1)} = 0.5$, $F_2 = F_3 = 0.25$. The position tracking (q_{m1}, q_{m2}, q_{m3}, q_s) and the torque tracking (τ_{m1}, τ_{m2}, τ_{m3}, τ_e) of the three joints of each robot are shown in Fig.6. After 2 seconds, the users start to drive the three robots to conduct free motion, and after 5 seconds, the slave robot comes in contact with the remote solid wall for four seconds. Then, all master robots are driven back to the original position. In this experiment, the position of the slave robot is controlled by the mixed signal of the three master robot's position. Due to the presence of time-varying delays, the PCs are launched by the POs to guarantee the system stability by dampening the robots. Therefore, the position tracking errors appear during free motion. The users can also feel feedback forces during free motion because of the damping effects of the PCs. During hard contact, accurate force tracking is derived as shown in Fig.5.15. The trainees felts the mixed force of Master 1 and the slave robot.

The final experiment tests the evaluation mode of the proposed multi-user teleoperation system, and the time-varying delays are further increased to 800 ms with 500 ms variation between every two robot. The dominance factor E_1 is 0, E_2 and E_3 are set to be 0.5, $F_1 = 0$, $F_2 = F_3 = 0.5$. In this experiment, Master 1 is fully controlled by the mixed signals from the other two master robots. The position tracking (q_{m1}, q_{m2}, q_{m3}, q_s) and the torque tracking (τ_{m1}, τ_{m2}, τ_{m3}, τ_e) of the three joints of each robot are shown in Fig.5.16. After 2 seconds, Master 2 and 3 control Master and the slave robot to conduct a free motion first and during the 7th second to the 12th second, the slave robot comes in contact with a solid wall. After 12 seconds, all of the robots move back to the origin. Due to the time-varying delays, large position tracking errors are shown in Fig.7, and the users also feels large feedback forces during free motion. The torque tracking during hard contact is still reasonable in Fig.5.16. When all of the robots go back to the original locations and stop moving, all of the tracking errors disappear.

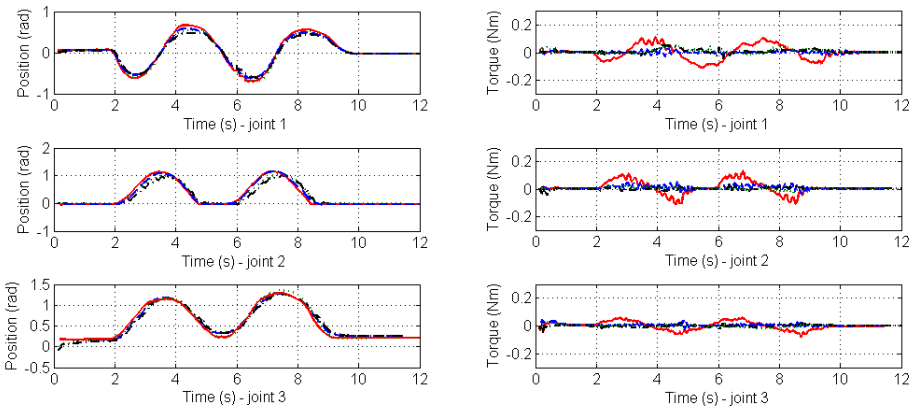

Figure 5.13. Position and torque tracking in training mode (red – Master 1, blue – Master 2, green – Master 3, Black – Slave)

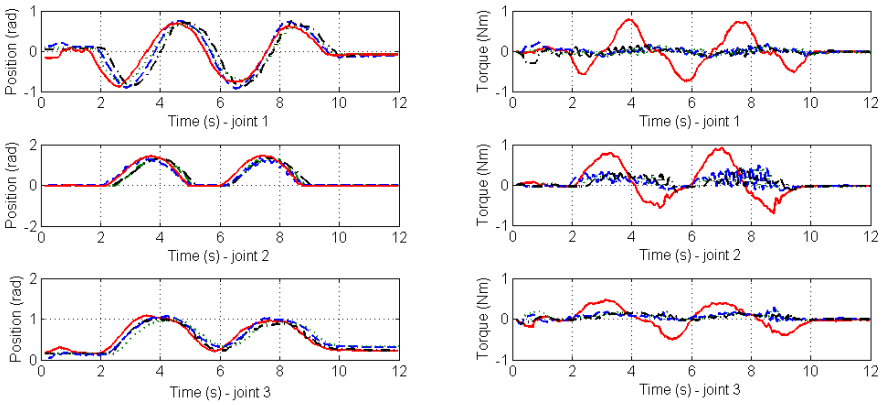

Figure 5.14. Position and torque tracking in training mode without FLs (red – Master 1, blue – Master 2, green – Master 3, Black – Slave)

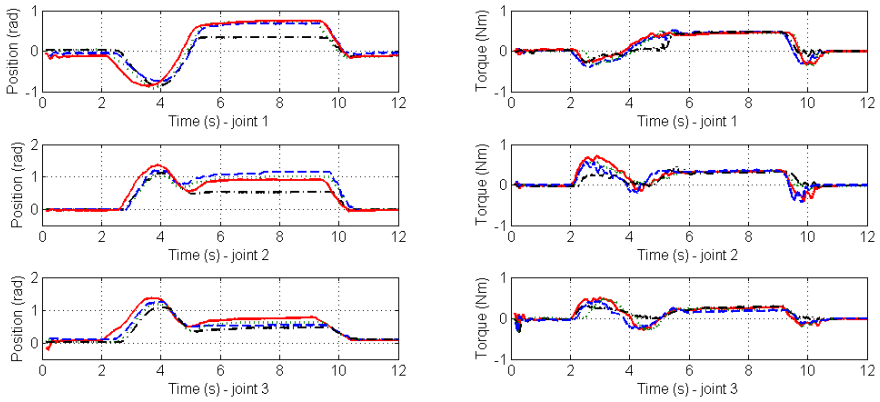

Figure 5.15. Position and torque tracking in guidance mode (red – Master 1, blue – Master 2, green – Master 3, Black – Slave)

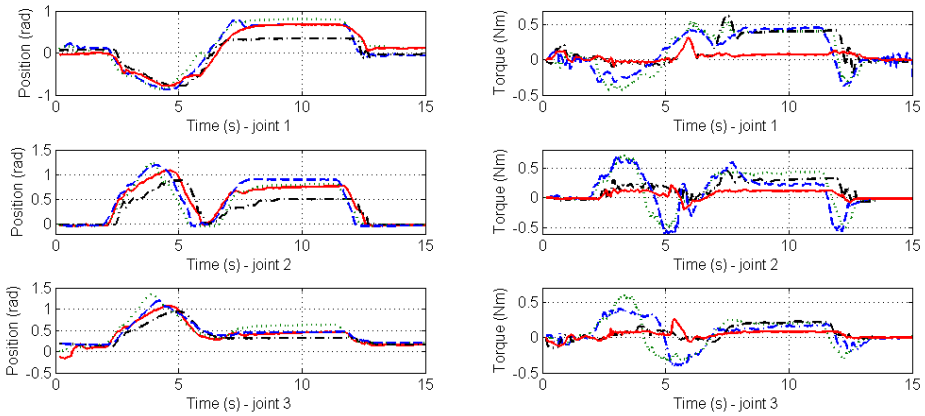

Figure 5.16. Position and torque tracking in evaluation mode (red – Master 1, blue – Master 2, green – Master 3, Black – Slave)

5.5 Summary

In chapter, the proposed passivity-based approach was applied to multilateral teleoperation systems. The reduced wave reflections architecture was applied to a SMMS system to achieve accurate position synchronization and reasonable force tracking. The wave-based TDPA was extended to guarantee the channel passivity of the multilateral teleoperation systems in the presence of random time delays. A DMDS system was proposed with variable dominance factors to enhance the system flexibility.

A multi-user teleoperation system was proposed to allow one mentor to simultaneously train multiple trainees in different locations to collaboratively control a slave robot. Lyapunov functions were used to analyse the stability of the multilateral teleoperation systems. The developed algorithms were validated by applying them to a multilateral teleoperation platform consisting of multiple haptic devices.

6 CONCLUSIONS AND FUTURE WORK

6.1 Overview

In the study reported in this thesis, a number of innovative passivity-based control architectures for bilateral and multilateral teleoperation systems were developed. The primary aim pursued was to simultaneously achieve high transparency and system stability in the presence of arbitrary time delays. The stability and transparency of the proposed method were analysed using passivity algorithms and Lyapunov functions. The performance of the developed methods were validated using 1-DOF and 3-DOF experimental platforms under different conditions. The major achievements of the work are reviewed in this Chapter.

6.2 Reduced Wave Reflections Architecture Design

In Chapter 3, the properties of different wave-based systems reported in literature were analysed and compared. Most of the wave-based systems developed previously had two main drawbacks, wave reflections and position drift. Wave reflections caused by imperfectly matched junction impedance can may send transfer useless information back to the communication channels to and introduce signal cause disturbance and vibration in the systems. Position drift happens when no position information is transmitted in the wave-based systems. Hence, an innovative wave variable transformation architecture was for the 4-CH linear teleoperation system was developed to solve wave reflections and position drift. In the proposed wave variable transformation, the outgoing wave variables do not contain any unnecessary information from the incoming wave variables to the extent that the signal variations caused by wave reflections can be effectively eliminated. By adding the hybrid signals transmission containing position and velocity information, the position drift issues can also be solved. The passivity analysis has been introduced to prove that the proposed wave variable transformation architecture can robustly guarantee channel passivity under arbitrary constant time delays. Compared with the wave transformation schemes

in literature, the proposed wave transformation architecture does is not adversely affected by the biased terms and can have higher time-delay-based transparency. Unlike the previous wave-based systems, the proposed system can also accurately transmit high frequency information. Most of the wave-based architectures reported in literature do not work effectively under to deal with time-varying delay issues.

In this chapter, the proposed wave variable transformation architecture was further extended to nonlinear teleoperation systems in the presence of time-varying delays. A sliding mode algorithm was also applied to compensate for the dynamic uncertainties in order to enhance transparency and guarantee the synchronization in finite time. The optimal balance between system stability and transparency was achieved by the proposed bilateral teleoperation system applying the deploying innovative wave variable transformation in the presence of time-varying delay.

6.3 Wave-based Time Delay Passivity Approach Design

The main drawback of the passivity-based approaches proposed in the literature is low transparency due to over-pursuing passivity under time delays, particularly in the wave variable method. Those methods over-dissipate energy to guarantee the passivity of the teleoperation system by considering the worst-case scenario. TDPA is a new method with a superior performance compared the wave variable method in balancing the trade-off between passivity and transparency in the presence of random time delays. Although, the TDPA-based systems could guarantee system stability, largely reduced transparency is their main drawback that cannot be ignored. Even under small constant or no time delay where ideal transparency could be easily achieved by many non-passivity based schemes, TDPA-based systems have large errors in tracking position and force.

In Chapter 4, a novel wave-based TDPA with new passivity observers and passivity controllers was applied to the 4-CH nonlinear bilateral teleoperation system. The proposed system had three main contributions.

Firstly, under constant time delays, the approach could maintain the passivity of the communication channels and ensure that the energy dissipation detected by the proposed observer was positive so that the proposed passivity controllers had no

influence on the torque and trajectory tracking. The new wave transformation also had no biased terms by matching impedances so that the proposed system could achieve higher transparency than the previous TDPA-based systems and wave-based systems proposed in the literature.

Secondly, in the presence of arbitrary time-varying delays, the proposed passivity observers could observe negative energy dissipation according to different time delays and robustly guarantee the system passivity. The new wave-based TDPA could adaptively dissipate energy to the extent that the proposed system was not as over-conservative as the conventional wave-based systems.

Thirdly, the consistent problems of the wave-based system, i.e. wave-based reflections and position drift were simultaneously solved in the proposed system.

Therefore, the proposed wave-based TDPA teleoperation system proved to have a better performance than previous wave-based systems and TDPA systems in achieving transparency and stability in the presence of arbitrary time-varying delays.

Moreover, since the original wave-based TDPA was mainly used to guarantee the channel passivity and knowing that without proper control algorithm, extra energy still could be injected into the master and slave side to jeopardize stability, the original wave based TDPA was extended to guarantee the overall system's passivity. This method was also combined with an extended PPC to enhance the position, velocity and torque tracking performances and to restrict the tracking errors in a pre-set boundary.

The proposed wave-based TPDA principally had two main drawbacks as it could seriously degrade the position and torque tracking during worst-case scenarios with large and sharply varying delays. Also, restriction on the rate of the time delays significantly undermined the practicability of the proposed system. Therefore, a new wave-based TDPA system was proposed with distinct passivity observers and controllers to largely enhance the system's tracking performance in the worst-case where the rate of time delays were larger than one. Neural networks were also deployed to eliminate the system's uncertainty.

6.4 Control Algorithm Design for Multilateral Teleoperation Systems

In Chapter 5, the concept introduced the multilateral teleoperation systems was studied and a number of control algorithms for different configurations were developed.

Deploying the reduced wave reflections architecture, a SMMS teleoperation system with characteristics of motion synchronization and force reflections under time delays was developed. With the reduced wave reflections architecture, the slave robots could accurately follow the master robot's motion without large vibrations. Control force signals were exchanged among all of the robots that could enforce the motion synchronization. In the proposed system, in the event of sudden change in the motion of one of the slave robots, the rest could be directly controlled using reflecting control force information guaranteeing accurate motion synchronization.

A DMDS system was proposed with variable dominance factors to enhance the flexibility of shared-control trainings. The variable dominance factors provided the system with two main characteristics. That is, 1) the system provided the ability for a second operator to correct the motion of the slave robots when necessary. 2) The three mode of training guidance and evaluation could be freely interchanged dynamically without the need to turn any parameter on or off.

A multi-user teleoperation system deploying the modified wave-based TDPA was introduced in Chapter 5. The main purpose of the development was to allow one mentor to lead multiple trainees in different remote locations to perform the remote tasks in the presence of different time delays. The proposed system contained three modes depending on the different values of the dominance factors, the training mode, the guidance mode and the evaluation mode. In the training mode, the mentor's master robot fully controlled the slave robot as well as other master robots. The trainees could only feel the dynamics of the mentor so that they could be trained by the motion of the mentor's master robot. In the guidance mode, all of the users cooperated to collaboratively perform the remote task. The mentor received the mixed dynamics of the slave robot and the other master robots while the trainees received the mixed dynamics of the slave and the mentor. In the evaluation mode, the mentor's robot was fully controlled by the mixed control information of other master robots so that the mentor could evaluate the performance of other users according to the received mixed

dynamics of other master robots. Fuzzy logic algorithm was also used to deal with the system uncertainties. An adaptive controller was designed in this system to address the problem of input saturation.

6.5 Future Work

The work presented in this thesis can be continued in the following directions:

i) The proposed algorithms in this thesis are applied to the 4-CH teleoperation system where force information is transmitted in the communication channel. The force signals containing acceleration information and noise can seriously affect the system stability. Therefore, methods to strengthen the external force transmission can be further explored and a less conservative stability condition can also be considered.

ii) In a telerobotic system the loss of data loss is a major drawback of the communication channel that can seriously affect the system performance. Unfortunately, there is no control method developed to effectively address this issue. In the work conducted in this thesis, the loss of data in the communication channels is ignored. As another extension of the current work, the development of an effective method to analyze and control the data loss in the communication channel can be considered..

iii) In Chapter 5, multi-user teleoperation systems was designed and implemented with enhanced user interaction featuring dominance factors that could adjust the control of the mentor over the trainee in execution of a task. The dominance factor is set manually based on the identified skills of the trainees. An online scheme that quantify the skill of the trainee and adjust the dominance factor automatically over the training period can improve the performance of a telerobotic system. It was suggested in Chapter 5 that variable dominance factors can enhance the flexibility of the system. Designing a variable dominance factors that can simultaneously guarantee flexibility and accuracy can be another important extension of this research.

iv) Balancing the optimal trade-off between transparency and stability is always the top priority in the passivity-based teleoperation research. However, it is difficult to further enhance the system transparency without sacrificing stability in the passivity-based teleoperation research. Future work can be considered to combine the passivity-based approaches with other methods to improve system transparency in the presence of arbitrary time delays.

REFERENCES

[1] G. Hirzinger, B. Brunner, J. Dietrich, and J. Heindl. (1993) Sensor-based space robotics-ROTEX and its telerobotic features. *IEEE Transactions on Robotics and Automation*, 9(5):649 – 663.

[2] W. S. Otaguro, L. O. Kesler, and D. D. (1988) Beebe. Telerobotics (supervised autonomy) for space applications. *IEEE Aerospace and Electronic Systems Magazine*, 3(11):11 – 15.

[3] Sheridan, T. B. (1993). Space teleoperation through time delay: review and prognosis. *Robotics and Automation, IEEE Transactions on*, *9*(5), 592-606.

[4] T. Shyu. Teleoperation at mount isa mines. (1997). In *Proceedings of Integrated Tech-nology in Mining Conference*, pages 757 – 762.

[5] L. Cragg and H. Huosheng. (2003) Application of mobile agents to robust teleoperation of internet robots in nuclear decommissioning. In *Proceedings of IEEE International Conference on Industrial Technology*, volume 2, pages 1214 – 1219.

[6] B. Espiau. An integrated experiment in advanced nuclear teleoperation. (1986) In *Proceedings of IEEE International Conference on Robotics and Automation*, volume 3, pages 996 – 996.

[7] B. Barnes, A. S. Menon, R. Mills, C. D. Bruyns, A. Twombly, J. Smith, K. Montgomery, and R. Boyle. (2003) Virtual reality extensions into surgical training and teleoperation. In *Proceedings of International IEEE/EMBS Special Topic Conference on Information Technology Applications in Biomedicine*, pages 142-145.

[8] A. Gupta and M.K. O’ Malley. (2006) Design of a haptic arm exoskeleton for training and rehabilitation. *IEEE/ASME Transactions on Mechatronics*, 11(3):280 – 289.

[9] W. S. Harwin, T. Rahman, and R. A. Foulds. (1995) A review of design issues in rehabilitation robotics with reference to north american research. *IEEE Transactions on Rehabilitation Engineering*, 3(1):3 – 13.

[10] Y Rybarczyk, E Colle, and P Hoppenot. (2002) Contribution of neuroscience to the teleoperation of rehabilitation robot. In *Proceedings of IEEE International Conference on Systems, Man and Cybernetics*, volume 4, pages 243 – 249.

[11] A. Casavola and M. Sorbara. (2005) Towards constrained teleoperation for safe longdistance robotic surgical operations. In Proceedings of IEEE International Conference on Robotics and Automation, pages 685 – 690.

[12] I. Font, S. Weiland, M. Franken, M. Steinbuch, and L. Rovers. Haptic feedback designs in teleoperation systems for minimal invasive surgery. (2004) In *Proceedings of International Conference on Systems, Man and Cybernetics*, volume 3, pages 2513 – 2518.

[13] O. Khatib. (2002). Human-centered robotics and haptic interaction: from assistance to surgery, the emerging applications. In *Proceedings of International Workshop on Robot Motion and Control*, pages 137 – 139.

[14] A. E. Quaid and R. A. Abovitz. (2002) Haptic information displays for computer assisted surgery. In *Proceedings of IEEE International Conference on Robotics and Automation*, volume 2, pages 2092 – 2097.

[15] Guthart, G., & Salisbury Jr, J. K. (2000, April). The IntuitiveTM Telesurgery System: Overview and Application. In *ICRA* (pp. 618-621).

[16] Deng, Q. W., Wei, Q., & Li, Z. X. (2007). Analysis of absolute stability for time-delay teleoperation systems. *International Journal of Automation and Computing*, *4*(2), 203-207.

[17] Oboe, R., & Fiorini, P. (1998). A design and control environment for internet-based telerobotics. *The International Journal of Robotics Research*, *17*(4), 433-449.

[18] Anderson, R. O. B. E. R. T. J., & Spong, M. W. (1989). Bilateral control of teleoperators with time delay. *Automatic Control, IEEE Transactions on*,*34*(5), 494-501.

[19] Shahdi, A., & Sirouspour, S. (2009). Adaptive/robust control for time-delay teleoperation. *Robotics, IEEE Transactions on*, *25*(1), 196-205.

[20] Zhang, B., Kruszewski, A., & Richard, J. (2012, July). H∞ control of delayed teleoperation systems under polytopic-type uncertainties. In *Control & Automation (MED), 2012 20th Mediterranean Conference on* (pp. 954-959). IEEE.

[21] Franken, M., Stramigioli, S., Misra, S., Secchi, C., & Macchelli, A. (2011). Bilateral telemanipulation with time delays: A two-layer approach combining passivity and transparency. *Robotics, IEEE Transactions on*, *27*(4), 741-756.

[22] Lee D, Spong M W. Passive bilateral teleoperation with constant time delay[J]. Robotics, IEEE Transactions on, 2006, 22(2): 269-281.

[23] Nuño, E., Basañez, L., Ortega, R., & Spong, M. W. (2009). Position tracking for non-linear teleoperators with variable time delay. *The International Journal of Robotics Research*, *28*(7), 895-910.

[24] Nuño, E., Basañez, L., & Ortega, R. (2011). Passivity-based control for bilateral teleoperation: A tutorial. *Automatica*, *47*(3), 485-495.

[25] Chopra, Nikhil, Mark W. Spong, and Rogelio Lozano. "Synchronization of bilateral teleoperators with time delay." *Automatica* 44.8 (2008): 2142-2148.

[26] Yang, Yana, Changchun Hua, and Xinping Guan. "Coordination control for bilateral teleoperation with kinematics and dynamics uncertainties." *Robotics and Computer-Integrated Manufacturing* 30.2 (2014): 180-188.

[27] Monfaredi, R., Razi, K., Ghydari, S. S., & Rezaei, S. M. (2006, October). Achieving high transparency in bilateral teleoperation using stiffness observer for passivity control. In *Intelligent Robots and Systems, 2006 IEEE/RSJ International Conference on* (pp. 1686-1691). IEEE.

[28] Chen, Y., Xi, N., & Li, H. (2012, December). Passive scattering transform bilateral teleoperation for an Internet-based mobile robot. In *Robotics and Biomimetics (ROBIO), 2012 IEEE International Conference on* (pp. 643-648). IEEE.

[29] Niemeyer, G., & Slotine, J. J. E. (2004). Telemanipulation with time delays. *The International Journal of Robotics Research*, *23*(9), 873-890.

[30] D. Lee and M. W. Spong. (2005) Bilateral teleoperation of multiple cooperative robots over delayed communication networks: theory. In *Proceedings of IEEE International Conference on Robotics and Automation*, pages 360 – 365.

[31] D. Lee and M. W. Spong. (2006) Semi-autonomous teleoperation of multiple cooperative robots for human-robot lunar exploration. In *Proceedings of AAAI Spring Symposium*.

[32] O. M. Palafox and M. W. Spong. (2009) Bilateral teleoperation of a formation of nonholonomic mobile robots under constant time delay. In *Proceedings ofIEEE/RSJ international conference on Intelligent robots and systems*, pages 2821 – 2826. IEEE Press.

[33] G. H. P. T. S. Noriaki and A. H. Hashimoto. (2007) Development of a single-master multi-slave tele-micromanipulation system. *Advanced Robotics,* 21(3-4):329 – 349.

[34] G. Hwang, D. Aarno, and H. Hashimoto. (2006) Haptic guidant bilateral teleoperation for single-master multi-slave system. In *Proceedings of Eurohaptics*, page 401-406.

[35] C. Gunn, M. Hutchins, D. Stevenson, M. Adcock, and P. Youngblood. (2005). Using collaborative haptics in remote surgical training. In *Proceedings of Joint Eurohaptics Conference and Symposium on Haptic Interfaces for Virtual Environment and Teleoperator Systems*, pages 481 – 482.

[36] S. S. Nudehi, R. Mukherjee, and M. Ghodoussi. (2005). A shared-control approach to haptic interface design for minimally invasive telesurgical training. *IEEE Transactions on Control Systems Technology*, 13:588 – 592.

[37] M. Tavakoli, RV Patel, and M. Moallem. (2008). *Haptics for teleoperated surgical robotic systems*. World Scientific Pub Co Inc.

[38] C. R. Carignan and P. A. Olsson. (2004). Cooperative control of virtual objects over the Internet using force-reflecting master arms. In *Proceedings of IEEE International Conference on Robotics and Automation*, volume 2, pages 1221 – 1226.

[39] A. P. Olsson, C. R. Carignan, and J. Tang. (2004) Cooperative control of virtual objects using haptic teleoperation over the Internet. In *Proceedings of*

Internationa Conference Series On Disability, Virtual Reality And Associated Technologies, pages 149 – 156.

[40] W. Lo, Y. Liu, I. Elhajj, N. Xi, Y. Wang, and T. Fukuda. (2004). Cooperative teleoperation of a multirobot system with force reflection via Internet. IEEE/ASME Trans. Mechatronics, vol. 9, no. 4, pp. 661–670.

[41] Sirouspour S. Modeling and control of cooperative teleoperation system. IEEE Transactions on Robotics 2005;21:1220–5.

[42] Sirouspour S, Setoodeh P. Multi-operator/multi-robot teleoperation: an adaptive nonlinear control approach. Proceedings of IEEE/RSJ International Conference on Intelligent Robots and Systems 2005:1576–81.

[43] Khademian, B., & Hashtrudi-Zaad, K. (2012). Dual-user teleoperation systems: New multilateral shared control architecture and kinesthetic performance measures. *Mechatronics, IEEE/ASME Transactions on*, *17*(5), 895-906.

[44] Ghorbanian, A., Rezaei, S. M., Khoogar, A. R., Zareinejad, M., & Baghestan, K. (2013). A novel control framework for nonlinear time-delayed Dual-master/Single-slave teleoperation. *ISA transactions*, *52*(2), 268-277.

[45] Li, Z., Ding, L., Gao, H., Duan, G., & Su, C. Y. (2013). Trilateral teleoperation of adaptive Fuzzy Force/Motion Control for nonlinear teleoperators with communication random delays. *Fuzzy Systems, IEEE Transactions on*, *21*(4), 610-624.

[46] Razi, K., & Hashtrudi-Zaad, K. (2014). Development of a Guaranteed Stable Network of Telerobots with Kinesthetic Consensus. *Haptics, IEEE Transactions on*, 7(4), pp.454-466.

[47] Ryu, J. H., Artigas, J., & Preusche, C. (2010). A passive bilateral control scheme for a teleoperator with time-varying communication delay.*Mechatronics*, *20*(7), 812-823.

[48] Van Valkenburg M. E. (1965). Network Analysis, Englewood Cliffs, NJ, USA: Prentice-Hall.

[49] Hannaford, B. (1989). A design framework for teleoperators with kinesthetic feedback. *Robotics and Automation, IEEE Transactions on*, *5*(4), 426-434.

[50] Lawrence, D. A. (1993). Stability and transparency in bilateral teleoperation.*Robotics and Automation, IEEE Transactions on*, *9*(5), 624-637.

[51] Ryu, J. H., Kwon, D. S., & Hannaford, B. (2004). Stable teleoperation with time-domain passivity control. *Robotics and Automation, IEEE Transactions on*, *20*(2), 365-373.

[52] Niemeyer, G., & Slotine, J. J. (1991). Stable adaptive teleoperation. *Oceanic Engineering, IEEE Journal of*, *16*(1), 152-162.

[53] Kamrani, E., Ramazani, A., & Monteiro, F. (2006, December). Teleoperation via Internet with Time-Varying Delay. In *Electronics, Circuits and Systems, 2006. ICECS'06. 13th IEEE International Conference on* (pp. 736-739). IEEE.

[54] Iiyama, N., Natori, K., & Ohnishi, K. (2009). Bilateral teleoperation under time‐varying communication time delay considering contact with environment.*Electronics and Communications in Japan*, *92*(7), 38-46.

[55] Hirche, S., & Buss, M. (2012). Human-oriented control for haptic teleoperation. *Proceedings of the IEEE*, *100*(3), 623-647.

[56] Willems, J. C. (2007). Dissipative dynamical systems. *European Journal of Control*, *13*(2), 134-151.

[57] Willems, J. C. (1972). Dissipative dynamical systems part I: General theory.*Archive for rational mechanics and analysis*, *45*(5), 321-351.

[58] Willems, J. C. (1972). Dissipative dynamical systems Part II: Linear systems with quadratic supply rates. *Archive for Rational Mechanics and Analysis*,*45*(5), 352-393.

[59] Hill, D., & Moylan, P. (1976). The stability of nonlinear dissipative systems.*Automatic Control, IEEE Transactions on*, *21*(5), 708-711.

[60] Hill, D. J., & Moylan, P. J. (1980). Dissipative dynamical systems: basic input-output and state properties. *Journal of the Franklin Institute*, *309*(5), 327-357.

[61] Vittorias, I., & Hirche, S. (2010, June). Stable teleoperation with communication unreliabilities and approximate human/environment dynamics knowledge. In *American Control Conference (ACC), 2010* (pp. 2791-2796). IEEE.

[62] Khalil, H. K., & Grizzle, J. W. (2002). *Nonlinear systems* (Vol. 3). Upper Saddle River: Prentice hall.

[63] Tzafestas, C., Velanas, S., & Fakiridis, G. (2008, May). Adaptive impedance control in haptic teleoperation to improve transparency under time-delay. In*Robotics and Automation, 2008. ICRA 2008. IEEE International Conference on* (pp. 212-219). IEEE.

[64] Kim, J., Chang, P. H., & Park, H. S. (2013). Two-Channel Transparency-Optimized Control Architectures in Bilateral Teleoperation With Time Delay.*Control Systems Technology, IEEE Transactions on*, *21*(1), 40-51.

[65] Hashtrudi-Zaad, K., & Salcudean, S. E. (2002). Transparency in time-delayed systems and the effect of local force feedback for transparent teleoperation.*Robotics and Automation, IEEE Transactions on*, *18*(1), 108-114.

[66] Hokayem, P. F., & Spong, M. W. (2006). Bilateral teleoperation: An historical survey. *Automatica*, *42*(12), 2035-2057.

[67] Passenberg, C., Peer, A., & Buss, M. (2010). A survey of environment-, operator-, and task-adapted controllers for teleoperation systems.*Mechatronics*, *20*(7), 787-801.

[68] Niemeyer, G., & Slotine, J. J. (1991, June). Transient shaping in force-reflecting teleoperation. In *Advanced Robotics, 1991.'Robots in Unstructured Environments', 91 ICAR., Fifth International Conference on* (pp. 261-266). IEEE.

[69] Niemeyer, G., & Slotine, J. J. (1997, April). Designing force reflecting teleoperators with large time delays to appear as virtual tools. In *Robotics and Automation, 1997. Proceedings., 1997 IEEE International Conference on*(Vol. 3, pp. 2212-2218). IEEE.

[70] Huang, J-C., Wu, C-I., Chang, Y-H., Lin, H-W., Wu, C-T. & Lee, S-T. (2010). Design and Implementation of Wave Variable Based Teleoperation Systems. *2010 International Coriference on System Science and Engineering*. pp.304-309.

[71] Tian, D., Yashiro, D., & Ohnishi, K. (2011, June). Frequency-domain analysis of wave variable based teleoperation and its equivalent implementation. In*Access Spaces (ISAS), 2011 1st International Symposium on* (pp. 41-46). IEEE.

[72] Hu, L., Liu, X. P., Liu, G., & Xu, S. (2011). Trajectory tracking compensation for teleoperation with transmission delays. *Robotica*, *29*(6), 863-871.

[73] Hu, L. Y., Liu, X. P., & Liu, G. P. (2010, June). The wave-variable teleoperator with improved trajectory tracking. In *Control and Automation (ICCA), 2010 8th IEEE International Conference on* (pp. 322-327). IEEE.

[74] Ye, Y., & Liu, P. X. (2010). Improving trajectory tracking in wave-variable-based teleoperation. *Mechatronics, IEEE/ASME Transactions on*, *15*(2), 321-326.

[75] Niemeyer, G., & Slotine, J. J. (1998, May). Towards force-reflecting teleoperation over the internet. In *Robotics and Automation, 1998. Proceedings. 1998 IEEE International Conference on* (Vol. 3, pp. 1909-1915). IEEE.

[76] Boukhnifer, M., & Ferreira, A. (2006). Wave-based passive control for transparent micro-teleoperation system. *Robotics and Autonomous Systems*, *54*(7), 601-615.

[77] Lozano, R., Chopra, N., & Spong, M. W. (2002, June). Passivation of force reflecting bilateral teleoperators with time varying delay. In *Proceedings of the 8. Mechatronics Forum* (pp. 954-962).

[78] Ganjefar, S., Najibi, S., & Momeni, H. (2011). A novel structure for the optimal control of bilateral teleoperation systems with variable time delay.*Journal of the Franklin Institute*, *348*(7), 1537-1555.

[79] Satler, M., Avizzano, C. A., Frisoli, A., Tripicchio, P., & Bergamasco, M. (2009, October). Bilateral teleoperation under time-varying delay using wave variables. In *Intelligent Robots and Systems, 2009. IROS 2009. IEEE/RSJ International Conference on* (pp. 4596-4602). IEEE.

[80] Satler, M., Avizzano, C. A., Frisoli, A., Tripicchio, P., & Bergamasco, M. (2010, September). Energy recovery in time-varying delay teleoperated system using wave-variables. In *RO-MAN, 2010 IEEE* (pp. 1-8). IEEE.

[81] Rodriguez-Seda, E. J., Lee, D., & Spong, M. W. (2009). Experimental comparison study of control architectures for bilateral teleoperators.*Robotics, IEEE Transactions on*, *25*(6), 1304-1318.

[82] Berestesky, P., Chopra, N., & Spong, M. W. (2004, April). Discrete time passivity in bilateral teleoperation over the internet. In *Robotics and Automation, 2004. Proceedings. ICRA'04. 2004 IEEE International Conference on* (Vol. 5, pp. 4557-4564). IEEE.

[83] Secchi, C., Stramigioli, S., & Fantuzzi, C. (2005, August). The problem of packets loss in scaled digital port-hamiltonian based bilateral telemanipulation. In *Proceedings of IEEE Conference on Control Applications, Toronto, Canada*.

[84] Tanner, N. A., & Niemeyer, G. (2005). Improving perception in time-delayed telerobotics. *The International Journal of Robotics Research*, *24*(8), 631-644.

[85] Chopra, N., Spong, M. W., Ortega, R., & Barabanov, N. E. (2006). On tracking performance in bilateral teleoperation. *Robotics, IEEE Transactions on*, *22*(4), 861-866.

[86] Fallahi, B., & Taghirad, H. D. (2011). Analytical Passivity Analysis for Wave-based Teleoperation with Improved Trajectory Tracking. *CCToMM Symposim*.

[87] MoafiMadani, S. M., Sabouri, B., Fallahi, B., & Taghirad, H. D. (2011, December). Implementation of wave-based teleoperation system by improved trajectory tracking method. In *Control, Instrumentation and Automation (ICCIA), 2011 2nd International Conference on* (pp. 999-1005). IEEE.

[88] Niemeyer, G., & Slotine, J. J. (1997, April). Using wave variables for system analysis and robot control. In *Robotics and Automation, 1997. Proceedings., 1997 IEEE International Conference on* (Vol. 2, pp. 1619-1625). IEEE.

[89] Yokokohji, Y., Imaida, T., & Yoshikawa, T. (1999). Bilateral teleoperation under time-varying communication delay. In *Intelligent Robots and Systems, 1999. IROS'99. Proceedings. 1999 IEEE/RSJ International Conference on*(Vol. 3, pp. 1854-1859). IEEE.

[90] Yokokohji, Y., Imaida, T., & Yoshikawa, T. (2000). Bilateral control with energy balance monitoring under time-varying communication delay. In*Robotics and Automation, 2000. Proceedings. ICRA'00. IEEE International Conference on* (Vol. 3, pp. 2684-2689). IEEE.

[91] Yokokohji, Y., Tsujioka, T., & Yoshikawa, T. (2002). Bilateral control with time-varying delay including communication blackout. In *Haptic Interfaces for Virtual Environment and Teleoperator Systems, 2002. HAPTICS 2002. Proceedings. 10th Symposium on* (pp. 285-292). IEEE.

[92] Zhang, T., & Li, Y. (2006, January). A control scheme for bilateral teleoperation systems based on time-varying communication delay identification. In *Systems*

and Control in Aerospace and Astronautics, 2006. ISSCAA 2006. 1st International Symposium on (pp. 6-pp). IEEE.

[93] Munir, S., & Book, W. J. (2001). Wave-based teleoperation with prediction. In*American Control Conference, 2001. Proceedings of the 2001* (Vol. 6, pp. 4605-4611). IEEE.

[94] Munir, S., & Book, W. J. (2002). Internet-based teleoperation using wave variables with prediction. *Mechatronics, IEEE/ASME Transactions on*, *7*(2), 124-133.

[95] Arioui, H., Kheddar, A., & Mammar, S. (2002). A predictive wave-based approach for time delayed virtual environments haptics systems. In *Robot and Human Interactive Communication, 2002. Proceedings. 11th IEEE International Workshop on* (pp. 134-139). IEEE.

[96] Smith, O. J. (1957). Closer control of loops with dead time. *Chemical Engineering Progress*, *53*(5), 217-219.

[97] Arcara, P., & Melchiorri, C. (2002). Control schemes for teleoperation with time delay: A comparative study. *Robotics and Autonomous Systems*, *38*(1), 49-64.

[98] Ching, H., & Book, W. J. (2006). Internet-based bilateral teleoperation based on wave variable with adaptive predictor and direct drift control. *Journal of Dynamic Systems, Measurement, and Control*, *128*(1), 86-93.

[99] Kuchenbecker, K. J., Fiene, J., & Niemeyer, G. (2005, March). Event-based haptics and acceleration matching: Portraying and assessing the realism of contact. In *Eurohaptics Conference, 2005 and Symposium on Haptic Interfaces for Virtual Environment and Teleoperator Systems, 2005. World Haptics 2005. First Joint* (pp. 381-387). IEEE.

[100] Kuchenbecker, K. J., & Niemeyer, G. (2006, May). Improving telerobotic touch via high-frequency acceleration matching. In *Robotics and Automation, 2006. ICRA 2006. Proceedings 2006 IEEE International Conference on* (pp. 3893-3898). IEEE.

[101] Oboe, R., & Fiorini, P. (1998). A design and control environment for internet-based telerobotics. *The International Journal of Robotics Research*, *17*(4), 433-449.

[102] Chopra, N., Spong, M. W., Hirche, S., & Buss, M. (2003). Bilateral Teleoperation over the Internet: the Time Varying Delay Problem1. *Urbana*,*101*, 61801.

[103] Eusebi, L., & Melchiorri, C. (1998). Force reflecting telemanipulators with time-delay: Stability analysis and control design. *Robotics and Automation, IEEE Transactions on*, *14*(4), 635-640.

[104] Yasrebi, N., & Constantinescu, D. (2011, May). Passive wave variable control of haptic interaction with an unknown virtual environment. In *Robotics and Automation (ICRA), 2011 IEEE International Conference on* (pp. 919-924). IEEE.

[105] Tanner, N. A., & Niemeyer, G. (2004, December). Practical limitations of wave variable controllers in teleoperation. In *Robotics, Automation and Mechatronics, 2004 IEEE Conference on* (Vol. 1, pp. 25-30). IEEE.

[106] Kontarinis, D. A., & Howe, R. D. (1995). Tactile display of vibratory information in teleoperation and virtual environments. *Presence: Teleoperators and Virtual Environments*, *4*(4), 387-402.

[107] Tanner, N. A., & Niemeyer, G. (2006). High-frequency acceleration feedback in wave variable telerobotics. *Mechatronics, IEEE/ASME Transactions on*,*11*(2), 119-127.

[108] Aziminejad, A., Tavakoli, M., Patel, R. V., & Moallem, M. (2008). Transparent time-delayed bilateral teleoperation using wave variables. *Control Systems Technology, IEEE Transactions on*, *16*(3), 548-555.

[109] Yokokohji, Y., & Yoshikawa, T. (1994). Bilateral control of master-slave manipulators for ideal kinesthetic coupling-formulation and experiment.*Robotics and Automation, IEEE Transactions on*, *10*(5), 605-620.

[110] Boroujeni, Z., Mohammadi, M., & Jalali, A. (2013, February). Stable adaptive time-variable delayed bilateral teleoperation for a surgery robot. In *Robotics and Mechatronics (ICRoM), 2013 First RSI/ISM International Conference on*(pp. 301-306). IEEE.

[111] Yalcin, B., & Ohnishi, K. (2009, November). Transparency issues of acceleration waves. In *Industrial Electronics, 2009. IECON'09. 35th Annual Conference of IEEE* (pp. 3174-3180). IEEE.

[112] Yalcin, B., & Ohnishi, K. (2010). Stable and transparent time-delayed teleoperation by direct acceleration waves. *Industrial Electronics, IEEE Transactions on*, *57*(9), 3228-3238.

[113] Katsura, S., Irie, K., & Ohishi, K. (2008). Wideband force control by position-acceleration integrated disturbance observer. *Industrial Electronics, IEEE Transactions on*, *55*(4), 1699-1706.

[114] Ohnishi, K., Shibata, M., & Murakami, T. (1996). Motion control for advanced mechatronics. *Mechatronics, IEEE/ASME Transactions on*, *1*(1), 56-67.

[115] Katsura, S., Matsumoto, Y., & Ohnishi, K. (2006). Analysis and experimental validation of force bandwidth for force control. *Industrial Electronics, IEEE Transactions on*, *53*(3), 922-928.

[116] Lew, J. Y., Repperger, D., & Berlin, J. (2004, March). Wave variables based teleoperation with time delay: application to space based laser maintenance. In *Aerospace Conference, 2004. Proceedings. 2004 IEEE* (Vol. 5, pp. 2912-2919). IEEE.

[117] Ye, Y., & Liu, P. X. (2009). Improving haptic feedback fidelity in wave-variable-based teleoperation orientated to telemedical applications. *Instrumentation and Measurement, IEEE Transactions on*, *58*(8), 2847-2855..

[118] Miyoshi, T., Terasima, K., & Buss, M. (2006, October). A design method of wave filter for stabilizing non-passive operating system. In *Computer Aided Control System Design, 2006 IEEE International Conference on Control Applications, 2006 IEEE International Symposium on Intelligent Control, 2006 IEEE* (pp. 1318-1324). IEEE.

[119] Kawashima, K., Tadano, K., Sankaranarayanan, G., & Hannaford, B. (2008, September). Bilateral teleoperation with time delay using modified wave variables. In *Intelligent Robots and Systems, 2008. IROS 2008. IEEE/RSJ International Conference on* (pp. 424-429). IEEE.

[120] Matiakis, T., Hirche, S., & Buss, M. (2006, June). Independent-of-delay stability of nonlinear networked control systems by scattering transformation. In *American Control Conference, 2006* (pp. 6-pp). IEEE.

[121] Matiakis, T., Hirche, S., & Buss, M. (2008). Networked Control Systems with Time-Varying Delay--Stability through Input-Output Transformation.

[122] Hirche, S., Matiakis, T., & Buss, M. (2009). A distributed controller approach for delay-independent stability of networked control systems. *Automatica*,*45*(8), 1828-1836.

[123] Stramigioli, S., van der Schaft, A., Maschke, B., & Melchiorri, C. (2002). Geometric scattering in robotic telemanipulation. *Robotics and Automation, IEEE Transactions on*, *18*(4), 588-596.

[124] Alise, M., Roberts, R. G., Repperger, D. W., Moore, C. A., & Tosunoglu, S. (2009). On extending the wave variable method to multiple-DOF teleoperation systems. *Mechatronics, IEEE/ASME Transactions on*, *14*(1), 55-63.

[125] Yang, F., Li, H., & Wang, Y. (2012, December). Wave-transformation-based control law for teleoperation with large time-varying delays. In *Robotics and Biomimetics (ROBIO), 2012 IEEE International Conference on* (pp. 1610-1614). IEEE.

[126] Hashemzadeh, F., Hassanzadeh, I., Tavakoli, M., & Alizadeh, G. (2012). A new method for bilateral teleoperation passivity under varying time delays.*Mathematical Problems in Engineering*, *2012*.

[127] Hinterseer, P., Hirche, S., Chaudhuri, S., Steinbach, E., & Buss, M. (2008). Perception-based data reduction and transmission of haptic data in telepresence and teleaction systems. *Signal Processing, IEEE Transactions on*, *56*(2), 588-597.

[128] Hirche, S., Hinterseer, P., Steinbach, E., & Buss, M. (2007). Transparent data reduction in networked telepresence and teleaction systems. part i: Communication without time delay. *Presence: Teleoperators and Virtual Environments*, *16*(5), 523-531.

[129] Burdea, G. (1996). *Force and Touch Feedback for Virtual Reality*. Wiley.

[130] Stanney, K. (2002). *Handbook of Virtual Environments*, Lawrence Erlbaum Associates.

[131] Vittorias, I., Kammerl, J., Hirche, S., & Steinbach, E. (2009, March). Perceptual coding of haptic data in time-delayed teleoperation. In*EuroHaptics conference, 2009 and Symposium on Haptic Interfaces for Virtual Environment and Teleoperator Systems. World Haptics 2009. Third Joint* (pp. 208-213). IEEE.

[132] Bate, L., Cook, C. D., & Li, Z. (2011). Reducing wave-based teleoperator reflections for unknown environments. *Industrial Electronics, IEEE Trans, on*, 392-397.

[133] Zheng, M., Chen, Q. H., Xiao, W., & Yang, H. N. (2013). Bilateral teleoperation with reducing wave-based reflections. *Advances in Manufacturing, 1*(3), 288-292.

[134] Chopra, N., & Spong, M. W. (2004, December). Adaptive coordination control of bilateral teleoperators with time delay. In *Decision and Control, 2004. CDC. 43rd IEEE Conference on* (Vol. 5, pp. 4540-4547). IEEE

[135] Xiong, W., Ju, H. H., & Liu, H. Y. (2012). Adaptive Nonlinear Teleoperation with Time Delay Using Modified Wave Variable Based Controller. *Applied Mechanics and Materials*, *110*, 2284-2295.

[136] Tian, D., Zhang, B., Shen, H., & Li, J. (2013). Stability Problem of Wave Variable Based Bilateral Control: Influence of the Force Source Design.*Mathematical Problems in Engineering*, *2013*.

[137] Chan, L., Naghdy, F., & Stirling, D. (2013). Extended active observer for force estimation and disturbance rejection of robotic manipulators. *Robotics and Autonomous Systems*, *61*(12), 1277-1287.

[138] Culmer P, Jackson A, Makower S, Richardson R, Cozens J, Levesley M, et al. A control strategy for upper limb robotic rehabilitation with a dual robot system. IEEE/ASME Transactions of Mechatronics 2010;15:575–85.

[139] Nudehi SS, Mukherjee R, Ghodoussi M. A shared-control approach to haptic interface design for minimally invasive telesurgical training. IEEE Transactions on Control Systems Technology 2005;13:588–92.

[140] Chebbi B, Lazaroff D, Bogsany F, Liu PX, Ni L, Rossi M. Design and implementation of a collaborative virtual haptic surgical training system.

Proceedings of IEEE International Conference on Mechatronics and Automation 2005;1:315–20.

[141] W. Lo, Y. Liu, I. Elhajj, N. Xi, Y. Wang, and T. Fukuda. Cooperative teleoperation of a multirobot system with force reflection via Internet. IEEE/ASME Trans. Mechatronics, vol. 9, no. 4, pp. 661–670, Dec. 2004.

[142] Buzan, F. T., & Sheridan, T. B. (1989, November). A model-based predictive operator aid for telemanipulators with time delay. In *Systems, Man and Cybernetics, 1989. Conference Proceedings., IEEE International Conference on* (pp. 138-143). IEEE.

[143] Raju, G. J., Verghese, G. C., & Sheridan, T. B. (1989, May). Design issues in 2-port network models of bilateral remote manipulation. In *Robotics and Automation, 1989. Proceedings., 1989 IEEE International Conference on* (pp. 1316-1321). IEEE.

[144] Suzuki, A., & Ohnishi, K. (2013). Frequency-Domain Damping Design for Time-Delayed Bilateral Teleoperation System Based on Modal Space Analysis. *Industrial Electronics, IEEE Transactions on*, *60*(1), 177-190.

[145] A. Suzuki and K. Ohnishi. (2013). Novel Four-Channel Bilateral Control Design for Haptic Communication Under Time Delay Based on Modal Space Analysis. *IEEE Tramsactions on control system technology*, VOL. 21, NO. 3.

[146] Iida, W., & Ohnishi, K. (2004, March). Reproducibility and operationality in bilateral teleoperation. In *Advanced Motion Control, 2004. AMC'04. The 8th IEEE International Workshop on* (pp. 217-222). IEEE.

[147] G. Niemeyer. Using wave variables in time delayed force reflecting teleoperation. Ph.D. dissertation, MIT, Cambridge, MA, Sep. 1996.

[148] A. Suzuki and K. Ohnishi. (2010) A constitution method of bilateral teleoperation under time delay based on stability analysis of modal space. in *Proc. IEEE Int. Symp. Ind. Electron.*, pp. 2277–2282.

[149] Zeltom Educational and Industrial Control Systems, viewed 29 November 2013, < http://zeltom.com/products/hilink>

[150] L. Bate and C. Cook. (2001). Exploration of intelligible force feedback for telesurgery over the Internet. in *Proc. Int. Conf. Inf. Technol. Mechatronics*. pp. 124–129.

[151] M. W. Spong, S. Hutchinson and M. Vidyasagar, *Robot Modeling and Control* (Wiley, New York, 2005).

[152] R. Kelly, V. Santibáñez and A. Loria, *Control of Robot Manipulators in Joint Space* (Springer, London,UK, 2005).

[153] Hashemzadeh, Farzad, and Mahdi Tavakoli. (2014). Position and force tracking in nonlinear teleoperation systems under varying delays. *Robotica*: 1-14.

[154] C. Simone and A. Okamura. (2002). Modeling of needle insertion forces for robot-assisted percutaneous therapy. *in Proc. IEEE Conf. Robot. Autom.*, vol. 2, pp.2085-2091.

[155] Y. Ye, Y.-J. Pan, and T. Hilliard. (2013). Bilateral teleoperation with time-varying delay: A communication channel passification approach. *IEEE/ASME Trans. Mechatronics*, vol. 18, no. 4, pp. 1431–1434.

[156] Chawda, V.; OMalley, M.K. (2015). Position Synchronization in Bilateral Teleoperation Under Time-Varying Communication Delays. *Mechatronics, IEEE/ASME Transactions on* , vol.20, no.1, pp.245-253.

[157] Polushin, Ilia G., Amir Takhmar, and Rajni V. Patel. "Projection-Based Force-Reflection Algorithms With Frequency Separation for Bilateral Teleoperation." *Mechatronics, IEEE/ASME Transactions on* 20.1 (2015): 143-154.

[158] L. Yang and J. Y. Yang, “Nonsingular fast terminal sliding-mode control for nonlinear dynamical systems,” *Int. J. Robust Nonlinear Control*, vol. 21, no. 16, pp. 1865–1879, 2011.

[159] R. Kelly, A tuning procedure for stable PID control of robot manipulators, *Robotica*, 13(2): 141-148, 1995.

[160] A. Ilchmann, E. P. Ryan and S. Trenn, Tracking control: performance funnels and prescribed transient behavior, *System control letter*, 54(7): 655-670, 2005.

[161] C. P. Bechlioulis and G. A. Rovithakis, Adaptive control with guaranteed transient and steady state tracking error bounds for strict feedback systems, *Automatica*, 45(2): 532-538, 2009.

[162] X. L. Xie, Z. G. Hou, L. Cheng, C. Ji, M. Tan and H. Yu, Adaptive neural network tracking control of robot manipulators with prescribed performance, *Proceedings of the Institution of Mechanical Engineers, Part I: Journal of Systems and Control Engineering*, 225(6): 790-797, 2011.

[163] C. P. Bechlioulis, Z. Doulgeri and G. A. Rovithakis, Neuroadaptive force/position control with prescribed performance and guaranteed contact maintenance, *IEEE Trans. Neur. Netw.*, 21(12): 1857-1868, 2010.

[164] Y. Karayiannidis and Z. Doulgeri, Model-free robot position regulation and tracking with prescribed performance guarantees, *Robotics and Autonomous systems,* 60(2): 214-226, 2012.

[165] A. K. Kostarigka, Z. Doulgeri and G. A. Rovithakis, Prescribed performance tracking for flexible joint robots with unknown dynamics and variable elasticity, *Automatica*, 49(5): 1137-1147, 2013.

[166] Yana, Yang, Hua Changchun, and Guan Xinping. "Adaptive prescribed performance control for nonlinear networked teleoperation system under time delay." *Control Conference (CCC), 2014 33rd Chinese*. IEEE, 2014.

[167] Yang, Yana, et al. "Adaptive neural network based prescribed performance control for teleoperation system under input saturation."*Journal of the Franklin Institute*352.5 (2015): 1850-1866.

[168] Yang, Yana, Changchun Hua, and Xinping Guan. "Synchronization control for bilateral teleoperation system with prescribed performance under asymmetric time delay." *Nonlinear Dynamics* (2015): 1-13.

[169] Veelenturf L P J. Analysis and applications of artificial neural networks[M]. Prentice-Hall, Inc., 1995.

[170] Lewis, Frank L., Aydin Yesildirek, and Kai Liu. "Multilayer neural-net robot controller with guaranteed tracking performance." *Neural Networks, IEEE Transactions on* 7.2 (1996): 388-399.

[171] Ciliz, M. Kemal. "Adaptive control of robot manipulators with neural network based compensation of frictional uncertainties." *Robotica* 23.02 (2005): 159-167.

[172] Yang, Yana, Changchun Hua, and Xinping Guan. "Finite Time Control Design for Bilateral Teleoperation System With Position Synchronization Error Constrained." *Cybernetics, IEEE Transactions on*, online first, 2015.

[173]"Adaptive Neural Network Control of Bilateral Teleoperation with Unsymmetrical Stochastic Delays and Unmodelled Dynamics", International Journal of Robust and Nonlinear Control, vol. 24, no. 11, pages 1628–1652.

[174] "Neural-adaptive Control of Single-master multiple slaves Teleoperation for Coordinated Multiple Mobile Manipulators with Time-varying Communication Delays and Input Uncertainty", IEEE Transactions on Neural Networks and Learning Systems, vol. 24 , no. 9, Sept. 2013, pp. 1400-1413.

[175] Li, Z., Xia, Y., Wang, D., Zhai, D. H., Su, C. Y., & Zhao, X. "Neural Network based Control of Networked Trilateral Teleoperation With Geometrically Unknown Constraints," IEEE Trans. Cybernetics, in publication process.

[176] Li, Zhijun, Yuanqing Xia, and Chun-Yi Su. *Intelligent Networked Teleoperation Control*. Springer, 2015.

[177] Hua, Chang-Chun, and Xiaoping P. Liu. "Delay-dependent stability criteria of teleoperation systems with asymmetric time-varying delays." *Robotics, IEEE Transactions on* 26.5 (2010): 925-932.